The University Of Sheffield.

Novel fibrinogen hydrogels for cell encapsulation and delivery

Sarah Louise Lindsay

A thesis submitted in partial fulfilment of the requirements for the degree of
Doctor of Philosophy

Faculty of Medicine, Dentistry and Health

The University of Sheffield

June 2017

Table of Contents

Abstract

Osteoarthritis is a debilitating disease that is predicted to affect 130 million people worldwide by 2050. Despite being a global problem, there is no cure for osteoarthritis. Therefore, there is a need for cell therapies to repair injured cartilage. Delivering and localising cells at the injury site is a major challenge, the use of hydrogels as cell carriers may overcome this challenge. Fibrin is a natural hydrogel and is formed by the proteolytic action of thrombin on fibrinogen creating a fibrous network of fibrin fibres. Cell encapsulation in fibrin has been demonstrated, these natural gels suffer from batch and manufacturer variability. Haemostatix Ltd. have developed novel cross-linked fibrinogen gels by attaching the active fibrinogen binding sequence (GPRP) to different molecules. This active sequence binds to fibrinogen without the need for thrombin, creating a multi-branched fibrin-like gel. This has the potential to provide opportunities to tailor gel properties for cell delivery. The aim of this research was therefore to investigate the potential use of the novel fibrinogen gels for the encapsulation and culture of chondrocytes and mesenchymal stem cells (MSCs).

The cell encapsulated fibrinogen gels were cultured under chondrogenic conditions for twenty-one days, fibrin gels were used as a reference material. This research has shown that chondrocytes and MSCs exhibited good survival and differentiation in both fibrinogen and fibrin gels. Chondrocytes remained in encapsulation throughout, and extracellular matrix (ECM) deposition was detected by measuring glycosaminoglycan (GAG) content and Toluidine blue staining. MSC's behaved differently, with evidence for cell migration from the fibrinogen and fibrin gels and degradation of the gels. This behaviour was inhibited by incubation with aprotinin. Gel degradation and MSC migration also occurred in serum-free culture conditions. In the presence of aprotinin, cell activity and GAG deposition suggested that the encapsulated MSCs survived and differentiated in the fibrinogen and fibrin gels.

The fibrinogen gels were comparable to fibrin for both chondrocyte and MSC encapsulation for cell activity and ECM deposition. The MSC migration and gel degradation was inhibited by aprotinin and therefore was most likely due to the activation of plasminogen. Removing plasminogen i.e. serum from the culture conditions resulted in gel degradation and MSC migration, suggesting that an aprotinin sensitive serine protease was produced that had activated fibrinogen and degraded the fibrinogen gels. The fibrinogen gels were comparable to natural fibrin, but offer the distinct advantage that the cross-linking density may easily be modified making the fibrinogen gel more versatile for use in different applications.

In conclusion, this novel fibrinogen system supported chondrocyte and MSC survival and differentiation, and these new biomaterials show great promise for use in cell encapsulation and delivery for cartilage regeneration.

Acknowledgements

I would like to thank my supervisors at the University of Sheffield: Dr. Aileen Crawford and Professor Paul Hatton, Haemostatix Ltd: Dr. Renata Zbozien, and the Medical Research Council for funding and giving me the opportunity to do this PhD. I am grateful to Aileen and Paul for all their encouragement, guidance and support throughout the research. I am thankful to Aileen, Katie, Rich and Saima for equipment and experimental training and continuous help within the laboratory. Thank you to Haemostatix Ltd: Sarah Middleton, Dr. Ben Nichols, Dr. Renata Zbozien, Steve Connick, Jonny Hunter and Greg Walker for providing the materials for this project but also their interest, support, warm welcome and training throughout my placement. The technical staff at the University of Sheffield have been great and always been willing to lend a helping hand including Kirsty Franklin, Brenka McCabe, Jason Heath, Dr. Robert Moorehead, Chris Hill, David Thompson, Dr. Jill Callaghan, Ian Brock, and Nicola Green. I would also like to thank Stuart Hunt for his advice and the great efforts he went to to help me and Gary Roche for his friendly words of encouragement.

A big thank you to the old and new D22 crew for their kind (and sometimes tough love) words of encouragement, ranting and de-stress drinks, as well as all the users of the busy and tropical TC. In particular, I am very grateful to Saima Ahmed for imaging my samples on the confocal microscope but also for all of her help, biology lectures, company to the abattoir, punchbowl times and friendship throughout. Thomas was a great support spending too many long days and nights typing in the Diamond together fuelled by coffee and biscuits with stressful breaks diffusing bombs. Joss has been a great friend, his chilled outlook and calm exterior emanated through the difficult times of PhD life.

Finally, I would like to express my appreciation to all of my amazing family and friends for everything they have done for me pre, during and post – PhD. A massive thank you to my mum, dad and brothers: Daniel and Chris, for always being there, answering the phone at all hours and showing an interest in my work. My grandparents have maintained their duties of spoiling me during my visits home; a welcomed break from experiments. Thank you to my best friend Amy, Emma and all of my lovely friends who have given me some great memories and provided so much support over the ups and downs of PhD and personal life. There are too many to list so those who have been a huge part of my PhD life make up a photo collage.

PhD by pictures

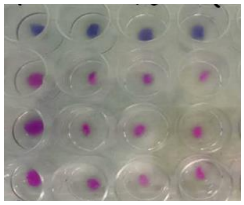

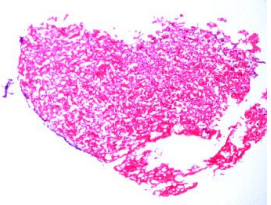

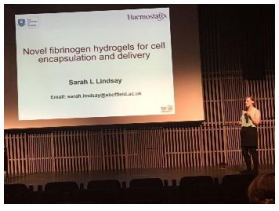

List of outputs

- British Society for Matrix Biology (BSMB) held in Chester, UK, April 2016. The conference was held in Chester, UK. I presented a poster and was awarded a writer's bursary to attend the conference.

- Tissue Engineering and Regenerative Medicine International Society (TERMIS) held in Uppsala, Sweden, June – July 2016. The conference was held in Uppsala, Sweden. I was awarded with an oral presentation in 'Hydrogels for TERM' session

List of abbreviations

- 2D – 2 dimensional
- 3D – 3 dimensional
- ACI – autologous chondrocyte implantation
- bBM-MSC – bovine bone marrow mesenchymal stem cell
- DMB - 1,9-Dimethylmethylene blue dye
- DMEM – Dulbecco's modified eagle medium
- DMSO - Dimethyl sulfoxide
- DNA - Deoxyribonucleic acid
- DTNB - 5,5′-Dithiobis(2-nitrobenzoic acid)
- ECM – extracellular matrix
- FBP – fibrinogen binding peptide
- FCS – foetal calf serum
- FPA – Peprostat bound to fibrinogen gel
- GAG – glycosaminoglycan
- H&E – Haematoxylin and Eosin
- IMS – industrial methylated spirit
- MACI – matrix induced autologous chondrocyte implantation
- MMP - Matrix metalloproteinases
- MSC – mesenchymal stem cell
- NICE – National Institute for Health and Care Excellence
- PBS – phosphate buffered saline
- PCL - Polycaprolactone
- PEG - Polyethylene glycol
- PLA - Poly(lactic acid)
- PLGA – poly(lactic-co-glycolic acid)
- PTFE – Polytetrafluoroethylene
- qRT-PCR – quantitative reverse transcriptase polymerase chain reaction
- RNA - ribonucleic acid
- SEM – scanning electron microscopy
- TGF-β – transforming growth factor beta
- tPA – tissue plasminogen activator
- uPA – urokinase plasminogen activator
- αMEM – alpha modified minimum essential eagle medium

List of Figures

List of Tables

1.0 Introduction

Articular cartilage is a highly specialised connective tissue providing structural support and absorbing compressive energy. Articular cartilage covers the ends of bones of diarthrodial joints. The main function of articular cartilage is to provide a smooth, near frictionless surface for joint articulation and to act as a biological "shock absorber" to protect articulating bones by absorbing the forces produced during movement. Articular cartilage has viscoelastic properties which enable it to withstand the forces placed on the joint due to every day movement. Cartilage is predominately avascular and aneural, therefore receiving nutrients and removing waste products is largely carried out by diffusion through the synovial fluid. This limits the regenerative capacity of articular cartilage because a typical cellular response of most tissues to injury usually involves vascularisation. Defects in articular cartilage due to trauma e.g. by sports injuries, may not heal and can result in eventual degeneration of the surrounding cartilage [1]. This process is considered the first step in a patient developing osteoarthritis.

Osteoarthritis is the commonest degenerative arthritis affecting joints of the body including the hand, feet, hip, shoulder and knee joints. Osteoarthritis places a huge economic burden and costs 1-2 % of GDP in developed countries [2] for treatment including assistive devices, medicine, and surgery but also for the time required for the patient to be off work [3]. Approximately 8.75 million people have requested treatment for osteoarthritis in the UK alone [4]. It is estimated that 8.3 million people aged 45 and over will have osteoarthritis of the knee alone by 2035, in the UK, placing a huge economic burden on the National Health Service [4]. Osteoarthritis is a global problem and it is predicted that by 2020 osteoarthritis will be the fourth leading cause of disability worldwide [5]. Further to this, by 2050 it is estimated that 130 million people will suffer from osteoarthritis worldwide [6]. Trauma, age and obesity are the highest risk factors associated with osteoarthritis [7] and affects a greater number of woman compared to men [8]. With an ever increasing aging population and obesity predicting to affect 11 million people in the UK by 2030 [9] osteoarthritis is going to continue to be a burden. Joint replacements are far from ideal as a solution to the disease particularly for younger patients. This is because the device loosens over time requiring revision surgery every ten to twenty years. Therefore, there is a huge need to find alternative treatment options for sufferers.

Regenerative medicine and tissue engineering technologies are focussed on stimulating tissue regeneration and repair of damaged tissues and tissue defects. One area

of focus of these technologies is that of the methodologies of delivering cells to a site of injury to aid in the regeneration of damaged tissue. Currently, one such area of cell delivery research is that of autologous chondrocyte implantation (ACI). ACI is undergoing clinical trials and has been successful in reducing pain and regaining joint mobility in patients with cartilage injuries [10]. By ACI becoming successful a cell delivery system must be researched in order to provide the cells with the optimum environment for cellular growth and differentiation. The extracellular matrix (ECM) of most tissues is a hydrogels and this is one of the reasons hydrogels are being investigated for cell encapsulation and delivery.

Many hydrogels are under investigation for cell encapsulation and delivery applications including fibrin. Fibrin is the first natural scaffold cells come across during the wound healing cascade and is a popular research material. Clinically, fibrin is used as a haemostat and has been used to encapsulate a variety of different cell types *in vitro*. However, due to fibrin being a natural material it suffers from batch and manufacturer variability. It is also difficult to alter the cross-linking density of fibrin gels. There are very few commercially available hydrogels with the advantages of natural materials and the tailorability of synthetic materials. Haemostatix Ltd. have developed a novel fibrinogen gel that takes advantage of the fibrinogen binding system. A synthetic molecule is linked to the active fibrinogen binding sequence (GPRP) that is available to bind to natural fibrinogen molecules. This creates a gel with the advantages of natural components and the tailorability of synthetic materials.

Therefore, the aim of this project was to investigate the potential of the novel cross-linked fibrinogen hydrogels provided by Haemostatix Ltd. for the cell encapsulation and delivery of chondrocytes and bone marrow-derived mesenchymal stem cells for the regeneration of articular cartilage. This novel cross-linked fibrinogen hydrogel was compared with the main competitor fibrin and agarose hydrogels.

2.0 Literature review

The literature review describes the structure and function of cartilage, the effects of osteoarthritis on patients, clinical current treatments and treatments in research for cartilage injury repair. The need for cell therapies and a novel delivery system will also be outlined. This will provide an overview of the background of the research allowing the impact of this work to be shown.

2.1 The structure and function of cartilage

Cartilage is a specialised connective tissue. There are four forms of cartilage: hyaline cartilage, fibrocartilage, elastic cartilage, and hypertrophic cartilage [11]. Hyaline cartilage is the most abundant type of cartilage within the body and can be found in the nose, trachea and at the ends of long bones. Elastic cartilage can be found in the ear and epiglottis, its main function is to provide support and be flexible whilst maintaining its shape. Fibrocartilage has the ability to absorb high levels of compressive energy and provides strength and support. This type of cartilage can be found in the spine as intervertebral discs and as the menisci in the knee joint.

Articular cartilage is classified as a hyaline cartilage, and is located on the ends of bones in diarthrodial joints. The main functions of articular cartilage are to 1) provide a smooth, low-friction surface for articulation and 2) to protect the bones by absorbing the compressive forces produced by joint movement, i.e. it acts as a biological 'shock absorber' [12]. Cartilage is made up of a sparse population of cells (chondrocytes) embedded in a dense ECM. The ECM of articular cartilage is composed predominantly of water which makes up approximately 80 % of its wet weight [13]. The remaining 20 % of the wet weight of the ECM is composed of proteins and proteoglycans and the oligoscaccharide hyaluronan. The major protein component of the ECM is collagen with 90 – 95 % of collagen in articular cartilage being collagen type II [14], collagen I, IV, V, VI, IX and XI make up the remaining collagen and contribute towards stabilising the collagen type II network [13]. Proteoglycans form a dense ECM [13] with aggrecan making up the majority of the proteoglycans, and comprises of a protein core bound to glycosaminoglycan (GAG) chains of chondroitin sulfate or keratan sulfate by covalent bonds [15] [13]. Its main function is to provide osmotic properties [13] and compressive strength [15] but also binds to hyaluronic acid via a protein linker to form a macromolecular aggregate [13]. The only cell type in cartilage is the chondrocyte and are

derived from mesenchymal stem cells (MSCs) [12]. MSCs secrete cartilage matrix and in doing this are known as chondroblasts which become surrounded in ECM known as the pericellular region. By chondroblasts being trapped in lacunae they are then known as chondrocytes. Chondrocytes are surrounded by a specialised ECM called the pericellular matrix [16]. This is important in protecting the chondrocytes during compressive loading and is involved in cell-ECM signalling and detection of compressive loads [16]. The pericellular matrix is formed from collagen fibrils of (mainly type VI collagen) and a dense proteoglycan matrix, providing protection to the chondrocytes during loading onto the joint [17]. The chondrocytes and surrounding pericellular matrix is known as a chondron. The territorial region of ECM surrounds the pericellular region protecting chondrocytes from mechanical forces.

Articular cartilage is composed of three different zones: superficial, middle and deep zones, see Figure 2.1 [13]. The superficial zone, approximately 10 – 20 % of articular cartilage, is the outermost zone and is in contact with the synovial fluid, its function is to protect the cartilage from shear stresses and tensile and compressive forces. The middle zone's main function is to resist compressive strength, this zone makes up 40 – 60 % of cartilage and is located between the superficial and deep zone. The deep zone is approximately 20 % of the total cartilage and provides the most resistance to compressive forces due to the organisation of collagen fibres, a low water concentration and high proteoglycan content. The mechanical properties of cartilage are due to the organisation of collagen fibrils in the interterritorial region, the ECM of the middle zone. The organisation of collagen fibrils differs in each zone: the collagen fibres run parallel to the surface of cartilage in the superficial zone; obliquely in the middle zone and perpendicular in the deep zone. Above the deep zone is calcified cartilage which contains hypertrophic chondrocytes and is separated from the deep zone by a tidemark. The function of the calcified cartilage is to adhere the articular cartilage to subchondral bone.

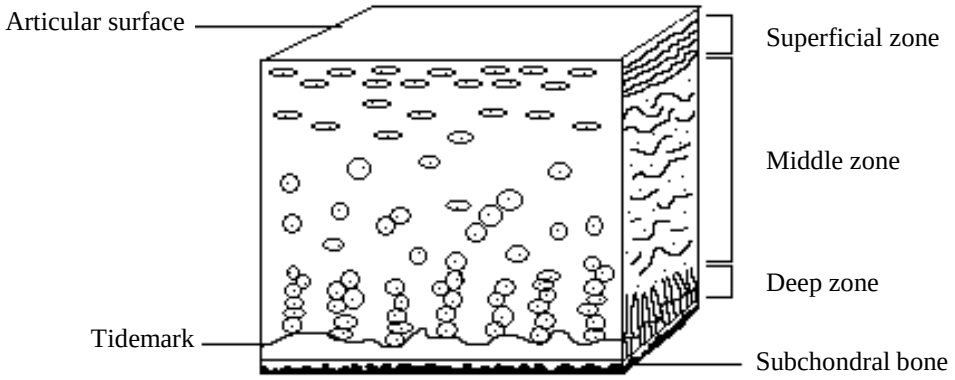

Figure 2.1 A schematic diagram of the structure of cartilage to show the morphology and distribution of chondrocytes (front of the diagram) and the orientation of collagen fibres (right hand side of the diagram)

Cartilage, unlike other connective tissues, is mostly avascular and aneural. Therefore, cartilage receives oxygen and nutrients, and waste products are removed by diffusion through the synovial fluid and matrix. Compression and regular movement of the joint is essential for the metabolism of the articular cartilage [18]. It is thought that the avascularity of cartilage is the cause of the limited capacity of the tissue to repair. Focal loss of articular cartilage causes lesions in the tissue and ultimately if the cartilage loss is severe, can lead to bone on bone grinding in the joints causing pain, discomfort and restricted articulation. Osteochondral defects consists of the full thickness of the cartilage and injuring the subchondral bone, in doing this bone marrow MSCs are released into the defect and begin to regenerate the cartilage. Unfortunately, this regeneration leads to the formation of fibrocartilage which has inferior properties to hyaline articular cartilage [19].

2.2 Cartilage injury and disease

Articular cartilage is an essential tissue for smooth, low friction joint articulation but this can be affected by injury or disease of the cartilage. The three major challenges associated with cartilage are: injury, rheumatoid arthritis and osteoarthritis. Cartilage injury is commonly associated with sports injuries and occurs in younger patients [20]. Three main types of cartilage injury can occur: matrix disruption, partial thickness and full thickness defects [21]. Matrix disruption is a small defect minimally injuring the articular surface. Partial thickness defects cause injury to the middle zone of the articular cartilage and full thickness defects injure the cartilage to the subchondral bone. Due to the limited capacity in which cartilage can repair itself these injuries do not heal, and currently the only treatment option for severe cartilage injuries is a joint replacement. Due

to patients with injuries to cartilage typically being younger, joint replacements are not a suitable treatment option, as discussed in more depth in section 2.3. But if the injury is not treated osteoarthritis may develop [22].

The main diseases affecting articular cartilage are osteoarthritis and rheumatoid arthritis. Both diseases result in the loss of articular cartilage from the diarthrodial joints causing decreased joint mobility and chronic pain. Rheumatoid arthritis is an autoimmune disease that results in the inflammation of diarthrodial joints [23]. Osteoarthritis is the loss of articular cartilage from diarthrodial joints which may be a result from previously untreated cartilage injuries, as previously stated.

The challenges of cartilage injury and disease requires intervention to aid in the repair of articular cartilage. There is a clear link between injury of the cartilage and osteoarthritis [24] and therefore osteoarthritis will be discussed in more depth below, section 2.2.1.

2.2.1 Osteoarthritis

Osteoarthritis is a debilitating complex disease which is characterised by loss of the articular cartilage. This leads to an increase in the friction coefficient, and loss of the ability of the diseased areas to withstand compressive loading which together, results in difficult and painful articulation of the joint. Age, obesity, sports injuries and trauma are risk factors for osteoarthritis [7]. It is still unknown as to why age is a contributing risk factor however, the majority of suffers are aged over 45. 49 % of women and 42 % of men aged over 75 have required treatment for osteoarthritis, these statistics suggest that age is contributing factor. Previously, it was suggested that osteoarthritis was an inevitable part of growing older this is because there is a general reduction of collagen synthesis contributing to other health problems such as cardiovascular disease [25]. However, it is now considered that osteoarthritis takes many years to develop into a symptomatic disease with a need for clinical intervention [26]. Obesity is a risk factor due to the increased weight being placed on the joint. A lack of exercise and sufficient movement and loading onto the joint may also cause cartilage degradation [13]. This is because regular movement and joint loading is required for metabolic activity. It is widely known that changes in the biomechanical and biochemical properties of the articular cartilage contribute towards the progression of the disease, these changes are still unknown and therefore it is difficult to find a cure. A defect may occur in the cartilage due to a disruption in chondrocyte metabolism affecting the chondrocyte – matrix

interactions [15] or due to chondrocyte apoptosis. Apoptosis occurs during the normal developmental stages of skeletal growth [27] but releases ECM degradative factors which can lead to the breakdown of the cartilage creating a defect [28]. Chondrocytes may respond to mechanical stress by synthesising proteinases involved in the degradation of the matrix [15] causing a defect in the cartilage. Once a defect has been established, the articular cartilage surface becomes much weaker so the injury can easily worsen. Synovial fluid MSCs are easily accessible to cartilage and it has been shown that they are present in a healthy joint [29]. During the early stages of osteoarthritis it has been shown that the number of synovial fluid MSCs increases [29] and continues to increase throughout the different stages of osteoarthritis [30]. But the role of synovial fluid MSCs in osteoarthritis is still uncertain.

Osteoarthritis can be categorised into stages depending on the severity and progression of the disease, these stages are a guide and stages can overlap throughout the progression of the disease [31]. The first stage is the formation of micro-cracks known as fibrillation in the superficial zone of the articular cartilage. Chondrocyte aggregation can occur at this stage causing a lack of chondrocytes within the chondron. Stage two is defined as fibrillation of the superficial zone. Matrix can break off the articular cartilage surface and into the synovial fluid causing inflammation. As fibrillation in the articular cartilage reaches the middle zone, the third stage of osteoarthritis has been reached. Chondrocyte death is also a feature of stage three. Stage four is a crucial stage for matrix degradation, a build-up of excess water in the middle zone and further matrix erosion into the synovial fluid. Complete cartilage degradation to the subchondral bone is stage five of the disease. This is where an attempt at cartilage repair occurs by microfracture: the subchondral bone can release MSCs which differentiate to form fibrocartilage. Stage six is a further change in the articular cartilage structure with the formation of fibrocartilage. Osteophytes also develop during the progression of the disease but are not stage specific and can appear at any time [32]. Osteophytes may form due to remodelling of the joint caused by osteoarthritis, or as a result of the biochemical and biomechanical changes in the joint stimulating the growth. This means that osteophytes may be formed as a response to compensate for the injured articular cartilage.

Fundamentally, the end result of osteoarthritis is the degradation of articular cartilage, with the formation of bony osteophytes and subchondral bone cysts [33]. This causes stiffness of the joint, painful articulation and inflammation. Currently, there is no cure for osteoarthritis and a full joint replacement is often required. There are treatments which

aim to extend the life of the joint to prolong the inevitable invasive joint replacement surgery.

2.3 Current treatments for osteoarthritis

The main symptom for osteoarthritis is chronic pain both when the joint is bearing weight and when the joint is at rest. Current treatments for osteoarthritis do not provide a cure, but provide valuable symptomatic relief by alleviating pain, helping them to maintain their mobility and independence. Nonsteroidal anti-inflammatories such as ibuprofen and pain relief medications, for example paracetamol, may be effective in the early stages of the disease as well as the use of assistive devices such as walking sticks to aid mobility [34]. To help relieve pain, patients are also advised to exercise to reduce the weight bearing on the joints and to build muscle strength around the joint to relieve pressure. These treatments are for patients with osteophytes and those progressing to damage, and thinning, of the cartilage [31], [35]. Even though these treatments do not provide a cure for osteoarthritis, they aid in pain reduction and prolonging the function of the joint before a joint prosthesis is required. Other treatments which are available on the National Health Service are arthroscopic debridement, hyaluronic acid injections, microfracture, and osteotomy, to realign the joint tissues if clinically indicated, and the cartilage transplantation technique, mosaicplasty. Eventually replacement of an arthritic joint with a joint prosthesis may be required.

2.3.1 Intra-joint injections of hyaluronic acid

Hyaluronic acid is a main component of synovial fluid and aids in; the lubrication of articular joints; the protection of cartilage; and provides the viscoelastic properties of synovial fluid [36]. When the concentration of hyaluronic acid in synovial fluid is decreased or the hyaluronic acid is degraded the viscosity is lowered. This has an effect on the biomechanics of the joint and leaves it susceptible to damage. Hyaluronic acid injections aims to replenish the hyaluronic acid in the synovial fluid to re-establish the lubrication of the joint and shock absorbance [37]. Joint homeostasis is only established for approximately three months after a hyaluronic acid injection due to the short half-life of the hyaluronic acid molecule.

2.3.2 Arthroscopic debridement and joint lavage

Arthroscopic debridement of the joint is when areas of damaged cartilage or bone in the joint are surgically removed and the joint surface smoothed by abrasion. [38]. Debris found within the joint can be removed by joint lavage. However, the National Institute for Health and Care Excellence (NICE) guidelines indicate that this procedure is not an effective procedure for alleviating pain for sufferers of osteoarthritis [39].

2.3.3 Microfracture

Microfracture involves drilling holes through subchondral bone causing a wound site in the area of the damaged cartilage [40]. The wound site stimulates healing by forming a blood clot and releasing MSCs from the bone marrow which migrate into the wound. The MSCs proliferate and differentiate to form fibrocartilage composed mainly of type I collagen. The disadvantage with this procedure is that fibrocartilage has inferior properties to hyaline articular cartilage due to the absence of appropriate viscoelastic and biochemical properties under compressive loading during joint movement. The success of the procedure is dependent on surgical technique and the rehabilitation after surgery.

2.3.4 Osteotomy

Osteotomy is a procedure where the bone is shortened in length and the joint realigned to relieve pressure on the joint [41]. This surgery is carried out when osteophytes have formed in the joint and this bone is removed to increase the space and reduce excess friction inside the joint. Removal of osteophytes alleviates pain and lengthens the life of the joint [42]. This procedure is only suitable for a small number of patients with osteoarthritis.

2.3.5 Mosaicplasty

Mosaicplasty is a procedure which involves transplanting an allograft or autograft of cartilage to the injured areas [26]. Osteochondral disks are removed from a non-weight-bearing area and implanted into the injury site, until the site is covered. The graft tissue integrates into the joint and behaves as the natural tissue. This procedure has had very good results in a follow up study of up to seventeen years [43]. However, due to the nature of the treatment the potential donor site morbidity is a potential significant problem with

time. It is not known whether the donor sites for the osteochondral plugs develop in to osteoarthritis.

2.3.6 Joint replacement

As osteoarthritis progresses, the articular cartilage is eroded and the joint space between the bones of the joint become closer together reducing the space in the joint capsule, decreasing the volume of synovial fluid in the joint. This reduces joint mobility making articulation very difficult and painful for the patient. A total joint replacement is the final treatment option and the only treatment that provides a solution to the problem but is not ideal as a long-term solution for osteoarthritis. Between 2003 and 2014, 772,818 artificial joint replacements of the knee and 708,311 replacements of the hip were carried out, of which 96 % and 93 %, respectively, of cases were due to osteoarthritis [44]. Joint replacements have been very successful for patients over the age of 65, increasing the patient's quality of life. For younger, more active patients the joint replacements loosen over time due to increased pressure on the artificial joint [45]. Revision surgery is required to replace the joint which is an invasive procedure and approximately 5 % of those that have a joint replacement will require revision surgery within 10 years of surgery [46]. Between 2003 and 2014, 47,829 revision surgeries of the hip and 79,859 revision surgeries of the knee were carried out [44]. Research is being undertaken into new materials for artificial joints or techniques for repairing the cartilage particularly in younger patients [45]. Other concerns over total joint replacements is the invasive surgical procedure with a 20 cm – 30 cm incision required, however mini-incision surgery is now recommended decreasing the incision to 10 cm – 12 cm [47]. Concerns over a greater risk of revision surgery and infection for mini-incision surgery have been reduced as NICE have reported that less than 1 % of patients treated with mini-incision surgery or the conventional joint replacement surgery were treated for an infection. However, patients required revision surgery sooner in mini-incision surgery in comparison to the conventional joint replacement. Research is focusing on increasing the longevity of the artificial joint or finding new methods for repairing cartilage for patients who require the artificial joint to last longer than 20 years to reduce the economic burden on the National Health Service.

The current treatments for osteoarthritis are currently far from ideal. They enable sufferers to maintain their independence and mobility but have a finite life-span. Younger

patients will require revision surgery which is an invasive procedure and not as effective as the first joint replacement surgery. This is why research in this area is crucial for osteoarthritis sufferers and the burden on the social and healthcare systems for example the National Health Service.

Tissue engineers are currently researching techniques based on the theory that natural tissue is much better at doing its job compared to joint prostheses. Cartilage is made up of chondrocytes which are derived from MSCs. This is why it is thought that cell therapies such as autologous chondrocyte implantation (ACI), that deliver chondrocytes or MSCs to the site of injury, could enable the regeneration of the damaged area given the appropriate environment. ACI is a potential treatment for the repair of the initial cartilage injury to prolong the joint and reduce the development into osteoarthritis.

2.4 Tissue engineering and regenerative medicine

Tissue engineering and regenerative medicine focuses its research on repairing and regenerating damaged tissue in the body this is because there is a limited availability of organs and tissues for transplantation. Due to an increasingly aging population there has become a much higher demand for tissue grafts and organs for repair or replacement of damaged tissues [48]. Regenerative medicine is an emerging field which seeks to find alternative methods to repair damaged, diseased or missing tissue and organs using various technologies, such as tissue engineering. Tissue engineering uses the knowledge of both cellular and molecular biology combined with materials and mechanical engineering to fabricate tissue grafts formed *in situ* or *in vitro* [49]. This technique is currently being researched for the treatment of cartilage injuries. ACI is the delivery of chondrocytes to the cartilage defect to aid in the repair of the tissue. This has been discussed in more detail below, section 2.4.1.

2.4.1 Autologous chondrocyte implantation

ACI is under investigation because it is thought that the results will produce a more hyaline cartilage structure and function compared to other treatments such as microfracture which produces fibrous cartilage. The type of cartilage produced during repair is important for the function of the joint. Brittberg et al was the first to publish ACI in 1994 and involves the implantation of cells, specifically chondrocytes, to the cartilage

defect [50]. The cells are isolated from an autologous biopsy of cartilage taken from a non-weight bearing area of the joint, cultured in the laboratory and implanted back into the patient [51]. After isolation, chondrocytes are cultured in monolayer on tissue culture plastic in the laboratory. During this culture the cells take up a fibroblast like morphology and after four passages the morphology changes and the cells dedifferentiate and begin to lose their phenotype [52]. However, it is known that the early passages of chondrocytes can regain full mature chondrocyte phenotype once cultured on a 3-dimensional (3D) substrate such as a fibrous or gel scaffold. This is why ACI is feasible and has the potential to regenerate injured cartilage. By isolating chondrocytes from an autologous cartilage biopsy, the risk of rejection is very low. However, this does mean a donor morbidity site is established in a non-load bearing area of the joint. Not only is this an additional surgical procedure for the patient, the lesion created may increase the risk of osteoarthritis in the future [53].

Research into this method has been conducted since the 1990's and therefore there are studies with follow up times of up to twenty years [54], [55], [56], [57]. The studies involve delivery of chondrocytes to an injury in the cartilage. Comprehensive clinical trials into ACI for osteoarthritis have not yet been conducted. The first generation of ACI involves the use of a periosteal flap [58]. The surgical procedures in the studies are invasive using a parapatellar arthrotome approach of creating a lesion [59] this approach opens up the knee joint completely. The injured cartilage is trimmed and neatened during the surgical procedure and an autologous periosteal flap was sutured over the defect allowing the chondrocytes to be injected between the flap and the injured cartilage [54]. Thus keeping the cells localised in the damaged area. Using an autologous periosteal flap means a reduced chance of rejection and infection however, it also means a potential site of morbidity which can cause further complications and procedures. A periosteal flap has been shown to undergo hypertrophy in a number of patients and has required further surgical procedures [57] highlighting the need for further research into cell delivery and localisation of cells to the defect.

ACI for cartilage defects has given good results in clinical trials and has been compared to microfracture as a treatment method in random clinical studies. The studies are mostly based on pain, improvement and satisfaction outcomes from questionnaires filled in by the patient over the follow up period. A five-year follow up study has shown no significant differences between ACI and microfracture treatment methods in terms of patient pain and procedure failures [60]. Both treatments significantly reduced the pain

for the patient compared to pain before treatments. Unfortunately, rehabilitation was not enforced or controlled on this study and therefore it is not possible to determine if these results are due to the success of the procedure and satisfactory or lack of rehabilitation. Other studies have found long-term benefits to ACI including reduced pain and increased mobility but these studies have not seen a complete regeneration of the cartilage [56]. It has also been shown that ACI can form hyaline-like cartilage [55] however some cartilage repairs did not achieve this [54] [61]. The periosteal flap was thought to encourage chondrocyte de-differentiation and benefit the ACI process. However, due to complications such as hypertrophy, other techniques are under investigation instead of the use of a periosteal flap such as matrix-induced autologous chondrocyte implantation (MACI).

MACI is the second generation of ACI, and involves the use of a collagen scaffold to seed the patient's chondrocytes after the cell numbers have been expanded in the laboratory as previously described. The chondrocyte-seeded scaffold is then adhered in the joint using fibrin glue [62]. The use of the collagen scaffolds to deliver the chondrocytes to the joint keep the chondrocytes *in* situ and do not require further surgical intervention due to hypertrophy [63]. Patients experienced a reduction in pain after surgical intervention with MACI and hyaline-like cartilage or hyaline-like with fibro-cartilage was found to have formed over the defect [62]. These results suggest that a periosteal flap is not needed to encourage hyaline-like cartilage formation and other scaffolds have the benefit of less complications such as hypertrophy or sutures. Therefore, the surgical procedure can be quicker and the need for revision surgery for the removal of hypertrophy is not required.

ACI can be affected by a number of factors for example the size of the defect and age of the patient. Patients were analysed with defect areas of less than or greater than 15 cm^2 meaning that if the defect was a perfect circle the diameter of the defect would be 4.37 cm [57]. The mean defect area was measured at 8.4 cm^2. A larger defect area of greater than 15 cm^2 had significantly higher outcomes scores compared to those with defects with an area of less than 15 cm^2 however, the failure rate for larger defects was significantly higher over the fifteen year follow up. The age of the patient is a major factor in the regeneration of the cartilage using ACI, patients aged between thirty and forty five at the time of surgery had a significantly lower rate of success compared to those under the age of thirty. These studies are only investigating ACI for cartilage defects and not for the repair of cartilage for osteoarthritic patients. Other factors include subchondral treatments

attempting to repair the cartilage prior to ACI which may affect the success rate of the treatment, for example microfracture. If microfracture has been carried out prior to ACI the treatment is less effective compared to that of just ACI [64] [65].

Research is being undertaken in MSC delivery to regenerate cartilage, this is the natural next step to using chondrocytes because chondrocytes are formed from the differentiation of MSCs. Microfracture releases MSCs from the subchondral bone but the cartilage formed is inferior to articular cartilage, and a scaffold material is not used to retain the MSC's in the cartilage lesion. MSCs have the ability to differentiate into many cell lineages including chondrogenic differentiation [66] and maintain their multipotency on tissue culture plastic [67]. Growth factors and the cellular environment determines MSC differentiation for example chondrogenic differentiation requires MSCs to be cultured in a 3D environment in the presence of transforming growth factor beta (TGF-β) [68]. MSCs are more readily available compared to chondrocytes and can be found from different sources for example bone marrow [69], synovial fluid [70], and adipose tissue [71]. Due to the variance in isolation of MSCs from different sources resulting in different characteristics, a broad set of criteria has been set in place to classify a cell as a MSC. The definition includes three criteria: adherence to tissue culture plastic; multipotent differentiation specifically osteogenic, chondrogenic and adipogenic differentiation; and the expression of specific surface antigens [72]. Human MSCs must adopt all three of these criteria however, when using animal models the expression of surface antigens may not be fully established and therefore this criteria may be removed. By introducing these criteria, MSC characteristics will become internationally standardised to ensure that all research and clinical practises are using MSCs. The differentiation capacities and versatility of MSCs makes them suitable for a wide range of applications. Currently research is focussing on how to utilise MSCs in tissue engineering. MSCs have been shown to migrate towards injury sites and undergo specific injury site differentiation [73]. The reason for migration to a site of injury is still unknown, however intracellular signalling pathways and chemoattractive factors have been shown to induce cell migration [74]. MSCs also have anti-inflammatory responses at injury sites making them attractive for delivery to wound sites or for tissue regeneration [73]. Cell migration and anti-inflammatory responses are also reasons why MSCs are being investigated for tissue regeneration.

ACI is a promising treatment for cartilage defects due to the positive and successful results with reduction of pain and increased joint mobility. However, the cartilage does

not fully regenerate over the long term follow up periods, and therefore more research needs to be carried out to find out why full cartilage regeneration may not occur. Part of this may be down to the delivery method, the chondrocytes used for implantation, and the donor morbidity site caused by a cartilage biopsy. Results with collagen scaffolds have shown more promising results compared to that of the periosteal flap. Further disadvantages of the periosteal flap are: the invasive surgical procedure; another donor morbidity site; the potential of the flap to undergo hypertrophy; and a desirable 3D environment is not created due to the chondrocytes being injected under a periosteal flap. This is why the third generation ACI is being investigated [75]. 3D scaffolds are being used to provide a more natural tissue-like environment for cell delivery and localisation of cells in the injury site via a less invasive method. It has been shown that implanting cells to a site of injury can aid in the regeneration of tissue. It is essential that there is a method of delivering cells safely and keep them localised in the injured area to help repair the damaged tissue.

2.4.2 Scaffolds

One way of regenerating tissue is by supplying appropriate cells to the damaged area however, the main challenge associated with this is ensuring cells remain localised at the injury site. Therefore, there is a need to develop novel scaffolds. The function of scaffolds is to provide a supporting system for cell adhesion, growth and differentiation. For the majority of tissue engineering applications, the basic process remains the same; cells are seeded onto a supporting 3D scaffold *in vitro* and then implanted to the site of injury [76]. At this point, cell adhesion, proliferation and differentiation occur across the scaffold and the tissue regeneration process can begin. An objective for tissue engineers is to create suitable 3D scaffolds to provide temporary support and guidance for tissue growth and regeneration [77]. There are two main ways in which scaffolds can be seeded with cells to encourage tissue regeneration: one way is to create a scaffold from either natural or synthetic materials and introduce cells *in vitro*, the other way is to encapsulate cells within the materials during the formation of the scaffold *in vitro* [77]. The materials used and the final biological application will determine which scaffold fabrication route will provide the best support for the desired cell type.

Scaffolds have a very important role in tissue engineering, and need the necessary chemical and physical properties to support cell adhesion, growth, migration,

differentiation [78], and vascularisation [79], all of which are essential for the regeneration of most body tissues. The chosen scaffold materials must be biocompatible, and degradable [80], with a controllable degradation rate [81], the material and degradation by-products must be non-toxic and non-immunogenic, [82]. The surface chemistry must promote cell adhesion [83], whilst the mechanical properties should ideally, mimic those of the ECM of the desired tissue [84]. Porosity and interconnected pores [85] are essential to ensure cell migration and the delivery of nutrients and oxygen to the cells as well as encouraging ECM production [86]. Scaffold materials need to be easily fabricated in 3D in a variety of different sizes and shapes [83]. Culturing cells on a 3D support is essential for promoting effective tissue formation. Research in two-dimensional (2D) cell culture has resulted in the addition of extensive scientific knowledge. However, 2D culture does not enable cells to fully function as they would in the human body [87]. Most tissue-derived cells rapidly de-differentiate in 2D culture systems. Cell-cell interaction, which is essential for cell function, is limited in 2D culture as communication can only occur between neighbouring cells. Cells naturally grow and exist as 3D cultures with ECM performing the supporting 'scaffold' function, within the human body. 3D culture allows cells to have virtually 100 % contact with each other or the developing ECM, and therefore increasing the cell-cell interactions and mimicking the natural environments for the cells [88].

Scaffolds are used for a variety of different applications including cartilage repair [89], nerve regeneration [90], skin tissue engineering [91], bone regeneration [92], wound healing [93], and drug [94], and growth factor delivery [95]. Each of these applications requires cell or drug delivery to encourage the tissue to regenerate and repair itself. Specifically cell encapsulation has been used to treat diabetes [96], growth factor deficiency [97] and Alzheimer's disease [98].

Fibre and porous material scaffolds including collagen [99], polyglycolic acid [100] and polylactic acid [101] have been studied for use in tissue engineering applications. These scaffolds have been successful as a supporting system for cell proliferation and differentiation. However, the focus of this research is on gel based scaffolds known as hydrogels and this is because hydrogels have the potential for use as injectable, cell delivery systems.

2.4.3 Gel based scaffolds

Hydrogels are becoming increasingly popular as a scaffold for cell encapsulation and delivery. Their high water content, water insolubility and tissue-like-nature make them

ideal for tissue engineering applications [77]. Hydrogels can be formed from both natural and synthetic materials, examples of which are shown in Table 2.1. Naturally occurring materials used in cell encapsulation typically consist of proteins or ECM components and have been shown to encourage cell survival to a greater extent than synthetic biomaterials [87]. Cellular interactions with the ECM and cell – cell communication is essential for survival and growth of tissues [102]. Integrins within the ECM are available for cell adhesion which allows cells to communicate with the matrix and surrounding cells [103]. Natural materials have the advantage in that they contain ligands for cell binding, encouraging cell survival [104]. Synthetic biomaterials do not naturally contain ligands, however methods such as ultraviolet radiation-induced degradation of polymers can promote cell adhesion to a synthetic ECM [105]. Despite these surface modification techniques, cellular behaviour is often more comparable to the native tissue when cells are encapsulated in natural materials compared to synthetic materials [104]. A limitation of natural materials is that they are usually derived from animal sources and therefore, can pose a risk of infection, disease or prion transfer and a possibility of immunogenic reactions in patients because of the animal-protein components [106]. It is also difficult to control mechanical properties and degradation rates of naturally derived hydrogels. However, an advantage of natural hydrogels is that the human body can naturally degrade the gels and excrete any waste products [107]. An advantage of synthetic hydrogels is that the properties can be more readily modified. For example, the mechanical properties can be altered to suit different applications and synthetic gels are highly reproducible with very little batch to batch variation [108]. Synthetic hydrogels are becoming the focus of research for these reasons. The properties of hydrogels make them ideal for cell encapsulation and delivery but only certain materials can be used for this application. The process of cell encapsulation requires the cells to be re-suspended in one of the components and this must be non-toxic, cytocompatible and cell friendly in its liquid state [109]. However, an advantage to this system is the gelation process will occur in and fill the desired area without the need to manufacture in the required shape or dimension. Liquid precursors will disperse the cells evenly throughout the gel and create an injectable system ideal for cell delivery.

Table 2.1 A summary of different materials used as scaffolds/cell delivery applications in tissue engineering

Gel	Source	Encapsulated cell types	Reference
Agarose	Red algae	Mesenchymal Stem Cells Human marrow stromal cells Chondrocytes	Huang et al. 2004. [110] Karoubi et al. 2009. [111] Mauck et al. 2002. [112]
Albumin	Human blood plasma	Islet cells Smooth muscle cells	Shapiro et al. 2000. [113] Gonen-Wadmany et al. 2007. [114]
Alginate	Brown algae	Fibroblasts Chondrocytes Mesenchymal Stem Cells Osteoblasts Schwann cells	Hunt et al. 2010. [115] Andrade et al. 2011. [116]. Jonitz et al. 2011. [117] Smith et al. 2007. [118].Yu et al. 2010. [119] Alsberg et al. 2001. [120] Pannunzio et al. 2005. [121]
Collagen	Animal/Human tissue	Fibroblasts Chondrocytes	Marenzana et al. 2006. [122] Galois et al. 2006. [123]
Fibrin	Animal/Human blood plasma	Smooth Muscle Cells Keratinocytes Chondrocytes Urethral Cells	Ahmann et al. 2010. [124] Voigt et al. 2006. [125] Park et al. 2005. [126] Bach et al. 2004. [127] Ho et al. 2006. [128]

		Mesenchymal Stem Cells	
Gelatin	Hydrolysation of Collagen	Chondrocytes Hepatocytes	Lien et al. 2009. [129] Wang et al. 2006. [130]
Hyaluronic Acid	Human/ Animal tissue including skin and cartilage	Chondrocytes Dorsal Root Ganglia	Yoo et al. 2005. [131] Horn et al. 2007. [132]
Poly(caprolactone)	Synthetic	Chondrocytes	Li et al. 2003. [133]
Poly(ethylene glycol)	Synthetic	Mesenchymal stem cells Chondrocytes Fibroblasts	Benoit et al. 2008. [134] Bryant et al. 2002. [135] Koh et al. 2002. [136]
Poly(lactic-co-glycolic acid)	Synthetic	Chondrocytes	Shin et al. 2012. [137]

2.5 Synthetic hydrogels

A range of synthetic hydrogels are used in research for cell encapsulation and delivery. By using synthetic products the materials can offer greater versatility and control over the porosity, cross-linking density and the degradation rate of the gels. The sample of synthetic hydrogels as shown in Table 2.1, are discussed below in more detail.

2.5.1 Poly (caprolactone)

Poly (caprolactone) (PCL) is a polyester rarely used in forming hydrogels [133]. PCL has been shown to be compatible with a range of cell types but there are concerns over the slow degradation rate. This may hinder the growth of tissue in the hydrogel resulting in reduced regeneration but this property makes PCL suitable for long-term drug or factor delivery [138]. Vaccines are another application where PCL is used because the environment created is not acidic making it ideal for antigens. Co-polymerisation, for example with PEG, has been shown to improve the mechanical properties of PCL

including the degradation rate and biocompatibility making it a more desirable material [139].

2.5.2 Poly (ethylene glycol)

PEG is the most commonly used synthetic polymer in cell encapsulation [77] and many successful results have been reported with various cell types, including chondrocytes [140]. However, the use of PEG is limited to cells which do not require cell adhesion due to the absence of ligands. It is possible to overcome this limitation with cross-linking 'arginine–glycine–aspartic acid' (RGD) peptide sequences into the gel. This peptide sequence is known to permit cell adhesion and this has given successful results with MSCs [141]. There are a number of ways in which PEG can be fabricated into a hydrogel and then tailored to a specific application [142]. Photopolymerisation is the most common method using light to transform PEG from a liquid state to a solid hydrogel creating a biocompatible gel [143]. PEG consists of two functional groups which can be modified for cross-linking by introducing reactive vinyl groups [144]. The density of cross-linked vinyl groups also determines the mechanical properties and the porosity of the hydrogel both properties of which are important for cell encapsulation and delivery. Therefore, being able to tailor the mechanical properties and porosities of the PEG gels is a big advantage [77]. However, an increase in mechanical strength is achieved by increasing the cross-linking of the hydrogel which in turn leads to decreased pore size which can compromise the diffusion of nutrients into or release of drugs or cells from the gel. It is important to achieve a balance of porosity and mechanical strength for a desired application. PEG is not a naturally degradable polymer and therefore will not degrade as tissue is forming in the hydrogel. However, it is possible to change the degradation properties with the addition of co-polymers [145]. PEG co-polymerised with polylactic acid (PLA) [146] or PCL [147] has been shown to degrade naturally. PEG can also exist as a stable liquid precursor prior to gelation allowing for an *in situ* injectable gel application [143]. More recently, Kar et al researched PEG hydrogels containing disulfide moieties enabling molecules secreted by MSCs to degrade the hydrogel [148]. Versatility of the gel can be established by altering the cell seeding density, and cross-linking density. PEG is a desirable material for use in cell encapsulation because it is biocompatible and can easily be modified to suit different applications.

2.6 Natural hydrogels

Cellular survival and differentiation has been demonstrated when encapsulated in natural hydrogels. Natural materials contain proteins and/or ECM components which allow for ECM – cell communication which is fundamental to cellular survival. Table 2.1 demonstrates a range of hydrogels in research for cell encapsulation applications and a sample of the hydrogels have been discussed in greater depth below.

2.6.1 Agarose

Agarose is a polysaccharide derived from red algae which forms a porous, soft gel with mechanical properties similar to tissue [149]. It is a promising gel in tissue engineering due to its ability to encapsulate cells and factors required for regeneration of injured tissue. Agarose is a temperature dependant gel; between 40 °C and 90 °C agarose exists as a polymer solution and as cooling takes place to approximately 30 °C to 40 °C a solid gel forms [150]. This temperature induced gelation makes it very difficult to encapsulate cells below temperatures which would injure the cells (i.e. below 40 ^{o}C) as gelation occurs very rapidly below 40 ^{o}C [107]. To overcome this problem a liquid nitrogen cooling system has been fabricated which solidifies the agarose in thirty seconds [149]. A disadvantage of agarose is that it is non-biodegradable by mammalian tissues, meaning the gel could hinder tissue formation reducing the rate and effectiveness of the regeneration process [151].

2.6.2 Albumin

Albumin is the most abundant protein found in human blood, constituting up to 60 % of blood plasma [152]. It is composed of a polypeptide chain arranged in α-helices, bound together by di-sulphide bonds [153]. Albumin's main roles include transport of various substrates and maintaining body fluid distribution [152]. Clinically, albumin is used as a blood substitute, in treating severe burns, diagnosing and treating breast cancer, diabetes and infectious diseases, and is also in clinical trials for further cancer treatments and drug delivery systems [154]. A desirable trait of albumin is its ability to bind to a number of different substrates including hormones, fatty acids, peptides, and drugs [155]. This property allows albumin to be used as a controlled release drug delivery system. Despite albumin having a high affinity for peptides and drugs, there is a lack of cell adhesion sites in the molecule which limits its potential in cell encapsulation and delivery [114]. To

overcome this problem, albumin could be cross-linked with other proteins such as fibrinogen which provides cell adhesion sites and supports cell migration, whilst the albumin moiety could control the release of bound drugs producing a potential cell and drug delivery system [155].

2.6.3 Alginate

Alginate is a water soluble polysaccharide sourced from brown algae and is currently widely used in the food and drink industry [156]. It is composed of two polymers D-mannuronic acid and L-guluronic acid, joined by 1, 4 – glycosidic linkages, alginate forms a gel in the presence of calcium ions [157]. Mechanical properties of the gel are dependent on the age, species and the location of the algae sourced [158]. However, it is possible to alter the mechanical properties by varying the concentrations of mannuronic acid and guluronic acid [108] or by using a co-polymer such as PEG [159]. An alginate gel is fabricated under mild conditions, is porous, and naturally degradable making it ideal for the release of proteins and cells [160]. A big advantage of this system is its pH sensitivity; protein release is inhibited at low pH enabling oral ingestion for pharmaceutical drug applications [161]. Retaining proteins [160] and cells [162] within the gel for a sustained release is the main challenge associated with this gel. The addition of the RGD sequence improved cell adhesion to the gel in long term cultures of up to forty-one days [163]. Alginate gels can be formed *in situ* [164] or *in vitro* by techniques such as 3D printing [165]. This versatility provides greater control over gelation and the structure of the gels making them ideal for tissue engineering applications.

2.6.4 Collagen

Collagen has received much attention for use in tissue engineering because it is the most abundant protein in ECM [166]. Over twenty different types of collagen are found in the body, however, type I collagen is the most common. Collagen hydrogels form at 37 ^{o}C and therefore they can be used to form gels *in situ* on injecting into the body [167]. However, this process takes around ten minutes and for most surgical applications a much quicker gelation process is desirable.

Collagen naturally binds to a variety of different cells making it an ideal scaffold to encourage cellular adhesion and growth [168]. Collagen hydrogels are degradable by proteolytic activity [169] and can be modified with the addition of fibronectin, chondroitin sulphate or hyaluronic acid to encourage the survival of different cell types

[170]. Collagen gels are mechanically weak despite being a native protein component of ECM. However, there are techniques which can improve the mechanical strength of collagen gels [171]. Cross-linking is one way to do this, which affects the covalent bonds between collagen molecules and the intramolecular bonds [172]. Another way is to 'reinforce' the collagen gel with components such as organic or synthetic polymers. Poly (lactic-co-glycolic acid) (PLGA) [173], GAGs [174] and glycation with ribose [175] have been shown to improve the mechanical strength of collagen gels. Another limitation of collagen gels is that cells may cause contraction of the gel after encapsulation and so prevent the gel from filling the required area [176]. Also, batch to batch variation in collagen is problematic [177].

2.6.5 Hyaluronic acid

Hyaluronic acid has been used in clinic for cosmetic applications [178] because of this hyaluronic acid has been investigated for use in tissue engineering and regenerative medicine. However, cross-linking is required to decrease its fast degradation rate [179]. Cross-linking with collagen decreases the degradation rate [180] and improves the mechanical properties of the gel [181]. Snyder et al. researched hyaluronic acid and fibrin gels but this resulted in a weak gel, the mechanical strength could be improved by modifying hyaluronic acid with methacrylic anhydride [182]. A modified hyaluronic acid gel was formed from photo-crosslinking with visible light, this creates a more feasible gelation system in clinic [183]. This hyaluronic acid gel was combined with plasma lysate, a known source growth factors, and cells to create a viscoelastic matrix that was successfully cryopreserved. This would enable an "off the shelf" product that could be used as an injectable system and gelled *in situ* with visible light. Hyaluronic acid is a versatile molecule in which the properties can be altered to suit different applications and therefore has promise in tissue engineering and regenerative medicine.

2.6.6 Chondroitin Sulfate

Chondroitin sulfate is a glycosaminoglycan and is present in ECM, as previously discussed. It has been shown that chondroitin sulfate has an anti-inflammatory effect and as a result could have a regenerative effect on delivery [184]. Chondroitin sulfate gels are mechanically weak [185] however, cross-linking with PEG increases the mechanical properties of the gel [186]. Lü et al researched a chondroitin sulfate – chitosan hydrogel that has the ability to self-repair in two hours [187]. Multiple aldehyde groups were

formed on chondroitin sulfate allowing imine bonds to form between the amine groups on N-succinyl-chitosan. Imine bonds continuously break and re-form when the gel remains in contact forming a strong, durable repair. This gel has a major advantage in tissue engineering for high load-bearing applications however, a lower repair rate would be desirable.

2.6.7 Fibrin

Fibrin is formed as the end product of the blood clotting cascade within the human body and it is the first natural scaffold cells adhere to during the wound healing cascade [188]. Fibrin formation requires two crucial components fibrinogen and the enzyme thrombin [189]. Fibrinogen monomers are 45 nm in length and are comprised of two D domains linked to a central E domain by a coiled-coil structure as shown in Figure 2.2 [190]. A fibrinogen molecule is composed of two sets of three polypeptide chains, Aα, Bβ, and γ, in the E domain. Aα contains a fibrinopeptide A sequence while Bβ contains a fibrinopeptide B sequence [191]. Fibrin is formed from the cleavage of fibrinopeptides A and B by the enzyme thrombin releasing a polymerization site which binds to the D domain of the adjacent fibrinogen monomer. This process creates a dense network of fibrin fibres and is further stabilized by factor XIIIa, also activated by thrombin, which cross-links α and γ chains forming a stronger clot [192].

Clinically, fibrin is used as a haemostat to reduce bleeding in surgical applications, and can come in a variety of forms such as sprays, thin films and gels [193]. Fibrin gels have been successfully used to encapsulate different cell types and have many properties which make it ideal as a cell delivery system. A desirable advantage of fibrin gels is that the structural and mechanical properties can be modified by altering the concentration of fibrinogen, thrombin or calcium present during gelation [189]. Rowe et al found that higher thrombin concentrations of 1 unit of thrombin per milligram (mg) of fibrinogen, formed more compact gels with: an increase mechanical stiffness; an increase in fibre bundles; thinner fibres; lower porosity; and also faster gelation times, compared to that of gels formed with lower thrombin concentrations of 0.001 units of thrombin per mg of fibrinogen [194]. Herbet et al researched the effect of calcium concentration on the structure of fibrin [195]. A calcium ion concentration of 2 millimolar (mM) resulted in a decreased fibre bundle diameter, increased fibre bundles and higher mechanical stiffness in comparison to fibrin gels formed with higher calcium concentrations of 10 mM, [195]. Fibrin scaffolds degrade naturally by fibrinolysis, however, the degradation rate can be

rapid [189]. Cross-linking or use of protease inhibitors such as aprotinin can reduce the degradation rate allowing tissue to form before the fibrin fully degrades [196] [197].

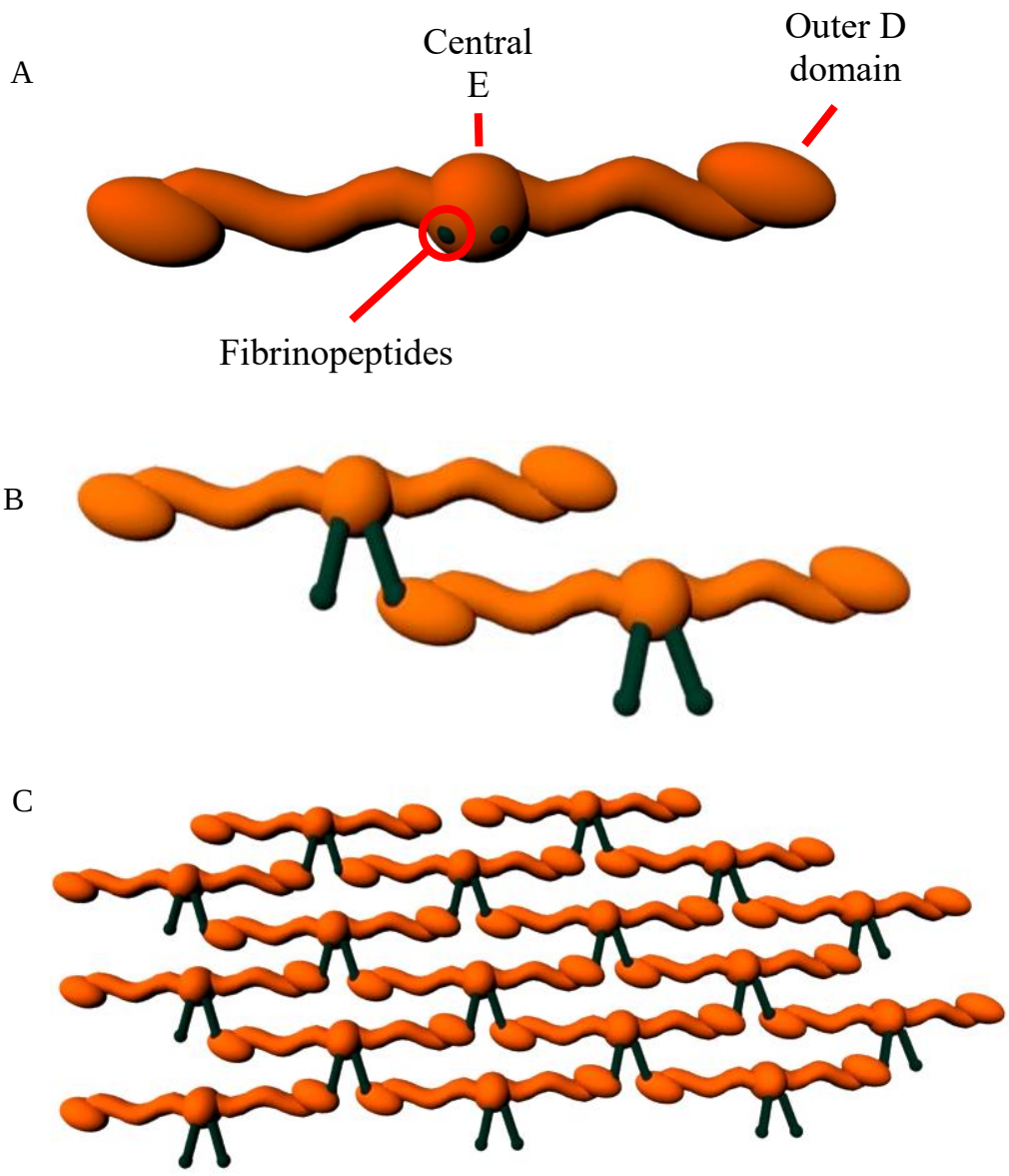

Figure 2.2 A fibrinogen monomer, with two outer D domains and a central E domain connected by a coiled-coil. The green circles represent the fibrinopeptides. B demonstrates the binding of the fibrinopeptides to the outer domains of adjacent fibrinogen molecules. C is a demonstration of a fibrin hydrogel forming fibres.

.

Fibrinogen can be isolated from the patient's own blood reducing the risk of transferring infection, making fibrin a highly desirable gel [198]. Fibrin is commercially available and has also been used widely in clinic and therefore is known to be biocompatible and non-toxic when used in the body. Fibrinogen and thrombin are

commercially available as kits as a high quality and quality assured product. Fibrin gels can be fabricated in two ways: creating the gel and implanting it into the body or injecting the gel precursors into the desired area and forming a gel *in situ* [199]. The latter procedure allows fibrin to gel in any shape and to fill small cavities which might not have been previously noticeable [200]. Cells would be required to be re-suspended in the liquid precursor aseptically meaning this must be biocompatible before gelation but would allow for more uniform spreading of the cells within the gel [77]. The main disadvantage of fibrin gels is that they are mechanically weak and therefore may not be able to withstand physiological conditions [201]. Increasing the density of cross-linking and the addition of a synthetic or natural cross-linker such as methacrylated hyaluronic acid increases the mechanical strength of the gel making it more suitable for use in the human body [202] [182].

2.7 Natural-synthetic hydrogels

Combinations of natural and synthetic hydrogels are one way to overcome the limitations of pure natural or synthetic gels. The main limitation of fibrin gels is the mechanical stiffness [201]. The mechanical stiffness of PEG–fibrinogen gels is increased as the PEG concentration is increased, because more functional groups are present from PEG creating a highly cross-linked structure [203]. Pure PEG hydrogels have a higher stiffness in comparison to PEG–fibrinogen gels because PEG carries five times more functional groups that are available for cross-linking. PEG–fibrinogen hydrogels should be able to withstand higher forces in the body compared to fibrin hydrogels. A limitation of synthetic hydrogels is the inability of cells to adhere however, the fibrinogen moiety provides the natural binding ligands for cell adhesion and to support cellular growth and differentiation [104]. An increase in PEG concentration increases the cross-linking in the network which results in an increase in mechanical strength of the gel but also a decrease in pore size limiting cell migration and also a decrease in the rate of degradation [204]. This means it is important to research the optimum functional groups present for cell survival.

Interpenetrating networks are fabricated from two or more components which form a network by intertwining [205]. Dinescu et al formed gels based on interpenetrating polymer network with gelatin, alginate and polyacrylamide [206]. Cells were able to adhere to the natural gelatin and alginate whereas the material structure and properties were provided by polyacrylamide, providing a gel that supported chondrogenesis. Wen et al investigated polymers such as PEG to reinforce thiolated chitosan to form a

biocompatible hydrogel for cell or drug delivery [207]. Also, an increased cross-linking density reduced the rate of drug release from the gel.

Natural and synthetic gels enable greater versatility and control over the degradation rate, and mechanical strength. Synthetic polymers provide the structural and mechanical properties required to withstand forces within the body and the natural component provides biocompatibility and enables cell adhesion and encourages differentiation. These properties are essential for an optimal gel for cell delivery applications.

2.8 Cross-linked hydrogels

As discussed in natural and synthetic hydrogels one material cannot provide the material properties and biocompatibility required for optimum material degradation, strength, cell adhesion, proliferation and differentiation. Therefore, a popular method to increase the strength, durability and to decrease the degradation rate of hydrogels is to cross-link natural or synthetic materials.

Pan et al. researched aldehyde dextran and amino gelatin as an *in situ* gel that formed within four minutes [208]. The importance of the concentrations of cross-linkers is highlighted in this study. The optimum concentrations had a quicker gelation rate and higher cross-linking density but a faster degradation rate. This is contradictory to other research where the higher the cross-linking density the slower the degradation rate [209] [210] [211]. Moghadam et al. cross-linked hydroxyethyl methacrylate with dimethacryloyl hydroxylamine to fabricate a gel with a long-term degradation rate and the ability to withstand load bearing applications [212].

Fibrin is another gel that suffers from rapid degradation rate and is mechanically weak, as previously discussed. The addition of aprotinin [213] or tranexamic acid [214] has been shown to reduce the degradation rate of the fibrin gels. Cross-linking is another way to overcome this problem. Genipin cross-linked with fibrin gels has been shown to reduce degradation rate and improve the mechanical properties of the gel [215]. The macroscopic structure of the cell encapsulated gel remained intact for up to 28 days in culture.

Self-assembling cross-linked gels are advantageous in tissue engineering applications. This will allow for gelation *in situ* which is highly desirable in a clinical setting, such as oxidised alginate and gelatin [216]. This gel formed *in situ* within twenty seconds without the need for external factors is highly advantageous in tissue engineering. Other self-assembly gels that are being investigated for use in tissue engineering and regenerative medicine require external factors to aid in their gelation. For example, chitosan and

gelatin self-assembly gels were prepared via ice segregation that required temperatures of -196 ºC [217]. Gelation requiring external factors such as photoresponsive, temperature, or pH changes are not desirable for a clinical setting. One way to overcome these problems is by using nanoparticles that can be injected to the site of injury after gelation has occurred.

Cross-linking can also be used to allow for a viscous or a weak gel cell delivery system that is thermo-responsive for gelation *in situ.* Cai et al have shown that a PEG based gel combined with a recombinant protein formed a weak, injectable network [218]. The cross-linking of the gel with poly(N-isopropylacrylamide) occurs *in situ* due to a thermal phase transition on injection into the body. This cross-linking improved cell retention and proliferation within the gels, creating an injectable, long-term delivery system. Kim et al also took advantage of a thermo-responsive gel formed from methylcellulose and ECM from adipose tissue, as the temperature was increased to 34 ºC a stronger gel formed making it ideal for gelation *in situ* [219]. These gels have many uses in tissue engineering and regenerative medicine by providing a non-toxic, easy delivery system and gelation ensures that cells remain localised at the injury site.

Cross-linking can also be achieved by click chemistry. Click chemistry is commonly used to form gels because: the reaction cannot produce toxic by-products; is carried out under simple reaction conditions; and does not require the use of solvents [220]. Chitosan and hyaluronic acid can be modified to enable a click chemistry reaction forming a gel that supports *in vitro* cell viability [221]. However, other click reactions require external factors such as UV light [222]. A controlled degradation rate has been a limitation for popular materials used in cell delivery, click chemistry is one way to overcome this. By incorporating nitrobenzyl moiety into a PEG – gelatin based gel, the introduction of UV light causes the complete degradation of the gel in 2 – 3 minutes [223]. This would enable complete control over the degradation of the gel and is highly advantageous in cell delivery applications.

The recent advances in hydrogel formation via cross-linking is a popular method to overcome the main limitations of materials used for cell delivery. As described throughout this section, a variety of different methods can be used to fabricate gels to allow for an injectable delivery system. Materials can be modified to provide gelation *in situ* without the need for external factors to ensure the hydrogels are suitable for and have potential use in clinic.

2.9 Commercial hydrogels

According to GlobalData the market value for osteoarthritis therapies is $5 billion and set to continue rising. But the expense and lack of comprehensive clinical trial data of using cell therapies is inhibiting its progress. There are a range of commercially available hydrogels as shown in Table 2.2, which are available for research purposes or are used in current clinical trials. Each hydrogel is a cell free scaffold or delivers the patient's own cells to the site of injury. The fabrication method and components of the scaffolds/hydrogels are not stated in Table 2.2 if they are unknown, this is because companies may not publish all aspects of their scaffolds for intellectual property reasons. All information displayed in Table 2.2 is publicly available.

Table 2.2 A table describing the current commercial hydrogels for use in research or clinic

Company	Product	Material	Application	Cell type	Comments
Organogenesis	Apligraf	PLA	Healing of venous leg ulcers and diabetic foot ulcers	Human keratinocytes and fibroblasts	The scaffold was made by solvent casting and sterilised with ethylene oxide Must be left in place for 5-7 days and then the dressing can be changed every 3 to 5 days. For 5-7 days the patient is unable to move and must remain in hospital until the wound has healed
Cellon	ArtiGEL	N/A	Research model	Human adipose derived stem cells	Available as two solutions: A - stored at room temperature B - stored at 4 ˚C. Different storage temperatures requires more set up time. Precursor solutions can be mixed with cell suspension in a 1:1 ratio, then placed in a well, a 100 µl solution in a 96-well plate takes 8 minutes to gel. This is a long gelation period.
ebers	Go Matrix	Gelatin	Research model	Fibroblasts	Gelatin from porcine skin, this is an animal product therefore a risk of cross species contamination. Scaffolds are 9 mm diameter and 1 mm thick. Uniform pores with sizes of 60, 90 or 130 µm
Cytograft	TESA	Cell extracellular matrix	Regeneration of damaged tissue	Dermal fibroblasts	Cells are cultured and matrix synthesis is encouraged. This is used to form sheets, threads or sprays to repair damaged organs or deliver cells. The cells used are either allogenic which will give a risk of rejection or autologous cells isolated from a biopsy and cultured.

3D Biotek	3D Inserts	PCL PLGA Polystyrene Hydroxyapatite discs Polystyrene and PCL	Research model	N/A	Sterilised via gamma radiation. PCL comes ready to use as well plate inserts. This is a 100 % porous structure and has batch to batch reproducibility. Scaffolds are mechanically strong and easy to handle. Polystyrene and PCL combination has been used for cancer research and stem cell research PCL - is rarely used due to its slow degradation rate
Histogenics	NeoCart	Collagen (type 1)	Cartilage regeneration	Patients own chondrocytes	This company are in stage 3 of clinical trials. A biopsy of non-load bearing cartilage is taken from the patient. The cartilage is digested into chondroctyes and are expanded in the laboratory and seeded onto the collagen scaffold. The scaffold is placed in a bioreactor under load bearing conditions for 1 week. The scaffold is then transferred to static culture for 1-2 weeks and is then re-implanted over the defect in the patient. Collagen - Gelation forms at 37 ˚C and therefore can form *in situ* in the body but this process takes about 10 minutes. It has the ability to bind to a variety of different cell types. There is batch to batch variation it is mechanically weak and as a gel contraction occurs after cell encapsulation.

ESI.BIO Stem Cell Solutions Sigma Biotime	HyStem HyStem -C HyStem - HP	Hyaluronic acid	In vivo and in vitro research	N/A	Customisable hydrogels. HyStem - animal free HyStem - C contains thiol modified collagen to encourage cell adhesion. Contains animal products. HyStem - HP contains collagen for cell adhesion and heparin. Gives a slow more controlled release, suitable for growth factor delivery. Contains animal products Hyaluronic acid is a naturally occurring polysaccharide and is found in the extracellular matrix of connective tissue
biotissue	AmnioGraft	Amniotic membrane	Protect, repair and heal damaged eyes	N/A	Ready to use membrane that is removed from the packaging and placed directly on the patient's eye to encourage healing. Usually used after surgery
Corbion	PURASORB	poly DL-lactide/glycolide (PDLG) poly DL - lactide (PDL)	Controlled release systems	N/A	N/A
	PURASORB	PLGA lactide/caprolactone copolymers	Tissue regeneration scaffolds	N/A	N/A
Organovo	Bioprinting	Human tissue	Tissue repair	N/A	3D printing of human tissue for repair of damaged tissue
DASILVA institue	Stem cell therapy	Adipose derived stem cells	Tissue regeneration	Adipose derived stem cells	Stem cells are isolated from the patient's naturally occurring adipose tissue. These are then re-implanted to the site of injury for regeneration

Advanced polymer materials INC.	N/A	PEG/PLA PEG/PCL PEG/PHB	Drug delivery and tissue engineering	N/A	Supply companies with biocompatible and biodegradable polymers PEG - has no cell adhesion sites and doesn't degrade naturally, requiring cross-linking to make this happen. The mechanical properties and porosity can easily be tailored but increasing the strength results in a decrease in porosity interfering with nutrient transfer.
DSM	Drug delivery platform	poly esteramide (PEA)	Drug delivery	N/A	Short and long term drug delivery
	OPTRIX	Porcine derived tissue	Tissue repair and regeneration	De-cellularised	Porcine tissue grafts that can be used for soft tissue repair. The graft is de-cellularised, disinfected and virus' inactivated. Contains collagen matrix and ECM components
Regenexx	Regenexx-SD	N/A	Cartilage regeneration	Bone marrow and blood samples from patient	A bone marrow and blood sample are taken from the patient and sent to the lab for processing and re-injected into the injured area. The cells can be injected on the same day or if more cells are required, after culturing. MSCs are isolated from the bone marrow and growth factors are isolated from blood.
Anika	Orthovisc	Highly purfied sodium hyaluronate	Alleviate symptoms of osteoarthritis	None	An injection of hyaluronic acid into the joint to alleviate symptoms of osteoarthritis. 3 to 4 injections are given 1 week apart to reduce symptoms for up to 6 months. Non-animal product Reduction in joint pain and increased mobility

Anika	Hyalofast	Hyaluronic acid	Scaffold for cartilage regeneration	Mesenchymal stem cells	The scaffold is a single 3D fibrous layer of a benzyl ester of hyaluronic acid. The scaffold can be cut to fit the injured area and implanted. MSCs can be entrapped on the scaffold, and the scaffold supports MSC adhesion, proliferation and differentiation. As the scaffold degrades hyaluronic acid is released into the joint providing a good environment for cells to grow. It is suggested that hyaline cartilage is formed from this method
biotissue	Bioseed	A polymer fleece and biological glue	Scaffold for cartilage regeneration	Patients own chondrocytes	The biological glue fixes the chondrocytes onto the fleece. Requires 28.8 million cells per scaffold The fleece and be implanted over the injury 4.5 weeks after the original biopsy. Fleece needs to be cut to fit injury
	Chondotissue	Polymer fleece and hyluronic acid	cartilage regeneration	Cell free	The fleece forms the network structure and the hyaluronic acid aids in regeneration of the cartilage. Fixation is with absorbable nails and involves an invasive surgery
ISTO technologies	RevaFlex	scaffold free	cell based cartilage	Patients own cells	A cell biopsy is taken from the patient and grown in the lab into a piece of cartilage and implanted over the site of injury

Haemostatix Ltd	Peprostat	Recombinant albumin coupled to fibrinogen binding peptides	Wound healing	N/A	Recombinant albumin is an artificial product coupled to the fibrinogen binding peptide. This peptide can bind to fibrinogen rapidly without the need for the enzyme thrombin, like fibrin. Peprostat is being developed as a haemostat for surgical applications.

2.9.1 HyStem

HyStem is a customisable hydrogel kit available from a variety of different companies. The basis of HyStem is hyaluronic acid which is thiolated making it highly versatile. Peptides can be linked onto thiolated hyaluronic acid by using simple chemistry for additional binding capabilities. As described previously, cross-linking has the additional advantages of increasing mechanical strength and providing cell adhesion sites. Hyaluronic acid is a component of synovial fluid and is known to encourage chondrogenic differentiation and therefore is a potential hydrogel for ACI.

2.9.2 Regenexx

The delivery of cells to a site of injury can be achieved without the use of a hydrogel or scaffold and has been done by Regenexx by obtaining bone marrow biopsies and blood samples and injecting these to the site of injury. The advantage of this is that the bone marrow can be injected to the site of injury on the day of isolation, reducing the patient's procedures and the need to isolate and culture the cells from the biopsy. This deceases the costs of cell delivery dramatically.

2.9.3 ISTO Technologies

ISTO Technologies are taking a different approach and isolating chondrocytes from healthy cartilage biopsies from the patient. The cells are then used to produce a piece of healthy cartilage in the laboratory and re-implanted into the patient at the site of injury. The disadvantage to this method is that potential morbidity sites are formed which may develop into osteoarthritis in the future creating more complications from the procedure. The isolating and culturing of chondrocytes in the laboratory to enable cartilage formation will be expensive.

2.9.4 Novel cross-linked fibrinogen gels

Fibrin gels have been used *in vitro* for cell encapsulation and as a biological sealant and are formed from the cleavage of fibrinogen by the enzyme thrombin (section 2.6.7). However, thrombin is unstable and must be stored at -20 °C [224]. Haemostatix Ltd. have developed a novel haemostat, known as Peprostat, for surgical and wound healing applications. This novel haemostat consists of a carrier bound to the highly active

fibrinogen binding peptide (FBP) sequence (GPRP) [224]. The peptide sequence GPRP interacts with the distal ends of fibrinogen monomers resulting in a dense, branched fibrillar network without the need for the enzyme thrombin as shown in Figure 2.3 [225]. Peprostat is currently in clinical trials as a topical haemostat and consists of recombinant albumin coupled to FBP. Peprostat rapidly forms a durable clot which stems bleeding in surgical applications. Peprostat is stable in liquid form and is available in ready-to-use formulations and therefore is a much faster and more convenient haemostat for use in surgery, in comparison to the leading competitor fibrin. Further carriers for FBPs are being developed by Haemostatix Ltd. such as peptide sequences known as P15, P17 and the commercially available HyStem. The peptide sequence P15 contains the RGD sequence known to encourage cell adhesion [226]. P17 contains DGEA which binds to α2β1 integrin [227] present on collagen type I [228] and is known to interact with various cells via binding to α2β1 integrins on the cell surface.

The research conducted for this thesis focused on the use of these novel cross-linked fibrinogen gels for cell encapsulation and delivery. *In vitro,* on introduction of the FBP carrier molecules to commercially available fibrinogen a novel fibrinogen cross-linked hydrogel is formed almost instantaneously. The stable, liquid precursor is a huge advantage in tissue engineering to allow cells to be re-suspended in the solution before gelation, adding to the ease of delivering cells to a site of injury. The liquid precursors also allow for an injectable system with gelation *in situ,* creating a less invasive procedure for patients. The fibrinogen – FBP carrier network is a cell friendly hydrogel and therefore has potential for tissue engineering applications. The structure and properties of the hydrogel are readily modified by altering the concentration of FBP available during gelation. In theory, the higher the concentration of FBP present during gelation, the greater the cross-linking density of the hydrogel producing a more compact and less porous gel. This allows the hydrogel to be tailored for specific cell types and applications. It is known that the environment in which the cells are in, can change cellular behaviour and therefore having a versatile hydrogel is important when a variety of different cell types can potentially be encapsulated [229]. The combination of natural and synthetic materials provides the benefits from the natural tissue-like environment for cell survival and the versatility of synthetic materials to ensure the porosity is optimal for cell survival and differentiation.

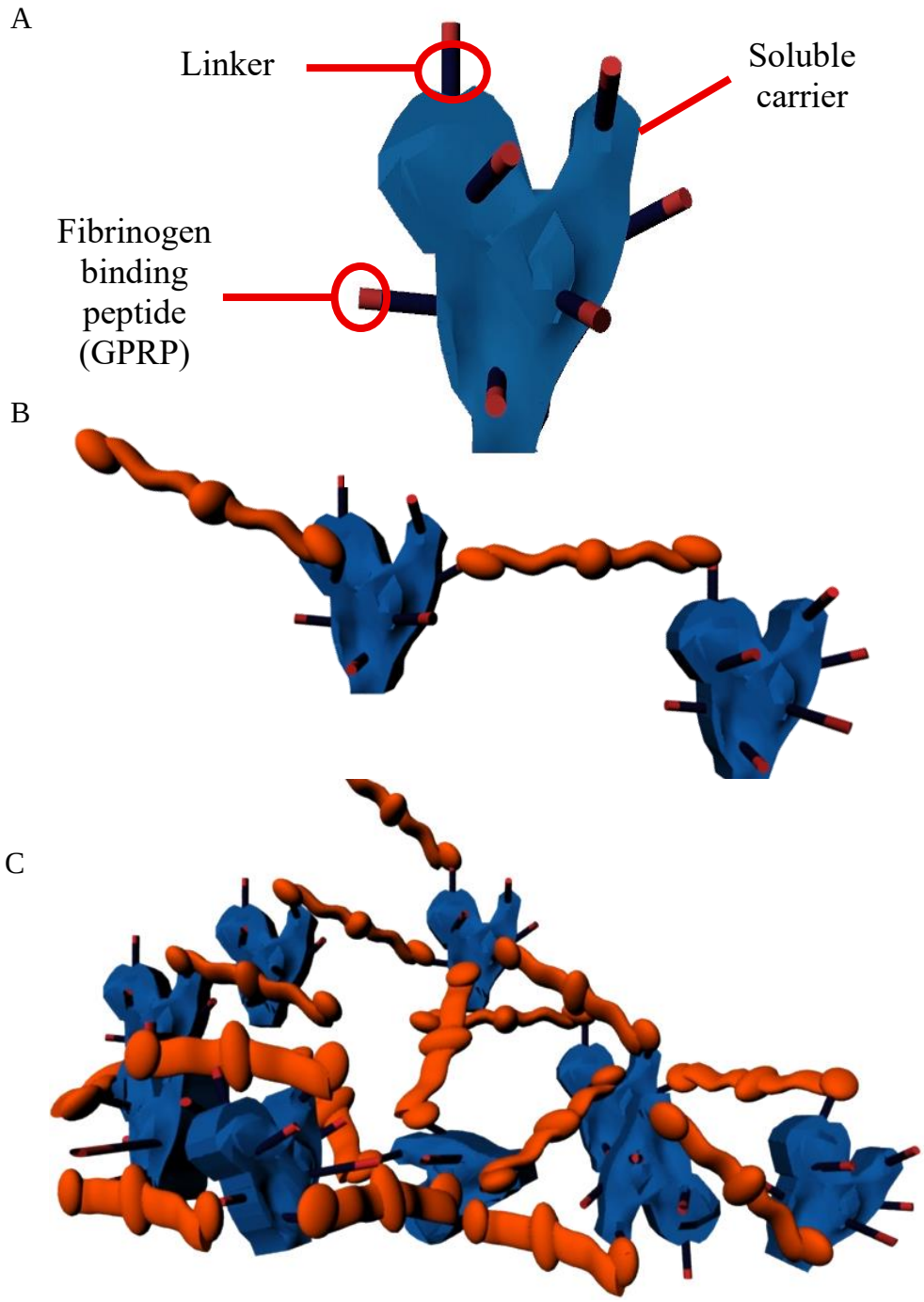

Figure 2.3 A schematic of the gelation process between FPA and fibrinogen molecules to create a cross-linked fibrous network A) shows the FPA molecule, the fibrinogen binding peptides are represented in red, B) shows the gelation process beginning with the active fibrinogen binding sequence binding the fibrinogen molecule, C) shows the highly cross-linked fibrous network.

The FBPs are bound to different carrier molecules including Peprostat, P15, P17, and HyStem and when individually combined with fibrinogen form the novel cross-linked fibrinogen gels. As described above, recombinant albumin is one carrier for the FBP and is known as Peprostat. On introduction to commercially available fibrinogen *in vitro* a hydrogel is formed, this hydrogel will be known as FPA. Other carriers for the FBP that were researched as part of this thesis and when combined with fibrinogen to for a gel will be known as P15 and P17. As described above, P15 contains the sequence RGD which has been incorporated into gels to encourage cell adhesion and cell viability [230] [231]. P17 contains the DGEA sequence which has been demonstrated to encourage cell differentiation [232]. Further information about these peptides are unavailable due to intellectual property sensitivity.

HyStem is a commercially available research product and contains chemically synthesised hyaluronic acid and a thiol-reactive cross-linker, refer to Figure 2.4. This enables the incorporation of the active fibrinogen binding sequence to bind to the thiol-reactive cross-linker. The FBP was linked to the hyaluronic acid molecule via the 12mer peptide sequence, refer to Figure 2.5. The thiol group binds to the 12mer peptide sequence using thiol-maleimide chemistry and the resulting molecule contains the FBP linked to the hyaluronic acid molecule, refer to Figure 2.6. On contact with fibrinogen the FBPs bind to the outer D domains of the fibrinogen molecules creating a hydrogel. HyStem is based on hyaluronic acid as a carrier for the fibrinogen binding peptide and was chosen because it has been shown to support chondrocyte differentiation and greater ECM deposition [233].

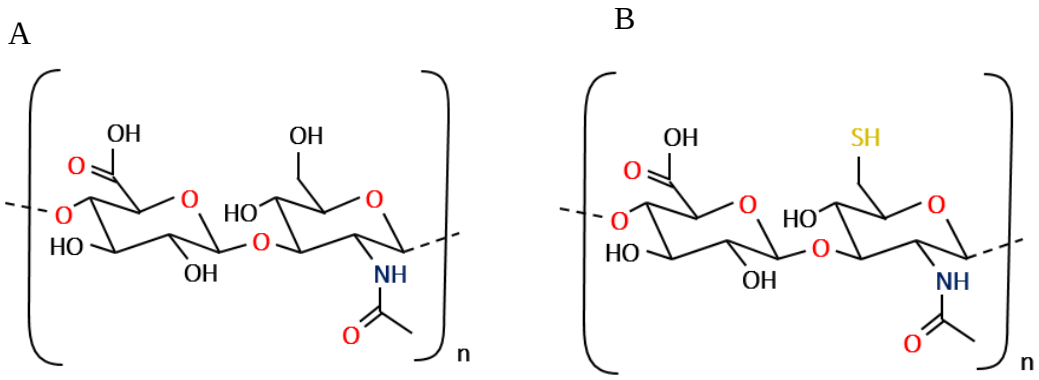

Figure 2.4 The molecular structure of a hyaluronic acid molecule (A) and the thiolated hyaluronic acid molecule (B)

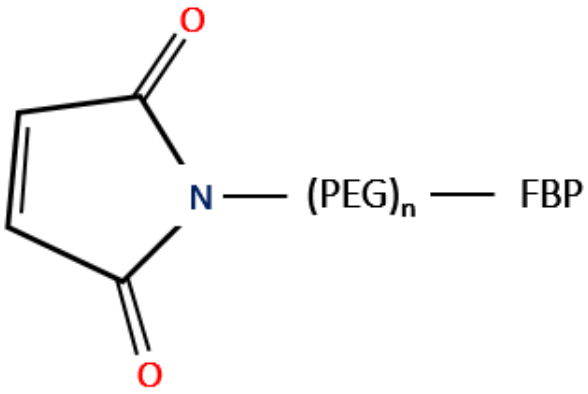

Figure 2.5 molecular structure of the 12mer peptide linked to the fibrinogen binding peptide (FBP)

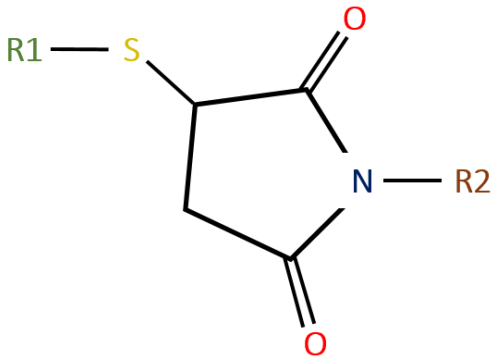

Figure 2.6 HyStem (R1) conjugated to the fibrinogen binding peptide (R2) via the 12mer peptide sequence

In summary, the cell encapsulation and delivery systems reported have limitations. Synthetic gels suffer from poor biocompatibility. Natural gels have the advantage of biocompatibility and provide a favourable environment for cell survival but have the added risk of disease transmission, and batch variability leading to challenges in quality assurance. Novel cross-linked fibrinogen gels based on the highly regulated and high quality commercial fibrinogen with synthetic cross-linkers, have the potential to overcome these issues to provide an innovative gel that is optimised for cell encapsulation. These novel cross-linked fibrinogen gels will not only provide the biocompatibility and tissue-like nature of natural materials but also the versatility of greater control over the cross-linking density. If developed further these novel fibrinogen gels should provide a superior cell delivery system that would improve the clinical outcomes of cell therapy and regenerative medicine approaches to hyaline cartilage repair. Therefore, this study will investigate the use for these novel fibrinogen gels for cell encapsulation and delivery focussing on cartilage repair.

3.0 Aims and Objectives

The literature review (chapter 2) outlines the need for cell therapies as a treatment for cartilage injury and the need for novel gels as a cell delivery system. Fibrin has been widely used for the encapsulation of cells *in vitro* with successful results but has limitations in that the enzyme thrombin is required for gelation, batch to batch variation of fibrin occurs and the cross-linking density of the gels cannot be readily modified. The novel cross-linked fibrinogen gels overcome the disadvantages of current gels used to encapsulate cells *in vitro*. Gelation occurs without the need for an enzyme and the porosity of the gels can readily be modified. The novel cross-linked fibrinogen gels have not been investigated for cell encapsulation, cell growth, and differentiation prior to this research. Therefore, this study focuses its research on the use of novel fibrinogen gels for cell encapsulation and delivery applications specifically for the regeneration of cartilage.

The specific aims of this research are outlined below.

1. To encapsulate bovine articular chondrocytes for the optimisation of the novel cross-linked fibrinogen gel fabrication technique and to create a cell friendly and reliable encapsulation system. Including the investigation of the role of calcium concentration on gelation and the effect this may have on chondrocyte survival.

2. To investigate the viability and differentiation ability of chondrocytes within the novel cross-linked fibrinogen gels using the leading competitor fibrin and agarose gels as reference materials. The optimisation methods used in aim 1 will be continued to investigate aim 2. Chondrocyte activity and differentiation will be analysed by PrestoBlue® assay, live/dead staining, glycosaminoglycan content and histological staining of Haematoxylin and Eosin to investigate cell morphology and distribution and Toluidine blue for visualisation of the proteoglycan content. Four concentrations of FPA used to form the FPA-fibrinogen gels will be investigated: 2.66 $mg.mL^{-1}$, 2 $mg.mL^{-1}$, 1.33 $mg.mL^{-1}$ and 0.7 $mg.mL^{-1}$ of FPA.

   Hypothesis: chondrocytes encapsulated in FPA-fibrinogen gels formed from 2.66 $mg.mL^{-1}$ FPA will have greater survival, differentiation and formation of ECM in comparison to the lower concentrations of FPA.

3. To investigate the encapsulation of bovine bone marrow mesenchymal stem cells within the novel cross-linked fibrinogen gels using fibrin as a reference material, using the optimised techniques from aim 1. The mesenchymal stem cells will be cultured under chondrogenic conditions and the analysis will be carried out using the techniques in aim 2. The hypothesis is that the mesenchymal stem cells will exhibit greater survival, differentiation and ECM formation in FPA-fibrinogen gels formed from 2.66 $mg.mL^{-1}$ FPA.

   Hypothesis: that both chondrocytes and mesenchymal stem cells will behave similarly when encapsulated in the FPA-fibrinogen and fibrin gels.

4. To investigate the potential mechanisms responsible for bovine bone marrow mesenchymal stem cell migration and subsequent gel degradation when mesenchymal stem cells are encapsulated in FPA-fibrinogen and fibrin gels. Serum-free conditions and inhibitors for plasmin and matrix metalloproteinases will be investigated. Cell migration will be determined by crystal violet stain and gel degradation will be analysed by light microscopy.

   Hypothesis: Gel degradation and mesenchymal stem cell migration from the fibrinogen gels was caused by fibrinolysis.

On completion of the research, the novel cross-linked fibrinogen gels will be optimised for chondrocyte and bone marrow mesenchymal stem cell encapsulation, survival and differentiation, under chondrogenic conditions. The optimisation process will be described in detail and will focus on biocompatibility and chondrocyte survival. The optimum method will be established and conducted for further in depth studies into chondrocyte and bone marrow mesenchymal stem cell survival and differentiation. This research will therefore determine if the novel cross-linked fibrinogen gels have potential for chondrocyte and bone marrow mesenchymal stem cell encapsulation and delivery for the repair of injured cartilage. This will add significant knowledge to the field of regenerative medicine by providing a versatile and innovative cell encapsulation and delivery system.

4.0 Materials and methods

4.1 Materials

A list of materials used throughout the research project.

Cell Isolation and Culture Methods

Tissue collection

- 10 % Trigene – Scientific Laboratory Supplies, UK
- 70 % Industrial methylated spirit – Genta Medical, York, UK
- Post mortem blades and handles – Swann Morton, Sheffield, UK
- Aluminium foil – Tesco
- Dissection tray - Scientific Laboratory Supplies, UK
- Scalpel handles - Scientific Laboratory Supplies, UK
- Scalpel blades, size 22 and 11 - Scientific Laboratory Supplies, UK
- Tweezers and Spatulas - Scientific Laboratory Supplies, UK
- Electric saw – Ryobi, B&Q, UK
- Record Junior 51 vice
- 50 mL Centrifuge tubes – BD Biosciences, Oxford, UK
- Petri dishes – ThermoFisher Scientific, Loughborough, UK
- Dulbecco's phosphate buffered saline – Sigma-Aldrich, Poole, UK
- Pasteur pipettes – Alpha Laboratories
- Class 2 laminar flow cabinet – Walker Safety Cabinets Ltd, UK

Chondrocyte isolation and expansion

- Galaxy R Plus CO_2 incubator – Eppendorf, UK
- Class 2 laminar flow cabinet – Walker Safety Cabinets Ltd, UK
- Trypsin – Sigma-Aldrich, Poole, UK
- Stuart orbital shaker - Scientific Laboratory Supplies, UK
- T75 flasks - Greiner Bio-One– Sigma Aldrich, Poole, UK
- Bacterial collagenase – Sigma Aldrich, Poole, UK

Culture medium used

- High glucose (4500 mg/l) Dulbecco's Modified Eagle Medium – Sigma Aldrich, Poole, UK

- Foetal calf serum, batch number F9665 – Sigma Aldrich, Poole, UK
- Penicillin- Streptomycin solution – Sigma Aldrich, Poole, UK
- 1 M HEPES buffer – Sigma Aldrich, Poole, UK
- Non-essential amino acids– Sigma Aldrich, Poole, UK
- L-alanyl-L-glutamine– Sigma Aldrich, Poole, UK
- Human basic fibroblastic growth factor – PrepoTech, London, UK

Bone marrow mesenchymal stem cell isolation and expansion

- Galaxy R Plus CO_2 incubator – Eppendorf, UK
- Trypsin – Sigma-Aldrich, Poole, UK
- Stuart orbital shaker - Scientific Laboratory Supplies, UK
- Petri dishes – ThermoFisher Scientific, Loughborough, UK
- Scalpel handles and size 22 blades - Scientific Laboratory Supplies, UK
- Phosphate buffered saline - Sigma-Aldrich, Poole, UK
- Tissue culture Cell+ growth surface treated T25 and T75 flasks for sensitive cells - Sarstedt, Germany

Culture medium used

- Low glucose (1000 mg/l) Dulbecco's Modified Eagle Medium – Sigma Aldrich, Poole, UK
- MSC qualified serum, batch number 12664 – ThermoFisher Scienctific, Loughborough, UK
- Penicillin- Streptomycin solution – Sigma Aldrich, Poole, UK
- L-glutamate - Sigma Aldrich, Poole, UK
- Human basic fibroblastic growth factor – PrepoTech, London, UK

MG63 expansion

- Human osteoblastic MG63 cell line - Sigma Aldrich, Poole, UK
- Galaxy R Plus CO_2 incubator – Eppendorf, UK
- Tissue culture T75 flasks - Greiner Bio-One

Culture medium used

- Alpha modified minimum essential medium eagle - Sigma Aldrich, Poole, UK
- Penicillin- Streptomycin solution – Sigma Aldrich, Poole, UK

- 1 M HEPES buffer – Sigma Aldrich, Poole, UK
- L-alanyl-L-glutamine– Sigma Aldrich, Poole, UK
- Human basic fibroblastic growth factor – PrepoTech, London, UK

Articular cartilage isolation and injury

- 6 mm and 3 mm disposable biopsy punches – Kai Medical
- Scalpel handles and size 22 blades - Scientific Laboratory Supplies, UK

Medium used

- High glucose (4500 mg) Dulbecco's Modified Eagle Medium – Sigma Aldrich, Poole, UK
- Foetal calf serum, batch number F9665 – Sigma Aldrich, Poole, UK
- Penicillin- Streptomycin solution – Sigma Aldrich, Poole, UK
- 1 M HEPES buffer – Sigma Aldrich, Poole, UK
- Non-essential amino acids– Sigma Aldrich, Poole, UK
- L-alanyl-L-glutamine– Sigma Aldrich, Poole, UK
- Dexamethasone - Sigma Aldrich, Poole, UK

Preparation of hydrogels

Preparation of fibrinogen gels

- Peprostat – Haemostatix Ltd, Nottingham, UK
- Polyethylene glycol-bound fibrinogen binding peptides – Haemostatix Ltd, Nottingham, UK
- Peptide sequences P15 and P17 – Haemostatix Ltd, Nottingham, UK
- HyStem – Sigma-Aldrich, Poole, UK

HEPES buffered saline solution containing calcium

- HEPES – Sigma Aldrich, Poole, UK
- Sodium Chloride - Sigma Aldrich, Poole, UK
- Calcium Chloride - Sigma Aldrich, Poole, UK

HyStem Preparation

- HyStem – Sigma-Aldrich, Poole, UK

- 12mer peptide sequence – Haemostatix, Nottingham, UK
- 5,5'-dithiobis-2 nitrobenzoic acid - Sigma-Aldrich, Poole, UK
- Cysteine - Sigma-Aldrich, Poole, UK
- N-ethylmaleimide- Sigma-Aldrich, Poole, UK
- Stuart heat stirrer – N/A
- Amicon® Ultra 0.5 mL Centrifugal Filters– Merck Millipore Ltd
- 0.22 µm Millipore filter – Merck Millipore Ltd

HEPES buffered saline solution

- HEPES – Sigma Aldrich, Poole, UK
- Sodium Chloride - Sigma Aldrich, Poole, UK

Fibrinogen

- TISSEEL ready to use tissue sealant solutions – Baxter Healthcare, UK

HEPES buffered saline solution containing calcium

- HEPES – Sigma Aldrich, Poole, UK
- Sodium chloride - Sigma Aldrich, Poole, UK

Agarose gels

- Agarose - Sigma Aldrich, Poole, UK
- Phosphate buffered saline - Sigma Aldrich, Poole, UK

Cell encapsulation in gels

Differentiation medium

Additives

- L-ascorbic acid – Sigma-Aldrich, Poole, UK
- Bovine Pancreatic Insulin - Sigma-Aldrich, Poole, UK
- Dexamethasone - Sigma-Aldrich, Poole, UK
- Human transforming growth factor β-1 – PeproTech, USA
- ITS liquid media supplement (100x) - Sigma-Aldrich, Poole, UK
- Bovine serum albumin - Sigma-Aldrich, Poole, UK
- β-glycerophosphate – Sigma-Aldrich, Poole, UK

Cell encapsulation in fibrinogen and fibrin gels

- 96-well culture plates - Greiner Bio-One

Cell encapsulation in 4 % agarose gels

- Agarose - Sigma-Aldrich, Poole, UK
- Phosphate buffered saline - Sigma-Aldrich, Poole, UK
- 24-well culture plates - Greiner Bio-One

Cell encapsulation and delivery to injured cartilage

- 100 mm micro spatula – Scientific Laboratory Supplies, UK

Fibrinogen based gels formed within well structures.

Agarose wells for forming fibrinogen gels

- Agarose - Sigma-Aldrich, Poole, UK
- Phosphate buffered saline - Sigma-Aldrich, Poole, UK
- 8 mm biopsy punch – Kai Medical
- 4-well culture plates - Greiner Bio-One

Polytetrafluoroethylene (PTFE) wells for forming fibrinogen gels

- Polytetrafluroethylene
- Bandsaw
- Pillar drill
- Elco plus saw handpiece – W&H, Hertfordshire, UK
- Glossy polishing paste - Henry Schein Inc. USA
- Grant ultrasonic bath XB2

Gels formed in 96-well plates and transferred to 24 well plate

- 96-well and 24-well culture plate - Greiner Bio-One
- 100 mm micro spatula – Scientific Laboratory Supplies, UK

Effect of calcium concentrations on fibrinogen gel formation

- TISSEEL ready to use tissue sealant – Baxter Healthcare, UK
- Peprostat – Haemostatix, Nottingham, UK

HEPES buffered saline solution containing calcium

- HEPES – Sigma Aldrich, Poole, UK
- Sodium Chloride - Sigma Aldrich, Poole, UK
- Calcium Chloride - Sigma Aldrich, Poole, UK

Gel degradation

- Marimastat – R&D Systems
- Aprotinin – R&D Systems
- Dimethyl sulfoxide - Sigma Aldrich, Poole, UK
- Plasminogen from bovine plasma - Sigma Aldrich, Poole, UK

Plasmin detection

- 96-well culture plates - Greiner Bio-One
- L-Lysine - Sigma Aldrich, Poole, UK
- Potassium Phosphate - Sigma Aldrich, Poole, UK
- Sodium Phosphate - Sigma Aldrich, Poole, UK
- D-Val-Leu-Lys p-nitroanilide dihydochloride plasmin substrate - Sigma Aldrich, Poole, UK
- Monopotassium phosphate - Sigma Aldrich, Poole, UK
- Sodium phosphate dibasic - Sigma Aldrich, Poole, UK
- Tecan Spectrophotometer Infinite M200 – Tecan, Switzerland

uPA and tPA detection

- Amiloride - Sigma Aldrich, Poole, UK
- Dimethyl sulfoxide (DMSO) - Sigma Aldrich, Poole, UK
- BIOPHEN - Urokinase chromogenic substrate – Aniara Dianostica, USA
- 96-well culture plates - Greiner Bio-One
- Tecan Spectrophotometer Infinite M200 – Tecan, Switzerland

Tris buffer

- Tris base – Fisher Scientific, USA
- Sodium Chloride - Sigma Aldrich, Poole, UK
- Tween-20 - Fisher Scientific, USA

KC4 coagulation

- KC4 coagulation analyser – N/A
- TISSEEL ready to use fibrinogen – Baxter Healthcare, UK
- Peprostat, P15 and P17 - Haemostatix, Nottingham, UK

Scanning electron microscopy

- Glutaraldehyde - Agar Scientific, Essex, UK
- 0.1 M cacodylate buffer

Cacodylate buffer

- Sodium cacodylate - Sigma Aldrich, Poole, UK
- Distilled water
- Hydrochloric acid - Sigma Aldrich, Poole, UK

Freeze dry dehydration

- VirTis benchtop SLC freeze dryer – Biopharma Process Systems Ltd, UK
- Scanning electron microscopy stubs – Agar Scientific, Essex, UK

Ethanol dehydration

- Ethanol - Fisher Scientific, USA
- Osmium Tetroxide - Agar Scientific, Essex, UK
- Scanning electron microscopy stubs – Agar Scientific, Essex, UK

Cell viability assay

- PrestoBlue® - Life Technologies, Paisley, UK
- 96-well culture plates - Greiner Bio-One
- Tecan Spectrophotometer Infinite M200 – Tecan, Switzerland

Live/Dead Staining and Confocal Microscopy

- 5-chloromethylfluorescein diacetate (CMFDA cell tracker Green) - Invitrogen Ltd
- Propidium Iodide - Invitrogen Ltd
- Formaldehyde - Fisher Scientific, USA

- Zeiss Axioskop LSM 510 meta confocal laser scanning microscope (Carl Zeiss Ltd, UK)
- x10 (EC Plan – Neofluar 10x/0.3 dry objective lens

Measurement of glycosaminoglycans using 1,9-dimethylmethylene blue dye

- Tecan Spectrophotometer Infinite M200 – Tecan, Switzerland
- Techne 60-well heat block – Scientific Laboratory Supplies, UK
- 96-well culture plates - Greiner Bio-One
- 1,9-dimethylmethylene blue - Sigma Aldrich, Poole, UK
- Papain - Sigma Aldrich, Poole, UK
- N-acetyl cysteine - Sigma Aldrich, Poole, UK
- Chondroitin sulfate A - Sigma Aldrich, Poole, UK

Phosphate buffer

- Disodium phosphate - Sigma Aldrich, Poole, UK
- Sodium dihydrogen phosphate - Sigma Aldrich, Poole, UK
- Ethylenediaminetetraacetic acid - Sigma Aldrich, Poole, UK

Histological examination

- Aluminum foil – Tesco
- Adhesive cork discs – Duratool
- Liquid nitrogen – British Oxygen, UK
- Optimal cutting temperature compound – ThermoFisher Scientific, Loughborough, UK
- Microm HM560 cryostat
- Microscope and camera
- SuperFrost Plus glass slides - ThermoFisher Scientific, Loughborough, UK
- Glass coverslips – VWR, USA
- Paraformaldehyde - Sigma Aldrich, Poole, UK

Haematoxylin and eosin stain

- H&E Shandon staining line
- Mayer's Haematoxylin – ThermoFisher Scientific, Loughborough, UK
- Eosin Y stain – ThermoFisher Scientific, Loughborough, UK

- Scott's tap water – ThermoFisher Scientific, Loughborough, UK
- Xylene - Fisher Scientific, USA

Alcian Blue

- Alcian blue – Merck Millipore Ltd
- Neutral red – Merck Millipore Ltd
- Distilled water
- Xylene - Fisher Scientific, Loughborough, UK
- DPX slide mounting medium - ThermoFisher Scientific, Loughborough, UK

Toluidine blue

- Toluidine blue – Merck Millipore Ltd
- Distilled water
- Xylene - Fisher Scientific, Loughborough, UK
- DPX slide mounting medium- ThermoFisher Scientific, Loughborough, UK

Crystal Violet

- Crystal Violet – Merck Millipore Ltd
- Distilled water

TRIzol RNA Extraction

- TRIzol – Life Technologies, Paisley, UK
- Jencons Ultrasonic processor
- Ethanol - Fisher Scientific, USA
- Isopropanol - Fisher Scientific, USA
- Distilled water
- NanoDrop 1000 spectrophotometer – Thermo Scientific, USA
- Water saturated 1-butanol - Fisher Scientific, USA
- Water saturated diethylether – May & Baker Ltd, UK
- Nuclease free water

Extraction Isolate II RNA mini kit

- Isolate II RNA mini kit – Bioline, London, UK
- 2-Mercaptoethanol – Sigma-Aldrich, Poole, UK

Electrophoresis of RNA

- Agarose – Sigma-Aldrich, Poole, UK
- Distilled water
- Formaldehyde – Sigma-Aldrich, Poole, UK
- Ethidium bromide – Sigma-Aldrich, Poole, UK
- SNCRWA electrophoresis machine – BioRad
- Syngene INGENIUS 3

MOPS buffer

- MOPS - Fisher Scientific, USA
- Sodium Acetate - Sigma Aldrich, Poole, UK
- Ethylenediaminetetraacetic acid - Sigma Aldrich, Poole, UK

4.2 Cell Isolation and Culture Methods

4.2.1 Tissue collection

Bovine metacarpophalangeal joints (from the 3rd metacarpal to the hoof) were obtained from a local abattoir from skeletally mature animals (18-24 months within six hours of slaughter for the meat industry). The joints were sprayed with 10 % Trigene and 70 % industrial methylated spirit (IMS) and the skin was removed from the joint using a post mortem blade, the ends were wrapped in aluminium foil leaving only the joint uncovered to reduce the risk of infection. The skinned joints were transferred to a class 2 laminar air cabinet and all subsequent procedures were carried out aseptically.

The metacarpophalangeal joints were fully opened using a scalpel and the articular cartilage was removed from the joint surfaces using a scalpel and tweezers. The pieces of articular cartilage were transferred into Ca^{2+}/Mg^{2+}- free phosphate buffer saline (PBS) until the tissue collection was completed. The metacarpophalangeal joint was then removed from the laminar air cabinet and the 3rd metacarpal bone was removed from the lower bones using a post-mortem blade. All the soft tissue was then removed and the bone was clamped in a vice. The end of the bone was removed using an electric saw to gain access to the bone marrow and the cut bone immediately transferred back to aseptic conditions. The surface of the bone marrow was discarded to reduce the risk of infection, and the underlying bone marrow was collected using a spatula into a 50 mL centrifuge tube.

4.2.2 Chondrocyte isolation and expansion

The PBS was removed from the articular cartilage pieces and replaced with 2.5 % (w/v) trypsin followed by incubation of the tissue at 37 °C for 30 minutes. The trypsin was removed and the cartilage pieces washed thoroughly with PBS. High glucose Dulbecco's Modified Eagle Medium (DMEM) containing 1000 units.mL^{-1} penicillin, 1000 µg.mL^{-1} streptomycin solution with 10 % foetal calf serum (FCS) and 2 mg.mL^{-1} of bacterial collagenase was added to the cartilage pieces. The container containing the cartilage was transferred to an orbital shaker and incubated with gentle shaking at 30 rotations per minute (rpm) at 37 degrees (°C) for 24 hours to digest the tissue. The cell-containing medium was removed and transferred to centrifuge tubes followed by centrifugation at 1,000 rpm, 192 g (g-force) for 10 minutes to pellet the chondrocytes. After centrifugation, the supernatant solution was removed and the cell pellet resuspended in PBS. The cells were pelleted by centrifugation at 1,000 rpm, 192 g for 10 minutes. This washing procedure and centrifugation was repeated again in the same manner. The final chondrocyte pellet was resuspended in high glucose DMEM and the cell number determined using a haemocytometer. The chondrocytes were then plated in tissue culture T75 flasks and cultured in monolayer culture in basic medium [high glucose DMEM containing 1000 units.mL^{-1} penicillin, 1000 µg.mL^{-1} streptomycin solution, non-essential amino acids, and 10 mM HEPES buffer pH 7.4. and 10 % v/v FCS]. The cell cultures were incubated at 37 ^{o}C in a humidified atmosphere of 95 % air/ 5 % CO_2 until confluent. The cells were then passaged or used for experimentation as described in sections 4.4.2.

4.2.3 Bone marrow mesenchymal stem cell isolation and expansion

The bone marrow was transferred to a petri dish and minced using a scalpel blade. Low glucose basic medium [low glucose DMEM containing 1000 units.mL^{-1} penicillin, 1000 µg.mL^{-1} streptomycin solution, and non-essential amino acids, buffer pH 7.4. and 10 % v/v MSC-qualified FCS and 5 ng.mL^{-1} FGF2] and 2 mg.mL^{-1} of bacterial collagenase was added to the bone marrow. The petri dish was placed on an orbital shaker and incubated at 37 °C for 4 hours to digest the bone marrow. The digestion was collected in a 50 mL centrifuge tube and centrifuged at 1,000 rpm, 192 g for 10 minutes. The supernatant was removed and the pellet re-suspended in PBS and centrifuged at 1,000 rpm, 192 g for 10 minutes, this was repeated twice. The cell pellet was then re-suspended with low glucose basic medium and plated in T25 flasks for sensitive cells. The cell

cultures were then incubated at 37 ºC in a humidified atmosphere of 95 % air/ 5 % CO_2 until confluent. The cells were then passaged or used for experimentation as described in section 4.4.2.

4.2.4 MG63 expansion

The human osteoblastic MG63 cell line were cultured in alpha modified minimum essential eagle medium (αMEM) containing 1000 units.mL^{-1} penicillin, 1000 µg.mL^{-1} streptomycin solution, non-essential amino acids, and 10 mM HEPES buffer pH 7.4 and 10 % v/v FCS. The cell cultures were incubated at 37 ºC in a humidified atmosphere of 95 % air/ 5 % CO_2 until confluent. The cells were then passaged or used for experimentation as described in section 4.4.2.

4.2.5 Articular cartilage isolation and injury

All procedures were carried out under aseptic conditions. The joint was opened as previously described in section 4.2.1. Articular cartilage was removed from the metacarpophalangeal joint (image A and C, Figure 4.1) by using a 6 mm disposable biopsy punch (image B, Figure 4.1) to create circular cartilage disc. The discs were removed from the underlying bone using a scalpel blade, image C, Figure 4.1 shows the result of the removed cartilage discs from the joint. Any pieces of cartilage that were removed with bone fragments attached were discarded. An example of this can be seen in image C, Figure 4.1, the white circle highlights the disruption of the bone during the removal of the cartilage discs by scalpel blades, the black circle shows that only the cartilage has been removed and therefore these cartilage discs were used for experimentation. This procedure created reproducible discs of cartilage, as seen in image D, Figure 4.1. The cartilage discs were incubated in basic medium containing 10 % FCS and 1 µM dexamethasone for 48 hours. The medium was then replaced with basic medium and 10 % FCS until required for experimentation. Injury to the cartilage was formed using a 3 mm sterile, disposable biopsy punch to create a 3 mm hole in the centre of the disc prior to experimentation. The black arrow in image E, Figure 4.1 shows the 3 mm injury created in the circular cartilage disc, shown by the white arrow. Finally, the hydrogel (black arrow) was formed as described in 4.5.3 and transferred onto the cartilage injury (white arrow) using a sterile spatula, this can be seen image F, Figure 4.1.

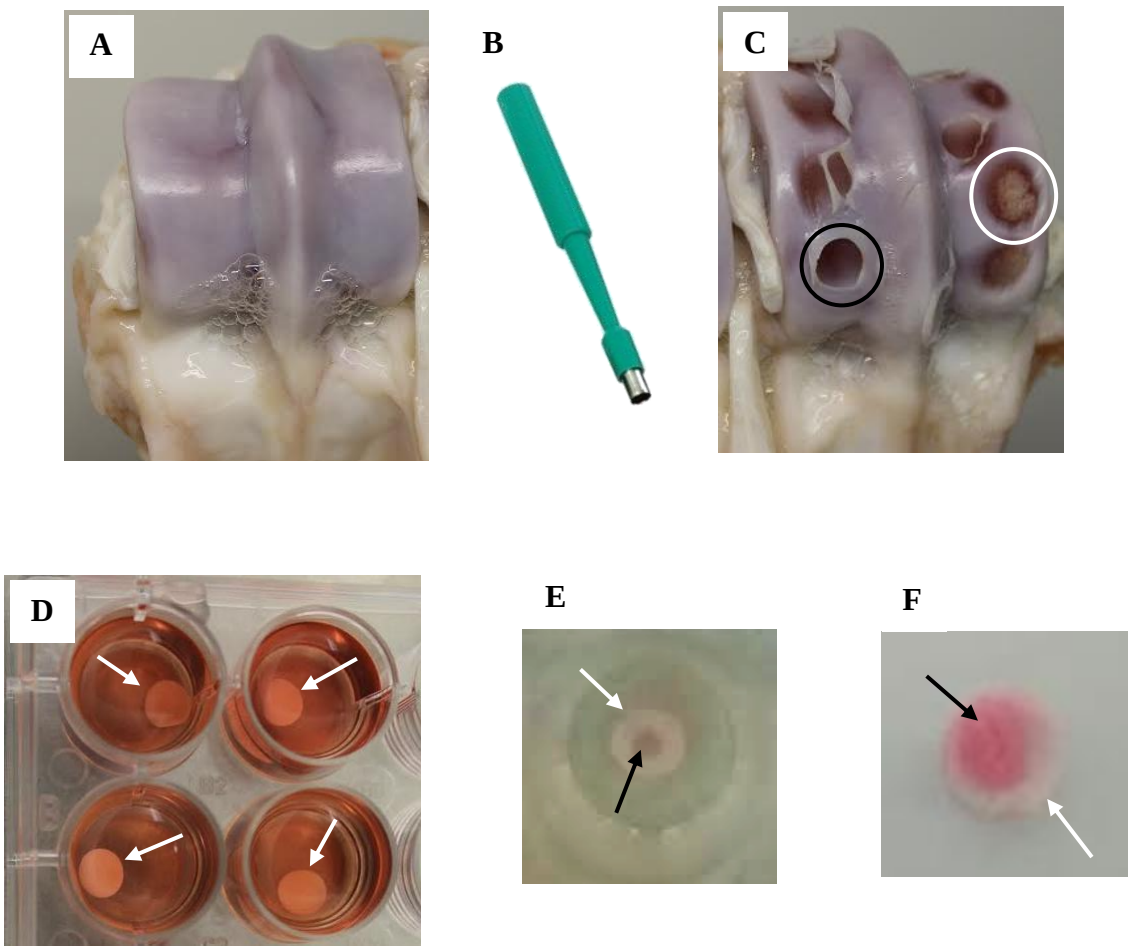

Figure 4.1 Bovine articular cartilage injury model taken from the metacarpophalangeal joint (A). A 6 mm biopsy punch (B) was used to obtain reproducible circular discs of cartilage (D, white arrows) from the joint (C). Cartilage discs were discarded if bone fragments were attached (C, white circle) and used for experimentation if only cartilage was removed (C, black circle). A 3 mm biopsy punch was used to create an injury (E, black arrow) in the cartilage disc (E, white Arrow), and the cell encapsulated fibrin or FPA-fibrinogen gels (F, black arrow) were placed over the injury (F, white arrow).

4.3 Preparation of hydrogels

4.3.1 Preparation of novel cross-linked fibrinogen gels

The FBP preparations used in this thesis (Peprostat, Polyethylene glycol, P15, and P17) were provided by Haemostatix Ltd. HyStem was purchased as a commercial kit and the FBP was linked to HyStem as described in section 4.3.2. The concentrations of FBPs were as follows:

- Peprostat is based on the coupling of multiple FBPs to a soluble carrier of recombinant albumin. Preparation of FPA were used at concentrations of 2.66 $mg.mL^{-1}$, 2 $mg.mL^{-1}$, 1.33 $mg.mL^{-1}$ and 0.7 $mg.mL^{-1}$ in 10 mM HEPES-buffered saline pH 7.4 containing 2 mM $CaCl_2$ unless otherwise stated.

- Polyethylene glycol-bound fibrinogen binding peptides (PEG) were used at 1 $mg.mL^{-1}$, 0.75 $mg.mL^{-1}$, 0.5 $mg.mL^{-1}$ and 0.25 $mg.mL^{-1}$ in 10 mM HEPES-buffered saline pH 7.4 containing 10 mM $CaCl_2$ as indicated in individual experimental results.

- P15 is a peptide containing the sequence RGD, the nature of this carrier is undisclosed due to intellectual property but it is coupled to the active FBP sequence. P15 was used at concentrations of 0.75 $mg.mL^{-1}$, 0.5 $mg.mL^{-1}$ and 0.25 $mg.mL^{-1}$ in 10 mM HEPES-buffered saline pH 7.4 containing 2 mM $CaCl_2$

- P17 is a peptide containing the sequence DGEA, the nature of this carrier is undisclosed due to intellectual property but is coupled to the active FBP sequence. P17 was used at concentrations of 0.75 $mg.mL^{-1}$, 0.5 $mg.mL^{-1}$ and 0.25 $mg.mL^{-1}$ in 10 mM HEPES-buffered saline pH 7.4 containing 2 mM $CaCl_2$

- HyStem is a commercially available kit in which the FBP has been linked as described in section 4.3.2. This FBP was used at concentrations of 1 $mg.mL^{-1}$ and 0.75 $mg.mL^{-1}$ in 10 mM HEPES buffered saline pH 7.4 containing 2 mM $CaCl_2$ as indicated in individual experiments

Each concentration of the above materials was chosen based on its ability to form a hydrogel with 34 $mg.mL^{-1}$ fibrinogen. The concentrations used are summarised in table 4.1 below.

Table 4.1 shows the ratio of fibrinogen binding peptides to fibrinogen molecules present during gelation for the concentrations used for each hydrogel. To form the fibrinogen gels, equal volumes of fibrinogen at 34 $mg.mL^{-1}$ and the required concentration of the fibrinogen-binding peptides were mixed together.

Carrier	Fibrinogen: fibrinogen binding peptide	Concentration of carrier ($mg.mL^{-1}$)
Peprostat	1:8	2.66
	1:6	2
	1:4	1.33
	1:2	0.7
PEG	1:8	1
	1:6	0.75
	1:4	0.5
	1:2	0.25
P15	Unknown	0.75
	Unknown	0.5
	Unknown	0.25
P17	Unknown	0.75
	Unknown	0.5
	Unknown	0.25
HyStem	Unknown	0.75
	Unknown	0.5
	Unknown	0.25

4.3.2 HyStem preparation

A HyStem vial containing 10 mg of hyaluronic acid and 9.6 mg of phosphate buffer salts was thawed at room temperature and 1 mL of 20 mM phosphate buffer was added to the vial which left at 40 ˚C to dissolve the vial contents. Once dissolved, the thiol concentration was determined by Ellman's assay. 4 $mg.mL^{-1}$ of 5,5'-dithiobis-2 nitrobenzoic acid (DTNB) was made up in Ellman's buffer consisting of 0.1 M sodium phosphate buffer and 2 mM EDTA at pH 8. 3 mM cysteine was used as a standard. 980 µL of Ellman's buffer, 10 µL of sample and 10 µL of DTNB was pipetted into a cuvette and the absorbance was measured at 412 nm. The thiol number was estimated and the 12-mer peptide was added at 1.5 times the mole concentration of the estimated thiols. This was left at 40 ˚C for fifteen minutes followed by incubation overnight on a gentle orbital shaker at ambient temperature. An Ellman's assay was carried out to determine if there was any unreacted thiols in the solution. Filter centrifuge tubes were pre-washed in distilled water overnight. The filter centrifuge tubes were centrifuged for 14,000 rpm for

five minutes to remove the water. 500 µL of 0.9 % NaCl containing 10 mM HEPES-NaOH pH 7.4 was added to the filter centrifuge tubes and the tubes centrifuged again at 14, 000 rpm for five minutes. This washing procedure was repeated once more. 400 µL of HyStem – 12mer peptide was then added to three of the filter centrifuge tubes and centrifuged at 14, 000 rpm for three minutes. 150 µL of 0.9 % NaCl containing 10 mM HEPES pH 7.4 was added to each filter centrifuge tube and centrifuged at 14, 000 rpm for five minutes, this was repeated. The HyStem – 12mer peptide was collected and the concentration calculated. The solution was passed through a 0.22 µm Millipore filter to remove any gelled components and the gelation of the resultant Hystem-12mer peptide preparation was tested with 34 mg.mL^{-1} fibrinogen.

4.3.3 Fibrinogen

Human fibrinogen was purchased as "TISSEEL ready to use solutions" from Baxter Healthcare UK. The TISSEEL was supplied as in a dual syringe with a fibrinogen solution in one syringe and a solution of thrombin in the other syringe. The thrombin and fibrinogen solutions were removed individually and stored separately in aliquots at -20 ^{o}C for experimental use. The TISSEEL fibrinogen was supplied at 90 mg.mL^{-1} and diluted to 34 mg.mL^{-1} with 10 mM HEPES buffered saline solution pH 7.4

4.3.4 Fibrin gels

The fibrin-based tissue sealant preparation "TISSEEL ready to use solutions" was used to form the fibrin gels. The thrombin and fibrinogen solutions were supplied in separate sections of a dual syringe system. As described above in section 4.3.3, the fibrinogen and thrombin solutions were removed individually from the dual syringe system and stored separately in aliquots at - 20 ^{o}C for experimental use. The TISSEEL fibrinogen was supplied at 90 mg.mL^{-1} and diluted to 34 mg.mL^{-1} with 10 mM HEPES buffered saline pH 7.4. The fibrin hydrogels were formed using fibrinogen at a concentration 34 mg.mL^{-}, which is the same concentration used for forming the fibrinogen gels. To form the hydrogels, thrombin at 192 IU.mL^{-1} was mixed with the fibrinogen solution in a 1:1 volume ratio.

4.3.5 Agarose gels

4 % agarose gel was made in non-sterile PBS by mixing 4 g of agarose powder with 100 mL of non-sterile PBS. A 1 % agarose gel was also used to coat the well bottoms of the tissue culture multi-well plates to prevent cell adhesion to the tissue culture plastic, 1 g of agarose powder was mixed with 100 mL of non-sterile PBS. The 1 % and 4 % agarose preparations were sterilised by autoclaving the gels at 115 °C for 15 minutes, and then leaving the gel solutions to cool overnight.

4.4 Cell encapsulation in gels

4.4.1 Differentiation medium

- Chondrocyte medium consisted of basic medium as described in section 4.2.2 with 10 % FCS, 50 $\mu g.mL^{-1}$ L-ascorbic acid and 1 $\mu g.mL^{-1}$ insulin
- bBM-MSC medium containing FCS consisted of low glucose basic medium as described in section 4.2.3 with 10 % MSC qualified FCS, 100 nM dexamethasone, 10 $ng.mL^{-1}$ transforming growth factor (TGFβ-1), 10 $\mu g.mL^{-1}$ insulin, 5.5 $\mu g.mL^{-1}$ transferrin, 5 $ng.mL^{-1}$ selenium and 25 $\mu g.mL^{-1}$ ascorbic acid.
- bBM-MSC serum free medium consisted of low glucose basic medium as described section 4.2.3 containing 1 $mg.mL^{-1}$ bovine serum albumin (BSA), 100 nM dexamethasone, 10 $ng.mL^{-1}$ transforming growth factor beta-1 (TGFβ-1), 10 $\mu g.mL^{-1}$ insulin, 5.5 $\mu g.mL^{-1}$ transferrin, 5 $ng.mL^{-1}$ selenium and 25 $\mu g.mL^{-1}$ ascorbic acid.
- MG63 medium consisted of αMEM as described in section 4.2.4 containing 2 % FCS, 1 $mg.mL^{-1}$ BSA, 10 nM dexamethasone, 25 $\mu g.mL^{-1}$ ascorbic acid, and 10 mM β-glycerophosphate.

4.4.2 Cell encapsulation in fibrinogen and fibrin gels

Cells were encapsulated in fibrinogen gels formed from either FPA, PEG, P15, P17, or HyStem coupled with fibrinogen. Cells were also encapsulated in fibrin gels and 4 % agarose gels.

Chondrocytes and MG63s were detached from the tissue culture plastic by the following procedure. The culture medium was removed and the cell layer washed with PBS. The PBS was removed and replaced with a 0.05 % trypsin- 0.02 % EDTA solution

and the cultures incubated at 37 °C for 5 minutes. When the cells had detached, the cell/trypsin-EDTA solution was transferred into a centrifuge tube and FCS added to 1-5 % vol/vol to inhibit the trypsin. The cells were pelleted by centrifugation at 1,000 rpm, 192 g for 5 minutes. After centrifugation, the supernatant was removed and the cell pellet was resuspended in basic culture medium for chondrocytes and αMEM for MG63s ready for re-plating in monolayer culture or encapsulation into the gels. Chondrocytes at passage 2-3 were used for gel encapsulation experiments as it has been found in house that the chondrocytes at these passages will re-differentiate to gain a full mature chondrocyte phenotype during culture in 3D. MG63s at passage 30-40 were used for gel encapsulation experiments.

Bovine bone marrow MSCs (bBM-MSCs) were removed from the tissue culture flask as follows: the culture medium was removed and the cell layer washed with PBS. The PBS was removed and replaced with 3 mL 0.025 % trypsin- 0.01 % EDTA solution in 1 mL PBS to ensure the trypsin-EDTA does not cause cell death and the cultures were incubated at 37 °C for 3 minutes. When the cells had detached, the cell/trypsin-EDTA solution was transferred into a centrifuge tube and FCS added to 1-5 % vol/vol to inhibit the trypsin. The cells were pelleted by centrifugation at 1,000 rpm, 192 g for 5 minutes. After centrifugation, the supernatant was removed and the cell pellet was re-suspended in low glucose basic culture medium ready for re-plating in monolayer culture or encapsulation into the gels. bBM-MSCs at passage 2-4 were used for gel encapsulation experiments as it has been found in house that the bBM-MSCs at these passages will differentiate during culture in 3D

Chondrocytes, bBM-MSCs, and MG63s were re-suspended in the fibrinogen at $6x10^6$ cells per 1 mL, unless otherwise stated. Individual hydrogels were formed by simultaneously pipetting 50 µL of the required carrier with 50 µL of the fibrinogen-cell suspension in a single well of a 96-well plate. As a control, cell-free hydrogels were also formed in wells of the 96-well plate. The 96-well plate was transferred to 37 ˚C for 5 minutes to allow for complete gelation on an orbital shaker at 30 rpm and covered with 200 µL of culture media appropriate to the cell type. Each of the experimental conditions were carried out in triplicate.

4.4.3 Cell encapsulation in 4 % agarose gels

4 % agarose was slowly melted to form a solution in a microwave and cooled to 39 °C in a water bath. Once cooled, chondrocytes were re-suspended in the agarose solution at $3x10^6$ cells per 1 mL of 4 % agarose and an Eppendorf pipette was used to transfer 100 µL of the 4 % agarose – cell suspension to a well in a 12-well plate. 1 % agarose was used to cover the tissue culture plastic, to inhibit cells from adhering to the bottom of the 12-well culture plate. Cell-free 4 % agarose was used as a control and cell-containing 4 % agarose gels were produced in triplicate.

4.4.4 Cell encapsulation and delivery to injured cartilage

Cells were also delivered to the injured cartilage as previously described in section 4.2.5. To do this 300,000 chondrocytes or bBM-MSCs were encapsulated in either fibrinogen gels formed from FPA 2.66 $mg.mL^{-1}$ in 10 mM HEPES buffered saline solution pH 7.4 containing 2 mM $CaCl_2$ or 34 $mg.mL^{-1}$ fibrin gels in 10 mM HEPES buffered saline solution pH 7.4 containing 2 mM $CaCl_2$ in a well in a 96-well plate as described in section 4.4.2. When gelation was complete, the gels were then transferred to the cartilage injury site (image F, Figure 4.1), formed as described in section 4.2.5 by a sterile spatula. The cartilage and gels were then cultured in the appropriate medium for up to 14 days.

4.5 Fibrinogen based gels formed within well structures

Although gelation was almost instantaneous after mixing the Peprostat and fibrinogen, it was slow enough to allow spreading of the gel over the surface of the culture wells. The spreading of the gels was limited by using individual wells of a 96-well plate in which to cast the gels. However, the size of the well in relation to the number of cells (0.5×10^5 cells per well) meant that the encapsulated cells had to have media changes every day. In addition, nutrient exchange may be compromised due the small volume of culture media that could be added to the culture wells. Gelation in larger wells meant that the cell/gel solution spread over the bottom of the culture wells before gelation was complete, hence, a thin gel film rather than a gel ‘ball-like’ structure was formed. Therefore, methods in which gelation can occur and the gels transferred to larger culture wells were investigated and two methods that were investigated are described below:

4.5.1 Agarose wells for forming fibrinogen gels

A sterile 1 % agarose gel was formed as described in section 4.4.3. The agarose gel was melted by microwaving it at a low power for approximately 2 minutes. The agarose was quickly added at a volume of 1 mL to the bottom of the culture wells of a 24-well plate using an Eppendorf pipette and left to gel at room temperature for 30 minutes to form an agarose coating. A 6 mm diameter hole was created in the gel coating using a sterile biopsy punch and the agarose plug was removed. The FPA analogues were gelled with fibrinogen in the centre of the holes as seen in Figure 4.2, and as previously described in section 4.4.3. 1 mL of basic high glucose culture medium as described in section 4.2.2 was then added per well. Using this methodology larger volumes of culture medium could then be provided for the encapsulated chondrocytes compared to chondrocytes encapsulated in a 96-well culture plate. The medium was then changed daily or every two days.

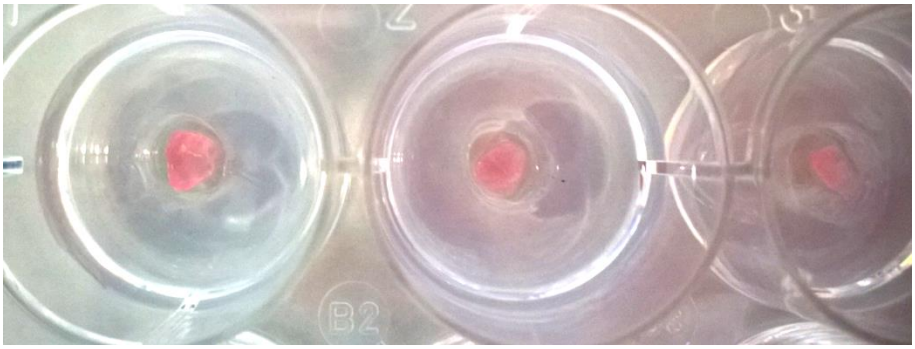

Figure 4.2 A 24-well plate with 1% agarose lining the bottom of the plate. A 6 mm hole was removed from the agarose 1% and fibrinogen based gels were gelled inside the hole (these appear pink in colour).

4.5.2 Polytetrafluoroethylene (PTFE) moulds for forming fibrinogen gels

6 mm diameter holes with a depth of approximately 8 mm were drilled into a small blocks of PTFE, as seen in Figure 4.3. These blocks were cleaned in a Grant ultrasonic bath for 5 minutes and was then polished using a hand-held polisher and Henry Schein glossy polishing paste until the surface became smooth. The PTFE blocks were then carefully rinsed and cleaned in the ultrasonic bath again for 5 minutes, and then autoclaved at 115 °C for 15 minutes to sterilise them. The gels were produced as described in section Preparation of hydrogels but mixed with the co-polymer in the PTFE well. It was then possible to transfer the gel pellet from the PTFE blocks to a 12-well plate using

a sterile spatula. After transfer to the 12-well culture plates the gel encapsulated cells were cultured with 2 mL of basic high glucose culture medium as described in section 4.2.2.

Figure 4.3 Blocks made from polytetrafluoroethylene, approximately 13 mm x 13 mm, the hole was drilled using a 6 mm drill piece to a depth of 8 mm and then polished.

4.5.3 Gels formed in 96-well plates and transferred to 24 well plate

Cells were suspended in the fibrinogen solution at $6x10^6$ cells per 1 mL of fibrinogen and the cell encapsulated gels formed in a 96-well plate as described in section 4.4.2. After gelation was complete, the gels were transferred to a 24-well plate, to contain one gel per well using a sterile micro spatula. This allowed 2 mL of medium to be placed on the hydrogels providing more nutrients for the cells.

4.6 Effect of calcium concentrations on fibrinogen gel formation

High calcium concentrations can be detrimental to cellular survival but calcium ions are crucial for gelation of the fibrinogen based gels. Therefore, different calcium concentrations of: 20 mM, 10 mM, 5 mM, 2 mM and 0 mM were investigated to determine the lowest level of calcium which is required for gelation. The experiment was set up as previously described in section 4.5.2 initially without the inclusion of chondrocytes to check if a gels were formed at the Ca^{2+} concentrations investigated. The fibrinogen gels were then formed from the fibrinogen binding peptides and a fibrinogen solution in 10 mM HEPES-buffered saline solution (pH 7.4) containing and $3x10^6$ chondrocytes.mL^{-1}.

4.7 Gel degradation

Gel degradation by encapsulated bBM-MSC and MG63 in FPA gels at a concentration of 2.66 mg.mL^{-1} and fibrin gels was investigated by the addition of Marimastat (a metalloproteinase inhibitor) or aprotinin (a serine-proteinase inhibitor) into the culture

medium. Marimastat was used at a final concentration of 1 μg.mL^{-1} or 10 μg.mL^{-1} in culture medium to inhibit matrix metalloproteinase (MMP) activity. Aprotinin was used at a final concentration of 5 μM, 204.48 KIU, or 30 μM, 1226.48 KIU, in low glucose DMEM to inhibit plasmin. To investigate the activation of plasminogen to plasmin in the samples, cell free and cell encapsulated hydrogels were prepared as previously described in section 4.4.2. At day three 50 μM plasminogen in 20 mM Lysine buffer was added to the medium of each hydrogel for 24 hours.

4.7.1 Plasmin detection

The medium samples were collected and 100 μL samples were pipetted into a 96-well plate in triplicate. 90 μL of lysine/phosphate buffer containing 10 mM potassium phosphate, 70 mM sodium phosphate and 100 mM lysine was added. The plate was read at 402 nm wavelength using the TECAN infinite 200 series for a complete zero time point. 10 μL of 6.5 mM D-Val-Leu-Lys p-nitroanilide dihydochloride plasmin substrate in 10 mM sodium phosphate dibasic, 70 mM monobasic potassium phosphate and 100 mM lysine at pH 7.5. This was then added to each well at a final concentration of 0.3 mM and the maximum absorbance measured at 402 nm every 10 minutes for 2 hours using the TECAN infinite 200 series. The plates were incubated at 37 ºC for the duration of the measurements.

4.7.2 uPA and tPA detection

The medium was collected from the 24 hour plasminogen incubation and 100 μL samples were pipetted into two 96-well plates in triplicate. 5 μL of 500 μM amiloride in DMSO was added into the samples in one of the 96-well plates and 85 μL of Tris-buffer containing 50 mM Tris, 150 mM NaCl, 0.02 % Tween-20 was added to these samples. 90 μL of Tris buffer was added to the plate which does not contain amiloride. The plates were read at an absorbance of 405 nm using the TECAN infinite 200 series to obtain an absolute 0 value. 10 μL of 0.1 mM urokinase substrate in Tris buffer was added to each sample. The plates were measured every 10 minutes for 1 hour at an absorbance of 405 nm using the TECAN infinite 200 series. The plates were incubated at 37 ºC for the duration of the measurements.

4.8 KC4 coagulation

A cuvette was placed in the KC4 coagulation analyser and a ball bearing is inserted into the cuvette. 100 μL of 3 mg.mL^{-1} fibrinogen was pipetted into the cuvette, the timer

was started and at 10 seconds 30 µL of the fibrinogen binding peptide was pipetted into the cuvette. A magnet in the KC4 coagulation analyser held the ball bearing in place until a gel forms and releases the ball bearing. Once clotting had taken place, the timer automatically stopped to determine the clotting speed of the sample and is accurate to 0.1 second. This was to ensure that the fibrinogen is biologically active with the clotting agent and was also a measure of gelation time.

4.9 Scanning electron microscopy

Cell free hydrogels were formed as previously described in section 4.4.2 and left in basic DMEM containing 10 % FCS for 48 hours. The DMEM was removed and the hydrogels fixed in 3 % glutaraldehyde for 1 hour. Two methods for hydrogel dehydration were investigated: freeze drying and ethanol dehydration as described below.

Freeze dry dehydration

Samples for freeze drying were left at -20 ˚C overnight. The plate was covered in parafilm and pierced over each hole with a needle. The plate was then placed in the VirTis benchtop SLC freeze dryer overnight. The samples were mounted on SEM stubs ready for imaging.

Ethanol dehydration

For ethanol dehydration fixed samples were stored at 4 ˚C overnight. 1 % osmium tetroxide was pipetted onto the hydrogels and left for 1 hour. Hydrogels were washed 3 times in distilled water followed by a dehydration series of 30 %, 50 %, 70 %, 90 %, 95 % and 100 % ethanol for 15 minutes at each step. The plate was left overnight in the fume cupboard to dry. The samples were then mounted on SEM stubs ready for imaging.

Before imaging on the SEM all samples regardless of dehydration protocol were gold coated using an emscope SC500 gold sputter coater for two minutes with a 15 mA current at 0.05 atm. Samples were imaged using Philips XL-20 SEM under vacuum. An electron beam was passed onto the sample and secondary electrons scattered in the chamber. These were detected and formed an image of the surface of the sample.

4.10 Cell viability

4.10.1 Cell activity

PrestoBlue® analysis was carried out to determine the cell viability of the chondrocytes encapsulated in the gel. PrestoBlue® is a commercially available preparation of the dye resazurin. Active cells take up the resazurin dye which is reduced within the mitochondria to resorufin which can freely diffuse chondrocyte out of the cells into the culture medium. The reduced resorufin dye is pink in colour can be detected fluorometrically. The cell viability assay was carried out according to the manufacturer's instructions. PrestoBlue® was added to the culture media at a final concentration of 10 % (vol/vol) and incubated at 37 °C for time periods from 30 minutes to 4 hours. At the required time point, 200 µL samples were removed from each of the wells and the amount of resosrufin determined fluorometrically using a TECAN infinite 200 series plate reader with an excitation wavelength of 535 nm and an emission wavelength of 590 nm.

Cell viability assays using PrestoBlue® were carried out on gel encapsulated cells after 24 hours, 3 days, 7 days, 10 days, 14 days, and 20 days after encapsulation. When the assay was completed any remaining dye was removed from the well and washed with PBS before culture medium was added to the wells.

4.10.2 Live Dead Staining and Confocal Microscopy

Live/dead stain was carried out to determine cellular survival and death within the gels. The gels were kindly imaged by Saima Ahmed on the confocal microscope. 10 µM 5-chloromethylfluorescein diacetate (CMFDA cell tracker Green) in DMSO and 10 µM propidium iodide (PI) was added to DMEM and incubated on the gels for 1 hour. The gels were then fixed in formaldehyde for 30 minutes. The fluorescently labelled samples were transferred to a glass microscope slide and imaged using an upright Zeiss Axioskop LSM 510 meta confocal laser scanning microscope. A x10 (EC Plan – Neofluar 10x/0.3 dry objective lens was used to image the samples. CMFDA was imaged using an excitation wavelength of 488 nm and an emission wavelength of 517 nm, to detect green fluorescence to visualise live cells. PI was imaged using an excitation wavelength of 543 nm and emission wavelength of 650 nm, to detect red fluorescence to visualise dead cells. The images were constructed using LSM image browser software to enable images of both live and dead cells.

4.10.3 Measurement of glycosaminoglycans using 1,9-dimethylmethylene blue dye

One of the main components of the extracellular matrix of hyaline cartilage are the proteoglycans, and in particular aggrecan. These proteoglycans are heavily glycosylated (mainly with chondroitin and keratin sulphate) and quantification of proteoglycans is achieved through determining the concentration of the glycosaminoglycan (GAG) components. 1,9-Dimethylmethylene blue dye (DMB) can be used to determine the concentration of GAG's present in a sample [234]. This is important to determine if the chondrocytes are undergoing differentiation or mesenchymal stem cells are undergoing chondrogenic differentiation in the gel and synthesising an extracellular matrix. After 21 days the gels were removed from the media, placed in small conical tubes and incubated with 200 µL of papain solution consisting of 200 mM phosphate buffer containing 1 mM EDTA, 0.05 w/v % papain and 0.96 w/v % n-acetyl cysteine, and left at 60 °C for 24 hours. Agarose gels were incubated with 0.2 $\mu g.mL^{-1}$ agarase at 40 ºC for 24 hours before incubation with 200 µL of papain solution consisting of 200 mM phosphate buffer containing 1 mM EDTA, 0.05 w/v % papain and 0.96 w/v % n-acetyl cysteine at 60 ºC for 24 hours. A chondrotin sulphate standard curve was formed using chondroitin sulphate concentrations from 0-50 $\mu g.mL^{-1}$. 20 µl of the chondroitin sulphate standards were added to a 96-well plate along with 20 µl of the samples. 250 µl DMB dye was added to each well using a multichannel pipette and the optical density measured at 525 nm immediately using the TECAN infinite 200 series.

4.11 Histological examination

After experimental termination, samples were fixed with 4 % formaldehyde for 30 minutes. Each hydrogel was fully submerged in OCT embedding matrix, surrounded by an aluminium foil structure formed by wrapping foil around a bijoux and folding the foil under the bottom leaving a small hole in the centre of the foil. The bijoux was removed leaving a cylinder of foil, the bottom was placed onto a piece of cork board enabling labelling of the sample. This was then placed in a glass beaker and lowered into liquid nitrogen at -196 ˚C and allowed to freeze to preserve the sample. These samples were then stored at -20 ˚C ready for cryosectioning on the microtome HM560 cryostat. Sections of 8 µm thickness were taken and collected onto SuperFrost Plus glass slides.

4.11.1 Haematoxylin and eosin stain (H&E)

Fixed sections were inserted in an automatic Shandon staining bath and emerged in baths of: running water, haematoxylin, running water twice, 0.1 % hydrochloric acid in 70 % alcohol, running water twice, Scott's tap water substitute, water, eosin twice, running water, 95 % alcohol, absolute alcohol, 1:1 absolute alcohol in xylene, and xylene twice. The sections were then mounted in DPX. Analysis of the images was carried out using imagej software to measure the pore diameter and number of pores per image.

4.11.2 Toluidine blue

Fixed sections were covered with 1 % toluidine blue in 0.5 % sodium borate made up in distilled water and stained for 5 seconds, immediately rinsed with distilled water, air dried, cleared in xylene and mounted in DPX.

4.11.3 Crystal Violet

Samples were fixed and left in the 24 well-plate for staining. The samples were covered with 0.1 % crystal violet in distilled water for 5 minutes, rinsed with distilled water, and immediately imaged.

4.12 Molecular biology

4.12.1 TRIzol RNA Extraction

Ribonucleic acid (RNA) extraction by TRIzol was carried out according to the manufacturer's instructions by adding 1 mL of TRIzol to the 300,000 chondrocytes encapsulated in 2.66 $mg.mL^{-1}$ and fibrin gels in nuclease-free Eppendorf's. The hydrogel was dissolved in the TRIzol by use of an ultrasonic processor. The samples were then stored at -80 ˚C until required. For RNA extraction 200 µL of chloroform was added to the TRIzol –gel solution and the Eppendorf was shaken vigorously for 15 seconds and left at room temperature for 3 minutes and then centrifuged at 12,000 g for 15 minutes at 4 ˚C. The upper colourless phase of the solution was transferred to a new nuclease-free Eppendorf with a filter pipette tip without disturbing the lower, pink phase. The lower phase contains phenol and will cause contamination of the RNA. 500 µL of isopropanol was added to the RNA solution and incubated at room temperature for 10 minutes before centrifugation at 12,000 g for 10 minutes at 4 ˚C. The supernatant was removed and the RNA pellet was washed with 1 mL of 75 % ethanol diluted with distilled water, this was briefly vortexed and centrifuged at 7,500 g for 5 minutes at 4 ˚C. The ethanol supernatant

was removed until a thin layer remained at the bottom of the Eppendorf and these were left to air dry for 10 minutes. 20 µL of nuclease-free water was used to re-suspend the RNA pellet. RNA concentration was then determined on the NanoDrop 1000 spectrophotometer. This was used to determine RNA concentration and if there are contaminants within the RNA solution. 1 µL of RNA solution was placed on the detector of the NanoDrop after using nuclease-free water as a blank. The programme then determined the concentration and purity of the RNA.

Phenol contamination was detected during the NanoDrop analysis. Therefore, the RNA solution was washed by adding 500 µL of water-saturated 1-butanol, made from mixing equal volumes of distilled water and 1-butanol vigorously and left for 15 minutes, the upper layer formed is water-saturated 1-butanol. The RNA – water-saturated 1-butanol solution was centrifuged for 30 seconds at 7,500 g. The upper layer was discarded leaving a thin layer on top of the RNA solution to minimise RNA loss. This was repeated three more times. The 1-butanol was removed from the samples by the addition of water-saturated diethylether, 50 mL of distilled water was mixed with 500 mL of diethylether vigorously and left for 15 minutes, and the upper phase is the water-saturated diethylether. This was removed and 500 µL of water-saturated diethylether was added to the RNA solution and titurated 5 times with a filter pipette tip. This was centrifuged at 7,500 g for 30 seconds and the upper phase removed leaving a thin layer to minimise RNA loss. This was repeated once more and the samples were then left to air dry in a fume cupboard for 15 minutes to remove the final layer of water-saturated diethylether.

4.12.2 RNA Extraction Isolate II RNA mini kit

RNA was extracted by Isolate II RNA mini kit. The extraction was carried out in accordance with the manufacturer's instructions and was as follows. The gels with 300,000 cells per gel were transferred to one nuclease-free Eppendorf. 350 µL of Lysis Buffer and 3.5 µL of 2-Mercaptoethanol was added to the samples to lyse the cells and break down any protein. Guanidinium thiocyanate is present in the Lysis Buffer which deactivates endogenous RNA leaving only pure RNA for collection. An Isolate II filter was placed in a collection tube and the lysate solution was added to the filter via a filter pipette tip. This was centrifuged for 11,000 g for 1 minute. The Isolate II filter was discarded and 350 µL of 70 % ethanol in nuclease-free water was added to the lysate solution in the collection tube and titurated 5 times. This solution was loaded onto an Isolate II RNA mini column inserted in a 2 mL collection tube and centrifuged at 11,000 g for 30 seconds. The column contains a silica membrane in which the RNA binds. The

Isolate II RNA mini column was transferred to a new collection tube and 350 µL of membrane desalting buffer was added to the column using a filter pipette tip and centrifuged at 11,000 g for 1 minute. To remove any DNA contaminates DNase I reaction mixture was prepared by adding 10 µL of reconstituted DNase I to 90 µL of reaction buffer for DNase I per sample in a nuclease-free Eppendorf and was gently mixed by flicking the Eppendorf. 95 µL of DNase I reaction mixture was added to each Isolate II RNA mini column and incubated at room temperature for 15 minutes. The RNA was then washed to remove any salt contaminants with 200 µL of Wash Buffer 1 and centrifuged at 11,000 g for 30 seconds, 600 µL of Wash Buffer 2 was added to the column and centrifuged again at 11,000 g for 30 seconds, the solution collected in the collection tube was discarded and the column was placed back into the collection tube. The final RNA wash was 250 µL of Wash Buffer 2 centrifuged at 11,000 g for two minutes. The RNA was then eluted with 60 µL of nuclease-free water into a nuclease-free centrifuge tube by centrifugation at 11,000 g for 1 minute.

4.12.3 Electrophoresis of RNA

An agarose gel was made to determine if RNA is present in the samples. The gel was made by heating 0.5 g of agarose in 36 mL of distilled water in the microwave to dissolve the agarose. 5 mL of MOPS/EDTA x10 solution, made from 0.4 M mops at pH 7, 0.1 M sodium acetate, and 0.01 M EDTA, was added with 9 µL of formaldehyde. This mixture was poured into an RNA mould with a comb at one end to create holes in the gel, this was left to gel for 30 minutes in a fume cupboard. 2 µL of RNA solution was mixed with 4 µL of ethidium bromide in a nuclease-free Eppendorf and placed in a heat block at 95 ˚C for 2 minutes. The comb was removed from the agarose gel and loaded into the tank of the SNCRWA electrophoresis machine (BioRad). The gel was covered in MOPS/EDTA x1 buffer and run for 45 minutes until the blue dye had travelled down the gel. The gel was then analysed using Syngene INGENIUS 3 to determine if any RNA bands were found.

4.13 Statistical analysis

All data was analysed by using GraphPad Prism 6. An unpaired t-test with Welch's correction was used to compare the cell encapsulated fibrinogen gels with their cell free equivalent. One-way ANOVA with Tukey post-hoc test was used to compare the means of groups of cell encapsulated fibrinogen gels. Significance has been highlighted throughout.

5.0 Results: Structure of the hydrogels

The concentrations of all the fibrinogen hydrogels used throughout the thesis was based upon the ability to form gels with 34 $mg.mL^{-1}$ fibrinogen. FPA gelled at concentrations of 2.66 $mg.mL^{-1}$, 2 $mg.mL^{-1}$, 1.33 $mg.mL^{-1}$ and 0.7 $mg.mL^{-1}$ with 34 $mg.mL^{-1}$ fibrinogen. These concentrations of fibrinogen and FPA were determined by Haemostatix Ltd for forming the FPA-fibrinogen hydrogels, and therefore were used for all investigations into the structure and cell encapsulation. Visually, P15 and P17 gelled at concentrations of 0.75 $mg.mL^{-1}$, 0.5 $mg.mL^{-1}$ and 0.25 $mg.mL^{-1}$ with 34 $mg.mL^{-1}$ fibrinogen, as recommended by Haemostatix Ltd.

HyStem was investigated at 1 $mg.mL^{-1}$, 0.75 $mg.mL^{-1}$, 0.5 $mg.mL^{-1}$, and 0.25 $mg.mL^{-1}$, which were concentrations recommended by Haemostatix Ltd. Visually, concentrations of 0.5 $mg.mL^{-1}$ and below formed very small, weak gels with fibrinogen at 34 $mg.mL^{-1}$ and therefore were not investigated further. However, HyStem 1 $mg.mL^{-1}$ and 0.75 $mg.mL^{-1}$ formed a good gel with fibrinogen at 34 $mg.mL^{-1}$ and were therefore investigated further and used throughout this project.

5.1 Coagulation rate

To measure the gelation capacity of the novel cross-linked fibrinogen gels a KC4 coagulation analyser was used. The time of gelation was measured by a magnetic force breaking once a solid gel had formed, the KC4 coagulation analyser was accurate to 0.1 seconds. It was observed that gelation occurred with all of the novel cross-linked fibrinogen gels. The gelation rate was analysed and Table 5.1 showed the mean gelation rate (expressed as coagulation rate) of each carrier of the FBP with fibrinogen. It was found that fibrin (formed using thrombin) formed more slowly in comparison to FPA-fibrinogen, (4.7 seconds vs 3.4 seconds for FPA system) and 4-5 times slower compared to P15 and P17 carriers. P15 and P17 had a similar gelation rates which was over 3 times faster than FPA, refer to Table 5.1.

A range of concentrations of FPA were tested to determine if the concentration of the FBPs had an effect on the ability to form a gel or the gelation time. The results are shown in Figure 5.1. It was observed that for the lowest concentration of FPA, 0.15 $mg.mL^{-1}$, the gelation time was very slow (at 8.4 seconds). As the concentration of FPA was increased the gelation rate plateaued, between 0.23 $mg.mL^{-1}$ and 2.55 $mg.mL^{-1}$ concentrations of FPA which gave a gelation time of 2.9 seconds. At the higher concentrations of

7.3 mg.mL^{-1} started to increase again Figure 5.1. Therefore, at the concentrations of FPA used in this project the gelation rates were: 2.66 mg.mL^{-1} at 2.9 seconds, 2 mg.mL^{-1} at 2.2 seconds, 1.33 mg.mL^{-1} at 2.1 seconds and 0.7 mg.mL^{-1} at 2.3 seconds, as calculated from Figure 5.1. The gelation rate of the novel cross-linked fibrinogen gels was similar.

Table 5.1 Average coagulation time of 30 IU thrombin, 0.25 mg.mL^{-1} FPA, 0.25 mg.mL^{-1} P15 and 0.25 mg.mL^{-1} P17 combined with 3 mg.mL^{-1} fibrinogen to determine the gelation speed.

Fibrinogen binding peptide carrier	Mean coagulation time (seconds)
Thrombin	4.7
FPA	3.4
P15	1.0
P17	1.2

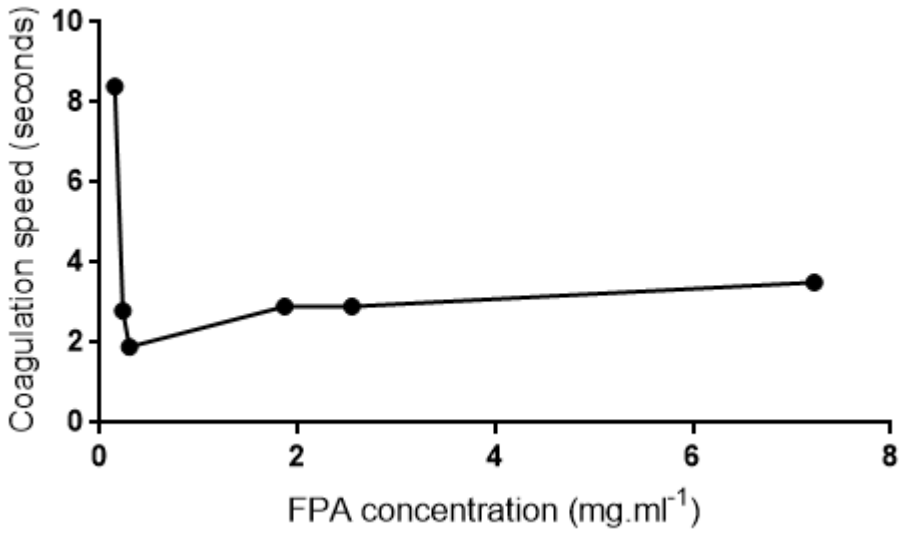

Figure 5.1 Mean coagulation rate of FPA at concentrations of 0.15 mg.mL^{-1}, 0.23 mg.mL^{-1}, 0.3 mg.mL^{-1}, 1.87 mg.mL^{-1}, 2.55 mg.mL^{-1} and 7.23 mg.mL^{-1} with 3 mg.mL^{-1} fibrinogen. N=1.

5.2 Scanning electron microscopy images

Fibrinogen gels formed using FPA at 2.66 mg.mL^{-1}, 2 mg.mL^{-1}, 1.33 mg.mL^{-1}, 0.7 mg.mL^{-1}, and fibrin gels were imaged using the SEM to investigate the structure of the hydrogels. Two methods for dehydrating the gels for the SEM were investigated. These were dehydration using ethanol and freeze drying the sample overnight. From observations after the dehydration processes, freeze dried samples still retained their 3D structure and macroscopically appeared more like the hydrogel before dehydration. Ethanol dehydrated samples turned into a thin flake of material with no macroscopic resemblance of the hydrated hydrogels. The SEM images of the microscopic structure reflect these macroscopic observations of the effect of dehydration methods on the gel structure. The fibrinogen fibres appear much clearer and less fused together in the freeze drying samples (Figure 5.2 C and D) in comparison to the ethanol dehydrated counterparts. SEM images for FPA-fibrinogen 2 mg.mL^{-1} for ethanol dehydration at a magnification of 3,000 was unable to be obtained, due to the fused surfaces the structure was not able to be seen. Therefore, only the freeze dried samples will be looked at in more detail.

The structures of fibrin and FPA-fibrinogen gels appear to be different. Fibrin gels have clear fibres which can be seen, Figure 5.2, whereas the FPA-fibrinogen gel structure is more foam-like in appearance, Figure 5.3 to 5.6. The structures of FPA-fibrinogen gels are very similar and the pore sizes of the gels do not appear to be very different, however it can be seen that gels formed with fibrinogen and FPA at 2.66 mg.mL^{-1}, 2 mg.mL^{-1} and 0.7 mg.mL^{-1} have larger pore sizes compared to FPA concentrations at 1.33 mg.mL^{-1}. It can also be observed that the FPA-fibrinogen gels formed using 1.33 mg.mL^{-1} have more pores on the surface of the gel in comparison to gels formed from FPA at concentrations of 2.66 mg.mL^{-1}, 2 mg.mL^{-1} and 0.7 mg.mL^{-1}. Therefore, gels formed from concentrations of FPA 2.66 mg.mL^{-1}, 2 mg.mL^{-1} and 0.7 mg.mL^{-1} seemed to create a more open porous structure in comparison to FPA at concentrations of 1.33 mg.mL^{-1}. However, a range of pore sizes can be seen in the SEM images for all gel structures.

Fibrinogen gels formed from P15-fibrinogen 0.75 mg.mL^{-1} (

Figure 5.7) and P17-fibrinogen 0.75 mg.mL^{-1} (Figure 5.8) gels had a much more open porous structure in comparison to FPA-fibrinogen gels and fibrin gels. There are areas of fibres and foam-like structures visible from both P15 and P17 – fibrinogen gels. Due to limitations in the amounts of available FBP materials, SEM could not be obtained with

gels formed from P15 and P17 – fibrinogen at concentrations of 0.5 $mg.mL^{-1}$ or 0.25 $mg.mL^{-1}$.

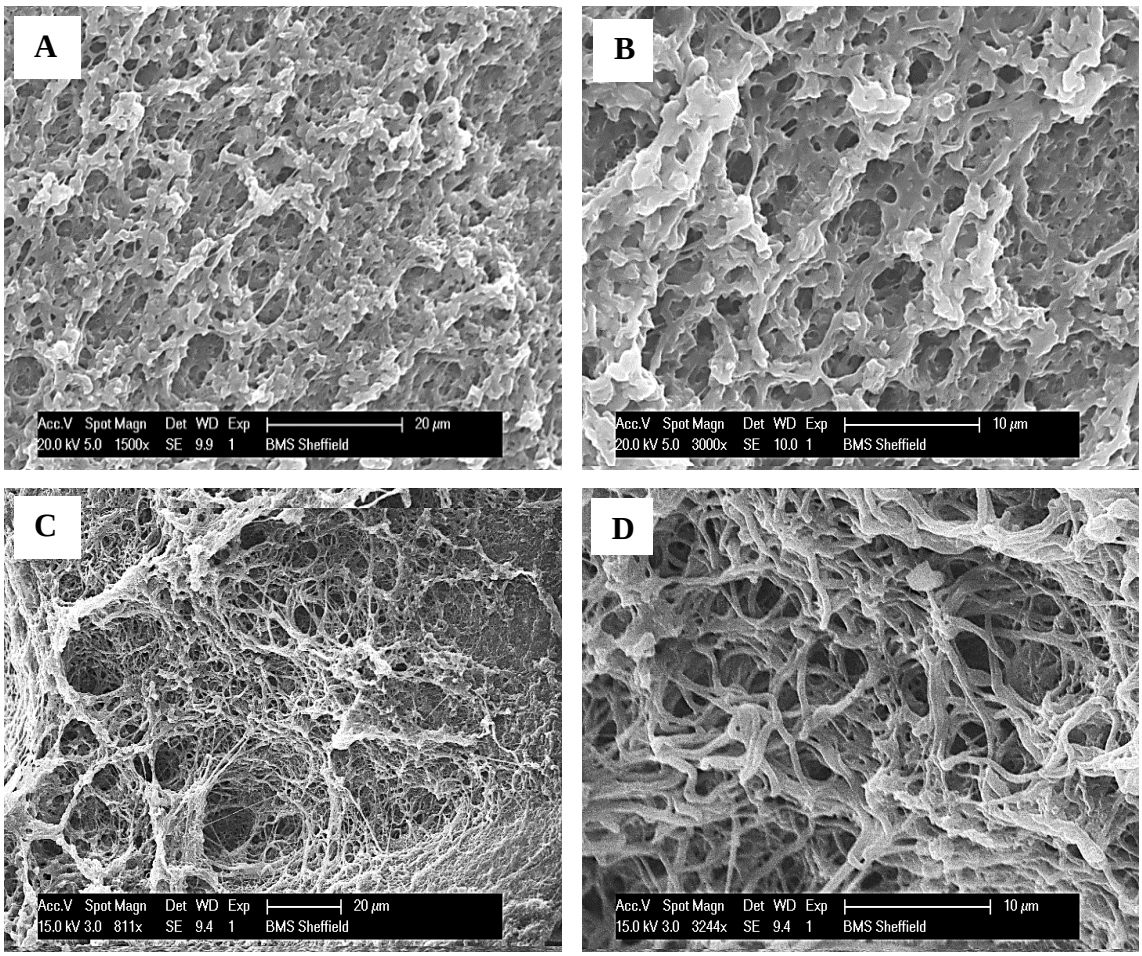

Figure 5.2 Scanning electron microscopy images of fibrin hydrogels dehydrated with ethanol (A and B) or freeze dried (C and D) taken at a magnification of A 1,500x, B 3,000x, C 811x and D 3244x, scale bars are shown on the image.

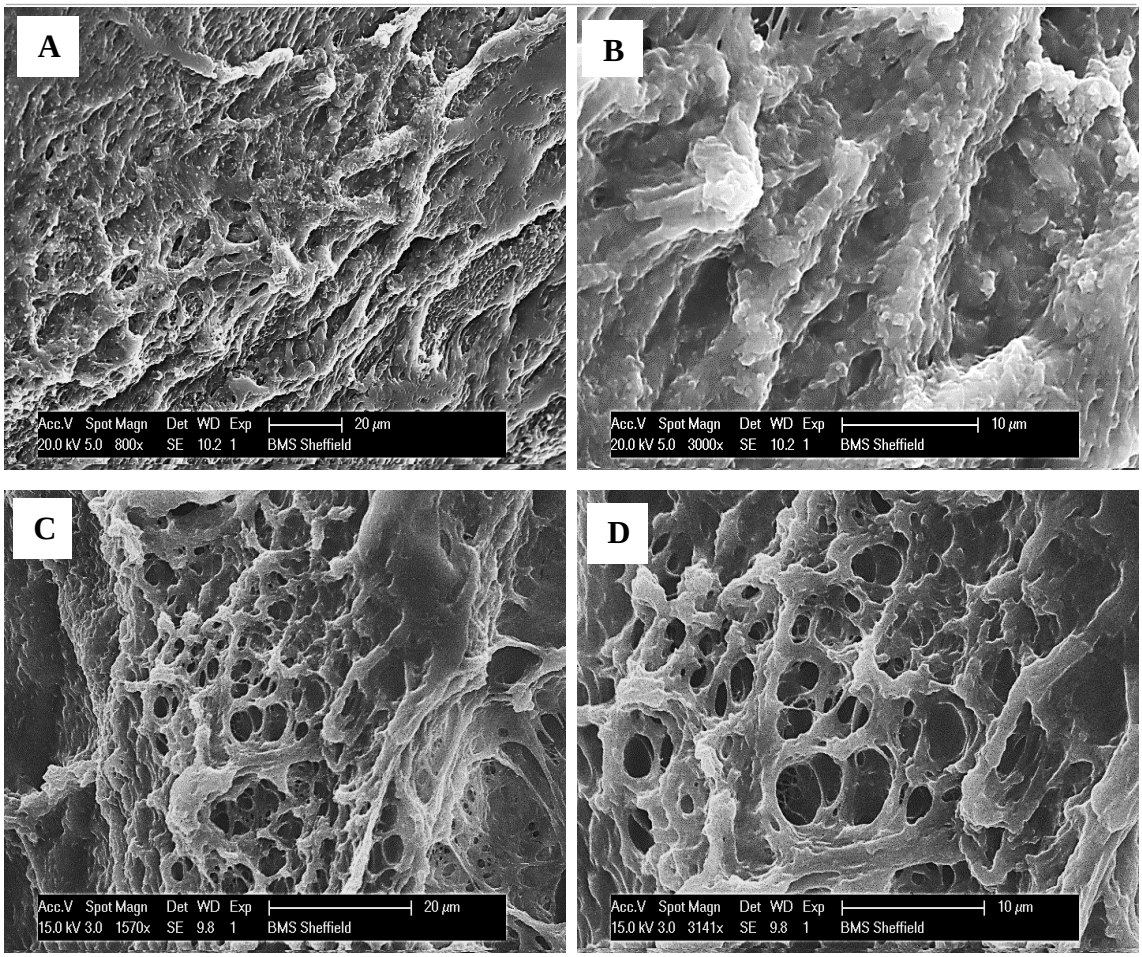

Figure 5.3 Scanning electron microscopy images of FPA-fibrinogen 2.66 mg.mL^{-1} hydrogels dehydrated with ethanol (A and B) or freeze dried (C and D) taken at a magnification of A 800x, B 3,000x, C 1,500x and D 3141x, scale bars are shown on the image.

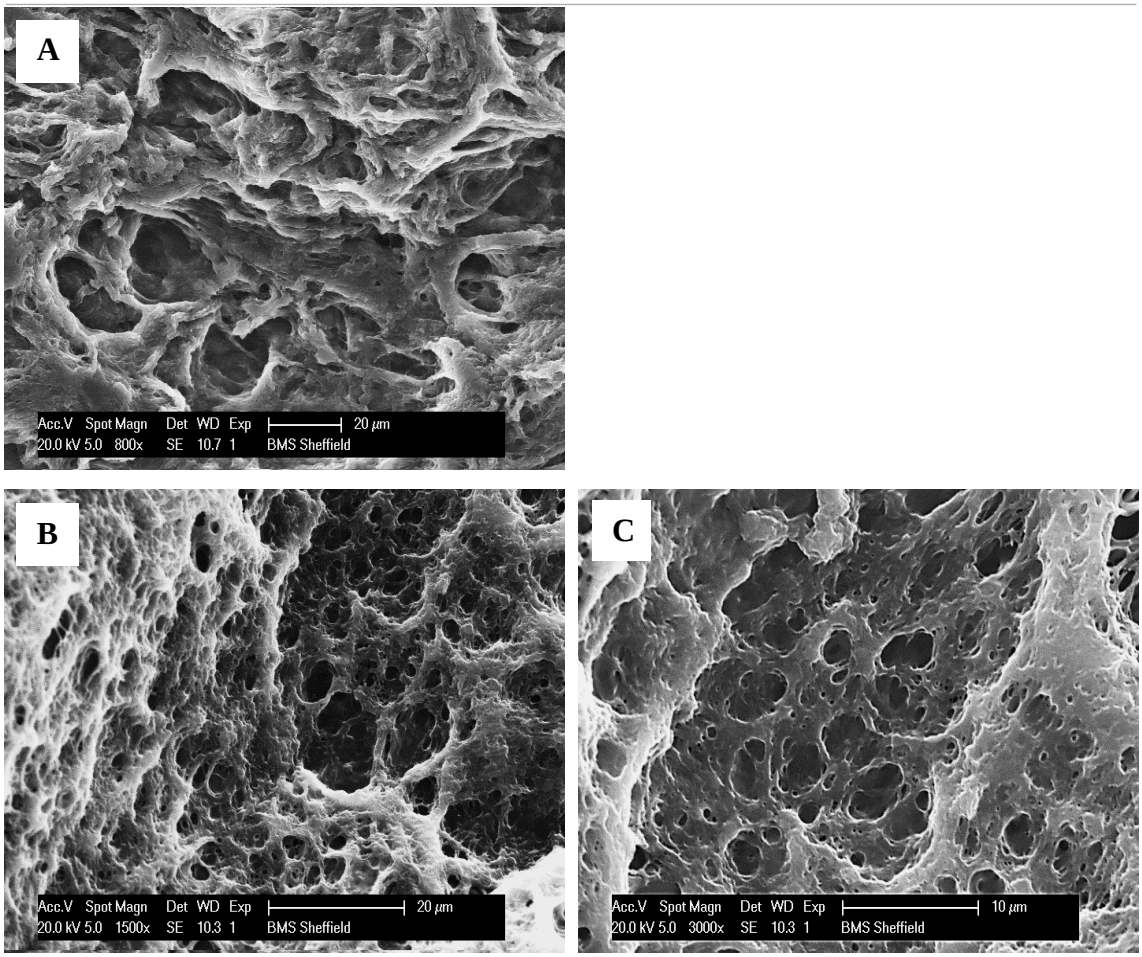

Figure 5.4 Scanning electron microscopy images of FPA-fibrinogen 2 mg.mL^{-1} hydrogels dehydrated with ethanol (A) or freeze dried (B and C) taken at a magnification of A 800x, B 1,500x, and C 3,000x, scale bars are shown on the image.

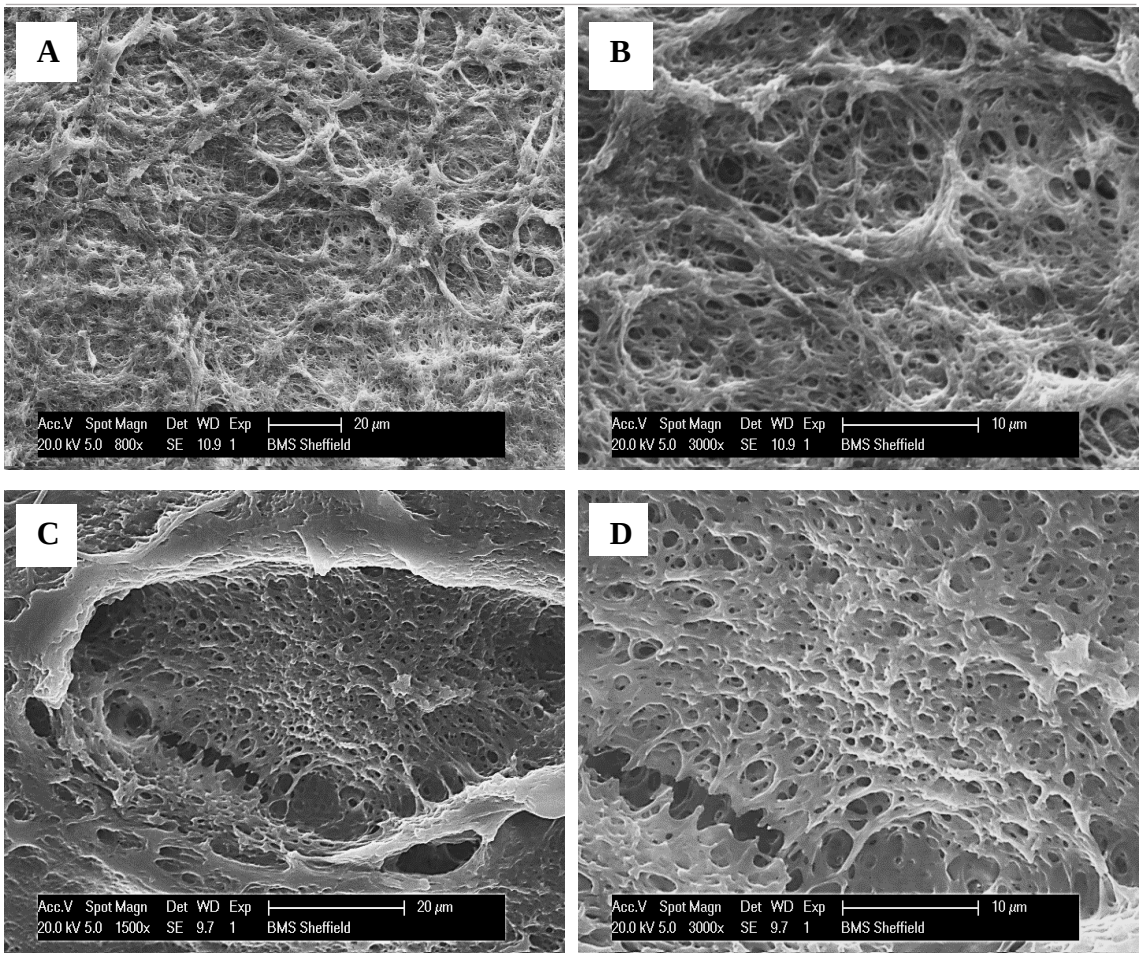

Figure 5.5 Scanning electron microscopy images of FPA-fibrinogen 1.33 mg.mL^{-1} hydrogels dehydrated with ethanol (A and B) or freeze dried (C and D) taken at a magnification of A 800x, B 3,000x, C 1,500x and D 3,000x, scale bars are shown on the image.

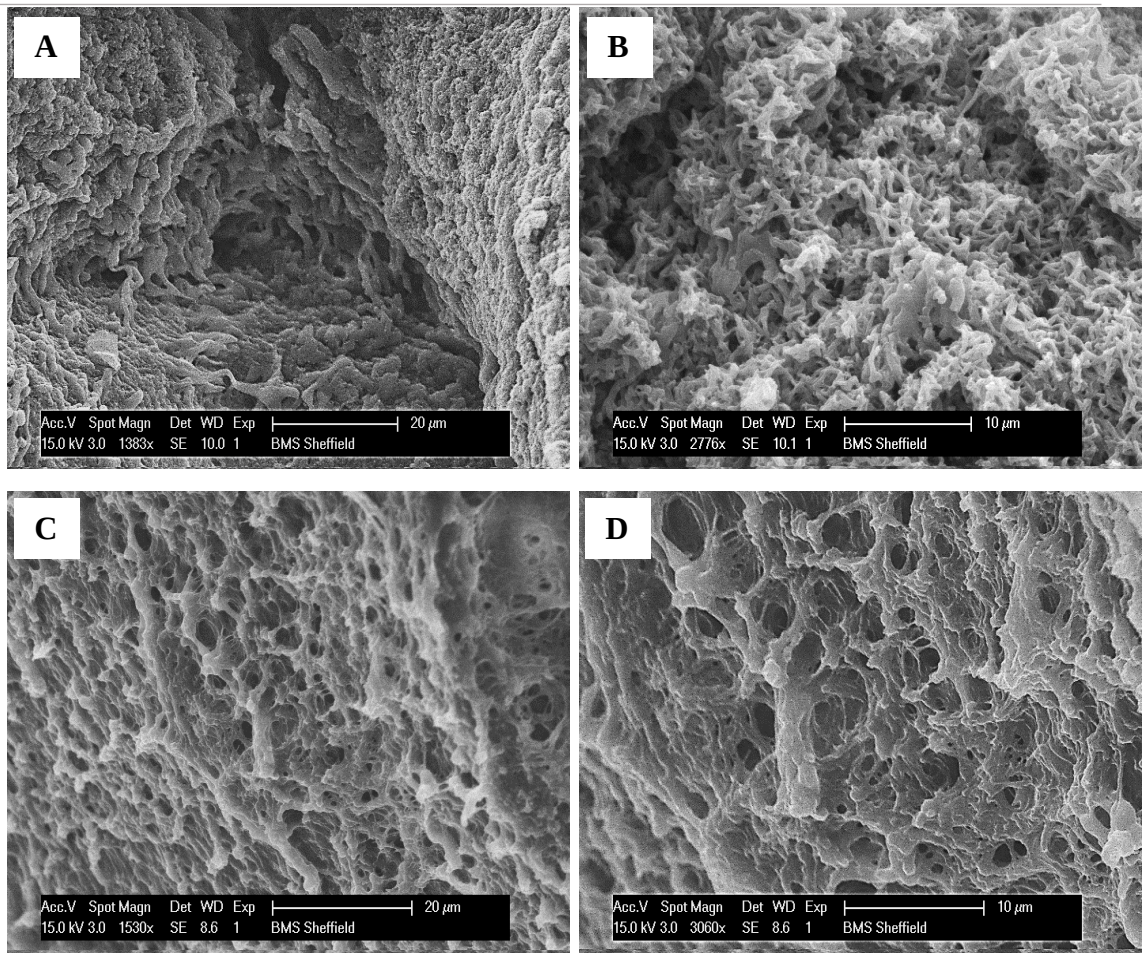

Figure 5.6 Scanning electron microscopy images of FPA-fibrinogen 0.7 mg.mL^{-1} hydrogels dehydrated with ethanol (A and B) or freeze dried (C and D) taken at a magnification of A 1,383x, B 2,776x, C 1,530x and D 3,060x, scale bars are shown on the image.

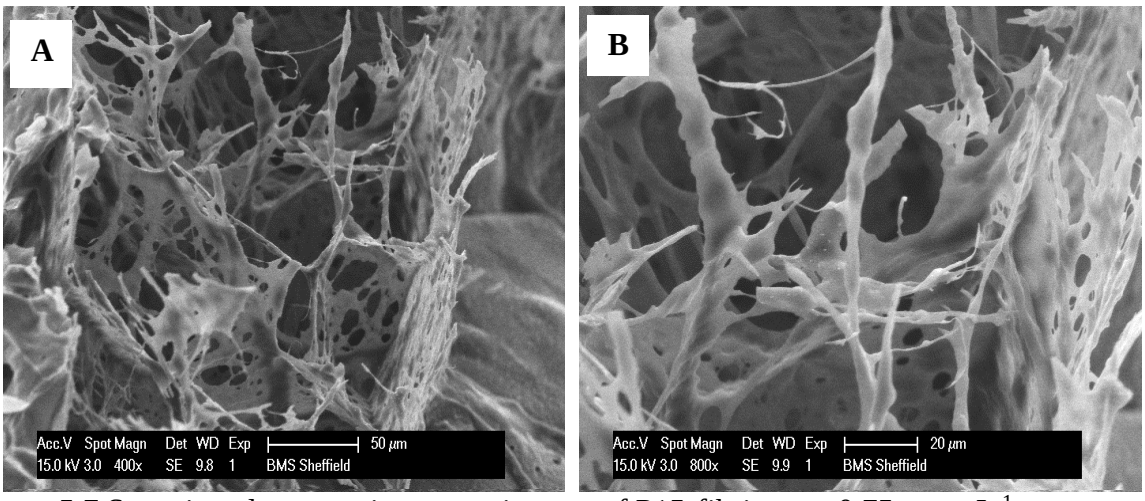

Figure 5.7 Scanning electron microscopy images of P15-fibrinogen 0.75 mg.mL^{-1} hydrogels freeze dried before imaging taken at a magnification of A 400x and B 800x, scale bars are shown on the image.

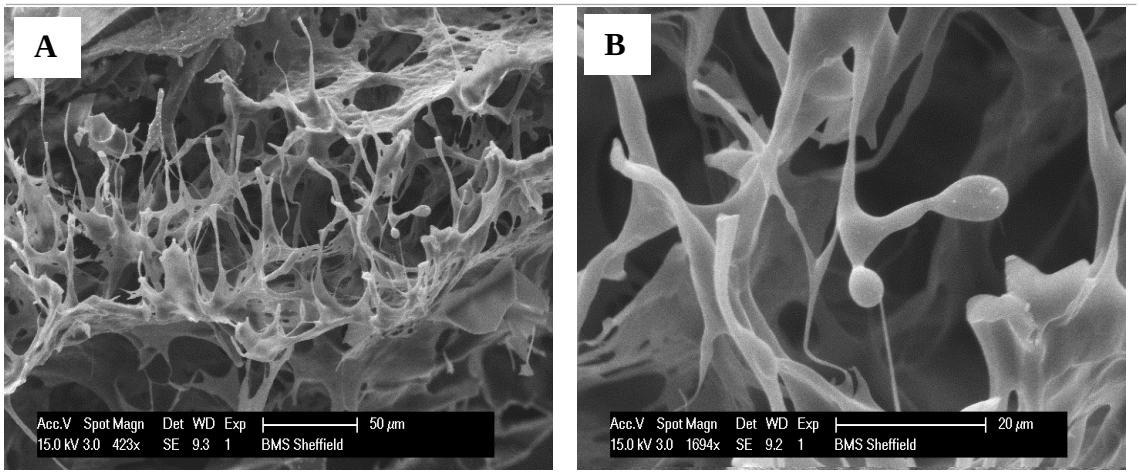

Figure 5.8 Scanning electron microscopy images of P17-fibrinogen 0.75 mg.mL^{-1} hydrogels freeze dried before imaging taken at a magnification of A 423x and B 1,694x, scale bars are shown on the image.

Key summary

- The gelation of fibrin gels was 1 second slower than the gelation of FPA-fibrinogen gels, and 3 seconds slower than the P15-fibrinogen and P17 fibrinogen gels.
- Dehydration via ethanol did not maintain the macroscopic or microscopic structure of the fibrinogen gels, artefacts prevented observations of the microscopic structure.
- Dehydration via freeze drying maintained the fibrinogen gels macroscopic structure and defined microscopic structure.
- Structure of fibrin was clear, defined fibres. FPA-fibrinogen gels had a more foam-like structure. The difference in structure between the various concentrations of FPA was difficult to investigate through the captured SEM images and therefore has been analysed in section 6.3.

6.0 Results: Chondrocyte encapsulation

As previously discussed in chapter 2, ACI is a technique being developed for the repair of injured cartilage. Successful results have been demonstrated within clinical trials. Therefore, the first investigation into cell encapsulation and delivery will be chondrocyte encapsulation. A range of novel fibrinogen gels will be used to encapsulate chondrocytes using fibrin and 4 % agarose gels as reference materials.

6.1 Poly (ethylene glycol)-FBP/fibrinogen hydrogels (PEG)

As previously described in section 4.4.2, chondrocytes were encapsulated in PEG - FBP - fibrinogen gels formed from concentrations of PEG at 1 $mg.mL^{-1}$, 0.75 $mg.mL^{-1}$, 0.5 $mg.mL^{-1}$, and 0.25 $mg.mL^{-1}$ with 34 $mg.mL^{-1}$ fibrinogen. Fibrin gels were formed from 34 $mg.mL^{-1}$ with 192 IU/mL thrombin. 50,000 chondrocytes were encapsulated per gel. The gels were formed and cultured in 96-well culture plates.

Cell viability

Cell activity was assessed using PrestoBlue® as described in section 4.10.1. Cell activity results are displayed as the average fluorescence values from the incubation of one hour with PrestoBlue®. Cell free gels were also incubated with PrestoBlue® reagent to determine if the gel interfered with the assay. The cell free gels produced very low fluorescence results, see Figure 6.1, therefore the gels did not interfere with the assay. The culture medium was also taken from each gel and assayed to determine if the medium contained any active cells, see Figure 6.1. This experiment was to determine if the chondrocytes had migrated from the gel. The low fluorescent results suggested that there are no active cells within the culture medium, see Figure 6.1, indicating that the chondrocytes remained in encapsulation. High levels of cellular activity were detected in all the concentrations of bovine chondrocyte encapsulated PEG gels in comparison to classical fibrin gels throughout the 20 day culture period (Figure 6.2). The data in Figure 6.2 also showed that over the 20 day culture period the rate of the reduced dye, resorufin, was increased with time in culture of the encapsulated cells in gels formed from all the PEG concentrations gelled with fibrinogen and fibrin gels. Therefore, all the gel formulations and the fibrin gels supported chondrocyte viability and proliferation for a 20 day culture period. However, the rate of resorufin formation was significantly lower for the fibrin encapsulated chondrocytes compared to PEG encapsulated cells at all time points (days 1, 7, 14, 20) (Figure 6.2, Table 6.1). In comparing the chondrocyte encapsulated gels formed from the different PEG concentrations, all gave similar results.

However, by day 20, PEG gels formed with 1 mg.mL^{-1} concentration showed the highest level of cellular activity which was significantly greater ($p<0.05$) than 0.25 mg.mL^{-1} (refer Figure 6.2 and Table 6.1). PEG 1 mg.mL^{-1} denotes there was a higher concentration of FBP groups present during gelation, which would create a more cross-linked, gel structure compared to the lower PEG concentrations.

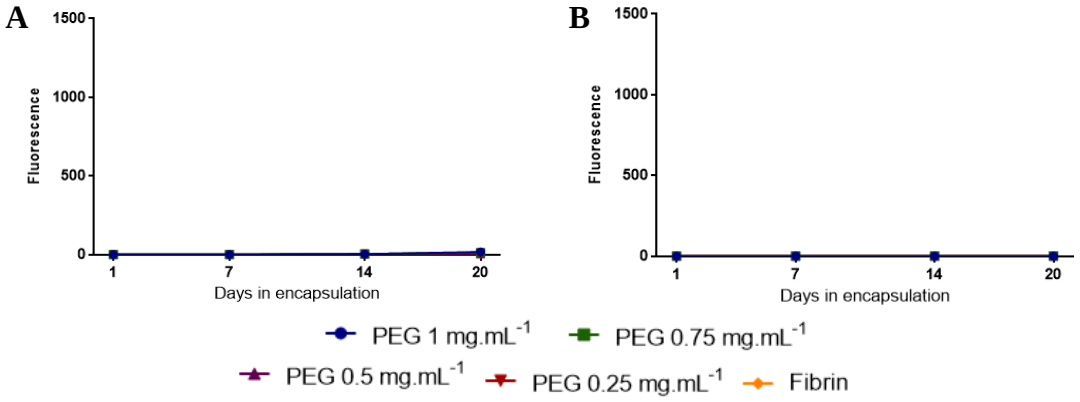

Figure 6.1 Effect of resazurin reduction (shown as relative fluorescence units per minute) over 21 days by cell free (**A**) fibrin and fibrinogen-PEG gels and the culture medium samples (**B**) taken from the incubation with fibrin and fibrinogen-PEG gels. The error bars represent the standard error of the mean. N=3

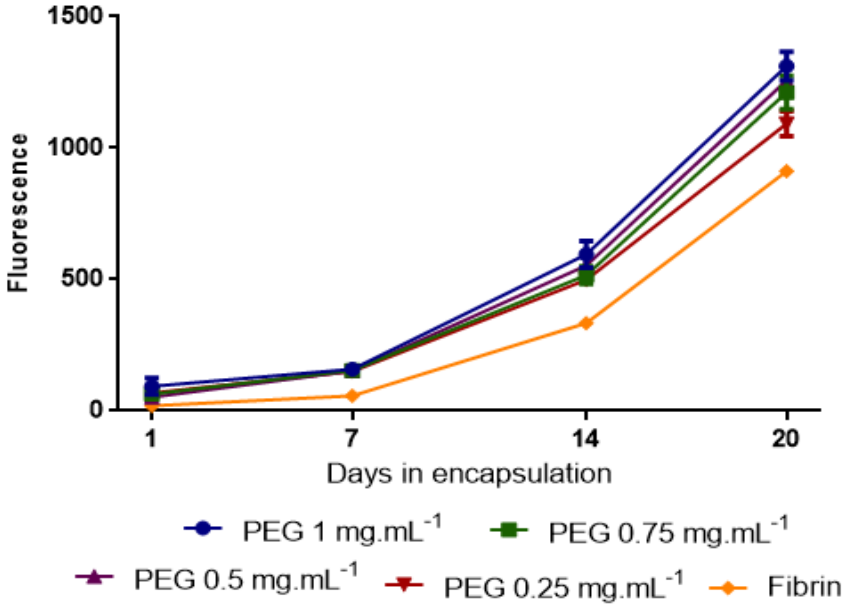

Figure 6.2 Cell activity of 50,000 chondrocytes per gel encapsulated for 20 days in fibrin gels and fibrinogen-PEG gels formed using concentrations of 1 mg.mL^{-1}, 0.75 mg.mL^{-1}, 0.5 mg.mL^{-1}, and 0.25 mg.mL^{-1}. Readings were taken at day 1, day 7, day 14 and day 20 of culture. The error bars represent the standard error of the mean. Statistical analysis with using one-way ANOVA with Tukey post test was conducted shown in Table 6.1. N=3

Table 6.1 Comparative analysis between the cell activity of chondrocytes encapsulated in PEG-fibrinogen gels and fibrin gels. The statistical analysis was carried out using one-way ANOVA with Tukey post hoc test comparing the group averages of gels formed from PEG 1 $mg.mL^{-1}$, PEG 0.75 $mg.mL^{-1}$, PEG 0.5 $mg.mL^{-1}$, PEG 0.25 $mg.mL^{-1}$, and fibrin, from the cell activity results taken at day 1, 7, 14, and 20 after encapsulation (refer to Figure 6.2). Significance: * P<0.05, ** P<0.01, *** P<0.001, **** P<0.0001. Results that are statistically not significant have not been shown in the table.

	Tukey's multiple comparisons test	95% CI of diff.	Summary
Day 1	PEG 1 $mg.mL^{-1}$ vs. Fibrin	1760 to 33937	*
Day 7	PEG 1 $mg.mL^{-1}$ vs. Fibrin	18725 to 29853	****
	PEG 0.75 $mg.mL^{-1}$ vs. Fibrin	17838 to 28967	****
	PEG 0.5 $mg.mL^{-1}$ vs. Fibrin	17321 to 28450	****
	PEG 0.25 $mg.mL^{-1}$ vs. Fibrin	16645 to 27774	****
Day 14	PEG 1 $mg.mL^{-1}$ vs. Fibrin	6964 to 24479	***
	PEG 0.75 $mg.mL^{-1}$ vs. Fibrin	2198 to 19713	**
	PEG 0.5 $mg.mL^{-1}$ vs. Fibrin	4424 to 21938	**
	PEG 0.25 $mg.mL^{-1}$ vs. Fibrin	1178 to 18692	*
Day 20	PEG 1 $mg.mL^{-1}$ vs. PEG 0.25 $mg.mL^{-1}$	307.3 to 12841	*
	PEG 1 $mg.mL^{-1}$ vs. Fibrin	5719 to 18253	****
	PEG 0.75 $mg.mL^{-1}$ vs. Fibrin	2707 to 15241	**
	PEG 0.5 $mg.mL^{-1}$ vs. Fibrin	4067 to 16601	***

Glycosaminoglycan content

The GAG content of the gel-encapsulated cells was determined to investigate whether the encapsulated chondrocytes could form and accumulate ECM components. Measurement of GAG is an indicator of proteoglycan accumulation in a putative ECM. The GAG content of cell free gels and culture medium from the cell-encapsulated gels was also determined. The GAG content of cell free gels was very low and suggested that the gels did not interfere with the assay (Figure 6.3). Culture medium was taken and analysed from both cell free and cell encapsulated gels, very little GAG was detected in the medium and there were no significant differences between cell encapsulated and cell free gels from the media samples (Figure 6.3). The total GAG content for chondrocyte encapsulated PEG gels showed high levels of GAG per gel, however all gels gave similar results and are not significantly different between groups (Figure 6.4). The cell encapsulated gels are significantly different from their cell free equivalent for 1 $mg.mL^{-1}$, 0.75 $mg.mL^{-1}$, and 0.5 $mg.mL^{-1}$ concentrations of PEG. Showing that the chondrocytes are synthesising ECM within the PEG and fibrin hydrogels.

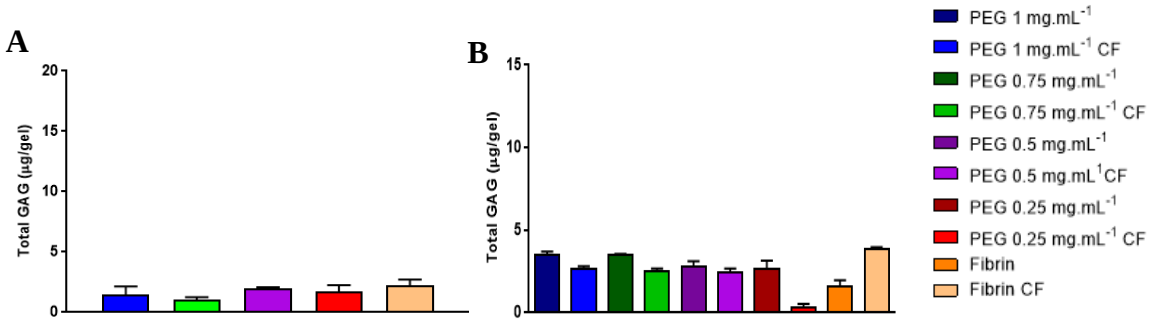

Figure 6.3 Effect of the cell-free (A) fibrin and PEG-fibrinogen gels on the DMB assay to measure GAG content. Total GAG content of the culture medium (B) taken at day 21 of culture from the incubation with cell free (CF) or chondrocyte encapsulated fibrin and PEG-fibrinogen gels. The error bars represent the standard error of the mean. Statistical analysis using one-way ANOVA with a Tukey post test showed no significant differences between the groups. N=3

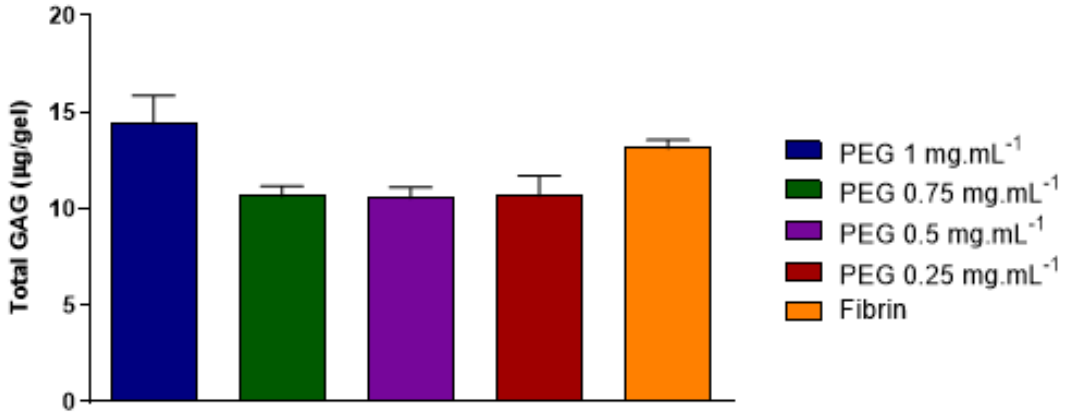

Figure 6.4 Total glycosaminoglycan content/gel of chondrocytes encapsulated in the PEG-fibrinogen gels formed with PEG 1 mg.mL^{-1}, PEG 0.75 mg.mL^{-1}, PEG 0.5 mg.mL^{-1}, PEG 0.25 mg.mL^{-1} or fibrin gels (shown as mean total GAG (µg/gel) indicating extracellular matrix deposition of 50,000 bovine chondrocytes per gel encapsulated for 21 days. The error bars represent the standard error of the mean. Statistical analysis using one-way ANOVA with a Tukey post test showed no significant differences between the groups. Refer to Table 6.2 for statistical analysis between the cell free counterparts. N=3

Table 6.2 Comparative analysis between the total glycosaminoglycan content of chondrocytes encapsulated in PEG-fibrinogen gels or fibrin gels after 21 days of incubation vs cell-free gels. The statistical analysis was carried out using an unpaired t-test with Welch's correction comparing fibrinogen gels formed with PEG 1 $mg.mL^{-1}$, PEG 0.75 $mg.mL^{-1}$, PEG 0.5 $mg.mL^{-1}$, and PEG 0.25 $mg.mL^{-1}$, or Fibrin, with their cell free equivalents from the total glycosaminoglycan content per gel measured at day 21 of culture. C denotes chondrocyte encapsulation, CF denotes the cell free gel. Significance: * P<0.05, ** P<0.01, **** P<0.0001. Non-significant results have not been shown in the table.

Unpaired t-test with Welch's correction	Significance
PEG 1 $mg.mL^{-1}$ C vs. PEG 1 $mg.mL^{-1}$ CF	**
PEG 0.75 $mg.mL^{-1}$ C vs. PEG 0.75 $mg.mL^{-1}$ CF	*
PEG 0.5 $mg.mL^{-1}$ C vs. PEG 0.5 $mg.mL^{-1}$ CF	*
Fibrin C vs. Fibrin CF	****

For strategic reasons, Haemostatix Ltd. decided that synthesis of the PEG-fibrinogen hydrogels would not be continued and therefore the investigation into the use of these gels was terminated.

6.2 Peprostat hydrogels

6.2.1 Initial biocompatibility

Chondrocytes were encapsulated in FPA hydrogels and formed from fibrinogen and FPA at concentrations of 2.66 $mg.mL^{-1}$, 2 $mg.mL^{-1}$, 1.33 $mg.mL^{-1}$ and 0.7 $mg.mL^{-1}$. Fibrin gels were formed from 34 $mg.mL^{-1}$ fibrinogen with 192 IU/mL of thrombin. 50,000 chondrocytes per gel were encapsulated in all gels to test biocompatibility of the hydrogels and their potential to support ECM formation by the chondrocytes. The gels were formed and cultured in 96-well culture plates.

Cell viability

Cell free gels were incubated alongside their chondrocyte encapsulated counterparts and were analysed to determine if the gels interfered with the assays used. Cell viability was determined by measuring the level of cell activity using PrestoBlue® as described in section 4.10.1. The cell free fibrin or FPA gels showed very low fluorescence indicating that the gels are not interfering with the assay by binding or reducing the resazurin (Figure 6.5). The medium from the chondrocyte encapsulated FPA gel cultures (refer to Figure 6.5) showed barely detectable fluorescence and therefore indicating that the chondrocytes remained encapsulated in the gel during the culture period. High levels of

cellular activity were detected in all FPA and fibrin gels encapsulated with bovine chondrocytes throughout the 21 day culture period (Figure 6.6). The rate of resorufin formation was significantly lower for the fibrin encapsulated chondrocytes compared to FPA encapsulated chondrocytes at day 7 and day 14 for FPA gels formed with 2.66 mg.mL^{-1} and 2 mg.mL^{-1} (Figure 6.6, Table 6.3).

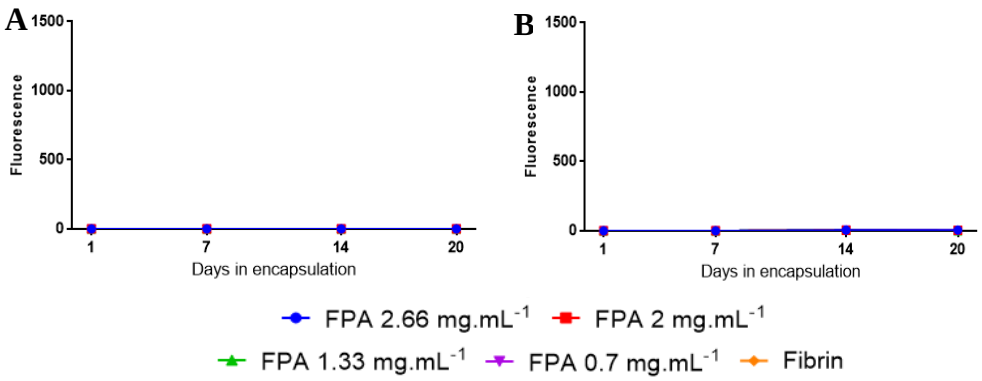

Figure 6.5 The effect of resazurin reduction dye (shown as fluorescence per minute) by cell free FPA-fibrinogen and fibrin gels (**A**) and the culture medium samples (**B**) incubated with the chondrocyte encapsulated FPA-fibrinogen and fibrin gels. The error bars represent the standard error of the mean. N=3

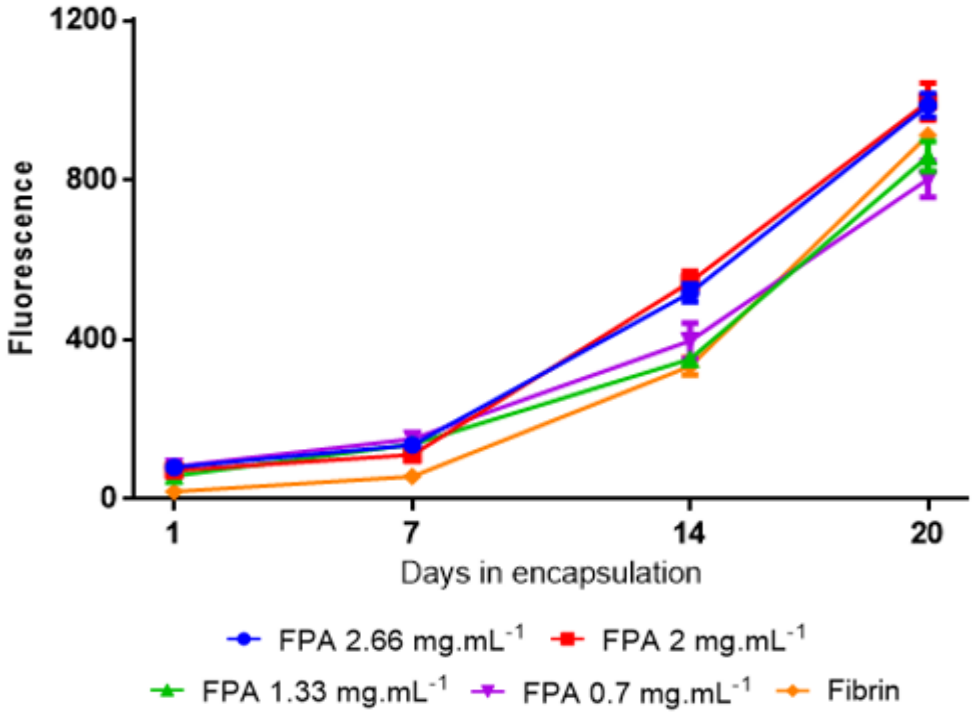

Figure 6.6 Rate of reduction of PrestoBlue® (shown as mean relative fluorescence units per minute) for chondrocytes encapsulated in fibrin gels and FPA gels formed using concentrations of 2.66 mg.mL^{-1}, 2 mg.mL^{-1}, 1.33 mg.mL^{-1}, 0.7 mg.mL^{-1} of FPA. Readings were taken on day 1, day 7, day 14 and day 20 of culture. The error bars represent the standard error of the mean. Statistical analysis with use of a one-way ANOVA with Tukey post test was conducted see Table 6.3 for results. N=3

Table 6.3 Comparative analysis between the cell activity of chondrocytes encapsulated in PEG-fibrinogen gels or fibrin gels vs cell-free gels during 21 days of incubation vs cell-free gels. The statistical analysis was by one-way ANOVA with Tukey post hoc test of the group averages. The cell viabilities were determined on days 1, 7, 14, 20 after encapsulation of chondrocytes (refer to Figure 6.6).

	Tukey's multiple comparisons test	95% CI of diff.	Summary
day 7	FPA 2.66 mg.mL^{-1} vs. FPA 2 mg.mL^{-1}	188.6 to 11317	*
	FPA 2.66 mg.mL^{-1} vs. Fibrin	13243 to 24371	****
	FPA 2 mg.mL^{-1} vs. FPA 1.33 mg.mL^{-1}	-11866 to -736.9	*
	FPA 2 mg.mL^{-1} vs. FPA 0.7 mg.mL^{-1}	-15114 to -3985	***
	FPA 2 mg.mL^{-1} vs. Fibrin	7490 to 18618	****
	FPA 1.33 mg.mL^{-1} vs. Fibrin	13791 to 24920	****
	FPA 0.7 mg.mL^{-1} vs. Fibrin	17039 to 28168	****
day 14	FPA 2.66 mg.mL^{-1} vs. FPA 1.33 mg.mL^{-1}	1238 to 18752	*
	FPA 2.66 mg.mL^{-1} vs. Fibrin	2309 to 19824	**
	FPA 2 mg.mL^{-1} vs. FPA 1.33 mg.mL^{-1}	2859 to 20373	**
	FPA 2 mg.mL^{-1} vs. FPA 0.7 mg.mL^{-1}	109.0 to 17624	*
	FPA 2 mg.mL^{-1} vs. Fibrin	3930 to 21445	**

Glycosaminoglycan content

The GAG content was measured and displayed as the total average content per gel. GAG content from cell free gels gave very low results (Figure 6.7) indicating that the gel is not interfering with the assay and that the chondrocytes in the cell encapsulated gels are synthesising ECM. The culture medium from day 21 of the culture of both cell free and chondrocyte encapsulated gels was also assessed for GAG content (Figure 6.7). The GAG content of culture medium from both cell free and chondrocyte encapsulated gels was very low and not significantly different from each other. The chondrocyte encapsulated FPA hydrogels (Figure 6.8) showed high levels of GAG content per gel and were significantly different from their cell free equivalents (Table 6.4) suggesting that the cells are synthesising ECM. The chondrocyte encapsulated gels in all FPA and fibrin gels gave similar results and were not statistically different from each other.

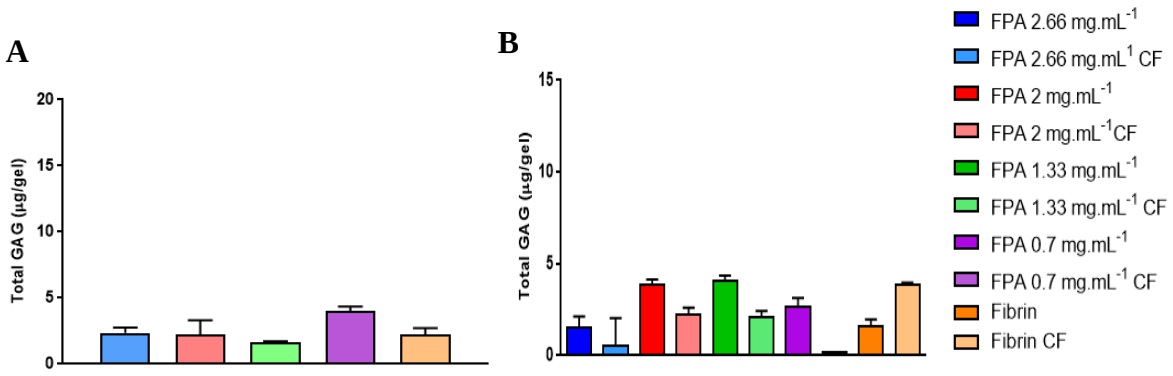

Figure 6.7 The effect of DMB (shown as mean total GAG (µg/gel)) on cell free (**A**) FPA-fibrinogen and fibrin gels. Total GAG content of the culture medium (**B**) taken at day 21 of incubation from the cell free (CF) and chondrocyte encapsulated FPA-fibrinogen and fibrin gels. The error bars represent the standard error of the mean. Statistical analysis by one-way ANOVA with Tukey post test was conducted. There was no significant differences between groups. Refer to Table 6.4 for statistical analysis comparison of cell free gels with cell encapsulated gels. N=3

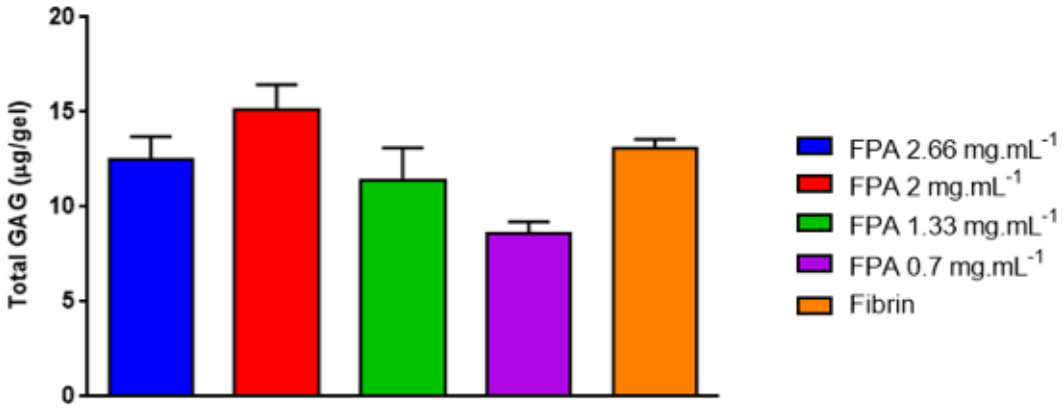

Figure 6.8 Total glycosaminoglycan content of 50,000 chondrocytes encapsulated in FPA and fibrin gels. Fibrinogen gels were formed with FPA at concentrations of 2.66 mg.mL^{-1}, 2 mg.mL^{-1}, 1.33 mg.mL^{-1}, and 0.7 mg.mL^{-1}. Results are shown as the mean total GAG (µg/gel) after 21 days in encapsulation. The error bars represent the standard error of the mean. N=3.

Table 6.4 Results of the statistical analysis of the data shown in Figure 6.7 and Figure 6.8. The data was analysed using one-way ANOVA with Tukey post hoc test to compare the group averages of FPA 2.66 mg.mL^{-1}, FPA 2 mg.mL^{-1}, FPA 1.33 mg.mL^{-1}, FPA 0.7 mg.mL^{-1} or fibrin gels with their cell free equivalents. C denotes chondrocyte encapsulation, CF denotes the cell free gel. Significance: *** P<0.001, **** P<0.0001. Non-significant results have not been shown in the table.

Tukey's multiple comparisons test	95% CI of diff.	Significance
FPA 2.66 mg.mL^{-1} C vs. FPA 2.66 mg.mL^{-1} CF	3.097 to 17.27	***
FPA 2 mg.mL^{-1} C vs. FPA 2 mg.mL^{-1} CF	5.819 to 19.99	****
FPA 1.33 mg.mL^{-1} C vs. FPA 1.33 mg.mL^{-1} CF	2.716 to 16.89	***
Fibrin C vs. Fibrin CF	5.866 to 15.89	****

6.2.2 Optimisation of gel fabrication

Forming the cell-encapsulated hydrogels in wells of a 96-well culture plate and the culturing the resultant gels in the same wells only allowed for 200 µL of media to surround the gel. Therefore, there was a relatively high cell number comparative to the maximum volume of culture medium which could be added to the culture wells. This meant that had to be changed daily as the medium became very acidic if left for longer than 24-36 hours which meant that cell proliferation and differentiation became compromised. Also, changing the culture medium every day was not always practical and higher cell numbers could not be encapsulated in the gels. Therefore, a method of forming the hydrogels in a larger culture plate or transferring the cell-encapsulated hydrogels to a larger well plate was required. Therefore, a series of experiments were carried out to investigate ways of ensuring the cell encapsulated hydrogels could be formed in, or transferred to larger culture wells.

Agarose wells

An agarose well system was investigated for casting fibrin and FPA-fibrinogen gels. As previously described, the gels were cast in the centre of 1 % agarose wells, formed as described in section 4.5.1. The chondrocytes were cultured in this environment for 7 days and the cell viability was determined at day 1 and day 7 after cell encapsulation. These results showed that there was very little detectable cellular activity after 7 days post-encapsulation in the agarose moulds, (Figure 6.9) and therefore the experiment was terminated after this period of time. The use of the agarose well-system in which to cast the gels was abandoned.

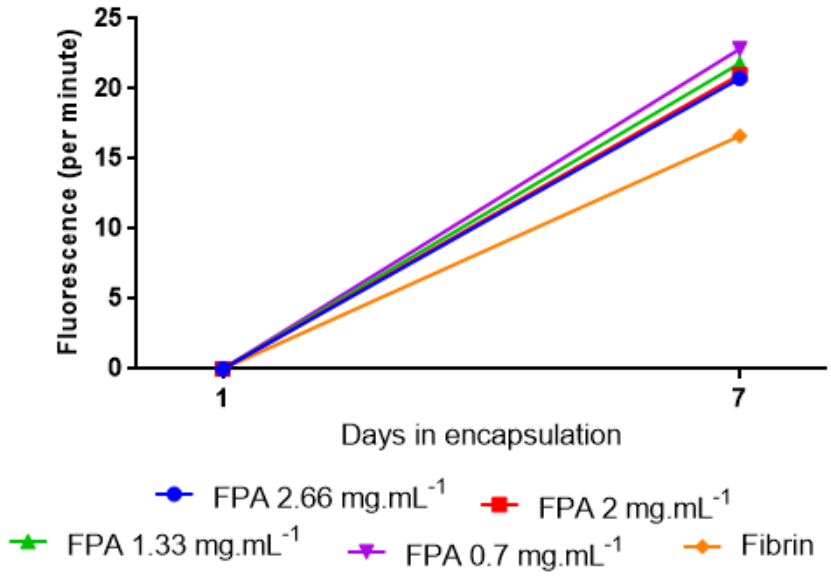

Figure 6.9 Cell viability measured as the rate of reduction of PrestoBlue® (shown as relative fluorescence units per minute) of 50,000 bovine chondrocytes per gel encapsulated in fibrin and FPA-fibrinogen gels formed with FPA at concentrations of 2.66 mg.mL^{-1}, 2 mg.mL^{-1}, 1.33 mg.mL^{-1}, and 0.7 mg.mL^{-1}. The gels were formed in a 1 % agarose well in a 24-well culture plate and cultured for 7 days. Readings were taken at day 1 and day 7 of culture. N=1.

PTFE moulds

The use of a PTFE mould in which to form the gels followed by transfer of the gels to a larger well in a culture plate was investigated. A custom-made PTFE mould was fabricated as described in section 4.5.2. The chondrocyte encapsulated gels were cast in PTFE moulds, after gelation was complete the gels were transferred to an individual well in a 24-well culture plate. It was observed that gelation was successful within the PTFE moulds and the gels were transferred with ease. However, the cellular activity was lower at days 1 and day 7 after chondrocyte encapsulation (Figure 6.10) compared to fabricating the gels in a well of a 96-well plate. Despite the lower cellular activity from the chondrocytes encapsulated in the PTFE moulds during preliminary experiments the PTFE moulds were used for further investigation into the concentration of calcium used during gelation, see section 6.2.4. This is because the FPA and fibrin gels formed within the PTFE wells were bigger and less visible solution was observed after gelation within the moulds. However, with successive usage, it became difficult to keep the PTFE wells clean and free from bacterial and fungal contaminants and therefore this method had to be abandoned.

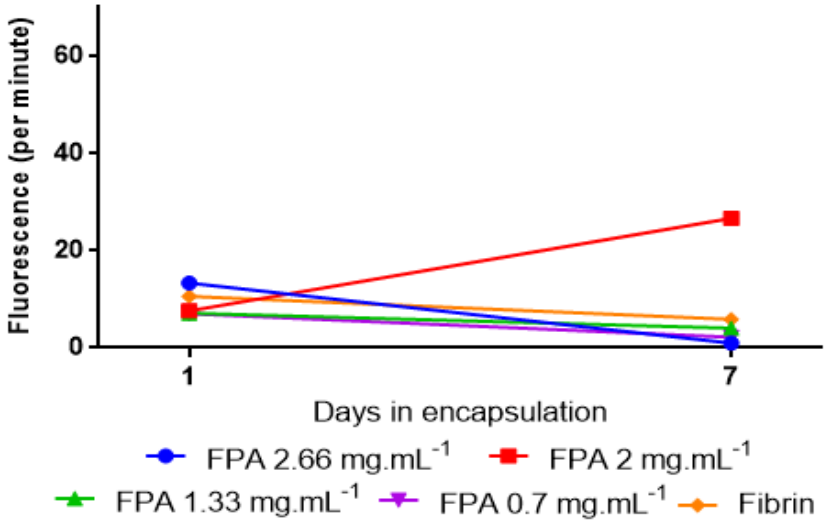

Figure 6.10 Cell viability measured as the rate of reduction of PrestoBlue® (shown as mean fluorescence per minute) indicating the cell activity of 50,000 bovine chondrocytes encapsulated in fibrin gels and FPA gels using concentrations of 2.66 mg.mL^{-1}, FPA 2 mg.mL^{-1}, FPA 1.33 mg.mL^{-1}, FPA 0.7 mg.mL^{-1}. The gels were formed in a PTFE well block, transferred to a well in a 24 well plate and cultures for 7 days. Readings were taken at day 1 and day 7 of culture. N=1.

Fabrication in 96-well culture plates

The final fabrication method of FPA and fibrin gels that was investigated was forming the FPA and fibrin gels in individual wells of a 96-well culture plate and transferring the gel to an individual well of a 24-well culture plate with a micro spatula (Figure 6.12). Chondrocyte encapsulated gels were fabricated and cultured in a well of a 96-well plate and used as a comparison, Figure 6.11. Gels formed from FPA at concentrations of 2.66 mg.mL^{-1}, 2 mg.mL^{-1}, 1.33 mg.mL^{-1}, and 0.7 mg.mL^{-1} and fibrin gels were then fabricated using this method alongside fabrication and culture in a well in a 96-well culture plate. The cell activity data suggested that chondrocytes survived in all gels regardless of their method of fabrication or culture. There were no significant differences between the gels cultured in 96-well plates and those cultured in 24-well plates. Therefore, the transfer of the FPA and fibrin gels and culture in a larger well did not affect cellular survival. The method of fabrication in a well in a 96-well culture plate and transferring the gels to a well in a 24-well culture plate was used for the remaining experiments.

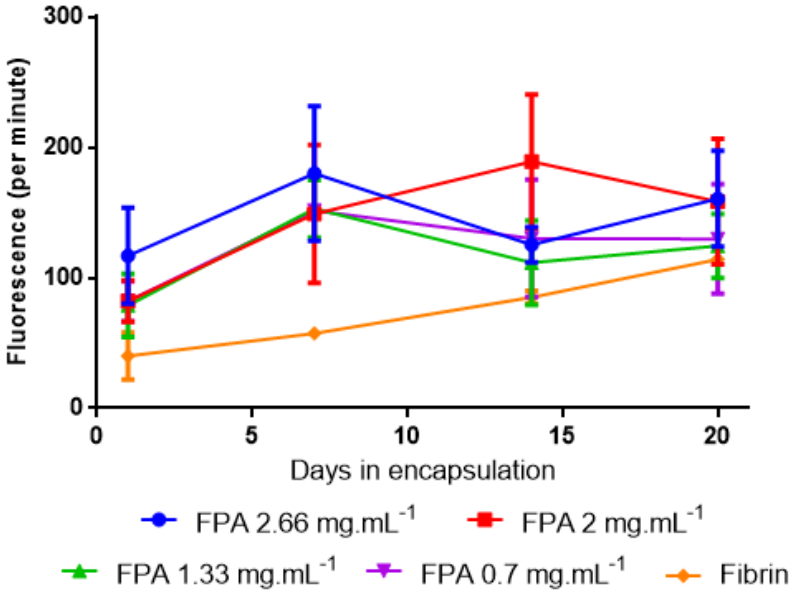

Figure 6.11 Cell viability of chondrocyte encapsulated fibrin gels and FPA gels measured as the rate of reduction of PrestoBlue®. 50,000 chondrocytes per gel were cultured in a well in a 96-well culture plate for 21 days. Readings were taken at day 1, 7, 14 and 20 of culture. The error bars represent the standard error of the mean. Statistical analysis with use of a one-way ANOVA with Tukey post test was conducted. No statistically significant differences were found between groups. N=2

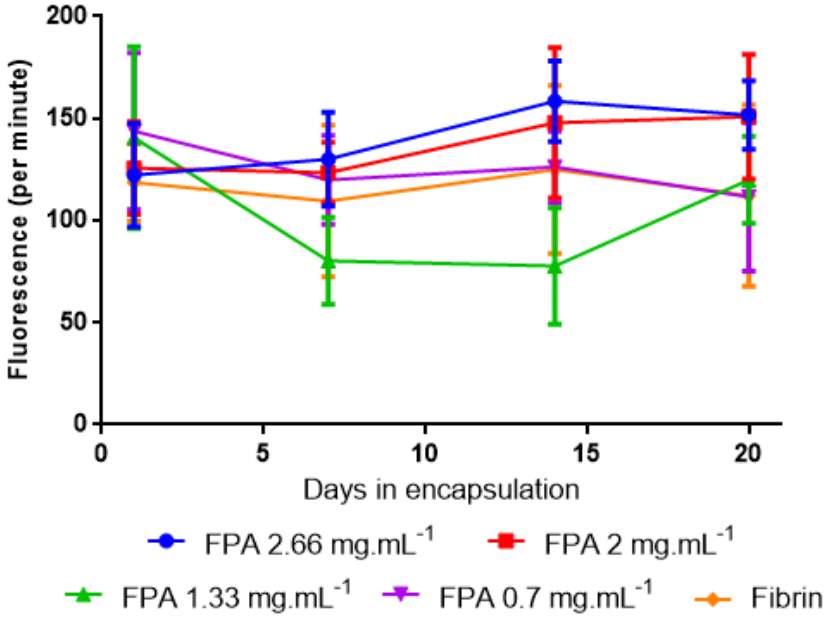

Figure 6.12 Cell viability measured as rate of reduction of PrestoBlue (shown as mean relative fluorescence units per minute) of 50,000 chondrocytes per gel encapsulated in FPA-fibrinogen and fibrin gels. The gels were cultured in 24-well plates for 21 days. Cell viability was assessed on day 1, day 7, day 14 and day 20 of culture. The error bars represent the standard error of the mean. Statistical analysis using one-way ANOVA with Tukey post tests showed no statistically significant difference between the hydrogel groups. N=2

6.2.3 Cell seeding density

To determine the optimum number of cells for encapsulating chondrocytes in the FPA and fibrin hydrogels cell seeding density experiments were carried out. 50,000, 150,000 and 300,000 chondrocytes per gel were encapsulated in fibrin, and gels formed from FPA at concentrations of 2.66 $mg.mL^{-1}$ and 0.7 $mg.mL^{-1}$ and cultured for 21 days in chondrogenic conditions. The hydrogels were formed in 96-well plates and then transferred to a 24-well plate after gelation.

Cell viability

Cell activity analysis was carried out on the hydrogels at day 1, 7, 14 and 20 after encapsulation and is a measure of fluorescence per minute of incubation. It can be seen that for all hydrogels, fibrin (Figure 6.13), and gels formed from FPA at concentrations of 2.66 $mg.mL^{-1}$ (Figure 6.14) and 0.7 $mg.mL^{-1}$ (Figure 6.15) that the higher the cell number the greater level reduction of the resazurin to resorufin. For each measurement (day 1, 7, 14, 20) the rate of reduction of encapsulation of 300,000 chondrocytes encapsulated per gel were significantly higher than the counterparts with 50,000 encapsulated cells per gel. It can also be seen from gels fabricated from FPA and fibrin that there is very little cellular activity in the gels containing 50,000 chondrocytes encapsulated, this suggested that the cell number needed to be increased. Interestingly, a drop in the cell activity between day 7 and day 14 is consistently observed which needs to be investigated further.

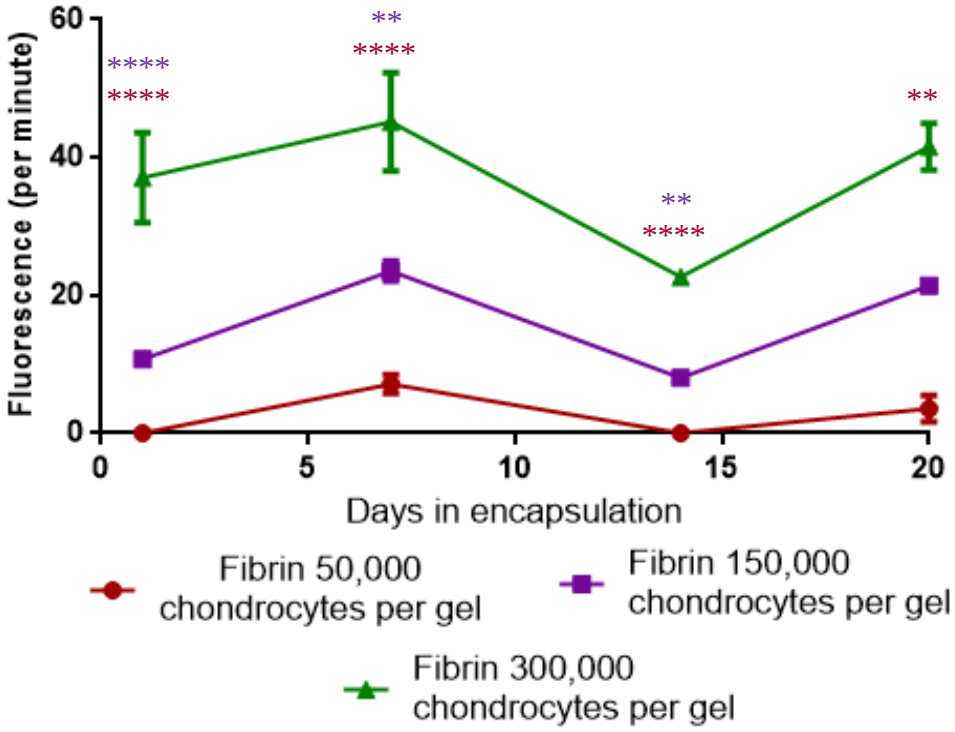

Figure 6.13 Effect of cell number on cell viability over 20 days of encapsulation in fibrin gels. Cell viability was determined by the rate of reduction of PrestoBlue® (shown as mean relative fluorescence units per minute). The error bars represent the standard error of the mean. Statistical analysis with use of a one-way ANOVA with Tukey post test was conducted. Significance: ** P<0.01, **** P<0.0001. Non-significant results have not been shown. Significance is displayed over the data plot and the colour corresponds to the condition in which the significance is compared to. N=2

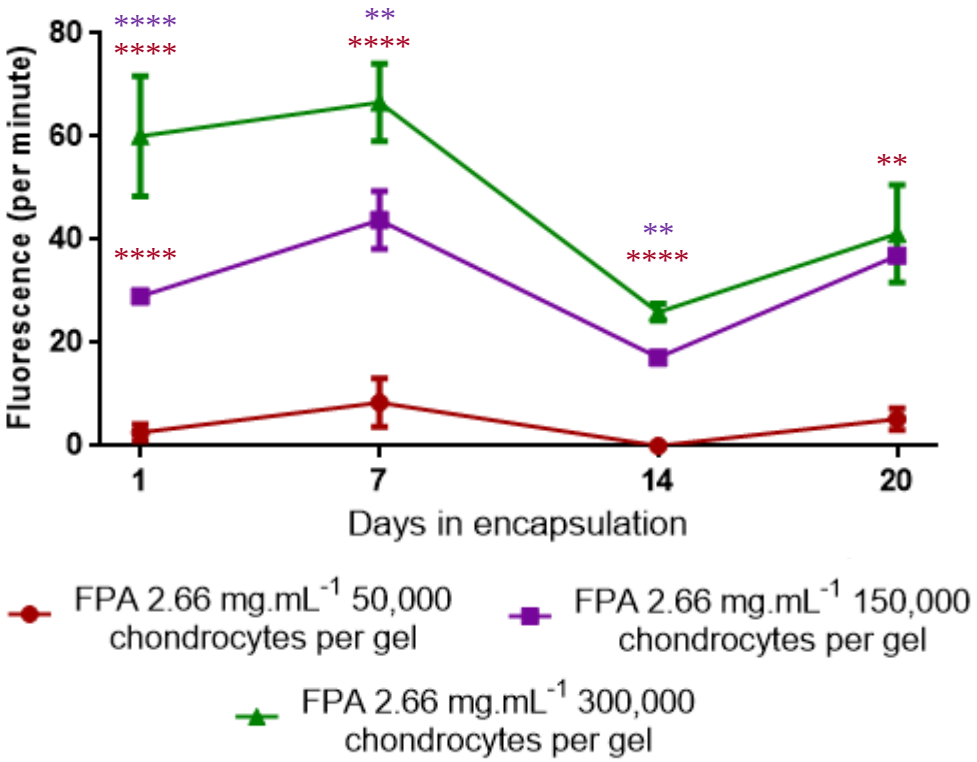

Figure 6.14 Effect of cell number on cell viability over 20 days of encapsulation in FPA gels. Cell viability was determined by the rate of reduction of PrestoBlue® (shown as mean fluorescence per minute). FPA gels were formed using 2.66 mg.mL^{-1} FPA. Measurements were taken at day 1, day 7, day 14 and day 20 of culture. The error bars represent the standard error of the mean. Statistical analysis with use of a one-way ANOVA with Tukey post test was conducted. Significance: ** P<0.01, **** P<0.0001. Non-significant results have not been shown. Significance is displayed over the data plot and the colour corresponds to the condition in which the significance is compared to. N=2

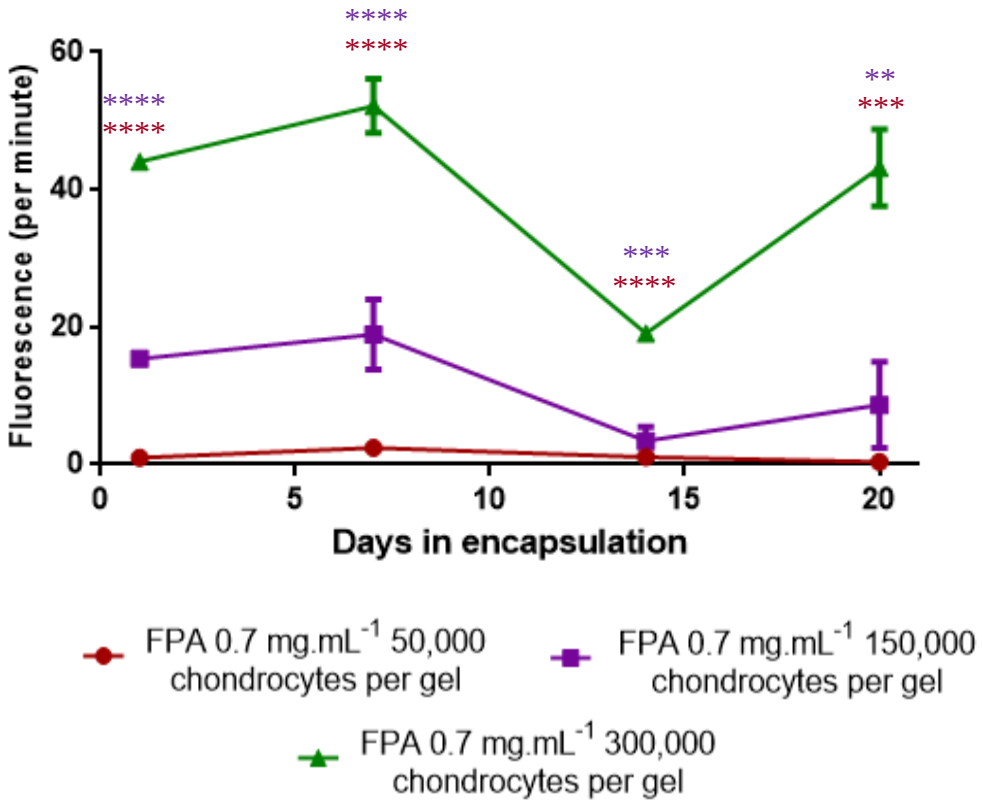

Figure 6.15 Effect of cell number on cell viability over 20 days of encapsulation in fibrinogen-FPA gels. FPA gels were formed using 0.7 mg.mL^{-1} FPA Cell viability was determined by the rate of reduction of PrestoBlue® (shown as mean fluorescence per minute). The error bars represent the standard error of the mean. Statistical analysis with use of a one-way ANOVA with Tukey post test was conducted. Significance: ** P<0.01, *** P<0.001, **** P<0.0001. Non-significant results have not been shown. Significance is displayed over the data plot and the colour corresponds to the condition in which the significance is compared to. N=2

Glycosaminoglycan content

For all fibrinogen based hydrogels, fibrin (Figure 6.16), and FPA at concentrations of 2.66 mg.mL^{-1} (Figure 6.17) and 0.7 mg.mL^{-1} (Figure 6.18), the average GAG content increased with increasing cell number. Chondrocytes encapsulated at 50,000 cells per gel synthesized less ECM in comparison to the counterpart with 300,000 encapsulated chondrocytes per gel. However, the differences in the level of GAG production between gels containing 50,000 chondrocytes and gels containing 300,000 cells were not statistically different. These results showed that the 100 µL gels used were capable of supporting chondrocyte viability at 300,000 chondrocytes/gel and indicated that the chondrocytes could dedifferentiate in the gels to produce ECM components. Therefore, in all further experiments 300,000 cells were encapsulated per gel.

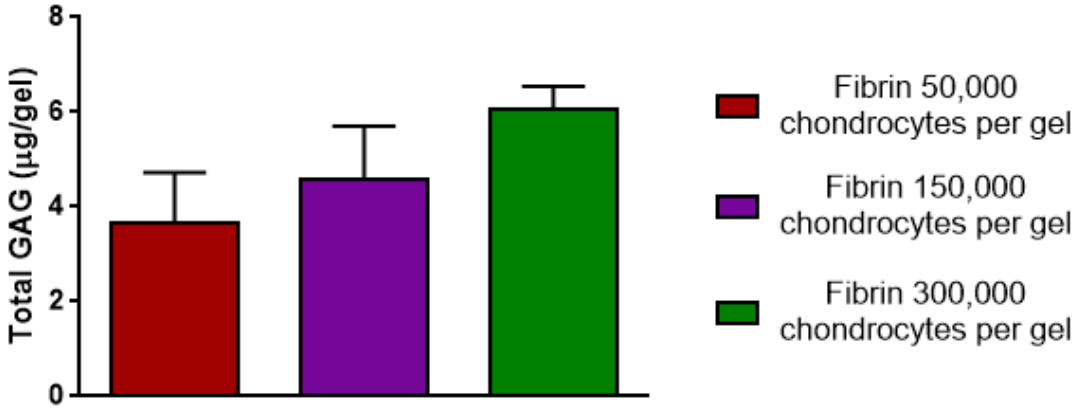

Figure 6.16 Effect of cell number of the GAG content of chondrocytes encapsulated in fibrin gels (shown as mean total GAG (µg/gel)) indicating ECM deposition after 21 days of culture in fibrin gels. The error bars represent the standard error of the mean. Statistical analysis with use of a one-way ANOVA with Tukey post-test was indicated that there was no statistical difference in the amount of GAGs produced by the higher number of chondrocytes encapsulated vs the lower number of chondrocytes. N=2

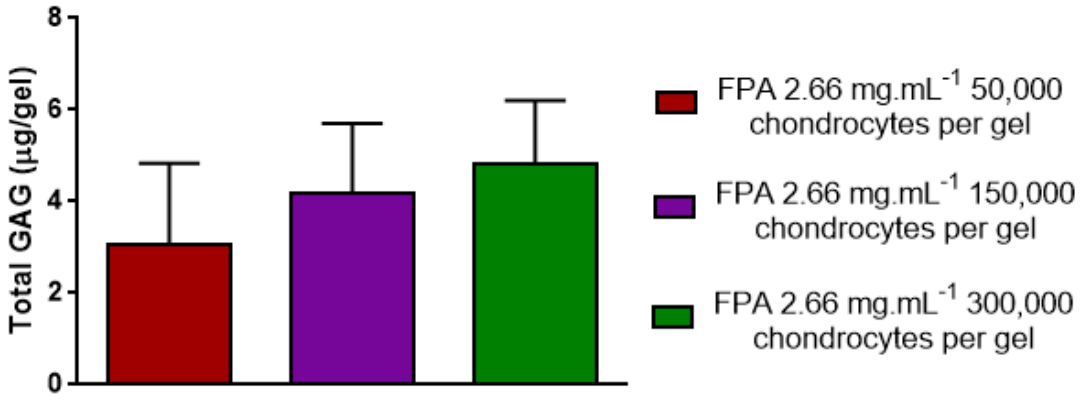

Figure 6.17 Effect of cell number on the glycosaminoglycan content of chondrocytes encapsulated in fibrinogen-FPA gels formed from 2.66 mg.mL^{-1} FPA (shown as mean total GAG (µg/gel) and cultured for 21 days. The error bars represent the standard error of the mean. Statistical analysis with use of a one-way ANOVA with Tukey post test was conducted to determine statistical significance between results N=2

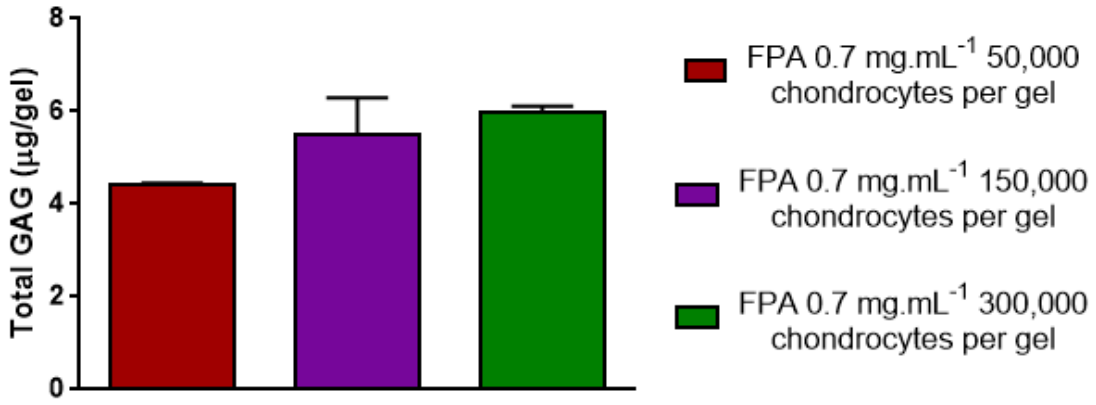

Figure 6.18 Effect of cell number on the glycosaminoglycan content of chondrocytes encapsulated in fibrinogen-FPA 0.7 mg.mL^{-1} gels (shown as mean total GAG (µg/gel) 50,000, 150,000 or 300,000 chondrocytes were encapsulated per gel and cultured for 21 days. The error bars represent the standard error of the mean. Statistical analysis was performed using of a one-way ANOVA with Tukey post test to determine statistical significance between results. N=2.

6.2.4 Calcium concentration

The initial gelation process for the fibrinogen gels took place in wells formed in PTFE blocks after which the gels were then transferred to individual wells of a 24-well plate (1 gel/well). Initial experiments used cell free gels to determine the minimum calcium concentration required for gelation. Gelation within the PTFE wells followed by transfer of the gels to 24-well plates was successful. Therefore, this method of casting fibrinogen gels was used to investigate the effect of calcium on the gelation process. The cell seeding density investigation determined that 300,000 chondrocytes encapsulated per gel was optimal for the culture conditions used and therefore was continued throughout the research.

The effect of 20 mM, 10 mM, 5 mM, 2 mM and 0 mM $CaCl_2$ on the gelation of fibrinogen by FPA was investigated. This experiment was undertaken to investigate whether the fibrinogen gelation could occur at low calcium ion concentrations which were more physiological and therefore less likely to cause toxic/adverse effects on the encapsulated cells. It was observed that all the concentrations of FPA (2.66 mg.mL^{-1}, 2 mg.mL^{-1}, 1.33 mg.mL^{-1}, and 0.7 mg.mL^{-1}) and fibrin, gelled at 20 mM, 10 mM, 5 mM, and 2 mM $CaCl_2$ concentrations. No gelation was observed in the absence of added calcium ions after 30 minutes under the conditions used. Therefore, bovine chondrocytes were encapsulated in fibrinogen-FPA gels and fibrin gels containing 2 mM $CaCl_2$ alongside gels made with 10 mM $CaCl_2$ as a comparison.

Cell viability

The results of the cell viability assay have shown that the chondrocytes have survived in all conditions for 21 days (Figure 6.20, Figure 6.19). Statistical analysis with a one-way ANOVA and Tukey post-test shows there are no significant differences in cellular activity between 2 mM and 10 mM concentrations of $CaCl_2$ present during gelation.

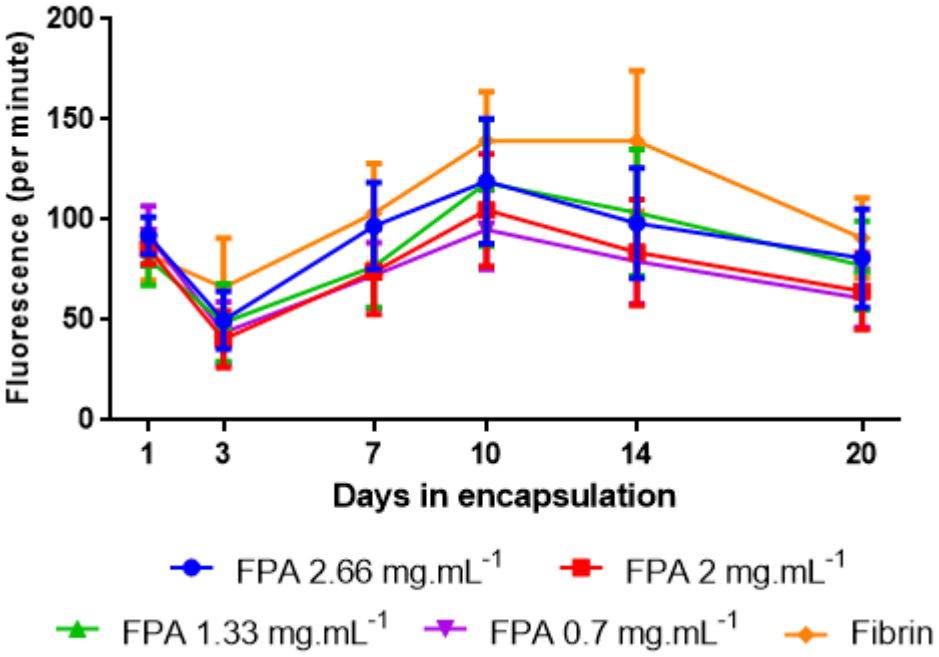

Figure 6.19 Rate of reduction of PrestoBlue® (shown as mean fluorescence per minute) of gels containing 300,000 bovine chondrocytes encapsulated for 21 days in fibrin gels and FPA-fibrinogen gels formed using FPA 2.66 mg.mL^{-1}, FPA 2 mg.mL^{-1}, FPA 1.33 mg.mL^{-1}, FPA 0.7 mg.mL^{-1} and fabricated with 2 mM $CaCl_2$buffered saline.The error bars represent the standard error of the mean. Statistical analysis with use of a one-way ANOVA with Tukey post test was conducted to detect any significant differences between 10 mM $CaCl_2$ and 2 mM $CaCl_2$ results. N=4.

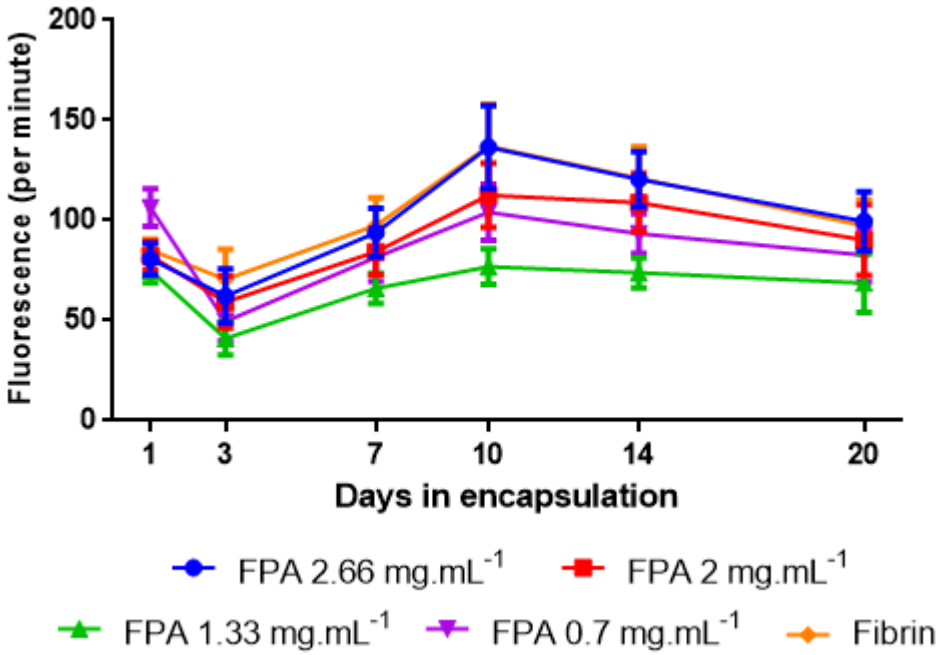

Figure 6.20 Rate of reduction of PrestoBlue® (shown as mean fluorescence per minute) of gels containing 300,000 bovine chondrocytes per gel and encapsulated for 21 days in fibrinogen gels formed using FPA 2.66 mg.mL^{-1}, FPA 2 mg.mL^{-1}, FPA 1.33 mg.mL^{-1}, FPA 0.7 mg.mL^{-1} and fibrin gels fabricated with 10 mM $CaCl_2$ buffered saline.. The error bars represent the standard error of the mean. Statistical analysis with use of a one-way ANOVA with Tukey post test was conducted between 10 mM $CaCl_2$ and 2 mM $CaCl_2$. N=4.

Glycosaminoglycan content

The GAG content suggested that the chondrocytes were synthesising ECM within all the FPA-fibrinogen and fibrin hydrogels (Figure 6.21, Figure 6.22). No statistical significant differences were found between the gels made from 2 mM and 10 mM $CaCl_2$ buffered saline. The results suggested that cellular viability was not affected by calcium concentration at 2 mM or 10 mM calcium ions. However, by lowering the concentration to physiological conditions the cells would be in a more physiological environment and are less likely to undergo apoptosis.

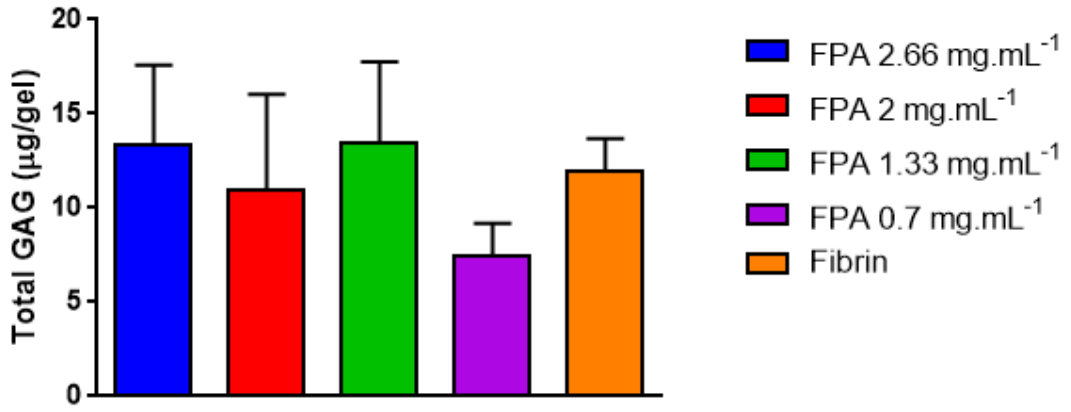

Figure 6.21 Total GAG content per gel from chondrocytes encapsulated in FPA-fibrinogen and fibrin gels fabricated with 2 mM $CaCl_2$ buffered saline. The error bars represent the standard error of the mean. Statistical analysis using one-way ANOVA with a Tukey post test was conducted to detect any statistical differences between between 10 mM $CaCl_2$ and 2 mM $CaCl_2$ results. N=4.

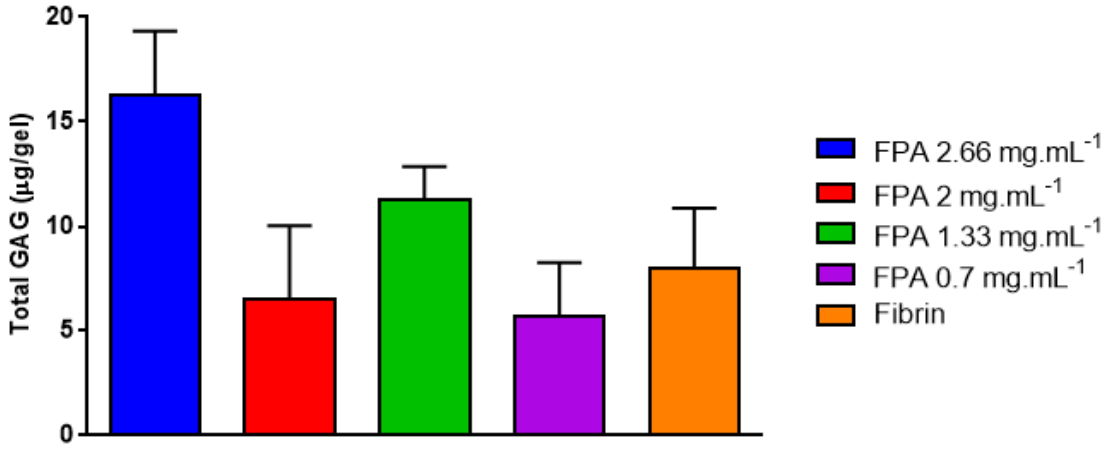

Figure 6.22 Total GAG content per gel from chondrocytes encapsulated FPA-fibrinogen and fibrin gels fabricated with 10 mM $CaCl_2$ buffered saline. The error bars represent the standard error of the mean. Statistical analysis using one-way ANOVA with a Tukey post test was conducted to detect any statistical differences between 10 mM $CaCl_2$ and 2 mM $CaCl_2$ results. N=4

Key Summary

- FPA-fibrinogen gels were optimised for chondrocyte encapsulation, the following parameters were investigated and deemed optimum for the gelation of FPA-fibrinogen gels and for cell survival and differentiation:
    - Gel fabrication in a well of a 96-well plate and transferred to a well in a 24-well plate
    - 300,000 chondrocytes encapsulated per gel
    - 2 mM $CaCl_2$ saline solution will be used to enable gelation – $CaCl_2$ was required for gelation
- These parameters were used to investigate chondrocyte survival and differentiation in greater depth (chapter 6.3) and to investigate the encapsulation bone marrow derived mesenchymal stems cells (chapter 7).

6.3 Chondrocyte encapsulated Peprostat and fibrin gels after optimisation

As seen previously in section 6.2.3 it was found that the optimum method for encapsulating the chondrocytes was to encapsulate 300,000 cells per gel with 2 mM $CaCl_2$ buffered saline. The formation of hydrogels was optimised in a 96-well culture plate and then transferred to a well in a 24-well plate (1 gel per well) using a sterile spatula. Transfer of the gels enabled 2 mL of medium to surround the chondrocyte encapsulated gels. Once the optimised method had been established the variability in chondrocyte survival was reduced.

Phase contrast images

Phase contrast images were taken at day 3 and day 21 after encapsulation with chondrocytes in fibrinogen gels formed from FPA 2.66 $mg.mL^{-1}$ (Figure 6.24), FPA 0.7 $mg.mL^{-1}$ (Figure 6.25) and fibrin gels (Figure 6.23). It can be seen from the phase contrast images that the chondrocytes remain in encapsulation in all hydrogels and do not migrate out of the gels.

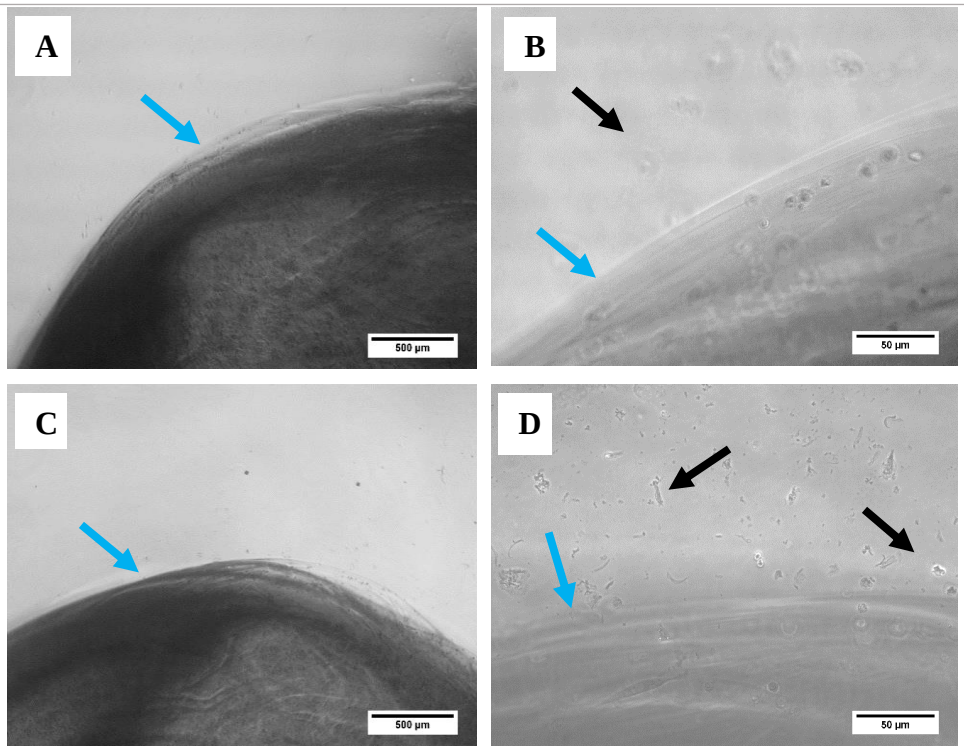

Figure 6.23 Phase contrast images of chondrocyte encapsulated fibrin gels, at day 3 after encapsulation (A and B) and day 21 after encapsulation (C and D) at x4 magnification (A and C) and x20 magnification (B and D). The blue arrows illustrate the edge of the hydrogel. Gel debris was observed by the black arrows in images B and D. Scale bars are shown on the image.

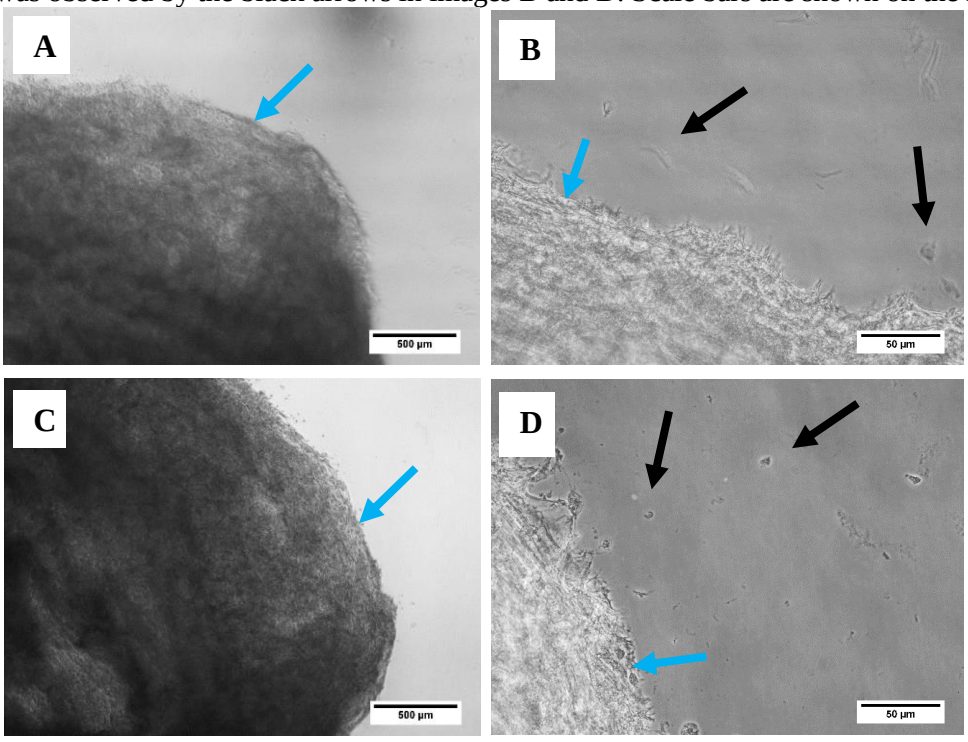

Figure 6.24 Phase contrast images of chondrocyte encapsulated FPA-fibrinogen gels at a concentration of 2.66 mg.mL^{-1} taken at day 3 after encapsulation (A and B) and day 21 after encapsulation (C and D) at x4 magnification (A and C) and x20 magnification (B and D). The edge of the hydrogel is illustrated by the blue arrow. Gel debris was observed by the black arrows in images B and D. Scale bars are shown on the image.

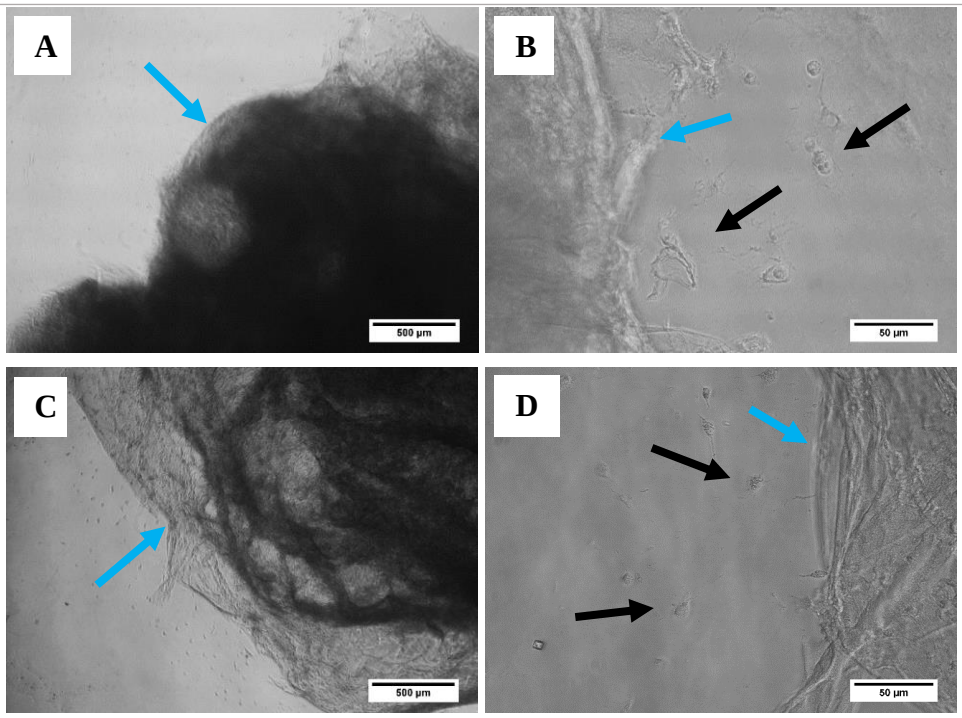

Figure 6.25 Phase contrast images of chondrocyte encapsulated FPA-fibrinogen gels at a concentration of 0.7 mg.mL^{-1} taken at day 3 after encapsulation (A and B) and day 21 after encapsulation (C and D) at x4 magnification (A and C) and x20 magnification (B and D). The edge of the hydrogel is shown by the blue arrows. Gel debris was observed by the black arrows in images B and D. Scale bars are shown on the image.

Chondrocyte viability

Resazurin reduction was observed in all FPA-fibrinogen hydrogels: FPA 2.66 mg.mL^{-1}, FPA 2 mg.mL^{-1}, FPA 1.33 mg.mL^{-1} and FPA 0.7 mg.mL^{-1} and fibrin (Figure 6.27). A peak in cell activity at day 10 was observed for chondrocyte encapsulated FPA-fibrinogen gels at all concentrations and fibrin gels after which the cellular activity decreased to day 21. Culturing chondrocytes in monolayer culture is well known to cause the cells to lose their chondrocyte phenotype which can be regained in 3D culture. Since differentiated chondrocytes tend to have a lower rate of metabolism it may be possible that the lower rate of resazurin reduction may be a reflection that the cells began synthesising ECM after this period of culture. There were no significant differences between the FPA-fibrinogen gels and fibrin gels which suggested that the FPA gels were comparable to fibrin in supporting cellular viability. Cell free gels exhibited very low results and therefore did not interfere with the assay, Figure 6.26. FPA 2.66 mg.mL^{-1}, FPA 2 mg.mL^{-1}, FPA 1.33 mg.mL^{-1} and FPA 0.7 mg.mL^{-1} and fibrin chondrocyte encapsulated gels were significantly different from their cell free counterparts at all time points, Table 6.5, this suggested chondrocyte survival. The medium was also analysed at

day 1, 3, 7, 10, 14, and 20 after encapsulation of chondrocytes, very little resazurin reduction was detected, see Figure 6.26, suggesting that the chondrocytes are not migrating from the FPA and fibrin gels and into the medium.

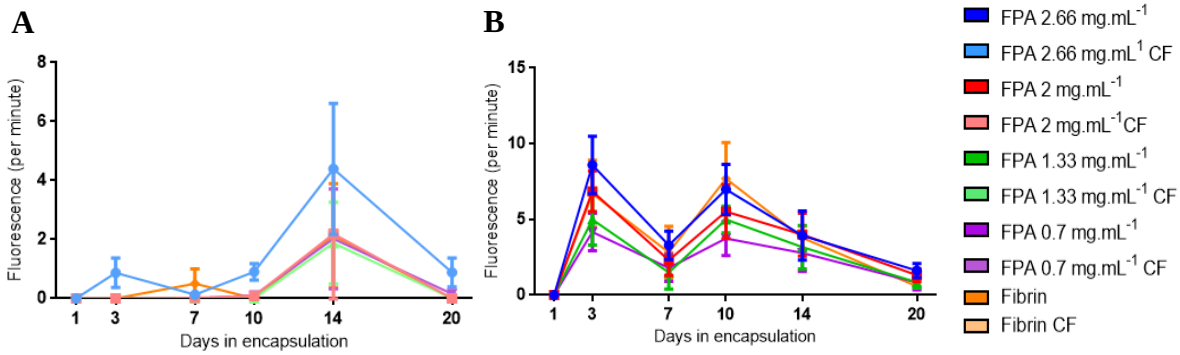

Figure 6.26 The effect of the rate of reduction of PrestoBlue® (shown as mean relative fluorescence units per minute) on cell free FPA-fibrinogen and fibrin gels (A) and the rate of reduction of resazurin on the medium samples (B) incubated with the chondrocyte encapsulated FPA-fibrinogen and fibrin gels. Measurements were taken at day 1, day 3, day 7, day, 10, day 14 and day 20 of culture. The error bars represent the standard error of the mean. Statistical analysis with use of a one-way ANOVA with Tukey post test was conducted. N=10

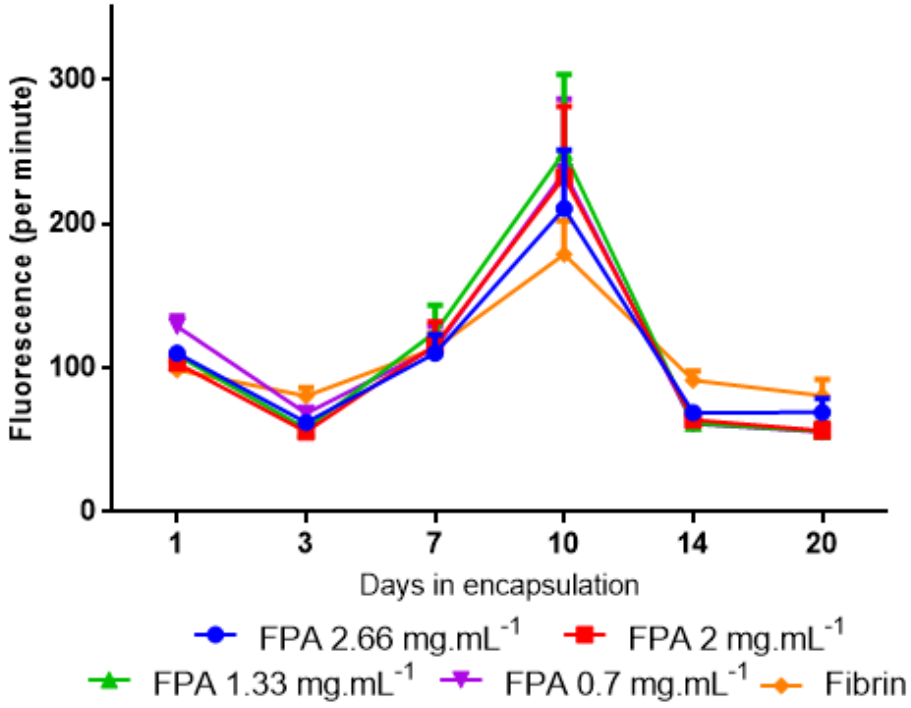

Figure 6.27 Rate of reduction of PrestoBlue® (shown as mean fluorescence per minute) indicating the cell activity of 300,000 bovine chondrocytes per gel encapsulated for 21 days in FPA 2.66 mg.mL^{-1}, FPA 2 mg.mL^{-1}, FPA 1.33 mg.mL^{-1}, FPA 0.7 mg.mL^{-1} and fibrin gels fabricated with 2 mM $CaCl_2$ buffered saline. Readings were taken at day 1, day 3, day 7, day, 10, day 14 and day 20 of culture. The error bars represent the standard error of the mean. Statistical analysis with use of a one-way ANOVA with Tukey post test was conducted. N=10

Table 6.5 Showing the statistical analysis of unpaired t-test with Welch's correction comparing FPA 2.66 mg.mL^{-1}, FPA 2 mg.mL^{-1}, FPA 1.33 mg.mL^{-1}, FPA 0.7 mg.mL^{-1}, and Fibrin, with their cell free equivalents from the cell activity results taken at day 1, 7, 14, 20 after encapsulation of chondrocytes refer to Figure 6.27 and Figure 6.32. Significance: *** P<0.001, **** P<0.0001

	Day of encapsulation	Significance
FPA 2.66 mg.mL^{-1} chondrocyte encapsulated against cell free gels	1	****
	3	****
	7	****
	10	***
	14	****
	20	***
FPA 2 mg.mL^{-1} chondrocyte encapsulated against cell free gels	1	****
	3	****
	7	****
	10	***
	14	****
	20	****
FPA 1.33 mg.mL^{-1} chondrocyte encapsulated against cell free gels	1	****
	3	****
	7	****
	10	***
	14	****
	20	****
FPA 0.7 mg.mL^{-1} chondrocyte encapsulated against cell free gels	1	****
	3	****
	7	****
	10	***
	14	****
	20	****
Fibrin chondrocyte encapsulated against cell free gels	1	****
	3	****
	7	****
	10	****
	14	****
	20	***

6.3.1 Live Dead stain

Observations from the live/dead stain suggested the majority of chondrocytes were seen to be viable, green, on days 1 and day 21 of encapsulation in fibrin gels, see Figure 6.28. Very few dead cells, red, are observed in the images. This has also been shown through the percentage of live cells in comparison to dead cells where as little as 2 % of chondrocytes were dead at day 21 of encapsulation in fibrin gels and 3 % in fibrinogen-FPA gels formed from 2.66 $mg.ml^{-1}$ FPA, refer to Figure 6.30. Similar cell viability results were observed for chondrocyte encapsulated FPA-fibrinogen gels at a concentration of 2.66 $mg.mL^{-1}$, see Figure 6.29. The number of chondrocytes increased by greater than 2-fold in fibrin and almost 2-fold in FPA 2.66 $mg.ml^{-1}$ gels from day 1 to day 21, see Figure 6.31. This result suggested cell proliferation, which is in accordance with the rise in apparent cell viability/cell activity by day 10. These results also suggested that the reduction in cell activity seen by day 21 is unlikely to be due to cell death.

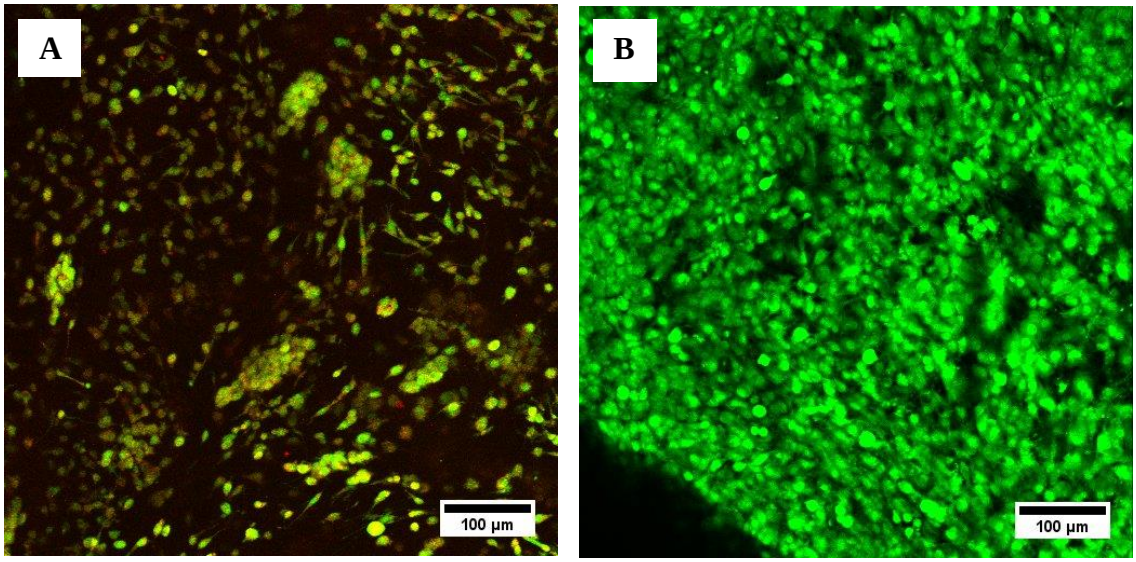

Figure 6.28 Live/Dead staining on chondrocyte encapsulated fibrin gels at day 1 (A) and day 21 (B) of encapsulation. Images taken on the confocal microscope. Scale bars shown on the image

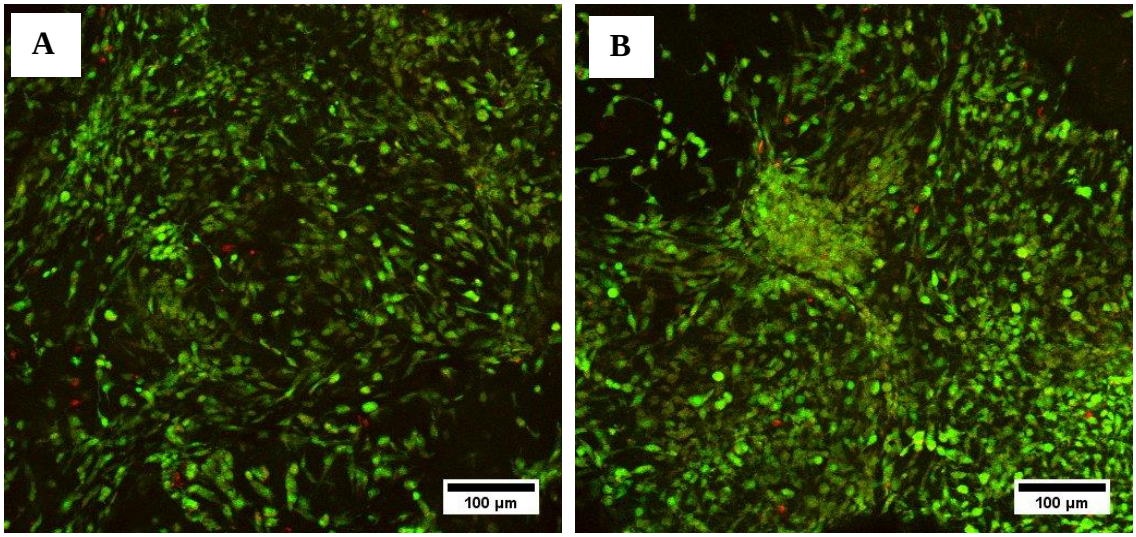

Figure 6.29 Live/Dead staining on chondrocyte encapsulated FPA-fibrinogen gels at a concentration of 2.66 mg.mL^{-1} FPA at day 1 (A) and day 21 (B) of encapsulation. Images taken on the confocal microscope. Scale bars shown on the image.

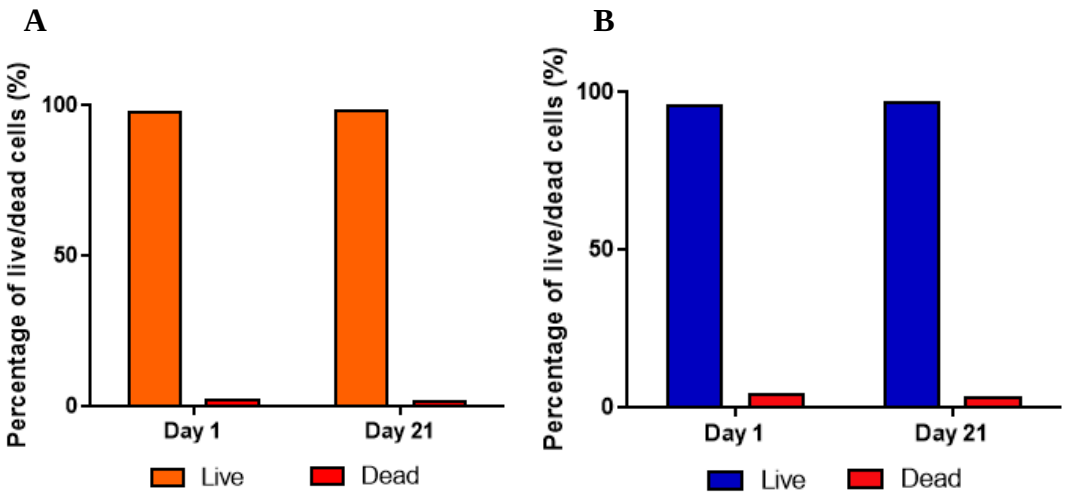

Figure 6.30 Percentage of live and dead chondrocytes at day 1 and 21 of encapsulation in (**A**) fibrin and (**B**) FPA-fibrinogen gels formed from 2.66 mg.mL^{-1} FPA. Cell number was quantified from live/dead stained images taken on the confocal microscope. N=1

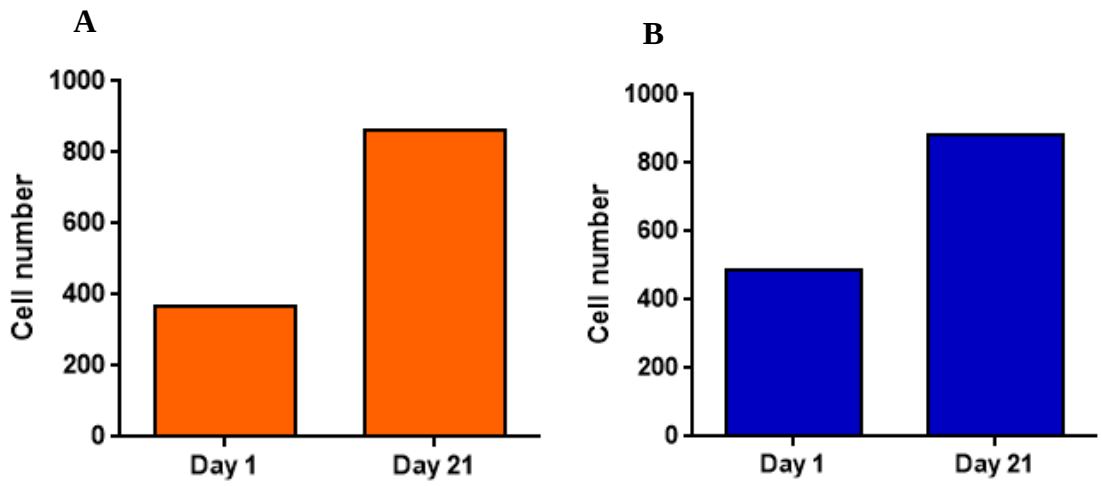

Figure 6.31 The number of live chondrocytes at day 1 and day 21 of encapsulation in (**A**) fibrin and (**B**) FPA-fibrinogen gel formed from 2.66 mg.mL^{-1} FPA. Cell number was quantified from live/dead stained images taken on the confocal microscope. N=1

6.3.2 Glycosaminoglycan content

All FPA-fibrinogen gels fabricated with FPA at concentrations of 2.66 mg.mL^{-1}, 2 mg.mL^{-1}, 1.33 mg.mL^{-1}, 0.7 mg.mL^{-1} and fibrin gels supported GAG deposition (Figure 6.33). Gels formed from FPA 2.66 mg.mL^{-1} and FPA 1.33 mg.mL^{-1} had a significantly higher ($P \leq 0.05$) mean GAG content in comparison to FPA 0.7 mg.mL^{-1}. Although gels formed from FPA 1.33 mg.mL^{-1} had a higher mean GAG content per gel in comparison to 2 mg.mL^{-1} and 0.7 mg.mL^{-1} the data is not significantly. The cell free counterparts of FPA 2.66 mg.mL^{-1}, FPA 2 mg.mL^{-1}, FPA 1.33 mg.mL^{-1}, FPA 0.7 mg.mL^{-1} and fibrin exhibited high effects from the DMB which suggested interference with the assay, Figure 6.32. No significant differences were observed between the chondrocyte encapsulated and the cell free counterparts from the FPA-fibrinogen and fibrin gels other than FPA 1.33 mg.mL^{-1}, refer to Table 6.6. Therefore, all the cell free data was subtracted from the counterparts of the chondrocyte encapsulated data.

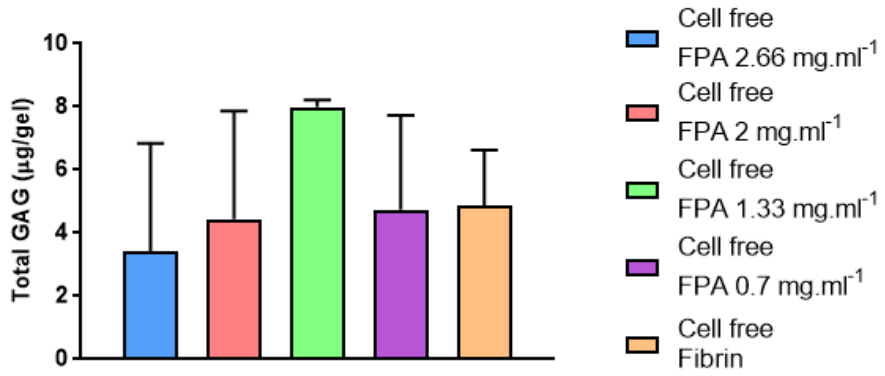

Figure 6.32 The effect of DMB (shown as Total GAG (µg/gel) on cell free FPA-fibrinogen gels and fibrin gels. The error bars represent the standard error of the mean. Statistical analysis with use of a one-way ANOVA with Tukey post test was conducted. N=6

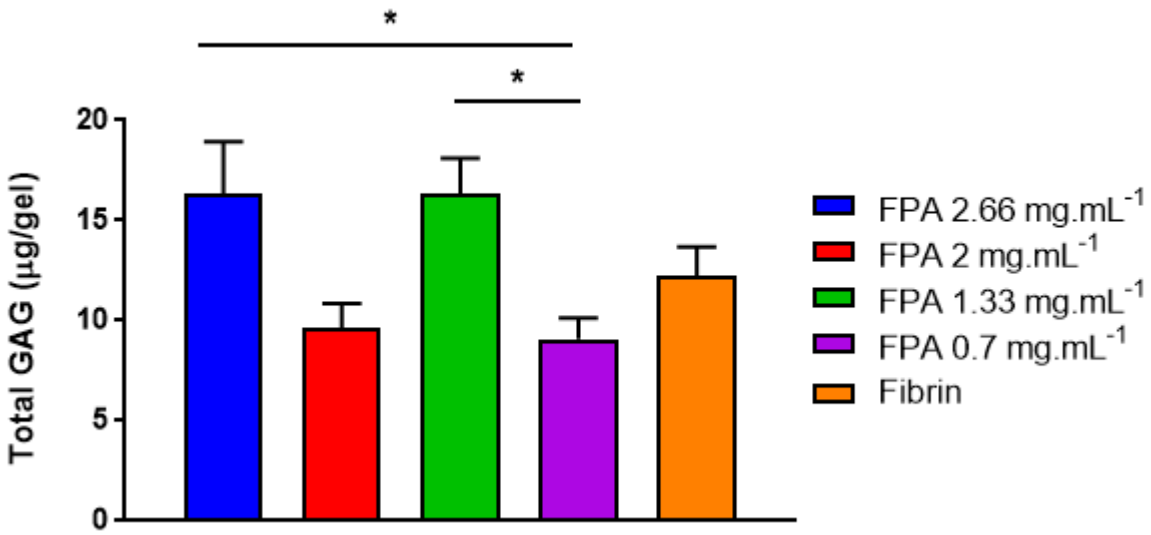

Figure 6.33 Total glycosaminoglycan content per gel of chondrocyte encapsulated FPA-fibrinogen and fibrin gels. Measurements were taken at day 21 of encapsulation. The error bars represent the standard error of the mean. Statistical analysis with use of a one-way ANOVA with Tukey post test was conducted. Significance: * P≤0.05. N=6

Table 6.6 Showing the statistical analysis of an unpaired t-test with Welch's correction comparing FPA 2.66 mg.mL^{-1}, FPA 2 mg.mL^{-1}, FPA 1.33 mg.mL^{-1}, FPA 0.7 mg.mL^{-1}, and Fibrin, with their cell free equivalents from the total GAG content measured at day 21 after encapsulation of chondrocytes refer to Figure 6.32 and Figure 6.33. Significance: ** P<0.01, ns is no significant differences

	Significance
FPA 2.66 mg.mL^{-1}	ns
FPA 2 mg.mL^{-1}	ns
FPA 1.33 mg.mL^{-1}	**
FPA 0.7 mg.mL^{-1}	ns
Fibrin	ns

6.3.3 Histological analysis

H&E staining in cell free gels (Figure 6.35) showed that the hydrogel structure stained, but this staining was less than observed in chondrocyte encapsulated hydrogels (Figure 6.36). Haematoxylin binds to chromatin and stains it purple whereas Eosin binds to ECM due to being an acidic dye and the stains ECM pink. It can be seen from the cell free images that the hydrogels stained pink due to the staining of fibrinogen and fibrin. From the H&E sections it is evident that the FPA-fibrinogen gels appeared more open-pored in comparison to the fibrin gels. Chondrocytes were seen evenly dispersed throughout the FPA-fibrinogen gels and fibrin gels (Figure 6.36). Due to the background staining from the hydrogel it is difficult to determine ECM formation. The cells appeared to be situated within the pores of the hydrogels individually and have maintained the spherical-like morphology, which is also observed in native articular cartilage Figure 6.34. It can also be observed that a dense cell layer had formed around the surface of the hydrogels surrounded by ECM synthesis, the chondrocytes have a flattened morphology similar to that of chondrocytes in the superficial zone of the articular cartilage.

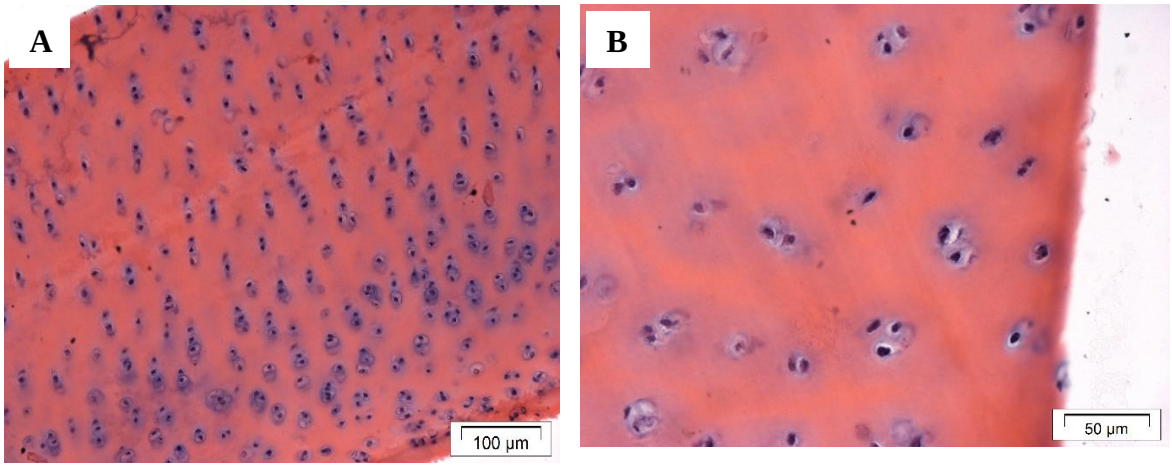

Figure 6.34 Histological H&E stained sections from native bovine articular cartilage from the metacarpophalangeal joint (A and B). Images taken at a magnification of x20 (A) and x40 (B). Scale bar shown on the image.

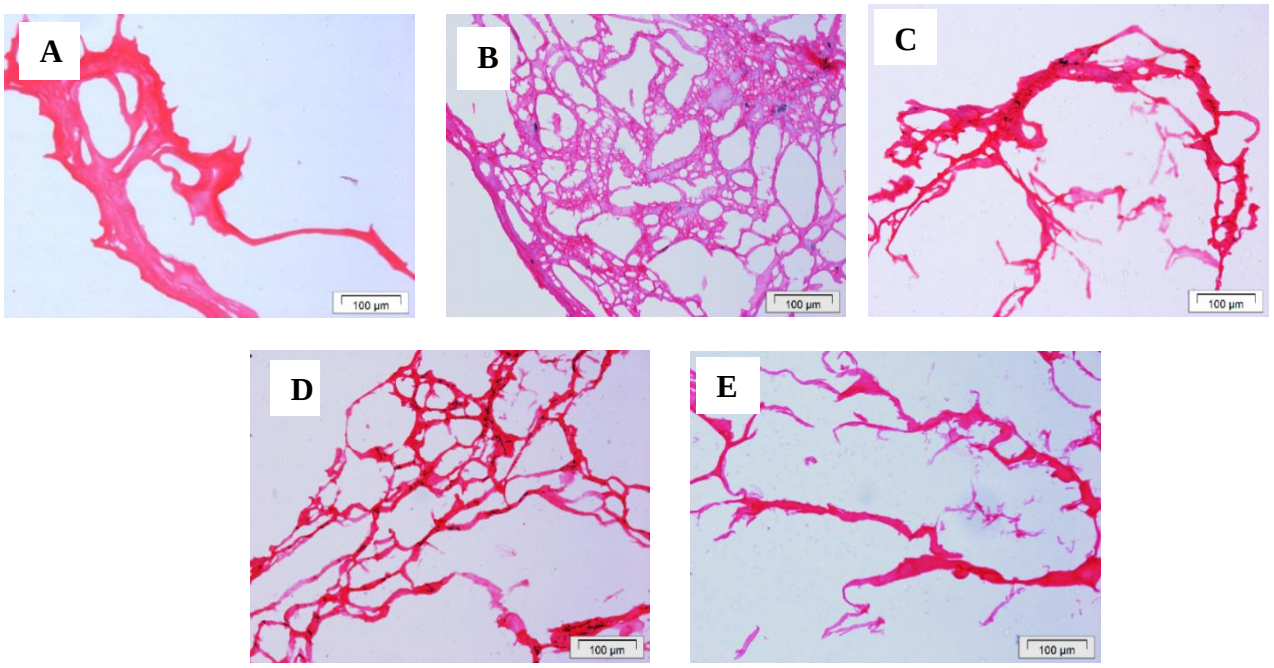

Figure 6.35 Histological H&E stained sections from cell free (A) fibrin, and FPA-fibrinogen gels formed from (B) 2.66 mg.ml^{-1} FPA, (C) 2 mg.ml^{-1} FPA, (D) 1.33 mg.ml^{-1} FPA and (E) 0.7 mg.ml^{-1} FPA. Images were taken at a magnification of x20 and scale bars are displayed on the image.

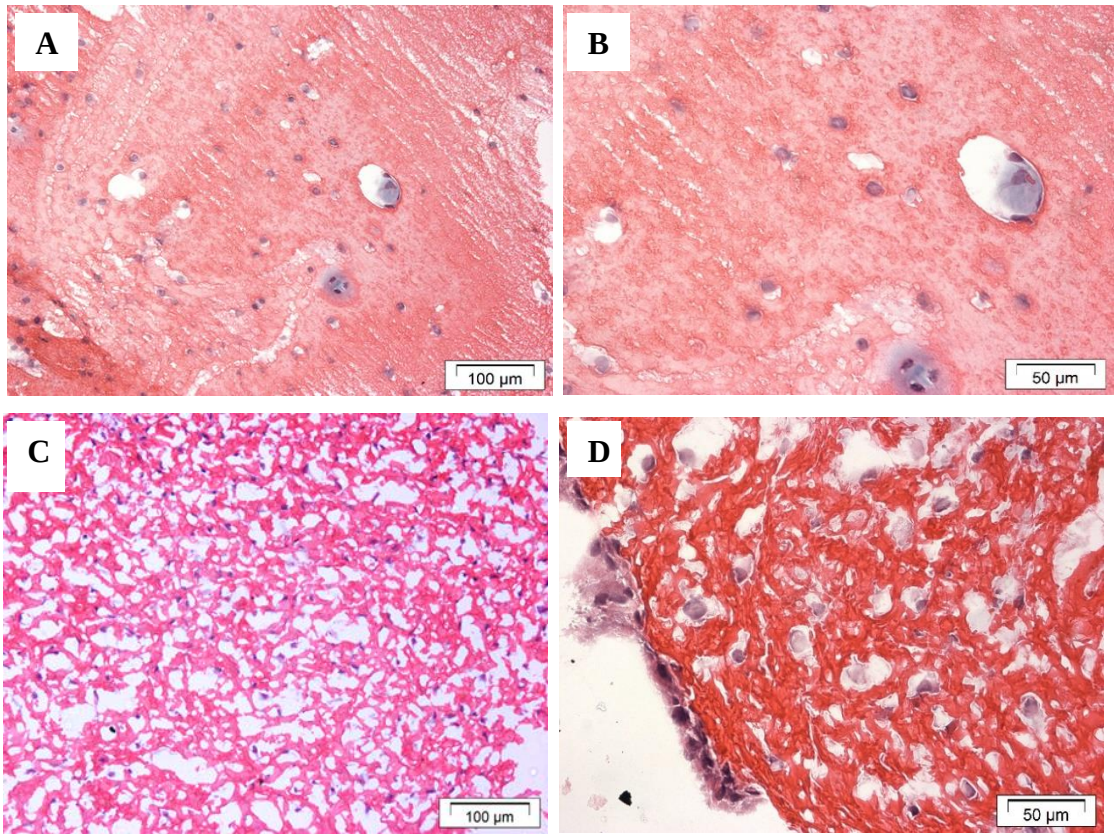

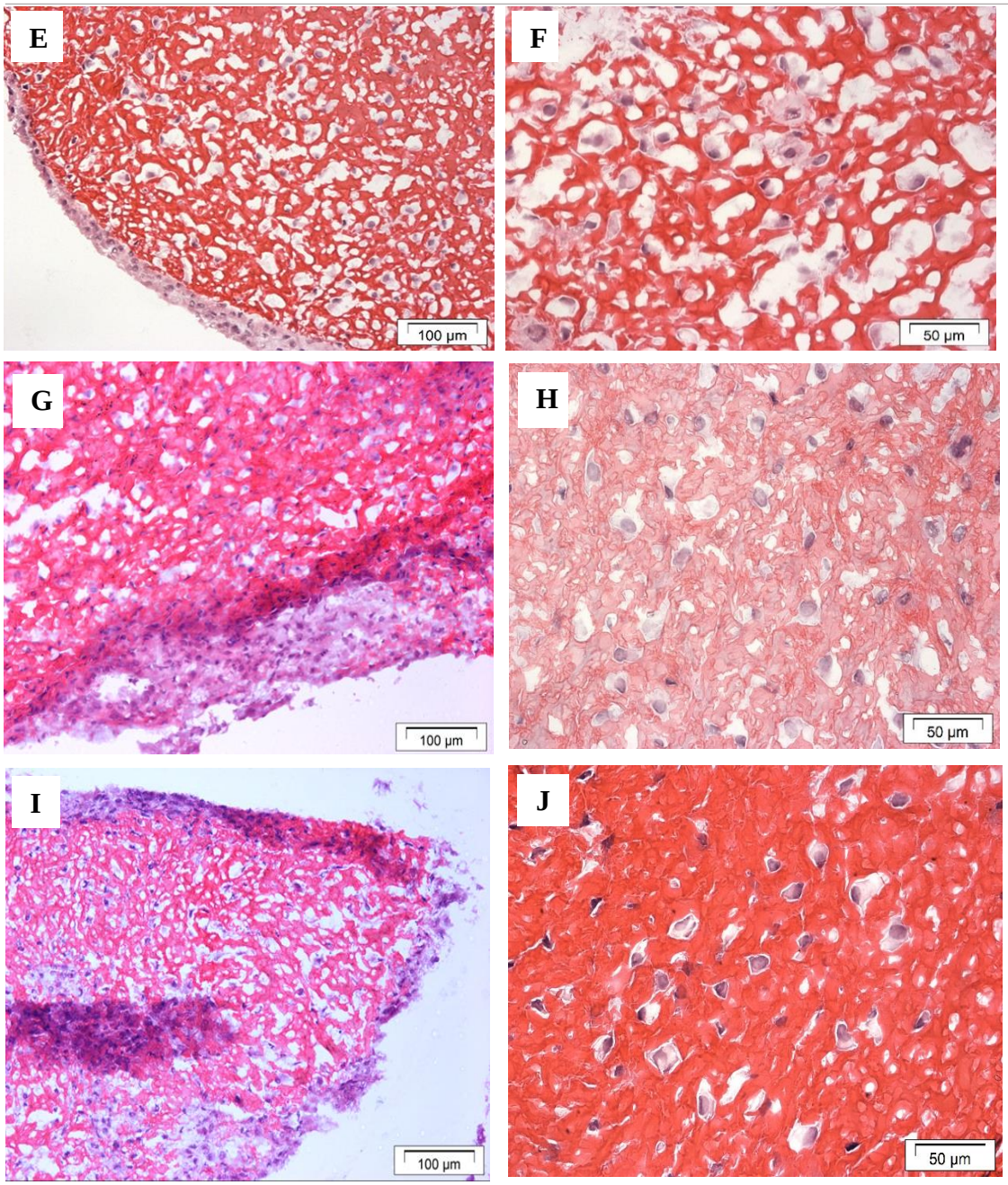

Figure 6.36 Histological H&E stained sections from chondrocyte encapsulated for 21 days (A, B) fibrin and FPA-fibrinogen gels formed from (C, D) 2.66 mg.ml^{-1} FPA, (E, F) 2 mg.ml^{-1} FPA, (G, H) 1.33 mg.ml^{-1} FPA and (I, J) 0.7 mg.ml^{-1} FPA. Images taken at a magnification of x20 (A, C, E, G, and I) and x40 (B, D, F, H and J). Scale bars shown on the image.

Toluidine blue stain was used for the detection of proteoglycans, in purple, and nucleic acids, in blue. Chondrocyte encapsulated FPA-fibrinogen and fibrin gels were stained at day 21 of culture as described in section 4.13. A high background due to the staining of the cell free hydrogels was observed (Figure 6.37). However, chondrocyte encapsulated FPA-fibrinogen and fibrin gels contain purple staining suggesting proteoglycans were deposited by the encapsulated chondrocytes. Proteoglycan formation suggests that the

chondrocytes are synthesising ECM over the 21 days in culture. A dense purple stained area is observed in sections of chondrocytes encapsulated in FPA-fibrinogen gels formed with 2.66 mg.mL^{-1} FPA (Figure 6.38, C, D) and 1.33 mg.mL^{-1} FPA (Figure 6.38, G, H) which is consistent with the higher total GAG content in comparison to fibrin, and FPA-fibrinogen gels formed with 2 mg.mL^{-1} FPA and 0.7 mg.mL^{-1} FPA (refer to Figure 6.38). FPA-fibrinogen gels formed from 2.66 mg.mL^{-1} appeared to have areas of dense proteoglycan formation surrounding chondrocytes. The histological staining of the hydrogels was consistent with the GAG content (Figure 6.33) suggesting that the chondrocytes are synthesising ECM within the FPA-fibrinogen gels and fibrin gels.

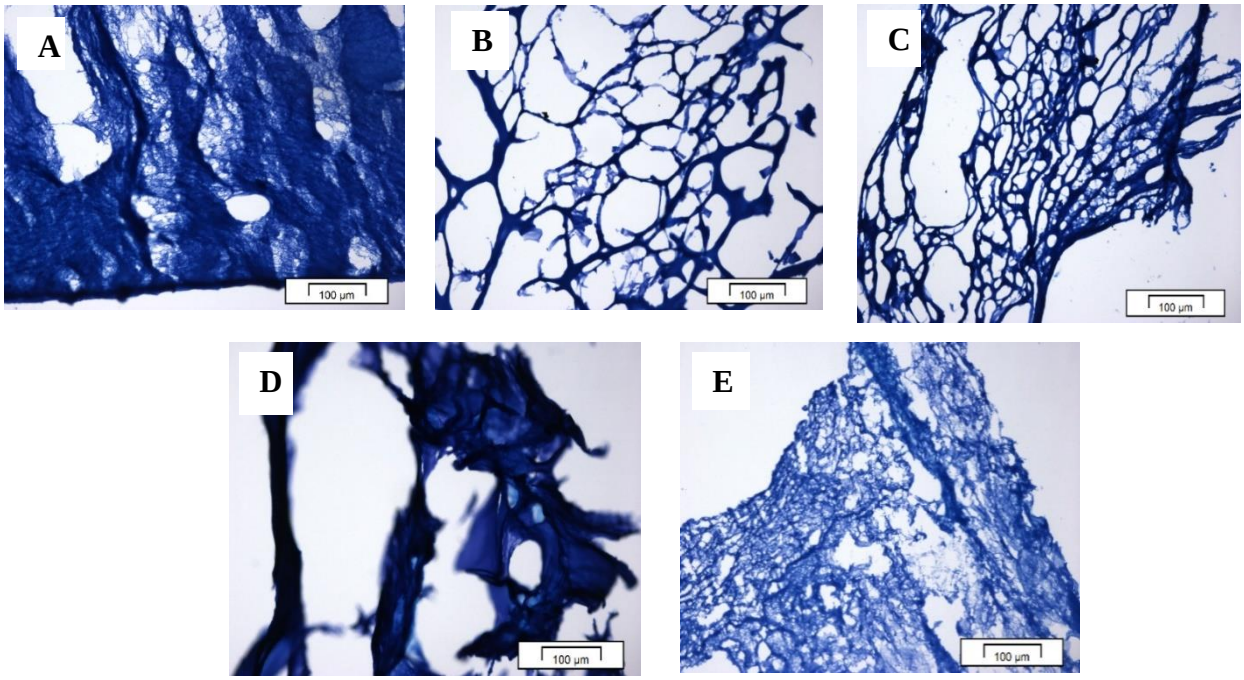

Figure 6.37 Histological Toluidine blue stained sections from cell free (A) fibrin and FPA-fibrinogen gels formed from (B) 2.66 mg.ml^{-1} FPA, (C) 2 mg.ml^{-1} FPA, (D) 1.33 mg.ml^{-1} and (E) 0.7 mg.ml^{-1} FPA. Images were taken at a magnification of x20 and scale bars are shown on the image.

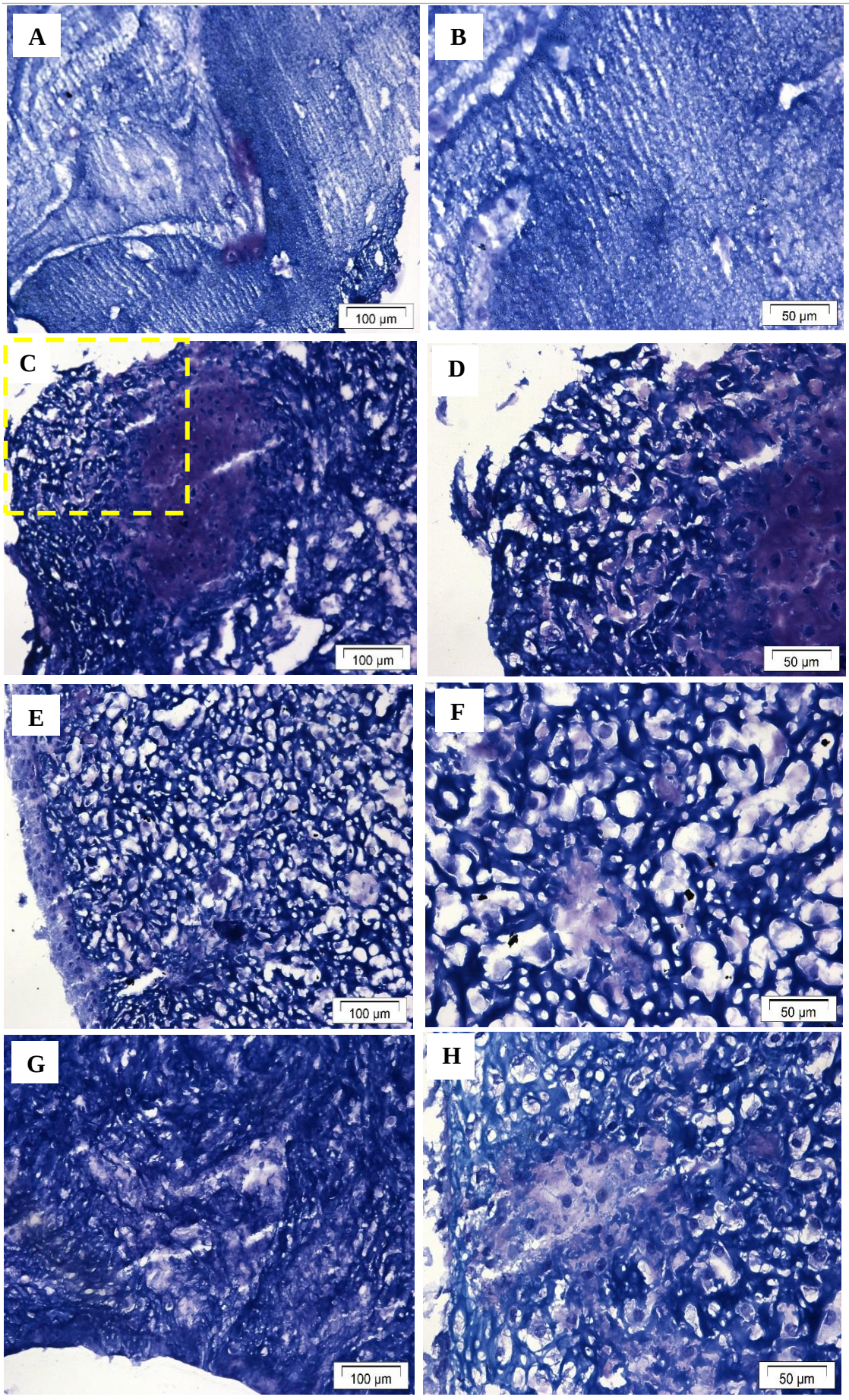
A
100 µm
B
50 µm
C
100 µm
D
50 µm
E
100 µm
F
50 µm
G
100 µm
H
50 µm

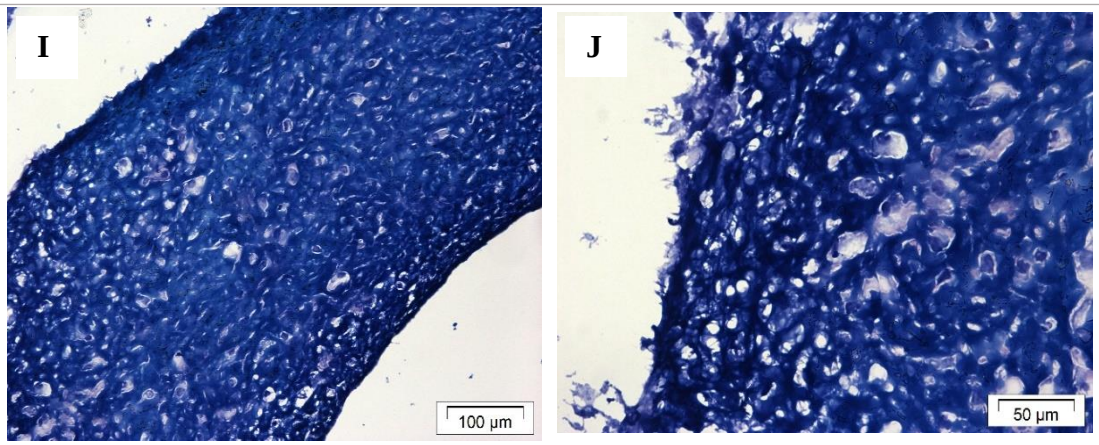

Figure 6.38 Histological Toluidine blue stained sections from chondrocytes encapsulated for 21 days in (A, B) fibrin and FPA-fibrinogen gels formed from (C, D) 2.66 mg.ml^{-1} FPA, (E, F) 2 mg.ml^{-1} FPA, (G, H) 1.33 mg.ml^{-1} and (I, J) 0.7 mg.ml^{-1} FPA. Images were taken at a magnification of x20 (A, C, E, G, and I) and x40 (B, D, F, H, and J). Magnification windows are shown on in yellow Scale bars are shown on the image.

The histological stained images were analysed for pore diameter and the average number of pores per image using imagej software. Pore diameter has been shown as a box plot with the minimum, maximum and median pore diameters and the interquartile range displayed. The analysis suggested that the chondrocyte encapsulated gels (Figure 6.39, B, D) had at least 5-fold more pores with a smaller pore diameter in comparison to the cell free counterparts (Figure 6.39, A, C). This suggested that the chondrocytes were occupying the pores and producing ECM within the pores. All chondrocyte encapsulated FPA-fibrinogen gels had virtually the same number and diameter of pores, however fibrin gels had larger pores but very few in comparison to the FPA-fibrinogen gels. This suggested that fibrin had a more compact and less porous structure in comparison to the FPA-fibrinogen gels.

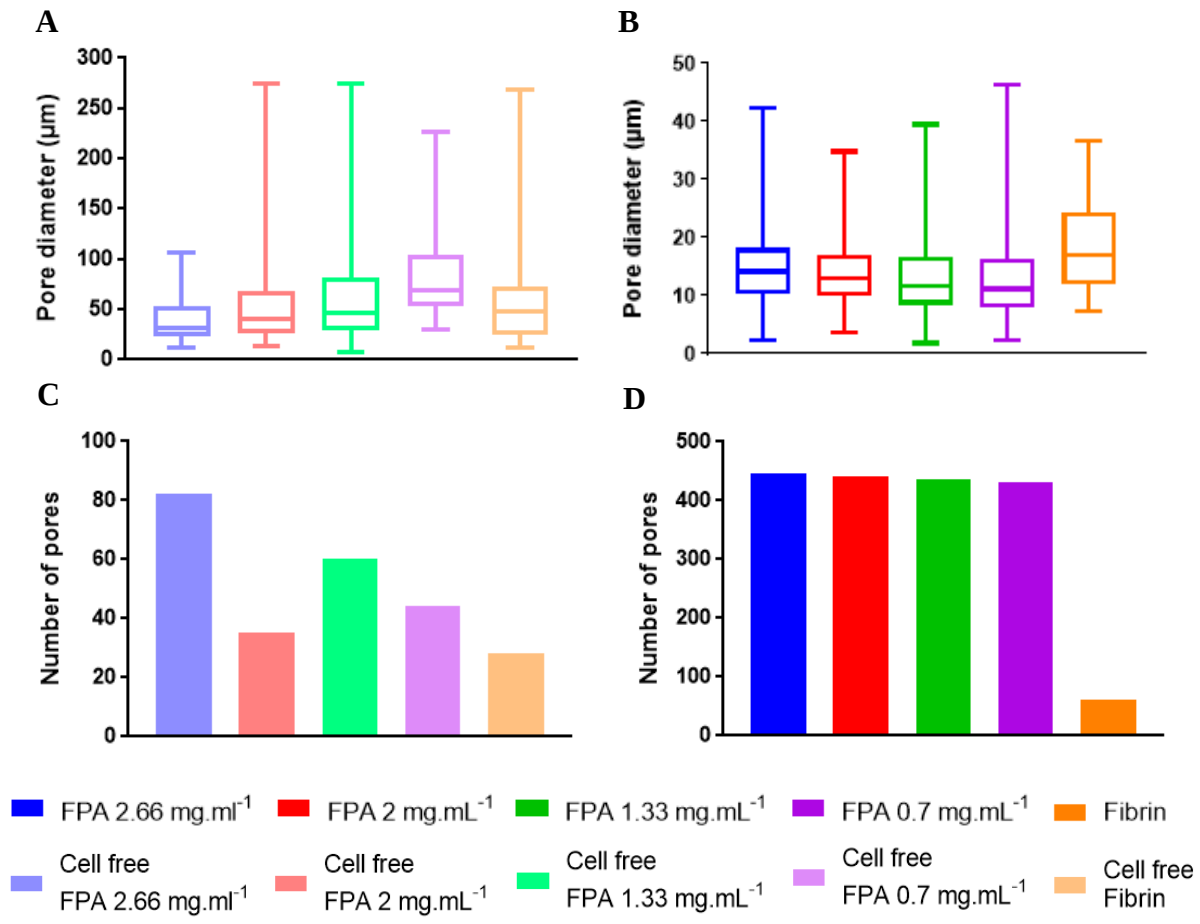

Figure 6.39 Measurements of pore diameter (A, B) and number of pores (C, D) from analysed from the histological staining of cell free (A, C) and chondrocyte encapsulated (B, D) fibrin and FPA-fibrinogen gels formed from 2.66 mg.mL^{-1}, 2 mg.mL^{-1}, 1.33 mg.mL^{-1}, and 0.7 mg.mL^{-1} FPA. Pore diameter (A, B) is shown as a box plot indicating the minimum, median and maximum pore diameter and the interquartile range.

The H&E and Toluidine blue stained chondrocyte encapsulated hydrogels have shown that the chondrocytes are evenly distributed throughout the gels and ECM formation can be observed in the centre and on the edges of the gels. Suggesting that the chondrocytes remained viable and were differentiating and forming ECM within the gels. Analysis of the stained images showed that the FPA-fibrinogen gels had a porous structure in comparison to fibrin and suggested that ECM formation had filled the pores of the gel.

In summary, the analysis of cell activity, GAG formation and proteoglycan staining it was observed that FPA-fibrinogen gels at a concentration of 2.66 mg.mL^{-1} was the optimal choice for chondrocyte encapsulation in comparison to FPA-fibrinogen gels at concentrations of 2 mg.mL^{-1}, 1.33 mg.mL^{-1}, and 0.7 mg.mL^{-1}. The structure and porosity of the gels were very similar and therefore FPA 2.66 mg.mL^{-1} with fibrinogen was chosen as optimal due to the formation of a larger gel compared to those formed with lower concentrations of FPA. This meant that the FPA-fibrinogen gel using 2.66 mg.mL^{-1} FPA was easier to handle and to observe any changes in gel size throughout culture. Therefore, further investigations for chondrocyte encapsulation was continued with FPA-fibrinogen gels formed using 2.66 mg.mL^{-1} FPA.

6.3.4 RNA extraction

Investigations into chondrogenic gene expression and whether the peak in cell activity at day 10 of encapsulation is due to de-differentiation (see section 6.3.2), RNA was extracted from the chondrocyte encapsulated FPA-fibrinogen (2.66 mg.mL^{-1} FPA) and fibrin gels. Two methods for RNA extraction were investigated: TRIzol reagent and Isolate II RNA mini kit. The data on RNA extraction is preliminary.

After extraction with TRIzol reagent, the RNA concentration at day 1 of chondrocyte encapsulation was very high for both FPA-fibrinogen gels formed from 2.66 mg.mL^{-1} FPA and fibrin, 1272 ng.mL^{-1} and 305 ng.mL^{-1} respectively. However, the first peak in the RNA NanoDrop as shown by the black arrows in Figure 6.40 and Figure 6.41 suggested contamination of the RNA pellet. Due to the phenol-based extraction method used, phenol contamination was suspected and this can cause a false high RNA concentration. Therefore, the RNA samples were passed through an RNA gel to determine if any RNA bands could be observed. Observations suggested that no RNA bands were found and therefore no RNA was present in the samples. TRIzol reagent extraction method was investigated again with a series of washes to remove the phenol contamination. A purer RNA sample was observed but the RNA concentration of the solution was very low at 2.1 ng.mL^{-1} at day 1 of chondrocyte encapsulation, (Table 6.7). Therefore, this method of extraction was abandoned and a different RNA extraction method was investigated.

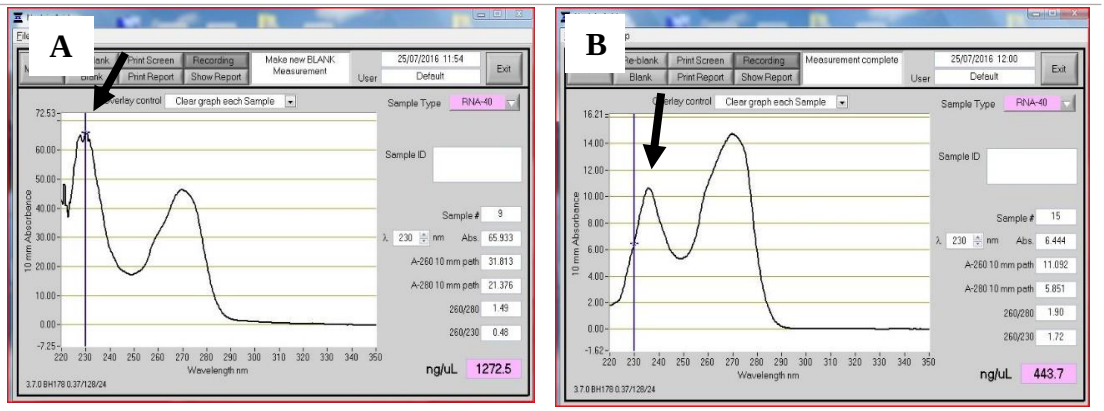

Figure 6.40 RNA extraction using TRIzol reagent of 300,000 bovine chondrocytes per gel encapsulated in 34 mg.mL^{-1} fibrin for (**A**) 1 day and (**B**) 7 days. The first peak in each graph, as shown by the arrow, is indicative of phenol contamination of the samples.

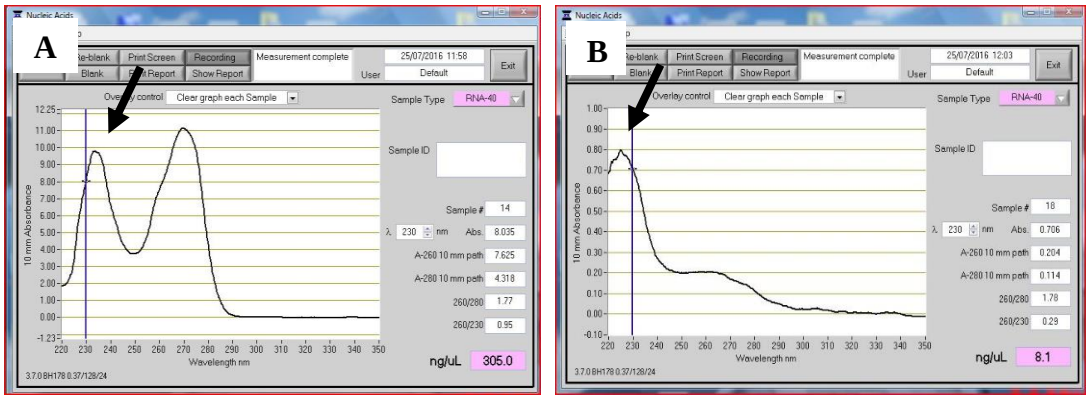

Figure 6.41 RNA extraction using TRIzol reagent of 300,000 bovine chondrocytes per gel encapsulated in 2.66 mg.mL^{-1} FPA for (**A**) 1 day and (**B**) 7 days. The first peak on each graph, as shown on the figure by arrows, is indicative of phenol contamination.

Table 6.7 300,000 chondrocytes encapsulated for 1 or 7 days in FPA 2.66 mg.mL^{-1}. RNA extraction was completed with TRIzol reagent and the RNA pellet washed. Showing the RNA concentration carried out on the NanoDrop and the 260/280 ratio reading.

FPA 2.66 mg.mL^{-1} hydrogel	RNA concentration (ng.µL^{-1})	260/280
BAC day 1	2.1	2.44
BAC day 7	1.4	1.68

To obtain higher concentrations of RNA 3 gels per extraction was investigated with another isolation method. An Isolate II RNA mini extraction kit was used, this method does not contain phenol and therefore should reduce the contamination of the pellets. The method increased the purity of the RNA samples and RNA was obtained as observed on the NanoDrop (Table 6.8). Three gels were required per RNA extraction to obtain a concentration of 77.3 $ng.mL^{-1}$ in comparison to one gel per extraction at 11.9 $ng.mL^{-1}$. Therefore, three gels per RNA extraction was required to obtain enough RNA to carry out quantitative reverse transcriptase polymerase chain reaction (qRT-PCR).

Table 6.8 RNA extraction using Isolate II RNA mini kit on 300,000 cells per gel encapsulated in FPA 2.66 $mg.mL^{-1}$. Showing the RNA concentration ($ng.\mu L^{-1}$) and the 260/280 ratio.

FPA 2.66 $mg.mL^{-1}$ hydrogel encapsulated with BAC	RNA concentration ($ng.\mu L^{-1}$)	260/280
1 gel per extraction	11.9	1.93
3 gels per extraction	77.3	1.5

After optimisation of the RNA extraction process from FPA 2.66 $mg.mL^{-1}$ and fibrin gels, RNA was extracted at day 0, day 10 and day 21 after 300,000 chondrocytes encapsulated per FPA-fibrinogen and fibrin gels. Three gels were used for one RNA extraction sample. RNA extraction at day 0 of encapsulation showed high RNA concentrations of 42.8 $ng.mL^{-1}$ for FPA-fibrinogen gels and 38.2 $ng.mL^{-1}$ fibrin gels. The results also suggested no contamination was found in the RNA pellets. However, cell activity of day 10 and day 21 of chondrocyte encapsulation suggested that the chondrocytes had died. RNA was extracted and very low concentrations of below 4 $ng.mL^{-1}$ was observed for both FPA-fibrinogen gels and fibrin gels (Table 6.9 and Table 6.10). There was also evidence of contamination suggested by the first peak of Figure 6.42.

Table 6.9 RNA extraction using Isolate II RNA mini kit on 300,000 chondrocytes encapsulated in FPA 2.66 mg.mL^{-1} gels, 3 gels per extraction. RNA concentration measured at day 0, day 10 and day 21.

FPA gel	RNA concentration (ng.µL^{-1})	260/ 280	RNA concentration (ng.µL^{-1})	260/ 280	RNA concentration (ng.µL^{-1})	260/ 280
Day 0	41.1	2.03	42.6	2.06	43.3	2.02
Day 10	0.09	4.02	1.59	2.77	0.253	1.6
Day 21	0.5	0.95	0.2	0.64	0.8	1.96

Table 6.10 RNA extraction using Isolate II RNA mini kit on 300,000 chondrocytes encapsulated in fibrin gels, 3 gels per extraction. RNA concentration measured at day 0, day 10 and day 21.

Fibrin gel	RNA concentration (ng.µL^{-1})	260/ 280	RNA concentration (ng.µL^{-1})	260/ 280	RNA concentration (ng.µL^{-1})	260/ 280
Day 0	36.7	2.05	40.6	1.99	37.2	1.97
Day 10	3.89	1.89	0.3	2.15	7.93	2.44
Day 21	0.4	1.32	0.1	0.16	0.4	0.48

A B

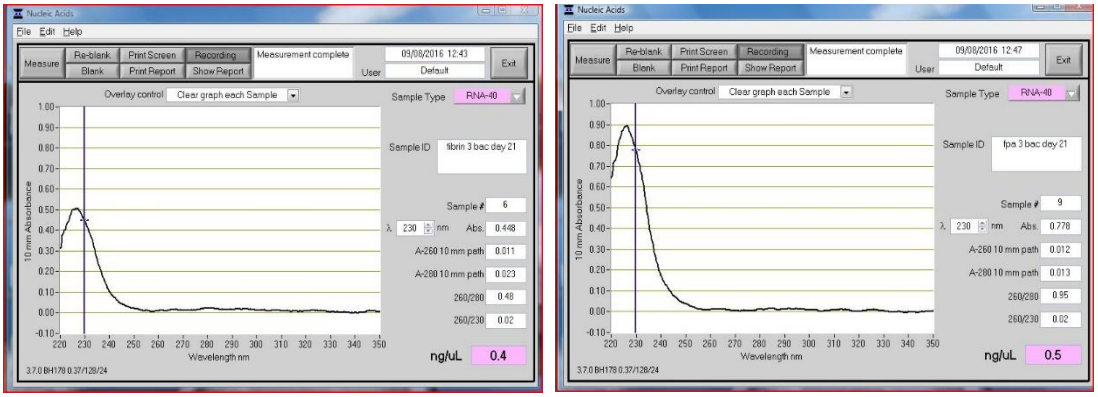

Figure 6.42 graphs showing the RNA extraction at day 21 of 300,000 chondrocytes encapsulated in fibrin (**A**) gels and FPA 2.66 mg.mL^{-1} (**B**) gels, 3 gels per extraction. The graphs show phenol contamination in the samples and no RNA.

The method to extract RNA was optimised by using the Isolate II mini kit with the chondrocyte encapsulated FPA-fibrinogen and fibrin gels. However, due to low RNA yields from day 10 and day 21, qRT-PCR could not be carried out in this investigation, therefore gene expression could not be determined.

Key Summary

- Chondrocytes remained in encapsulation throughout the 21 day culture period. The FPA-fibrinogen and fibrin gels did not visibly degrade during the culture period.
- Chondrocytes encapsulated in FPA-fibrinogen and fibrin gels were metabolically active and proliferated within the gels. ECM deposition was observed through total GAG content per gel, Toluidine blue and H&E staining.
- All concentrations of FPA and fibrin used to form gels performed similarly in terms of cell activity. FPA-fibrinogen gels formed from FPA 2.66 $mg.mL^{-1}$ and FPA 1.33 $mg.mL^{-1}$ had statistically significant higher mean GAG content in comparison to FPA 0.7 $mg.mL^{-1}$. All FPA concentrations total GAG content was comparable to fibrin.
- RNA extraction from FPA-fibrinogen and fibrin gels required more optimisation before gene expression could be analysed.
- FPA-fibrinogen and fibrin gels had similar average pore diameters. Fibrin had 10-fold fewer pores in comparison to FPA-fibrinogen gels. Therefore, the FPA-fibrinogen gels had a more open porous structure in comparison to fibrin.

6.4 Agarose gels

Agarose 4 % gels were used as a reference material to the fibrinogen-FPA gels. It is also known that chondrocytes survive and differentiate when encapsulated in 4 % agarose gels. Chondrocytes were encapsulated at 300,000 cells per gel in 100 µL gels.

Cell activity

Cell viability was measured by the reduction of resazurin to resarufin. Very little dye reduction was observed in cell free gels showing that 4 % agarose did not interfere with the assay, causing no binding or reduction of resazurin (Figure 6.43). Cell activity in chondrocyte encapsulated gels showed that the cells have survived over the 21 day period of encapsulation, (Figure 6.43). Interestingly, in common with chondrocytes encapsulated in fibrinogen-FPA and fibrin gels, a peak of cell activity was also seen at day 10 with the chondrocyte encapsulated 4 % agarose gels.

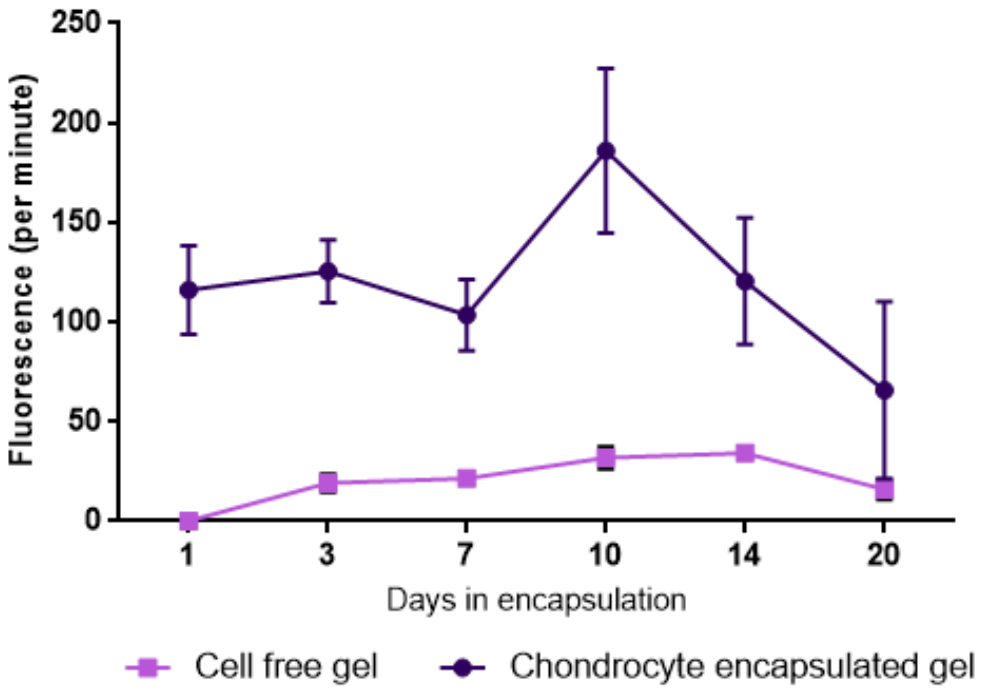

Figure 6.43 The effect of the rate of reduction of PrestoBlue on cell free 4 % agarose gels and the cell viability of 300,000 chondrocytes encapsulated in 4 % agarose gels. This was measured by the rate of reduction of PrestoBlue® over 21 days. The error bars represent the standard error of the mean. N=6.

Glycosaminoglycan content

Cell free gels did not interfere with the 1,9-dimethylmethylene blue assay to measure GAG (Figure 6.44). Figure 6.44 showed the GAG content of chondrocyte encapsulated in 4 % agarose gels. The results showed that the chondrocytes were synthesising ECM within the gels. Also, GAG levels in agarose were similar to those of the chondrocyte encapsulated fibrin and novel cross-linked fibrinogen gels, see section 6.3.

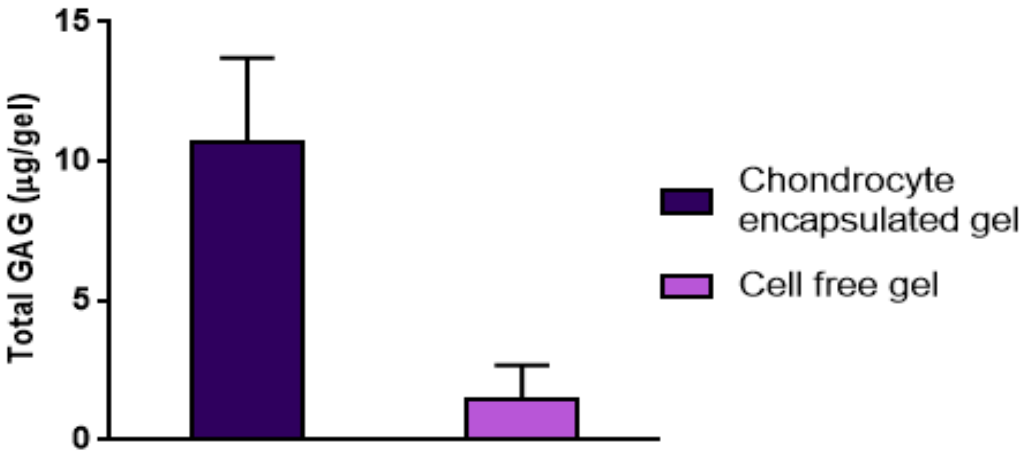

Figure 6.44 The effect of cell free 4 % agarose gel on the DMB assay and the total GAG content (shown as Total GAG (µg/gel)) of chondrocyte encapsulated 4 % agarose gels, measurements were taken at day 21 of encapsulation. The error bars represent the standard error of the mean. N=6

Histological staining

Histological staining provided further evidence for ECM deposition in the agarose gels. The results of the staining sections, with H&E staining (Figure 6.45) and Toluidine blue staining (Figure 6.46). Very little staining was observed for cell free gels stained with H&E and Toluidine blue and therefore have not been shown. H&E staining of the agarose encapsulated chondrocytes showed a blue/black staining of the cell nuclei and light purple of ECM. This staining was observed due to the complete lack of background staining from the cell free gel. The chondrocytes have a spherical morphology and are more disorganised throughout the 4 % agarose gel. Figure 6.46 shows sections of the 21 day chondrocyte encapsulated agarose gels showed a deep purple and blue colour. The metachromic shift in the dye colour is characteristic of the dye binding to proteoglycan components and was suggestive of proteoglycan formation in the gels.

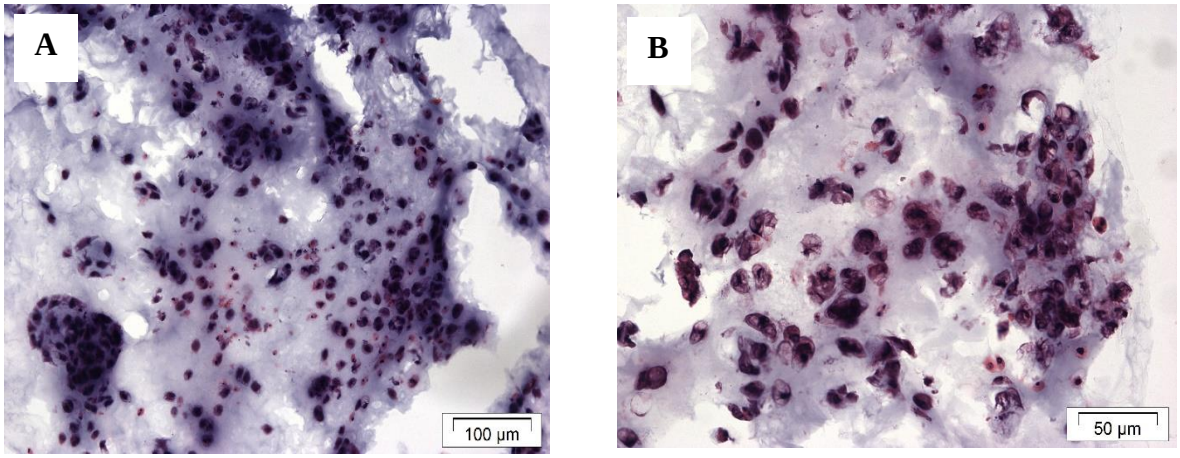

Figure 6.45 Histological H&E staining of sections of chondrocyte-encapsulated agarose gels. (300,000 chondrocytes encapsulated per gel) (A and B) Images were taken at a magnification of x20 (A) and x40 (B). Scale bars are shown on the images

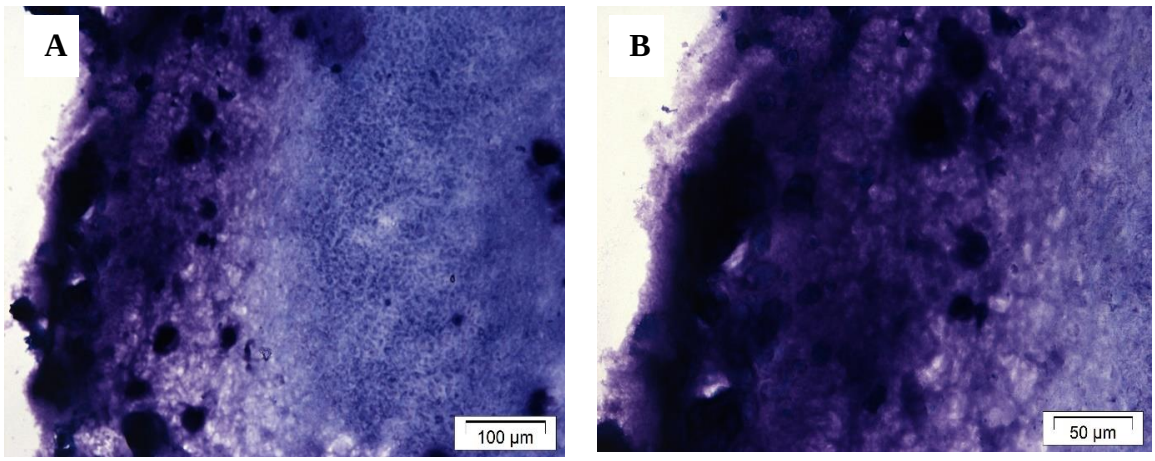

Figure 6.46 Histological Toluidine Blue staining of sections of chondrocyte encapsulated agarose gels (300,000 chondrocytes/gel) (A and B). Images were taken at a magnification of x20 (A) and x40 (B). Scale bars are shown on the image.

Key Summary

- Confirmation of chondrocyte survival and differentiation in 4 % agarose gels.
- Chondrocytes encapsulated in FPA-fibrinogen gels were comparable to fibrin and 4 % agarose gels for cell activity and total GAG content per gel.

6.5 P15, P17, and HyStem gels

Gelation experiments were carried out with P15 and P17 - fibrinogen hydrogels at concentrations of 0.75 $mg.mL^{-1}$, 0.5 $mg.mL^{-1}$, and 0.25 $mg.mL^{-1}$ of the FBP components of P15 and P17. All three concentrations of P15 and P17 formed gels however, it was observed that 0.25 $mg.mL^{-1}$ of P15 or P17 formed smaller gels with fibrinogen in comparison to 0.75 $mg.mL^{-1}$ of P15 and P17. HyStem formed considerably smaller and weaker gels below concentrations of 0.75 $mg.mL^{-1}$. Gelation was observed at 1 $mg.mL^{-1}$ and 0.75 $mg.mL^{-1}$ of HyStem which appeared to form larger and stronger gels compared to lower concentrations of HyStem. However, in comparison to P15, P17, fibrin and FPA the HyStem gels were much smaller. The concentrations of P15 and P17 that were investigated for chondrocyte encapsulation were 0.75 $mg.mL^{-1}$, 0.5 $mg.mL^{-1}$, and 0.25 $mg.mL^{-1}$ and the HyStem concentrations used were 1 $mg.mL^{-1}$ and 0.75 $mg.mL^{-1}$. FPA-fibrinogen gels formed using 2.66 $mg.mL^{-1}$ FPA and fibrin gels were used as reference materials.

Phase contrast, light microscopy images of the chondrocyte encapsulated P15, P17 and HyStem – fibrinogen gels (refer to Figure 6.47 to Figure 6.56, images A-D), showed that chondrocytes appeared to have adhered to the tissue culture plastic throughout the 21 day encapsulation period. This was not previously observed with chondrocyte encapsulated FPA-fibrinogen, PEG-fibrinogen or fibrin gels, see sections 6.1, 6.3, and 6.4. The hydrogels have shown very little apparent degradation throughout the culture period in terms of diminishing volume. At day 21, the gels were removed from the well and the tissue culture plastic was treated with crystal violet to stain any adherent chondrocytes to the surface of the tissue culture plastic. This allowed the observations of chondrocytes that migrated out of the fibrinogen gels (Figure 6.47 to Figure 6.56, images E-F). It can be seen that a ring-like distribution of chondrocytes was visible on the tissue culture plastic surrounding the areas occupied by the hydrogels. Therefore, the chondrocytes did not remain fully encapsulated during the 21 day incubation period. The ring-like distribution indicating that chondrocytes on the outer surface of the hydrogel may have been able to migrate out of the fibrinogen gels formed form P15, P17 or HyStem.

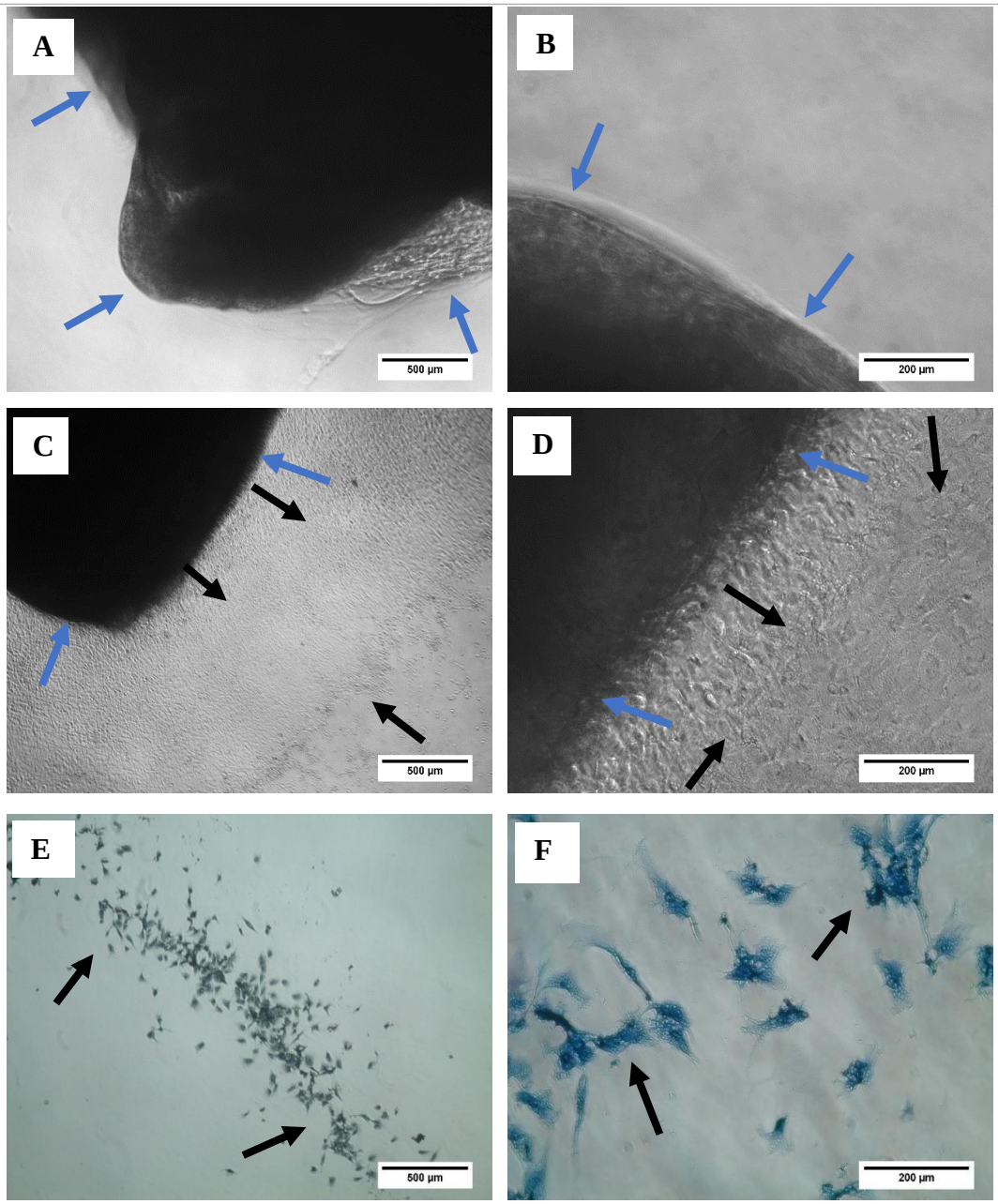

Figure 6.47 Phase contrast images chondrocyte encapsulated fibrin gels taken at day 1 (A and B) and day 21 (C and D) after encapsulation. Crystal violet on the tissue culture plastic after day 21 of encapsulation (E and F). The blue arrows show a representation of the hydrogel and the black arrows show the migrating chondrocytes. Images taken at x4 magnification (A, C and E) and x20 magnification (B, D and F). Scale bars are shown on the image.

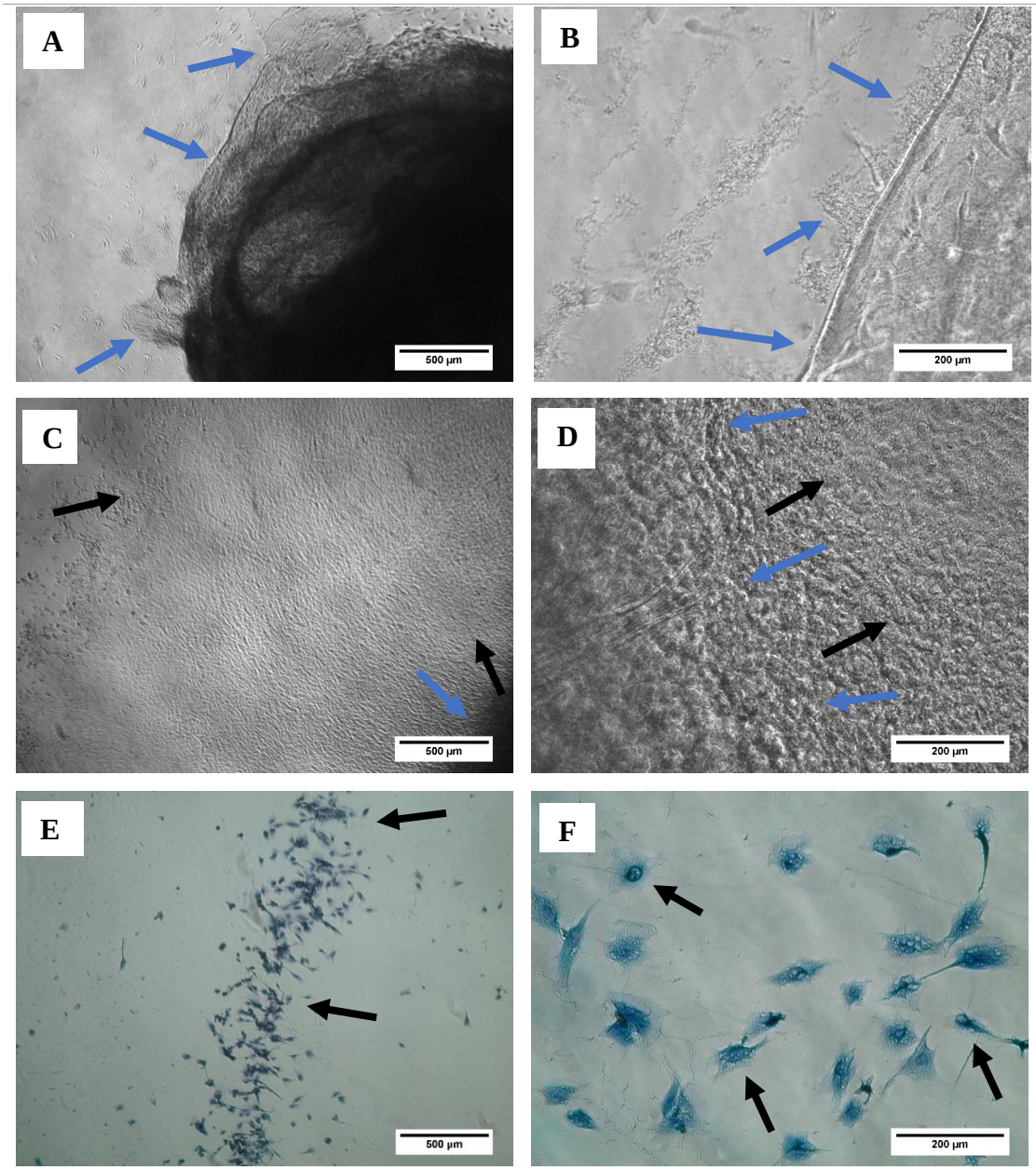

Figure 6.48 Phase contrast images chondrocyte encapsulated FPA-fibrinogen gels using 2.66 mg.mL^{-1} FPA. Images taken at day 1 (A and B) and day 21 (C and D) after encapsulation. Crystal violet on the tissue culture plastic after day 21 of encapsulation (E and F). The blue arrows show a representation of the hydrogel and the black arrows show the migrating chondrocytes. Images taken at x4 magnification (A, C and E) and x20 magnification (B, D and F). Scale bars are shown on the image.

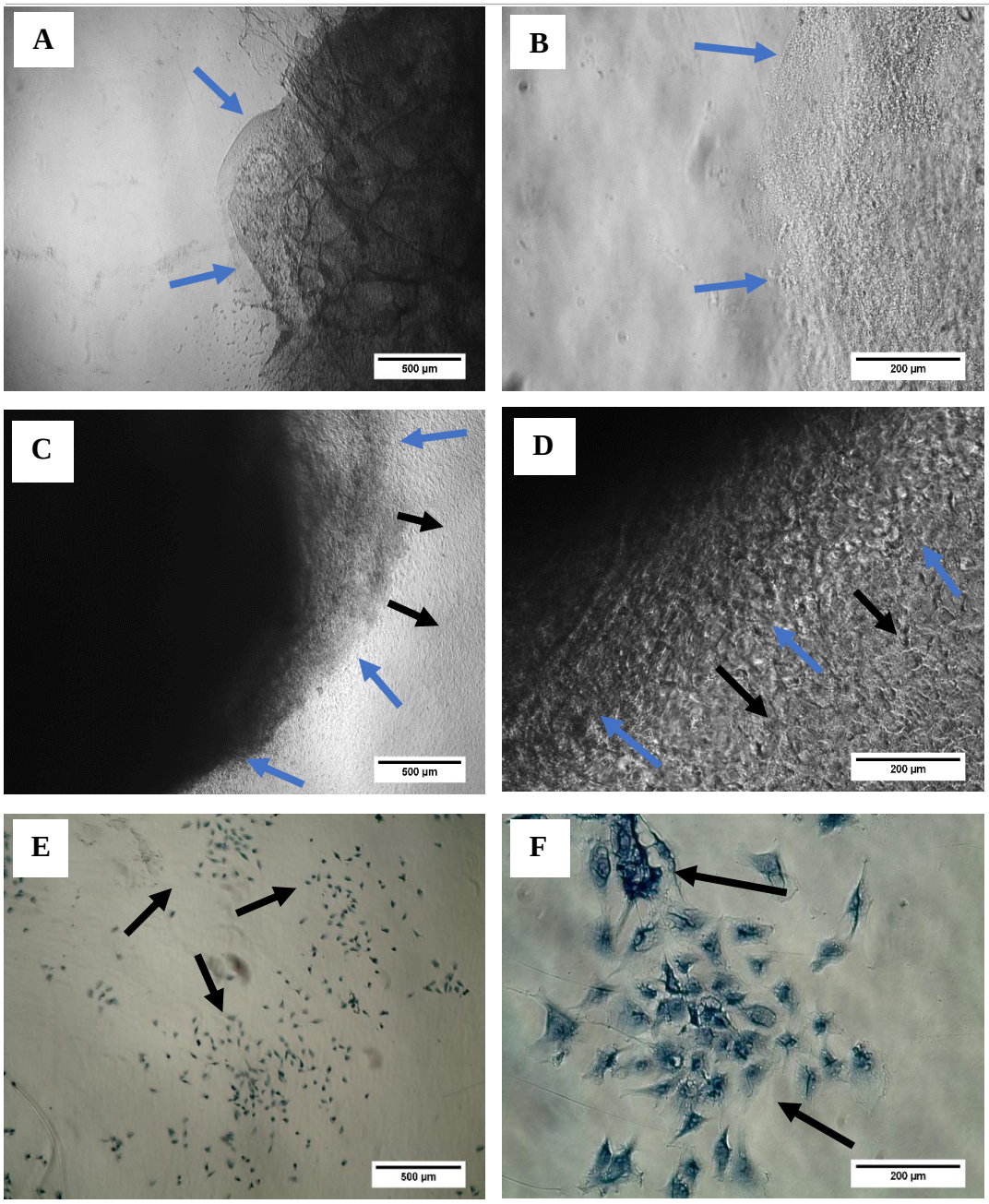

Figure 6.49 Phase contrast images chondrocyte encapsulated P15-fibrinogen gels using 0.75 mg.mL^{-1}. Images taken at day 1 (A and B) and day 21 (C and D) after encapsulation. Crystal violet on the tissue culture plastic after day 21 of encapsulation (E and F). The blue arrows show a representation of the hydrogel and the black arrows show the migrating chondrocytes. Images taken at x4 magnification (A, C and E) and x20 magnification (B, D and F). Scale bars are shown on the image.

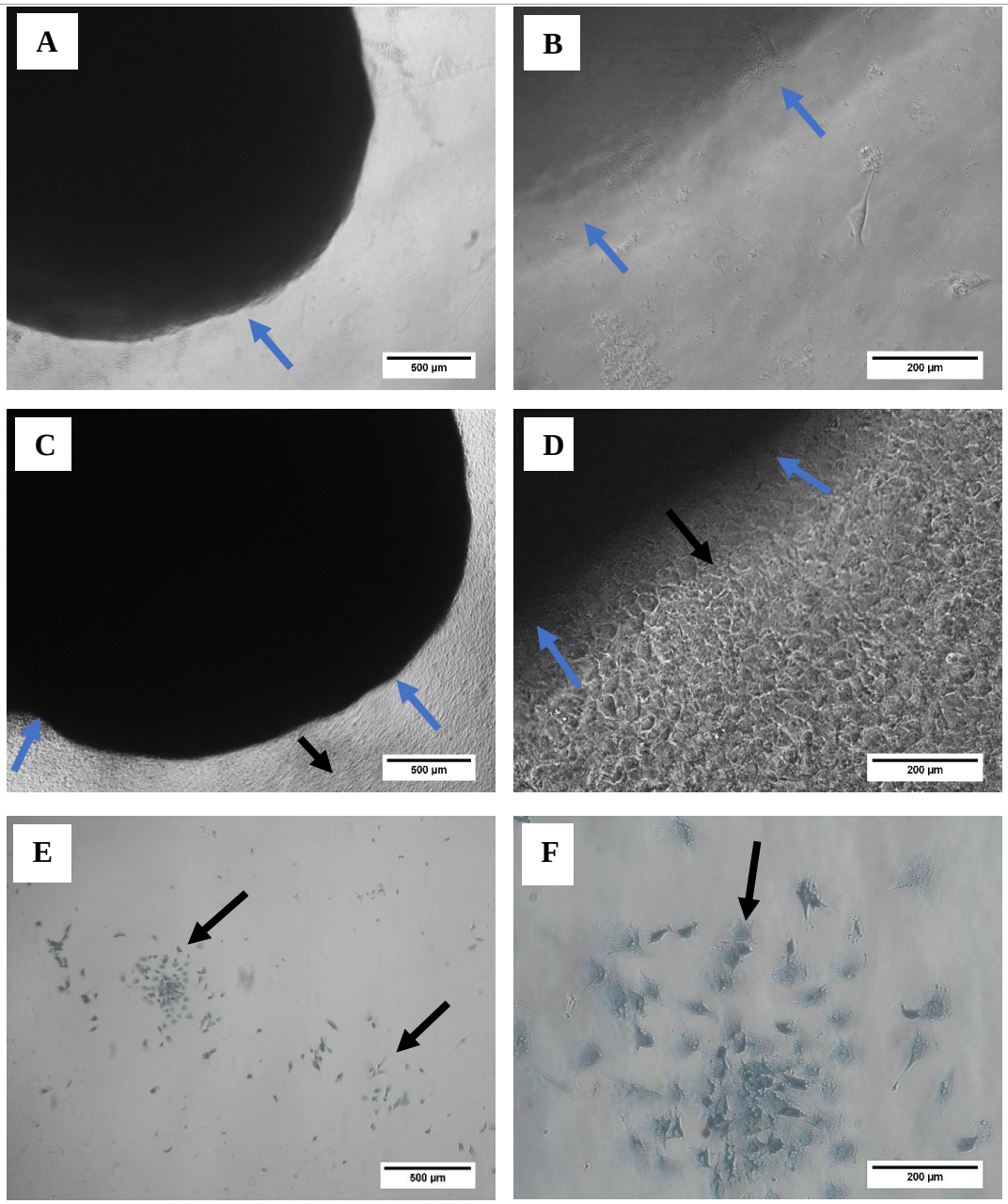

Figure 6.50 Phase contrast images chondrocyte encapsulated P15-fibrinogen gels using 0.5 mg.mL^{-1}. Images taken at day 1 (A and B) and day 21 (C and D) after encapsulation. Crystal violet on the tissue culture plastic after day 21 of encapsulation (E and F). The blue arrows show a representation of the hydrogel and the black arrows show the migrating chondrocytes. Images taken at x4 magnification (A, C and E) and x20 magnification (B, D and F). Scale bars are shown on the image.

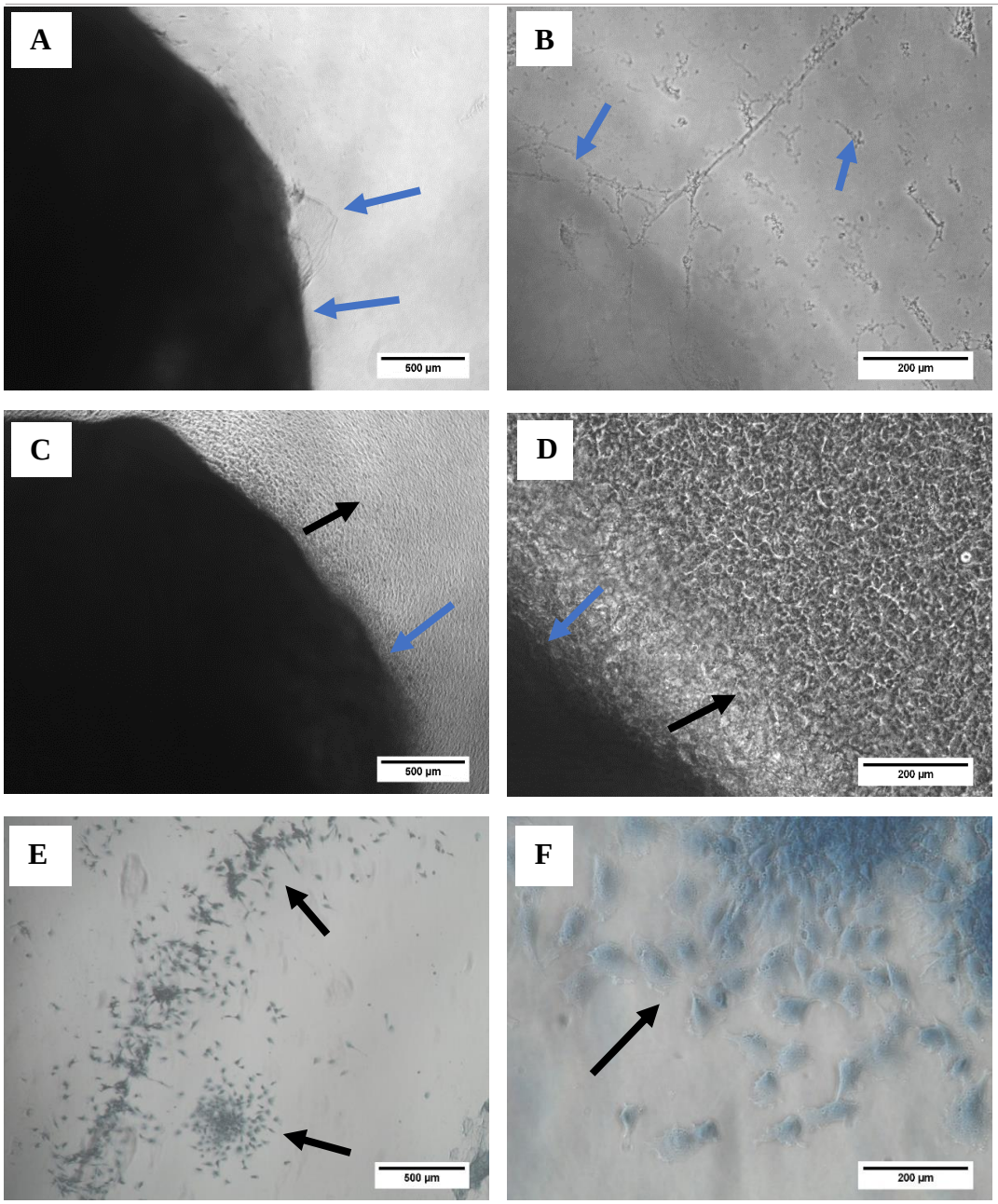

Figure 6.51 Phase contrast images chondrocyte encapsulated P15-fibrinogen gels using 0.25 mg.mL^{-1}. Images taken at day 1 (A and B) and day 21 (C and D) after encapsulation. Crystal violet on the tissue culture plastic after day 21 of encapsulation (E and F). The blue arrows show a representation of the hydrogel and the black arrows show the migrating chondrocytes. Images taken at x4 magnification (A, C and E) and x20 magnification (B, D and F). Scale bars are shown on the image.

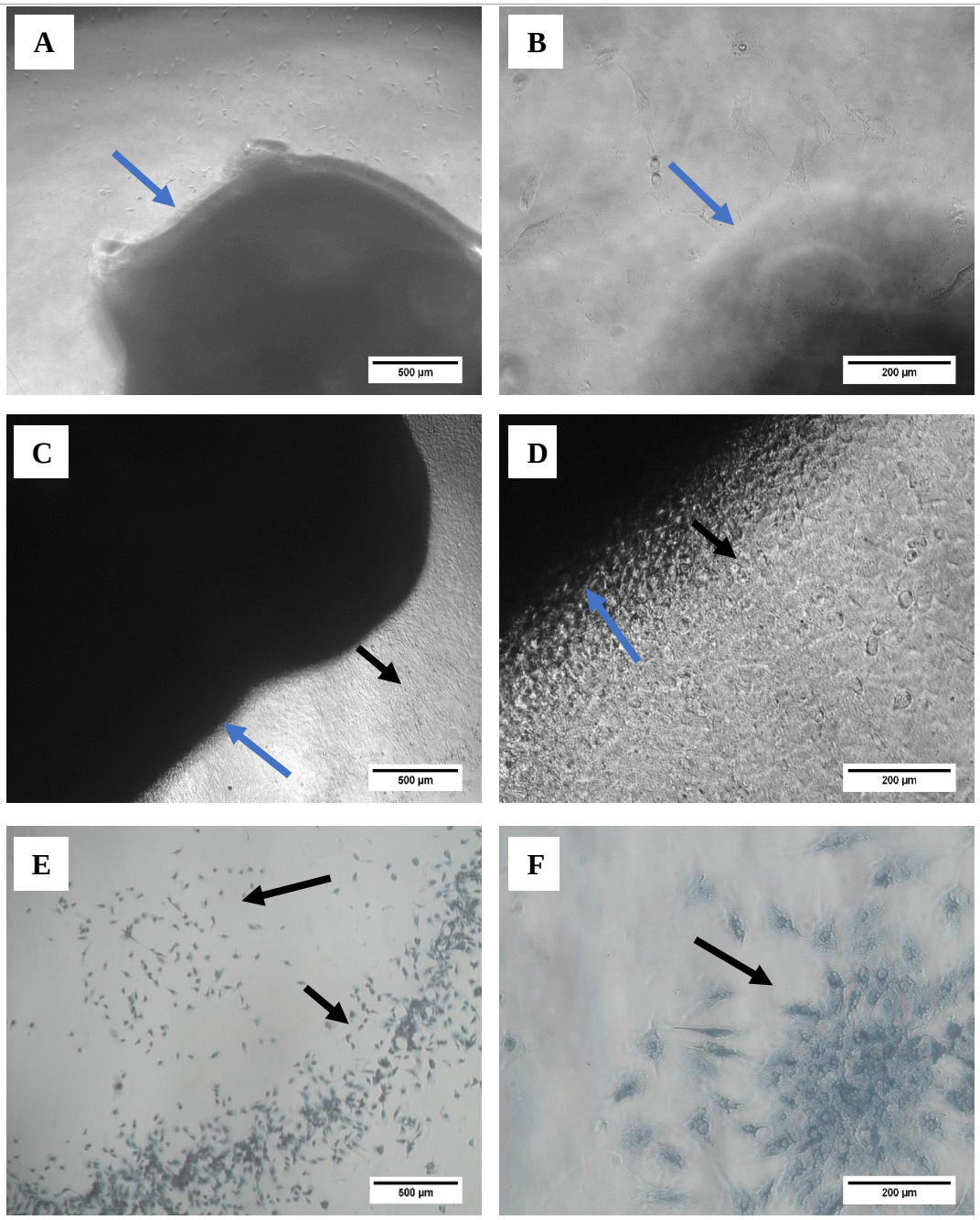

Figure 6.52 Phase contrast images chondrocyte encapsulated P17-fibrinogen gels using 0.75 mg.mL^{-1}. Images taken at day 1 (A and B) and day 21 (C and D) after encapsulation. Crystal violet on the tissue culture plastic after day 21 of encapsulation (E and F). The blue arrows show a representation of the hydrogel and the black arrows show the migrating chondrocytes. Images taken at x4 magnification (A, C and E) and x20 magnification (B, D and F). Scale bars are shown on the image.

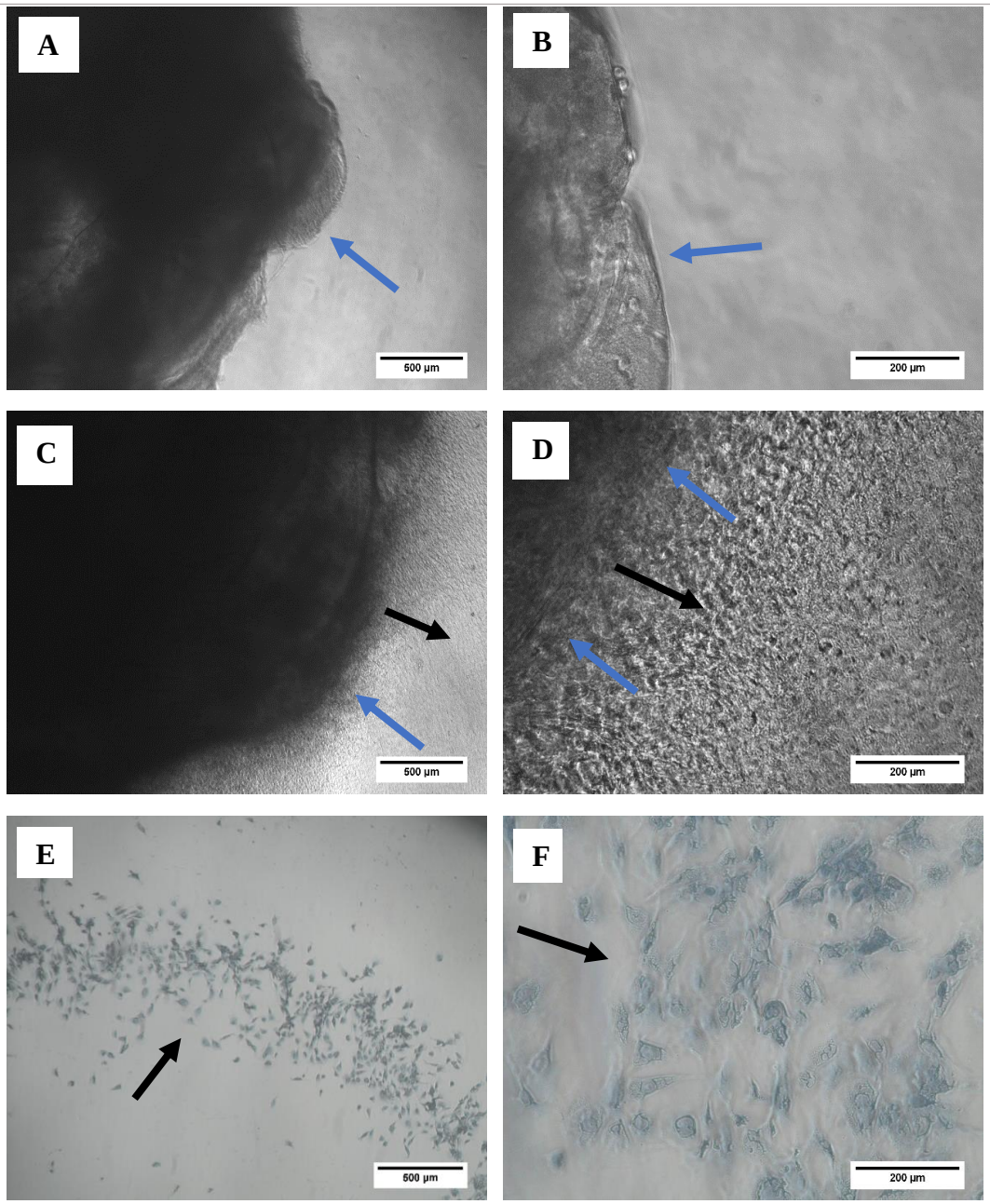

Figure 6.53 Phase contrast images chondrocyte encapsulated P17-fibrinogen gels using 0.5 mg.mL^{-1}. Images taken at day 1 (A and B) and day 21 (C and D) after encapsulation. Crystal violet on the tissue culture plastic after day 21 of encapsulation (E and F). The blue arrows show a representation of the hydrogel and the black arrows show the migrating chondrocytes. Images taken at x4 magnification (A, C and E) and x20 magnification (B, D and F). Scale bars are shown on the image.

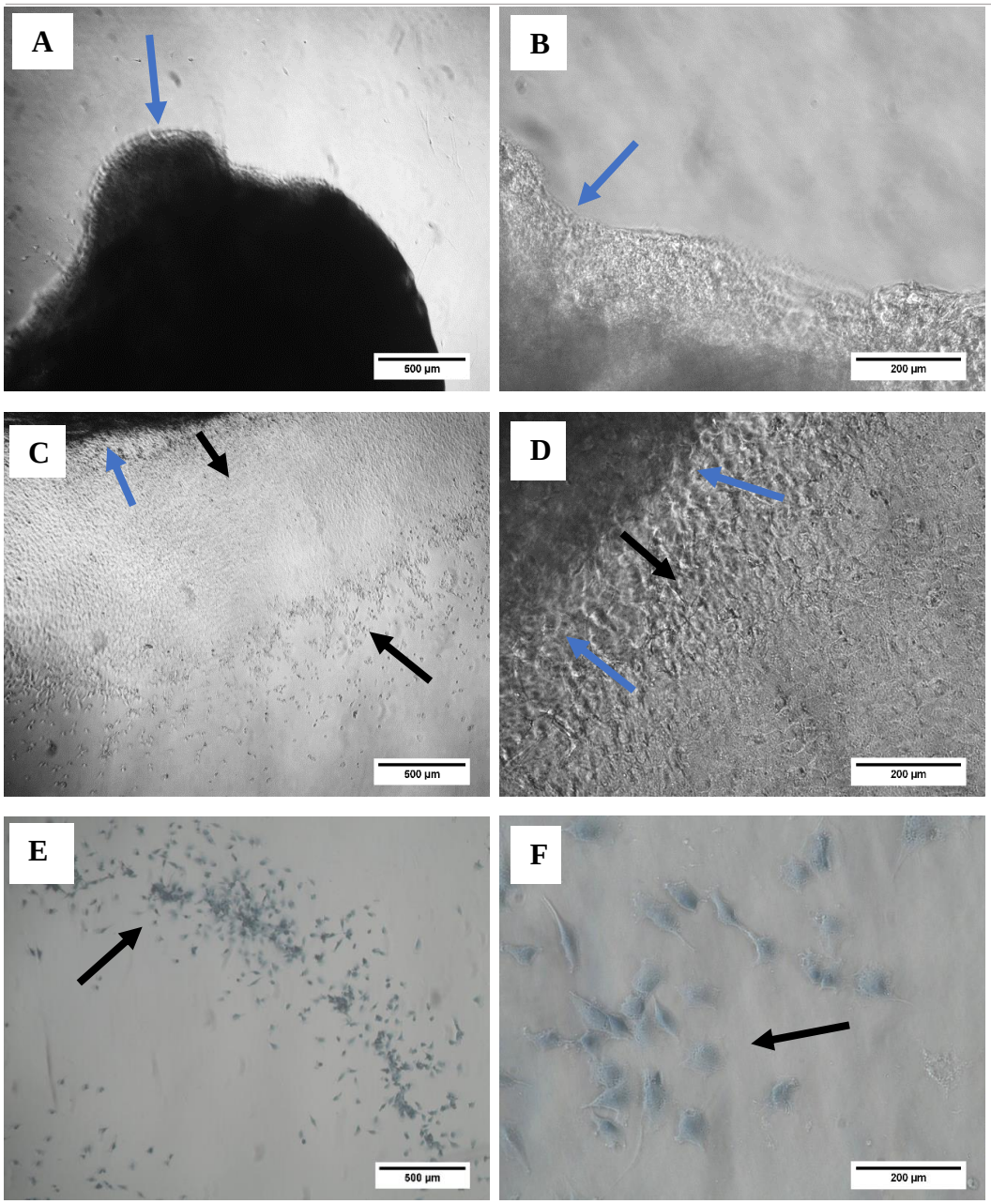

Figure 6.54 Phase contrast images chondrocyte encapsulated P17-fibrinogen gels using 0.25 mg.mL^{-1}. Images taken at day 1 (A and B) and day 21 (C and D) after encapsulation. Crystal violet on the tissue culture plastic after day 21 of encapsulation (E and F). The blue arrows show a representation of the hydrogel and the black arrows show the migrating chondrocytes. Images taken at x4 magnification (A, C and E) and x20 magnification (B, D and F). Scale bars are shown on the image.

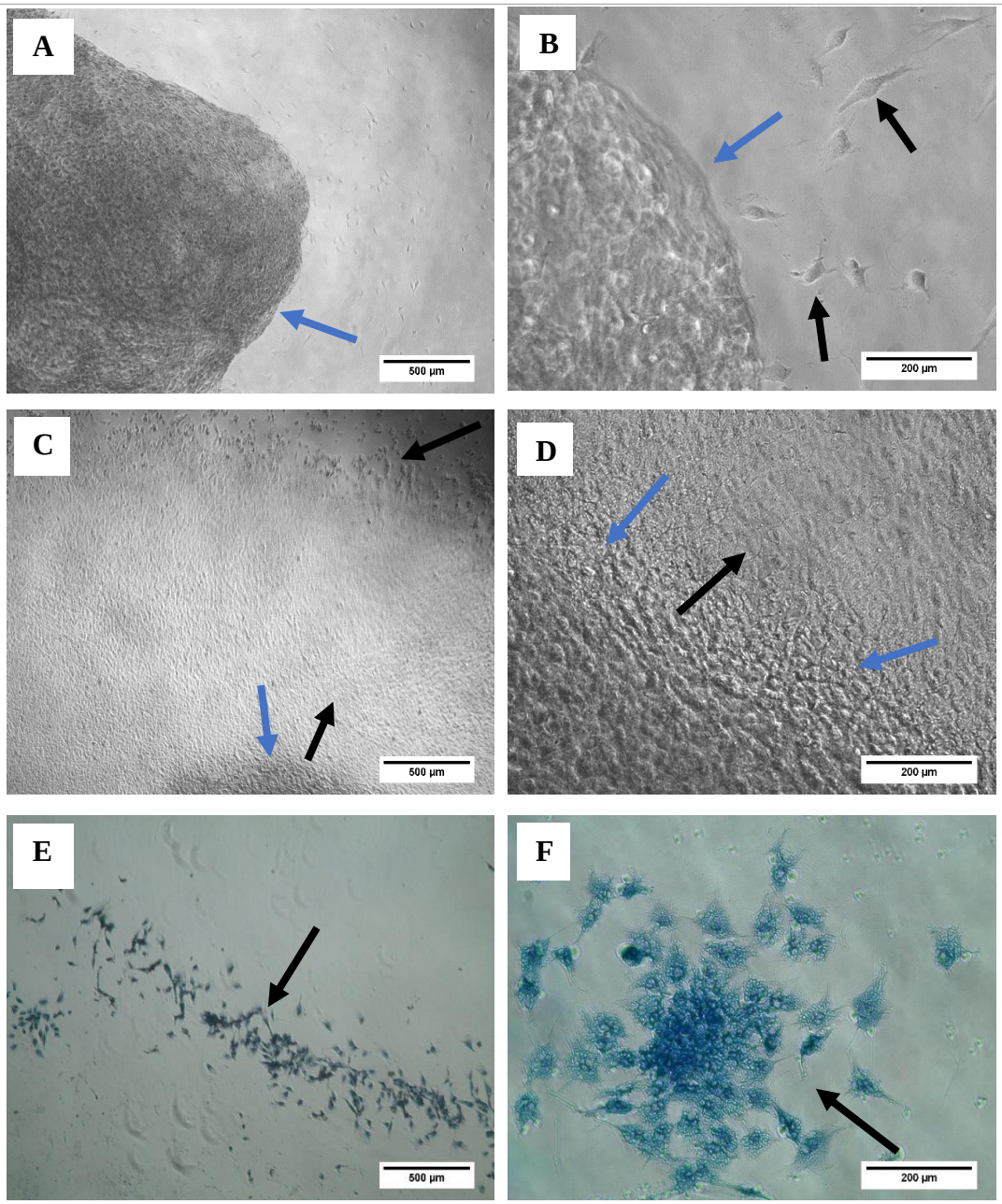

Figure 6.55 Phase contrast images chondrocyte encapsulated HyStem-fibrinogen gels using 1 mg.mL^{-1}. Images taken at day 1 (A and B) and day 21 (C and D) after encapsulation. Crystal violet on the tissue culture plastic after day 21 of encapsulation (E and F). The blue arrows show a representation of the hydrogel and the black arrows show the migrating chondrocytes. Images taken at x4 magnification (A, C and E) and x20 magnification (B, D and F). Scale bars are shown on the image.

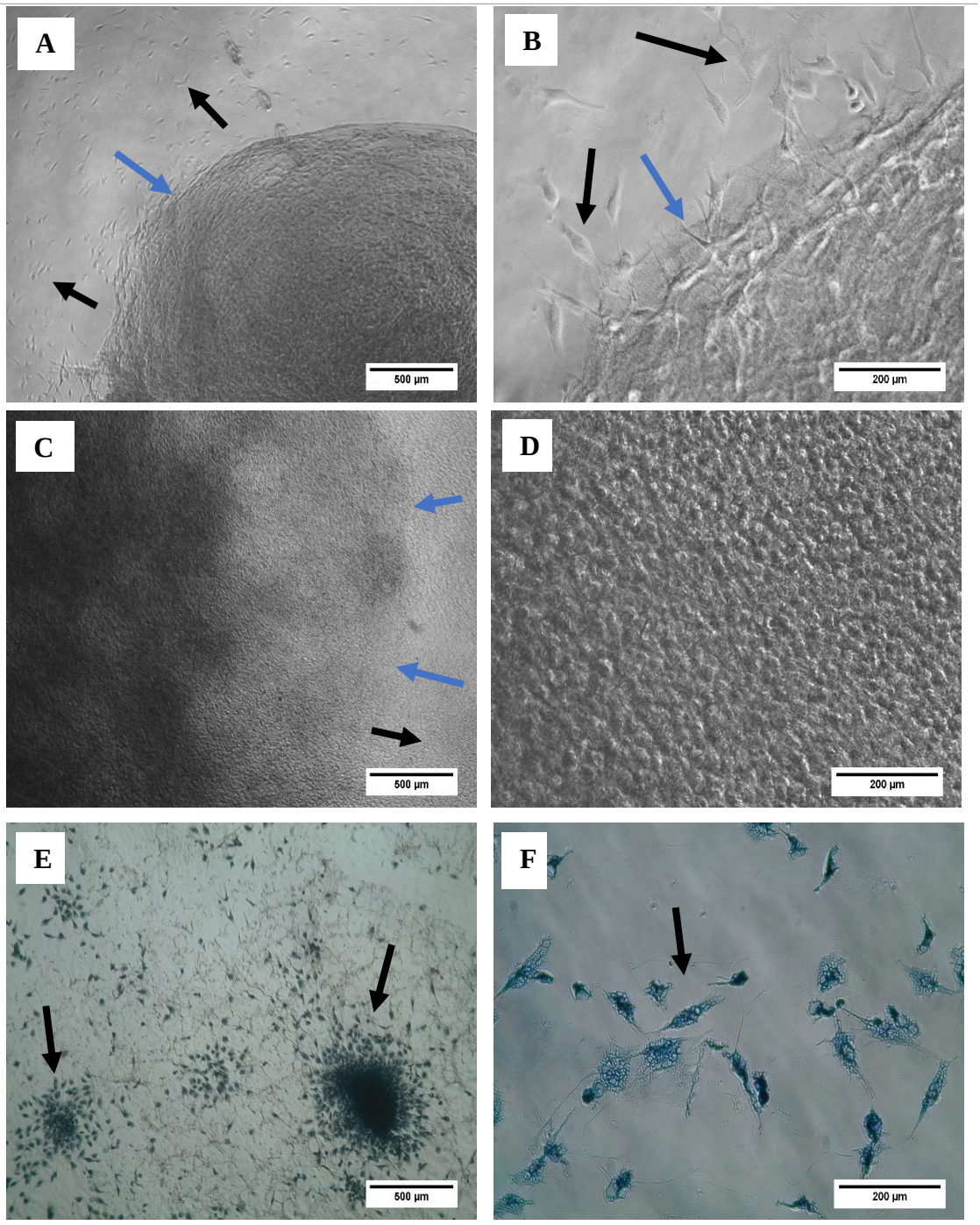

Figure 6.56 Phase contrast images chondrocyte encapsulated HyStem-fibrinogen gels using 0.75 mg.mL^{-1}. Images taken at day 1 (A and B) and day 21 (C and D) after encapsulation. Crystal violet on the tissue culture plastic after day 21 of encapsulation (E and F). The blue arrows show a representation of the hydrogel and the black arrows show the migrating chondrocytes. Images taken at x4 magnification (A, C and E) and x20 magnification (B, D and F). Scale bars are shown on the image.

Chondrocyte activity

All cell free P15-fibrinogen, P17-fibrinogen, HyStem-fibrinogen, FPA-fibrinogen (2.66 mg.mL^{-1} FPA) and fibrin gels exhibited low resazurin reduction in the cell viability assay suggesting that the gels did not interfere by binding or reducing the dye chemically (Figure 6.57). The cell viability of the chondrocyte encapsulated gels was assessed. It was observed that all the fibrinogen gels supported chondrocyte survival over the 20 day culture period of encapsulation, a gradual increase in cellular activity was observed (Figure 6.58, Figure 6.59, Figure 6.60). It was observed that the HyStem gels in particular degraded throughout the culture period and chondrocytes had adhered to the tissue culture plastic. This may account for the higher cellular activity observed in the 0.75 mg.mL^{-1} HyStem.

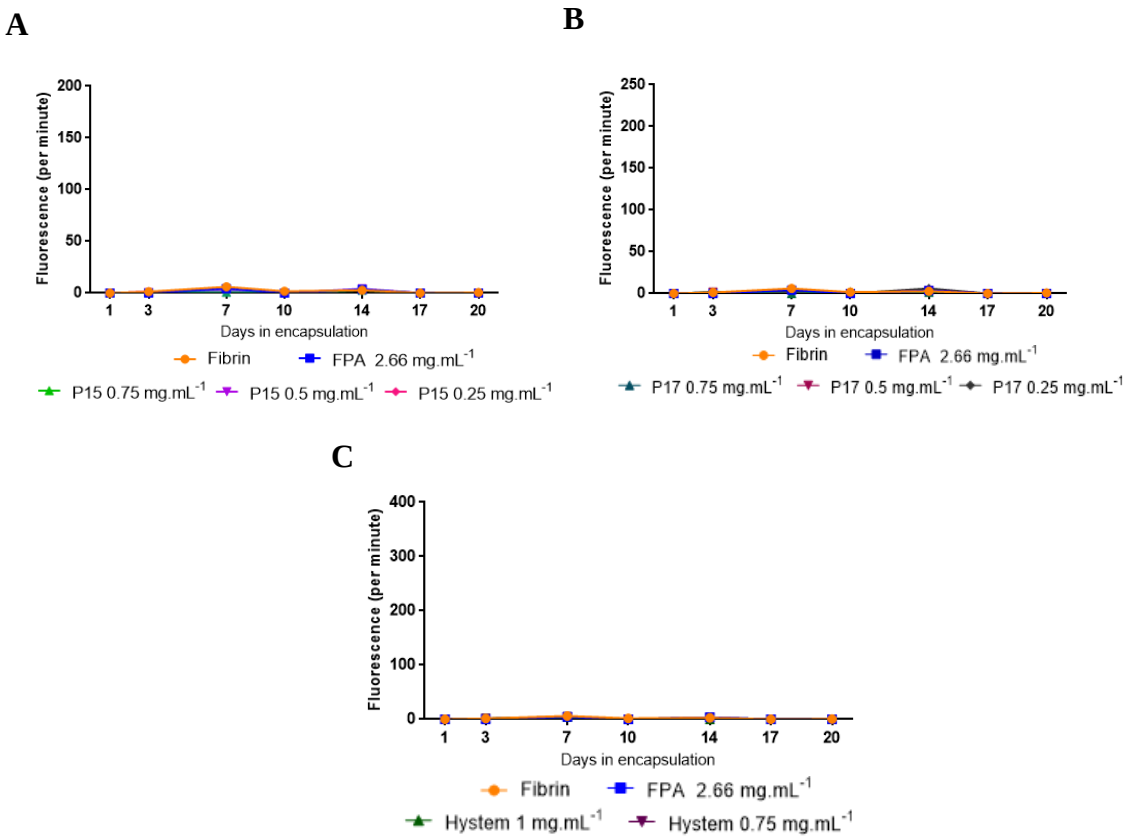

Figure 6.57 The effect of the rate of reduction of PrestoBlue (shown as mean relative fluorescence units per minute) of cell free P15-fibrinogen gels (**A**), P17-fibrinogen gels (**B**) and HyStem-fibrinogen gels (**C**). Measurements were taken at day 1, day 3, day 7, day, 10, day 14, day 17 and day 20 of culture. N=1

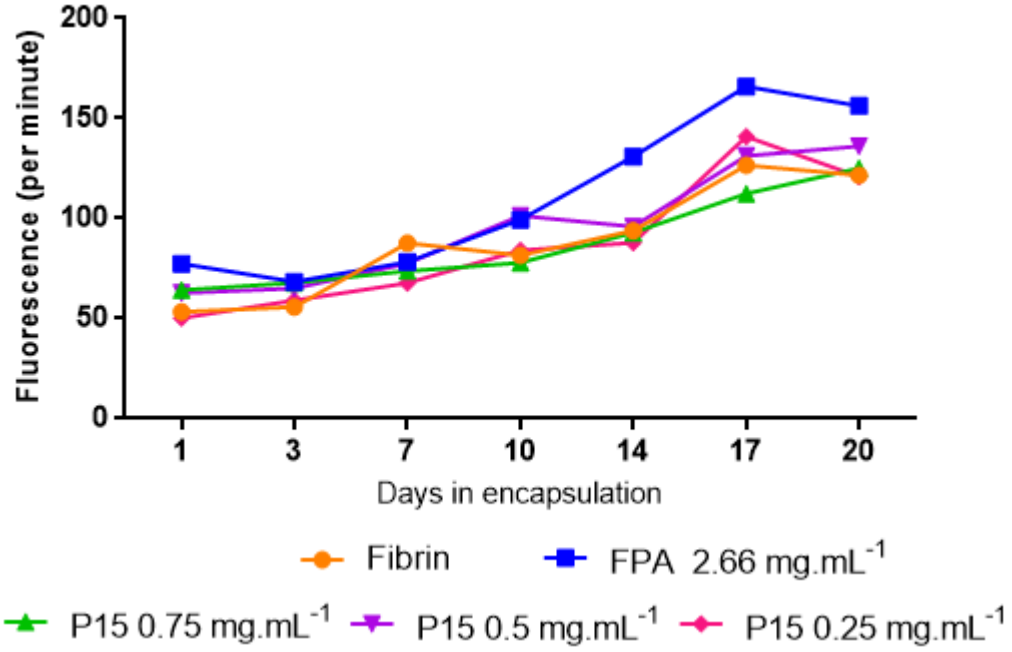

Figure 6.58 Rate of reduction of PrestoBlue (shown as mean fluorescence per minute) indicating the cell activity chondrocyte encapsulated fibrin, FPA-fibrinogen and P15-fibrinogen gels. The error bars represent the standard error of the mean. N=1

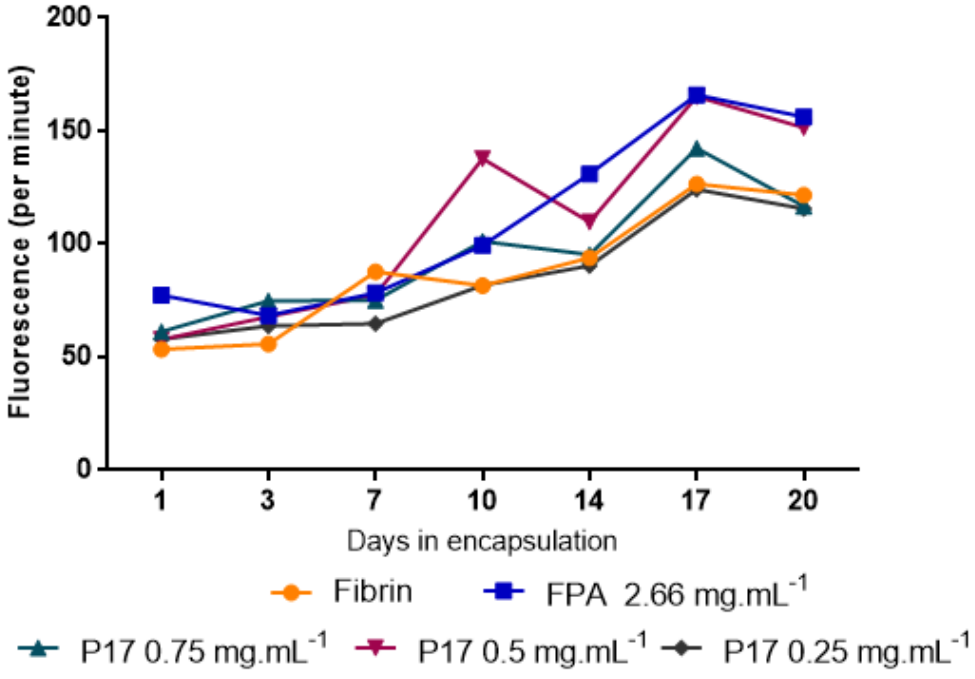

Figure 6.59 Rate of reduction of PrestoBlue (shown as mean fluorescence per minute) indicating the cell activity chondrocyte encapsulated fibrin, FPA-fibrinogen and P17-fibrinogen gels. The error bars represent the standard error of the mean. N=1

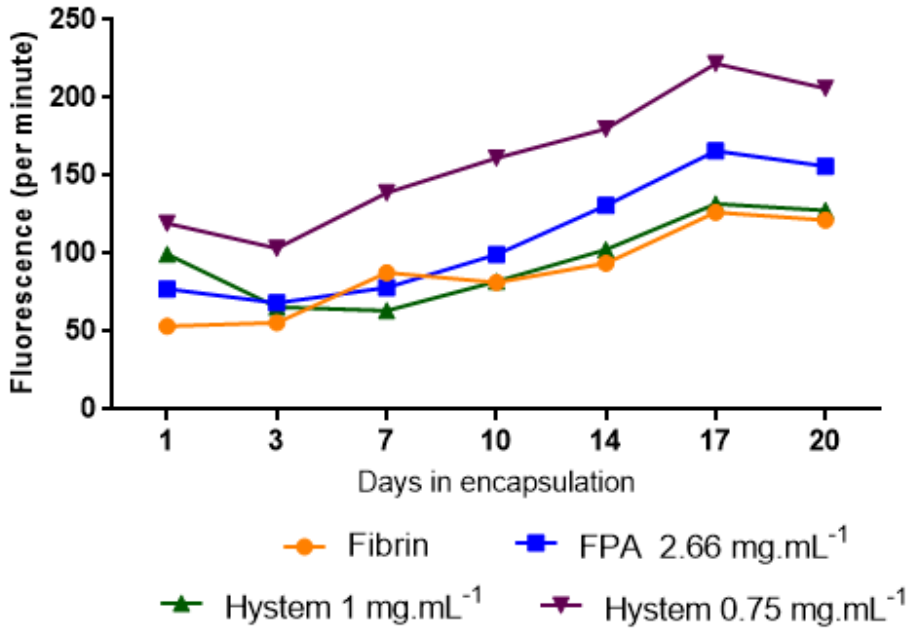

Figure 6.60 Rate of reduction of PrestoBlue (shown as mean fluorescence per minute) indicating the cell activity chondrocyte encapsulated fibrin, FPA-fibrinogen and P15-fibrinogen gels. The error bars represent the standard error of the mean.. N=1

Glycosaminoglycan content

Cell free gels were tested for GAG content and P15, P17, HyStem, FPA 2.66 mg.mL^{-1} and fibrin exhibited very little GAG in comparison to their chondrocyte encapsulated counterparts and therefore are not interfering with the assay (Figure 6.61). ECM synthesis was observed in P15, P17 and HyStem (Figure 6.63, Figure 6.64). The GAG content in P15, P17, HyStem, fibrin and FPA 2.66 mg.mL^{-1} under the conditions used showed very high values in comparison to those previously seen. However this could not be repeated due to insufficient material.

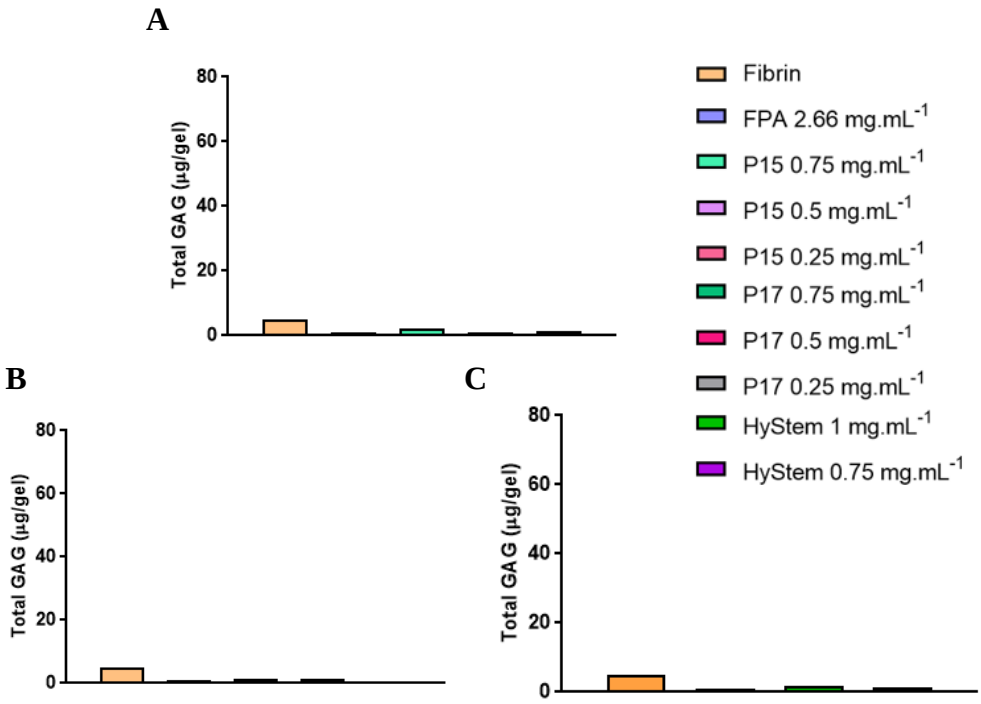

Figure 6.61 The effect of DMB on cell free P15-fibrinogen (A), P17-fibrinogen (B) and HyStem-fibrinogen (C) gels. N=1

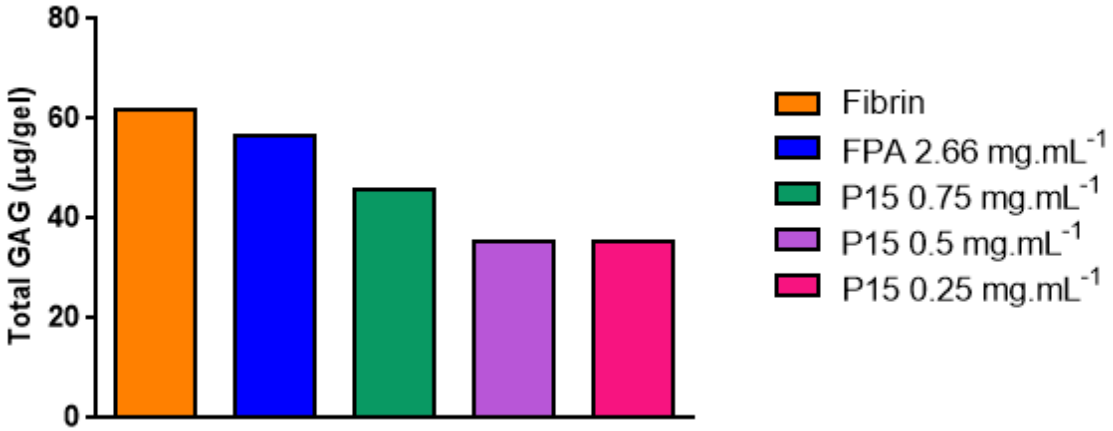

Figure 6.62 Total glycosaminoglycan content per gel of chondrocyte encapsulated in Fibrin, FPA-fibrinogen, and P15-fibrinogen gels. The error bars represent the standard error of the mean. Statistical analysis with use of a one-way ANOVA with Tukey post test was conducted. N=1

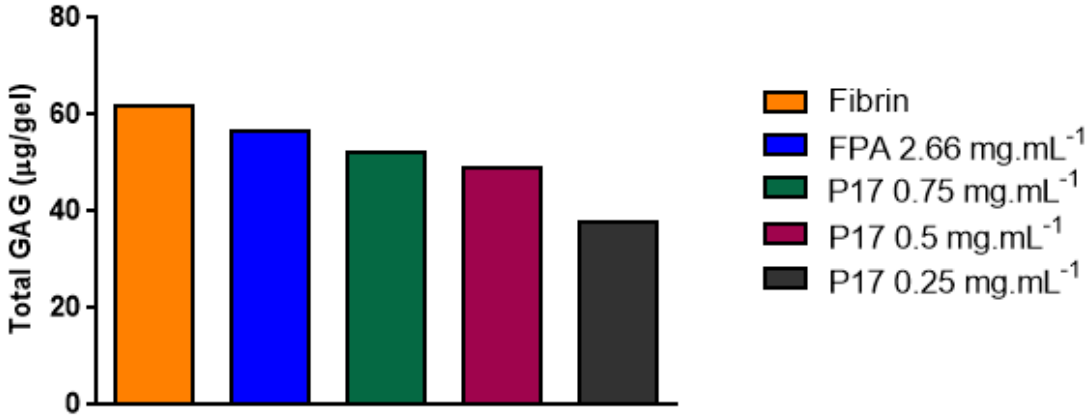

Figure 6.63 Total glycosaminoglycan content per gel of chondrocyte encapsulated fibrin, FPA-fibrinogen, and P17-fibrinogen gels. The error bars represent the standard error of the mean. Statistical analysis with use of a one-way ANOVA with Tukey post test was conducted. N=1

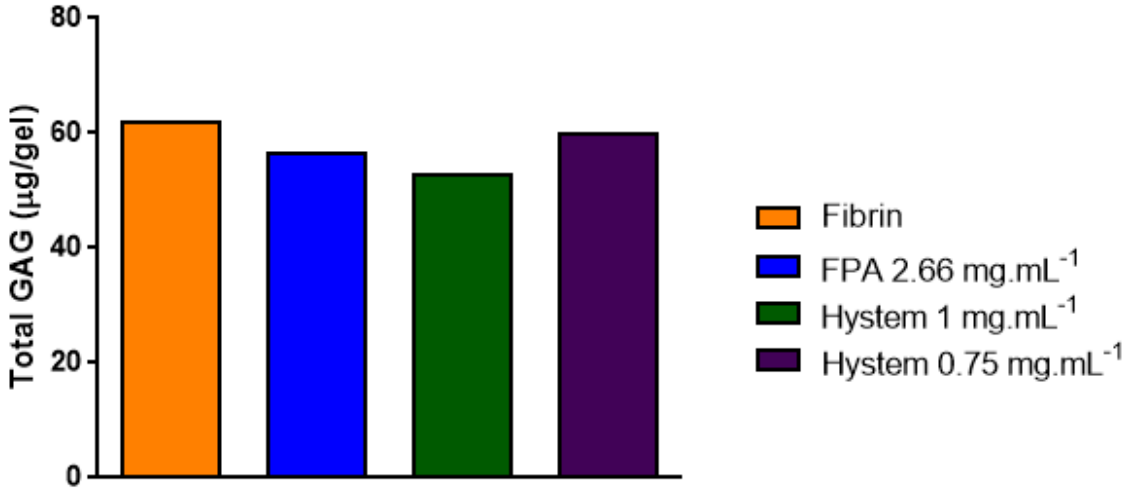

Figure 6.64 Total glycosaminoglycan content per gel of chondrocyte encapsulated in fibrin, FPA-fibrinogen, and HyStem-fibrinogen gels. The error bars represent the standard error of the mean. Statistical analysis with use of a one-way ANOVA with Tukey post test was conducted. N=1

Haematoxylin and Eosin Stain

Histological H&E stain was carried out after chondrocyte encapsulated P15, P17 and HyStem gels were cultured in chondrogenic conditions for 21 days. Unfortunately, cell free gels were unable to be stained due to samples being required for the DMB assay. Figure 6.65 illustrates the H&E staining. The chondrocytes appear to be disorganised when encapsulated in the P15, P17 and HyStem gels and had a spherical morphology. No

chondrocytes were stained from the H&E staining conducted on P17 0.75 mg.mL^{-1} and P17 0.25 mg.mL^{-1}.

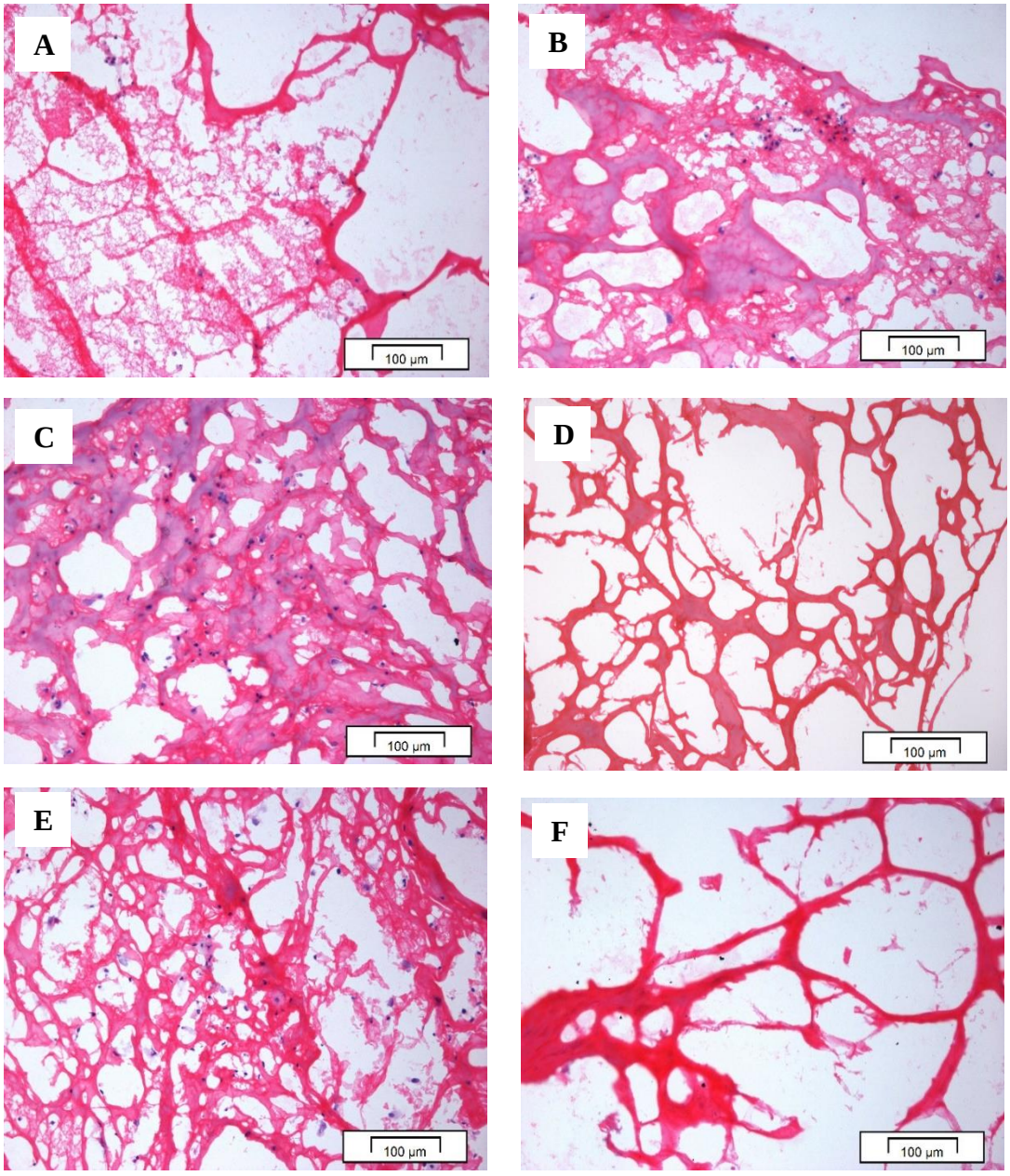

Figure 6.65 Histological H&E stained sections of chondrocyte encapsulated P15-fibrinogen gels formed from (A) 0.75 mg.mL^{-1} P15, (B) 0.5 mg.mL^{-1} P15 and (C) 0.25 mg.mL^{-1} P15 and P17-fibrinogen gels formed from (D) 0.75 mg.mL^{-1} P17, (E) 0.5 mg.mL^{-1} P17 and (F) 0.25 mg.mL^{-1} P17. Images were taken at a magnification of x20 and scale bars are shown on the image.

Toluidine blue stain

Toluidine blue staining was carried out on chondrocyte encapsulated P15, P17 and HyStem gels. Chondrocytes were not observed from the staining and very little proteoglycan staining was observed, Figure 6.66. This was inconsistent with the GAG content per gel, see Figure 6.61, Figure 6.63, and Figure 6.64. Unfortunately, cell free staining was unable to be obtained due to the samples being required for the GAG assay. There was limited materials available for the peptide work and therefore the histological staining could not be repeated.

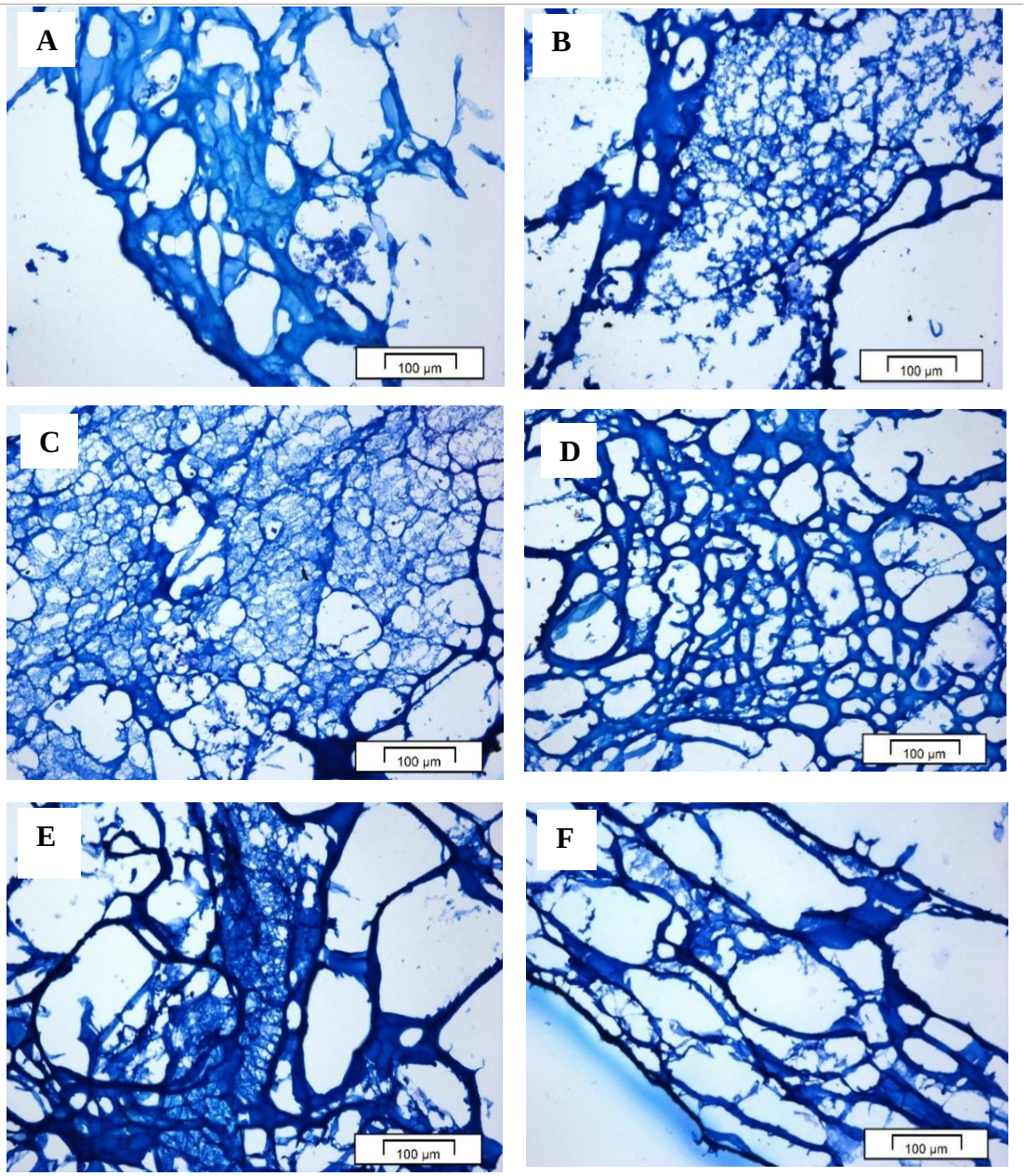

Figure 6.66 Histological Toluidine blue stained sections of chondrocyte encapsulated P15-fibrinogen gels formed from (A) 0.75 mg.mL^{-1} P15, (B) 0.5 mg.mL^{-1} P15 and (C) 0.25 mg.mL^{-1} P15 and P17-fibrinogen gels formed from (D) 0.75 mg.mL^{-1} P17, (E) 0.5 mg.mL^{-1} P17 and (F) 0.25 mg.mL^{-1} P17. Images were taken at a magnification of x20 and scale bars are shown on the image.

Key Summary

- Chondrocytes migrated from the P15, P17, and Hystem – fibrinogen gels.
- HyStem – fibrinogen gels formed much smaller gels in comparison to P15, P17, FPA – fibrinogen and fibrin gels. Chondrocyte encapsulated HyStem – fibrinogen gels also degraded throughout the 21 day culture period.

- Chondrocytes encapsulated in P15, P17, and HyStem – fibrinogen gels survived and differentiated in the gels.
- Proteoglycan staining by Toluidine blue did not reflect the high total GAG content by DMB assay.
- Experimental repeats are required to confirm the accuracy of the results.

6.6 Cell delivery to cartilage injury

A cartilage injury model was developed in order to investigate events in a cartilage injury after the delivery of chondrocytes encapsulated within FPA-fibrinogen and fibrin gels. As described previously in section 4.2.5, and shown in Figure 4.1, a 6 mm biopsy punch was used to remove reproducible discs of articular cartilage from bovine metacarpophalangeal joints. The discs of cartilage were then injured by using a 3 mm biopsy punch to create a circular injury in the centre of the cartilage disc. Chondrocytes were delivered to the site of injury via encapsulation in fibrinogen-FPA gels at a concentration of 2.66 mg.mL^{-1} FPA and fibrin gels containing 300,000 chondrocytes per gel for 14 days. As shown in Figure 6.67, the cartilage disc can be seen in pink and the hydrogel, in blue, was formed prior to be placed over the cartilage injury.

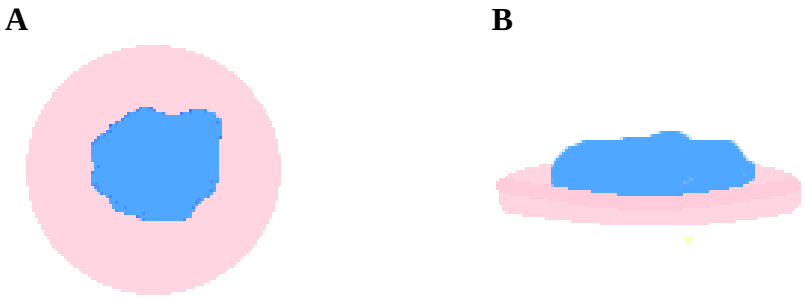

Figure 6.67 Schematic of the cartilage injury model. Top view (A) and side view (B) of the injured cartilage (pink) and chondrocytes delivered via the hydrogel (blue).

Cell viability

The viability of the chondrocyte encapsulated fibrin or FPA-fibrinogen gels and cartilage was assessed over the time course of the incubation using PrestoBlue® (see section 4.10.1). The culture medium was collected and assayed for the capability to reduce the resazurin-based PrestoBlue®. Any apparent resazurin-reduction activity in the

culture medium would be indicative of significant cell death in the model and release of cellular contents such as enzymes capable of the dye reduction or cells present in the medium. The culture medium showed very low level of resazurin reduction (Figure 6.68) which indicated no cell death or the release of cells into the medium had occurred during the culture of the injured cartilage and hydrogels. Figure 6.69 showed the viability of the cultured cartilage and chondrocyte-encapsulated fibrin and fibrinogen-FPA gels. The rate of PrestoBlue® reduction suggested that the cartilage and gel system remained viable throughout the incubation period with a trend for the rate of the dye reduction to increase over the 10 day incubation period.

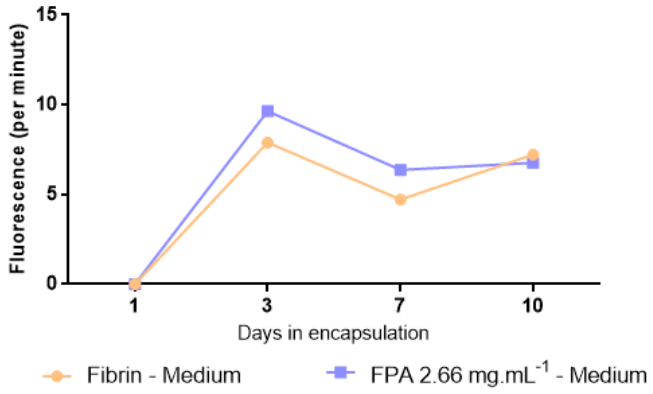

Figure 6.68 Rate of reduction of by culture medium removed during the time course of culture of fibrin and fibrinogen-FPA gels and injured articular cartilage. Readings were taken at day 1, day 3, day 7, and day 10 of culture. N=1.

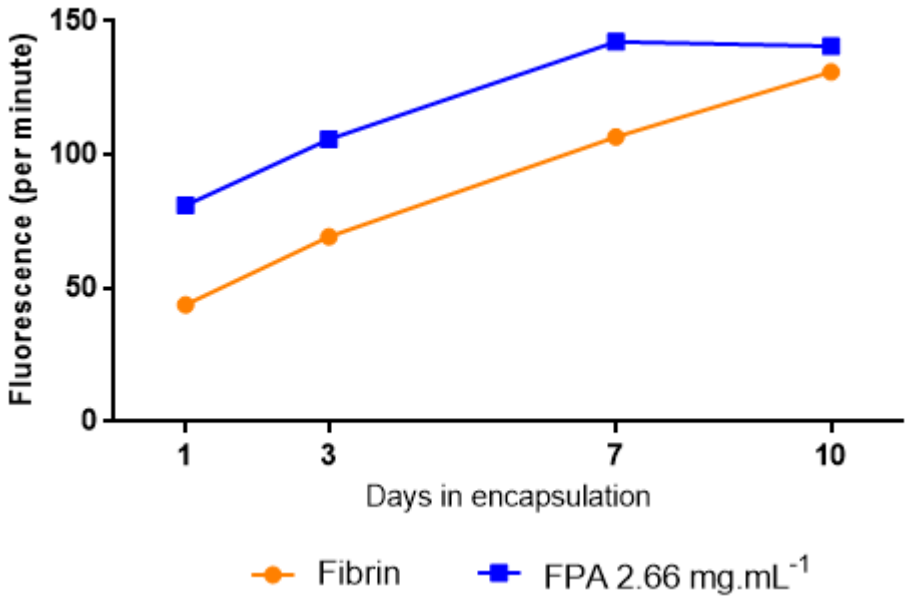

Figure 6.69 Viability of the injured articular cartilage and encapsulated chondrocytes. The data show the rate of reduction of PrestoBlue®. Readings were taken at day 1, day 3, day 7 and day 10 of culture. N=1

Phase contrast images

Phase contrast images were taken of the model injury site on days 4 and 10 of culture. It was observed at day 4 that the chondrocytes had remained in encapsulation in the fibrin and FPA-fibrinogen gels, refer to Figure 6.70 (A, C). Figure 6.70, image A has a clear gap between the hydrogel (blue arrow) and the cartilage injury (purple arrow), where it can be observed that no chondrocytes had adhered to the tissue culture plastic. However, by day 10, refer to Figure 6.70 image B, chondrocytes are observed adhering to the tissue culture plastic (as demonstrated by the black arrow) between the FPA-fibrinogen gel (blue arrow) and the cartilage (purple arrow). This is an interesting observation as the chondrocytes did not migrate out of fibrin of fibrinogen-FPA gels incubated alone. The fibrin gel had formed a thin film over the tissue culture plastic and the cartilage injury, this can be seen in the gap between the fibrin gel (blue arrow) and cartilage (purple arrow), see Figure 6.70 image C. No chondrocytes could be seen between this gap at day 4, by day 10 the fibrin gel had completely obstructed the gap between the gel and the cartilage and therefore the light microscopy images have not been included.

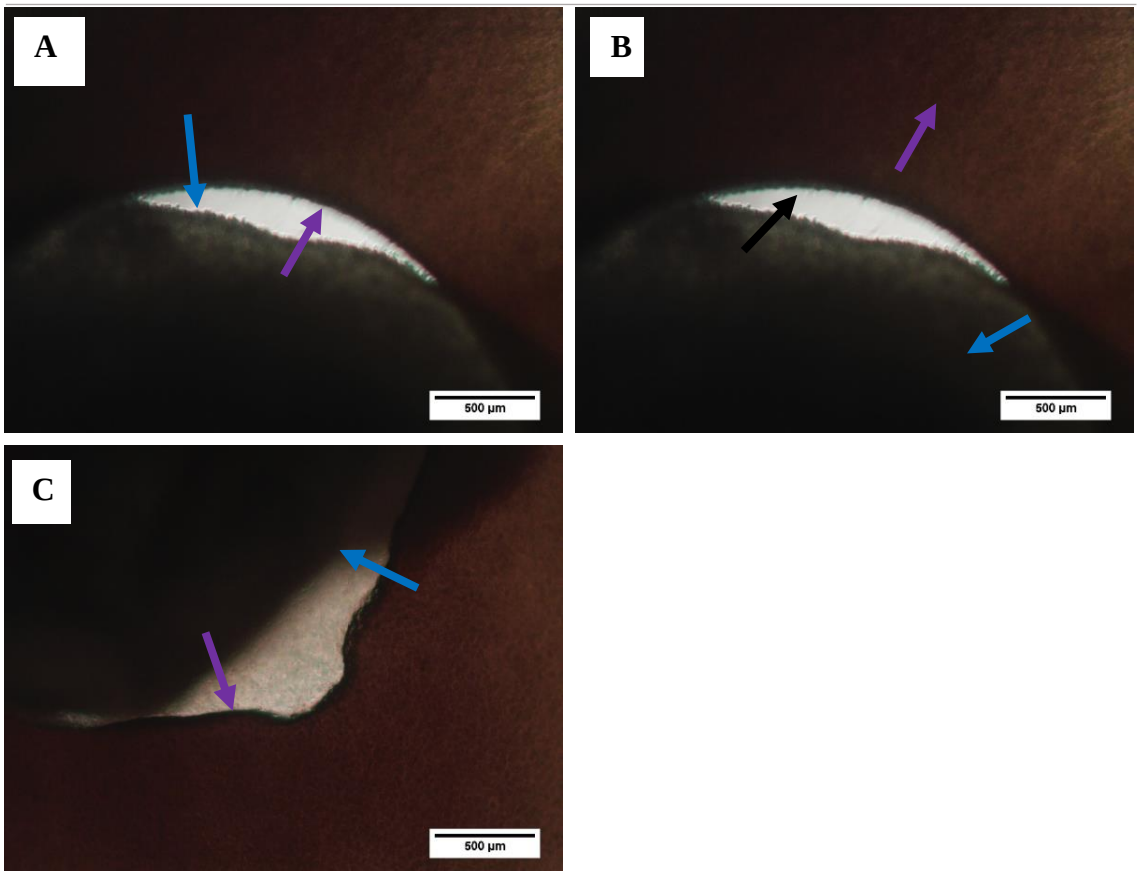

Figure 6.70 Phase contrast light microscopy images showing the chondrocyte encapsulated fibrin and FPA-fibrinogen gels (blue arrow) in position in the cartilage injury site (purple arrow). The black arrow shows migratory cells. Images A and B show the injury site with chondrocytes encapsulated in fibrinogen-FPA gels, and image C shows the injury site with the fibrin-encapsulated chondrocytes. Images were taken at day 4 (A and C) and day 10 (B) of culture. Scale bars are shown on the image.

Haematoxylin and Eosin staining

H&E staining of histological sections taken from the encapsulated chondrocytes in the cartilage injury site was carried out to determine if ECM formation had occurred. Figure 6.71 and Figure 6.72 shows stained sections from chondrocyte encapsulated fibrin and FPA-fibrinogen gels, respectively, for 14 days. Dense cell layers and ECM, green arrows Figure 6.71, can be seen from chondrocytes encapsulated in fibrin gels, blue arrow. Figure 6.72 showed that large volumes of the fibrinogen-FPA gel, blue arrow, have been occupied with developing ECM deposition, green arrows, after just 2 weeks of culture. In addition, the chondrocytes appeared to show some alignment as seen in native articular cartilage. The ECM deposition had integrated with the cartilage, red arrow, suggesting that this is the early stages of cartilage repair.

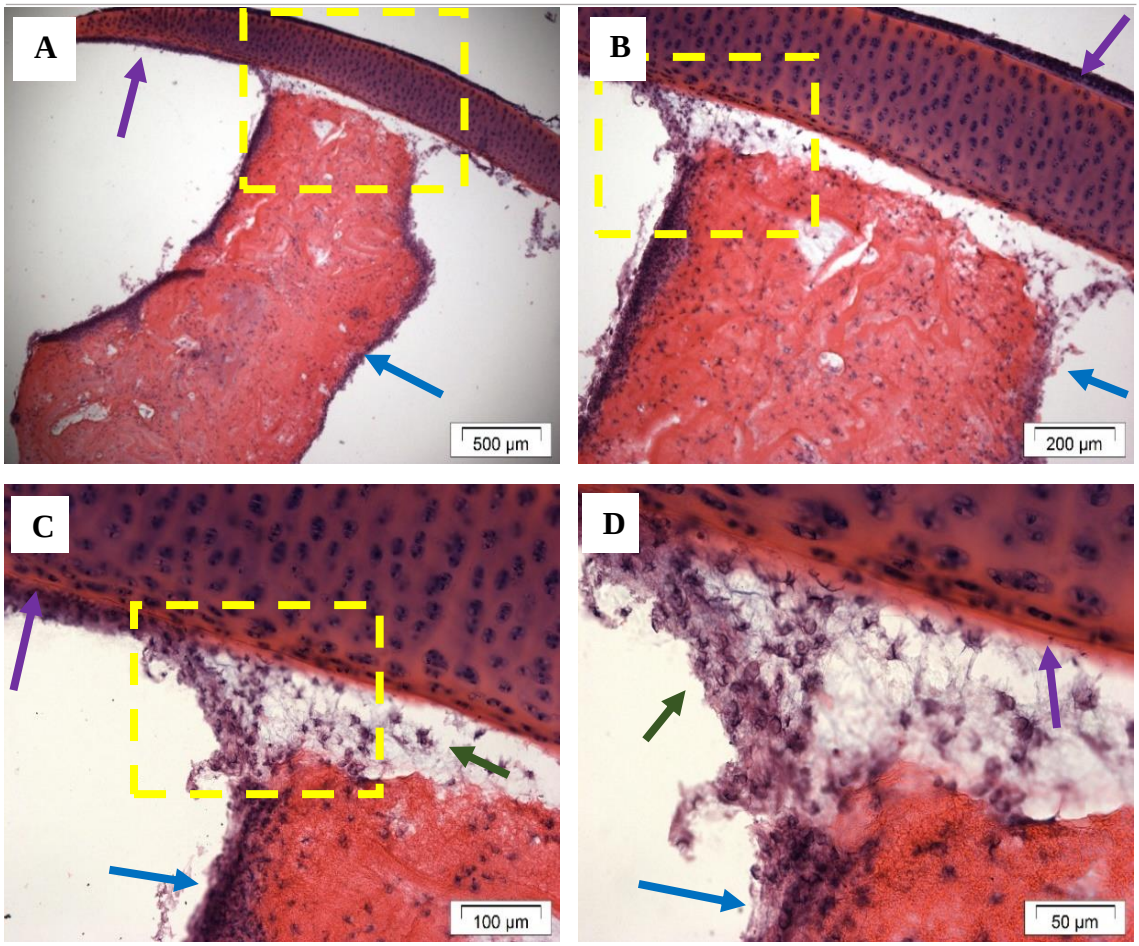

Figure 6.71 Images showing H&E stained sections of chondrocytes encapsulated in fibrin gels, blue arrow, at the cartilage injury site, purple arrow, for 14 days. ECM deposition is shown by the green arrows. Images were taken at a magnification of x4 (A), x10 (B), x20 (C) and x40 (D) and the magnification window is yellow. Scale bars are shown on the image.

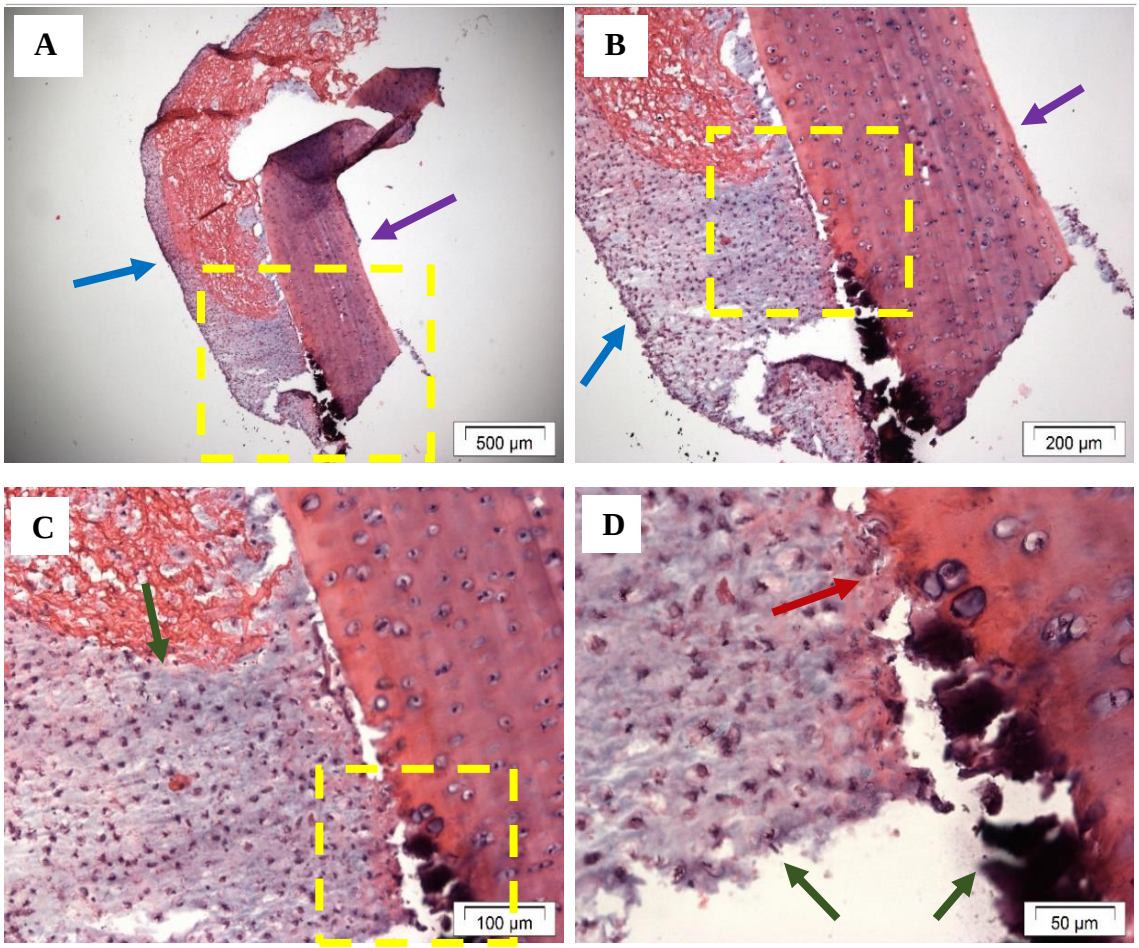

Figure 6.72 Histological H&E staining of 300,000 chondrocytes encapsulated in 2.66 mg.mL^{-1} FPA-fibrinogen gels, blue arrow, and delivered to an articular cartilage injury, purple arrow, cultured for 14 days. ECM deposition was observed and shown by the green arrow. Images taken at a magnification of x4 (A), x10 (B), x20 (C) and x40 (D), the magnification window is in yellow. Scale bars are shown on the image.

Key Summary

- The injured cartilage appeared to dramatically increase ECM formation from the encapsulated chondrocytes in FPA-fibrinogen and fibrin gels, in comparison to the gels cultured without injured cartilage.
- The integration of the hydrogel, chondrocytes and cartilage can easily be seen suggesting that cartilage repair is in progress.
- The cartilage explant injury model is a viable model to investigate cartilage repair *in vitro*.

7.0 Results: Encapsulation of MSC's and the osteoblastic cells MG63

MSCs are currently in research for cartilage regeneration due to the ability to undergo chondrogenic differentiation. MSC's are also released during the microfracture treatment for osteoarthritis. Therefore, bBM-MSCs were encapsulated in a range of novel fibrinogen gels to determine their potential for use in cell encapsulation and delivery to repair injured cartilage.

7.1 MSC encapsulation in FPA gels

Previous optimisation results from chondrocyte encapsulated FPA-fibrinogen and fibrin gels suggested that 300,000 cells per gel was optimal for encapsulation. Therefore, this cell number was used for the following experiments investigating the encapsulation of bovine bone marrow derived mesenchymal stem cells (bBM-MSCs) and human MG63 osteoblastic cells in fibrin and FPA-fibrinogen gels.

bBM-MSCs were encapsulated in fibrin, and fibrinogen–FPA gels formed from 2.66 $mg.mL^{-1}$, 2 $mg.mL^{-1}$, 1.33 [1], and 0.7 $mg.mL^{-1}$ FPA. The gels were incubated in basic culture medium for 7 days to allow for cell proliferation. However, in contrast to experiments with encapsulated chondrocytes, during this 7 day incubation period the bBM-MSCs started to migrate out of the all the FPA-fibrinogen and fibrin gels at day 3 of encapsulation, as shown by the black arrows on Figure 7.1 to Figure 7.5. All FPA-fibrinogen and fibrin gels were observed to show initial stages of degradation at this time (i.e. the gels were visibly smaller). The MSCs were observed to attach to the surface of the culture plates. By day 15 after MSC encapsulation all bBM-MSC encapsulated gels had almost completely degraded, this can be seen in the phase contrast, light microscopy images Figure 7.1 to Figure 7.5. These figures show the rapidly decreasing size of the gels during the incubation period. At day15 the cells attached to the culture surface were stained with crystal violet. In contrast, cell free gels, however, showed no signs of degradation in the culture condition used and therefore it must be the encapsulated bBM-MSCs which must be causing the degradation of the fibrin and fibrinogen-FPA gels.

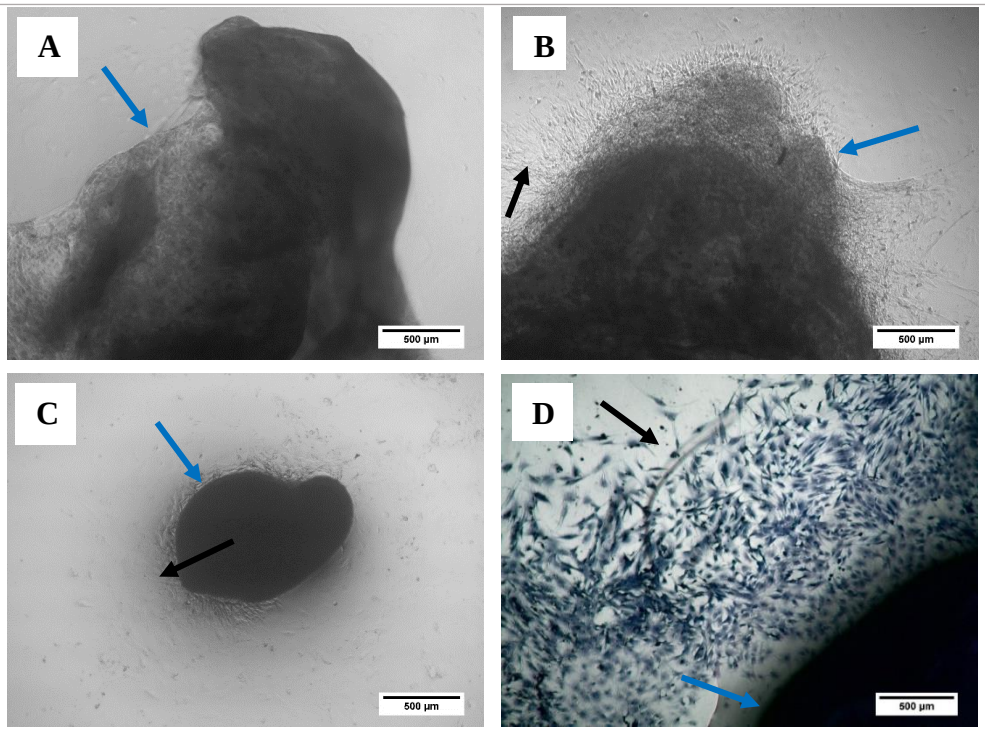

Figure 7.1 Light microscopy images of bBM-MSC encapsulated fibrin gels, blue arrow, taken at day 1 (A), day 3 (B), and day 15 (C). Cells were stained with crystal violet at day 15 of encapsulation (D), black arrows point to a representation of migratory cells. Images were taken at a magnification of x4. Scale bars are shown on the image.

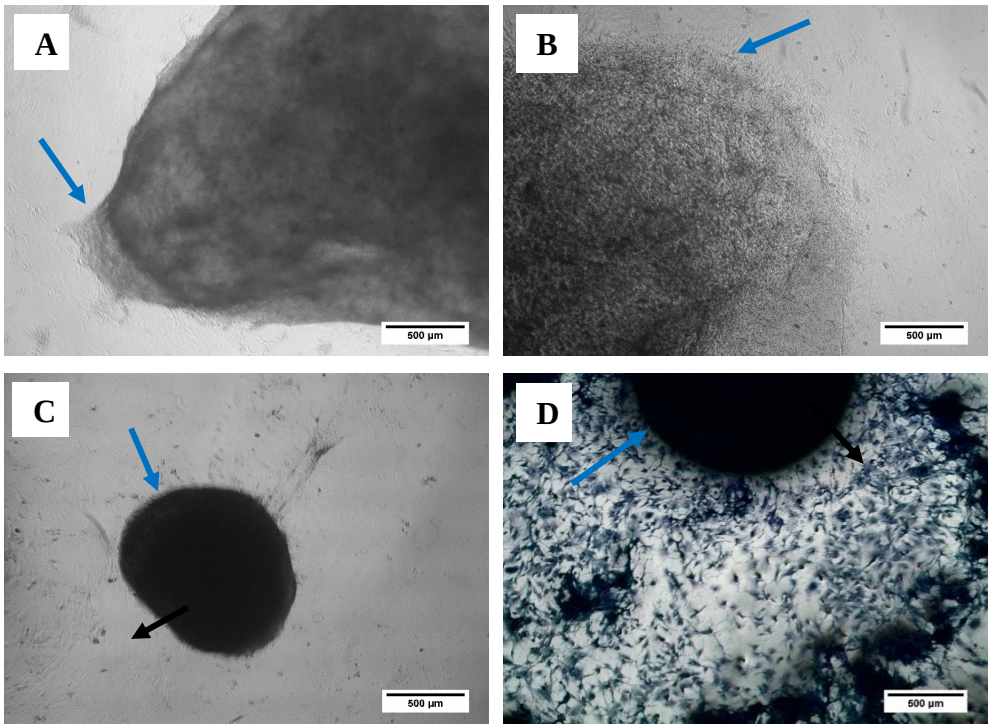

Figure 7.2 Light microscopy images of bBM-MSC encapsulated FPA-fibrinogen gels formed using 2.66 mg.mL^{-1} FPA, blue arrow. Images taken at day 1 (A), day 3 (B), and day 15 (C). Cells were stained with crystal violet at day 15 (D) black arrows point to a representation of migratory cells. Images were taken at a magnification of x4. Scale bars are shown on the image.

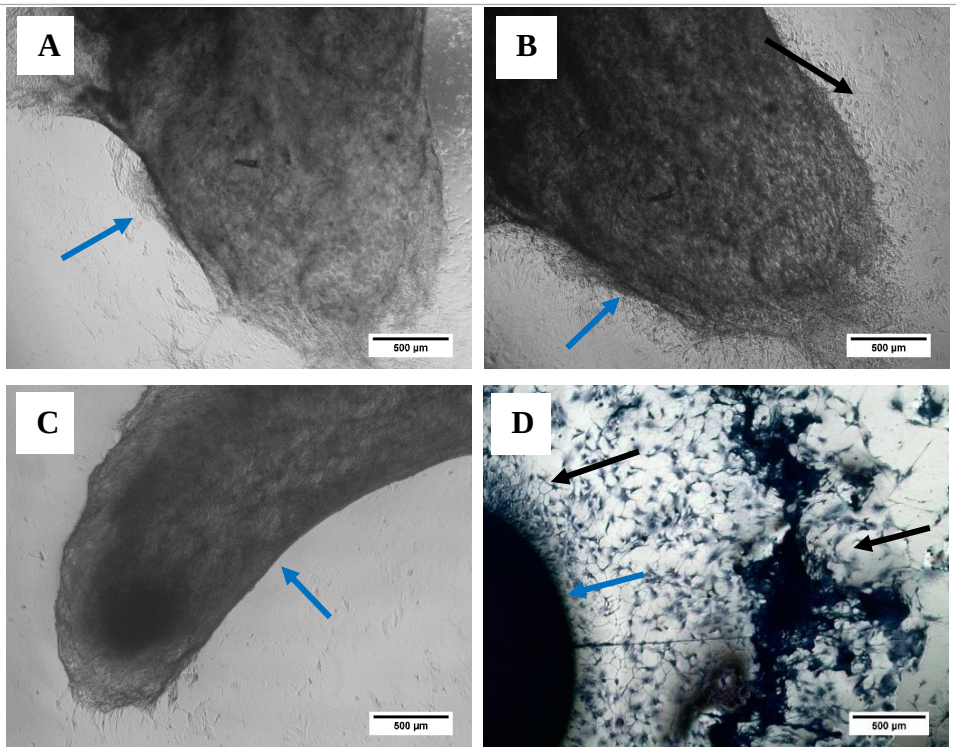

Figure 7.3 Light microscopy images of bBM-MSC encapsulated FPA-fibrinogen gels formed using 2 mg.mL^{-1} FPA, blue arrow. Images taken at day 1 (A), day 3 (B), and day 15 (C). Cells were stained with crystal violet at day 15 (D) black arrows point to a representation of migratory cells. Images were taken at a magnification of x4. Scale bars are shown on the image.

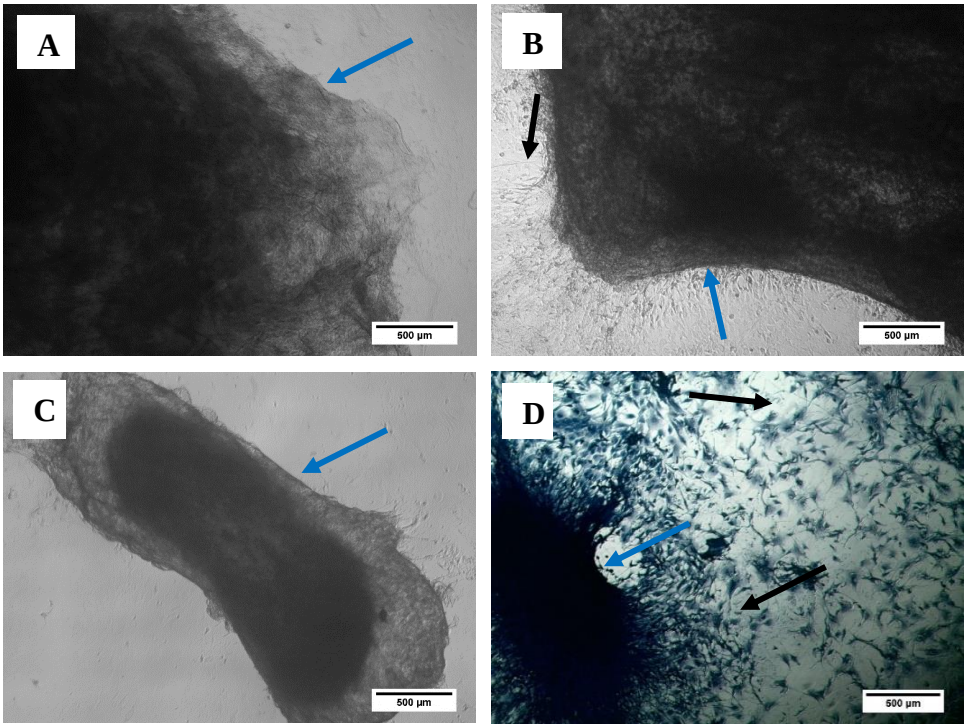

Figure 7.4 Light microscopy images of bBM-MSC encapsulated FPA-fibrinogen gels formed using 1.33 mg.mL^{-1} FPA blue arrow. Images taken at day 1 (A), day 3 (B), and day 15 (C). Cells were stained with crystal violet at day 15 (D) black arrows point to a representation of migratory cells. Images were taken at a magnification of x4. Scale bars are shown on the image.

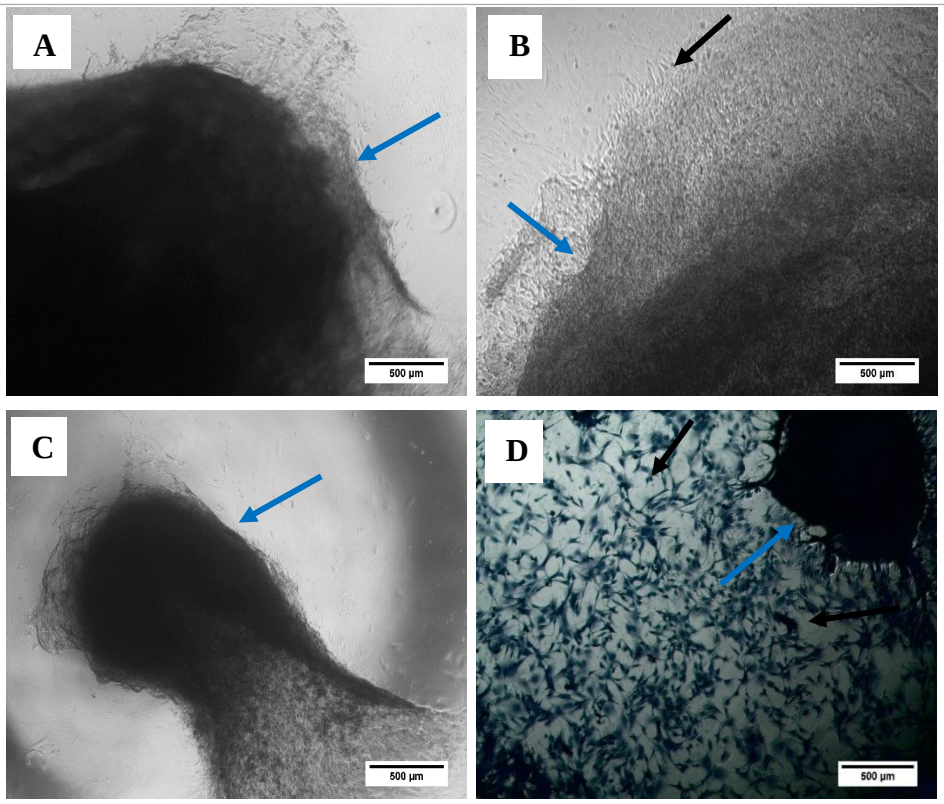

Figure 7.5 Light microscopy images of bBM-MSC encapsulated FPA-fibrinogen gels formed using 0.7 mg.mL^{-1} FPA, blue arrow taken at day 1 (A), day 3 (B), and day 15 (C). Cells were stained with crystal violet at day 15 (D) black arrows point to a representation of migratory cells. Images were taken at a magnification of x4. Scale bars are shown on the image.

7.1.1 Encapsulation of osteoblastic cell MG63

Osteoblastic MG63 cells were encapsulated in fibrin, and FPA-fibrinogen gels formed from 2.66 mg.mL^{-1}, 2 mg.mL^{-1}, 1.33 mg.mL^{-1}, and 0.7 mg.mL^{-1} FPA and incubated in basic αMEM culture medium as described in section 4.2.5. In common with the bBM-MSCs, the cells rapidly migrated from all the gels. By day 7 the gels had greatly diminished in size and the MG63 cells migrated outward on the surface of the culture wells, shown by the black arrows in image D, Figure 7.6 to Figure 7.10. In contrast, no apparent gel shrinkage/degradation was observed in the cell free gel controls. Figure 7.6 to Figure 7.9 shows phase contrast microscopy images of the encapsulated MG63 and cell free controls. These figures clearly show the shrinkage of the encapsulated gels and the migration of the MG63 cells. Therefore, it was decided to investigate the mechanism of gel degradation that was occurring in the fibrin and FPA-fibrinogen gels encapsulated with MG63s and bBM-MSCs. The actual decrease in size of the cell encapsulated gels suggested a fibrinolysis mechanism

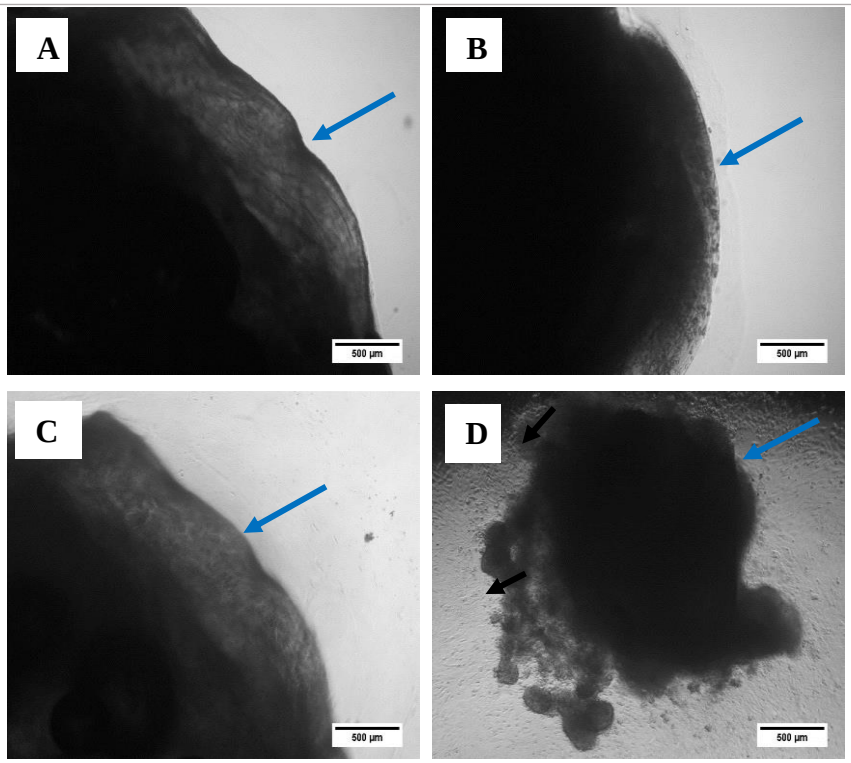

Figure 7.6 Light microscopy images of cell free (A and C) and MG63 encapsulated (C and D) fibrin gels, blue arrow, at day 1 (A and B) and day 7 (C and D) of encapsulation. Black arrows show MG63s adhering to the tissue culture plastic surrounding the gel. The images were taken at a magnification of x4. Scale bars are shown on the image

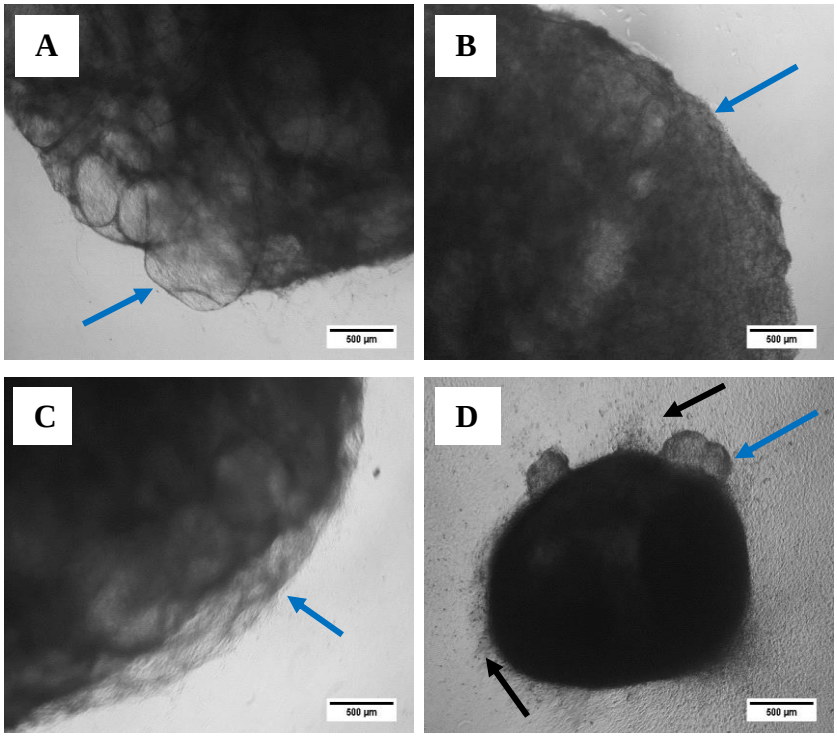

Figure 7.7 Light microscopy images of cell free (A and C) and MG63 encapsulated (C and D) FPA-fibrinogen gels, blue arrows, formed using 2.66 mg.mL^{-1} FPA at day 1 (A and B) and day 7 (C and D) of encapsulation. Black arrows show the cells adhering to the tissue culture plastic surrounding the gel. The images were taken at a magnification of x4. Scale bars are shown on the image.

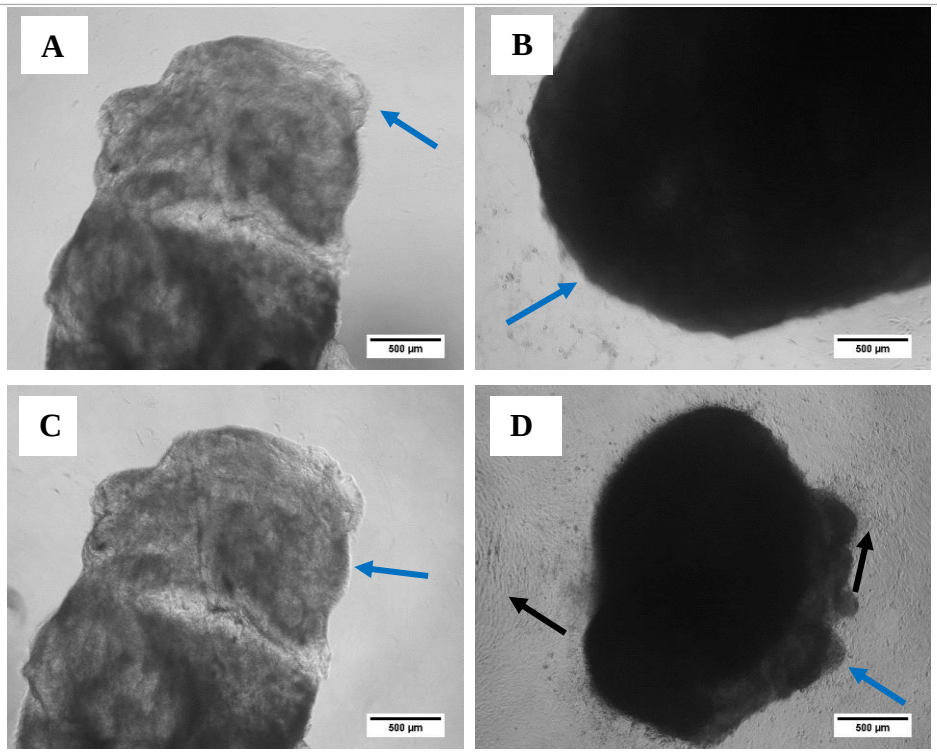

Figure 7.8 Light microscopy images of cell free (A and C) and MG63 encapsulated (C and D) FPA-fibrinogen gels, blue arrows, formed using 2 mg.mL^{-1} FPA at day 1 (A and B) and day 7 (C and D) of encapsulation. Cells escaping from the gel in image D, have been shown by the black arrow. The images were taken at a magnification of x4. Scale bars are shown on the image.

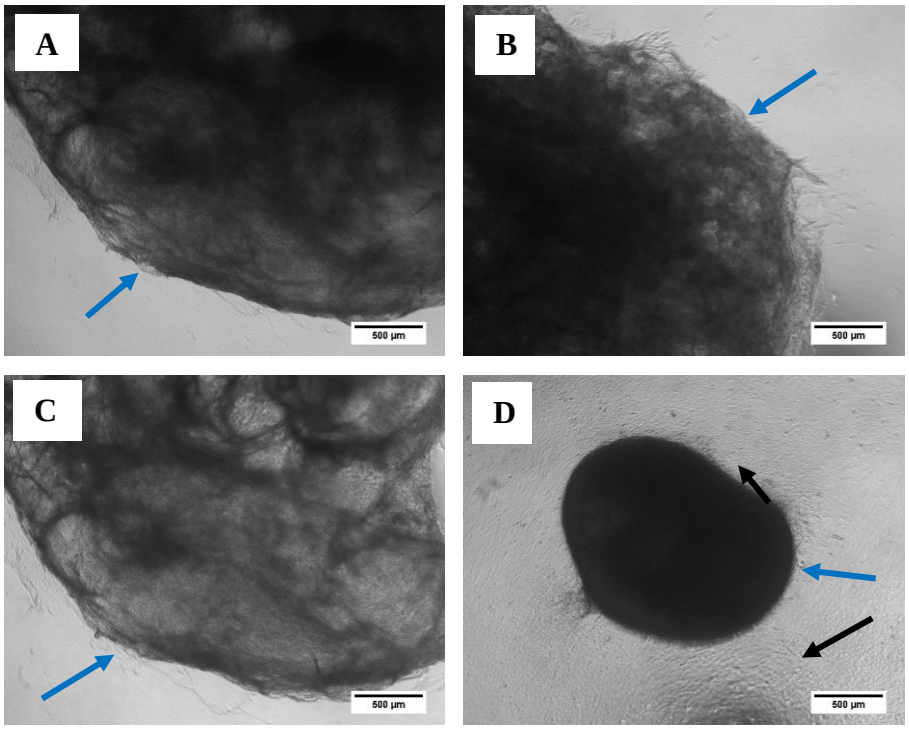

Figure 7.9 Light microscopy images of cell free (A and C) and MG63 encapsulated (C and D) FPA-fibrinogen gels formed using 1.33 mg.mL^{-1} FPA, blue arrow, at day 1 (A and B) and day 7 (C and D) of encapsulation. The black arrows show the MG63s that have escaped from the gel. The images were taken at a magnification of x4. Scale bars are shown on the image.

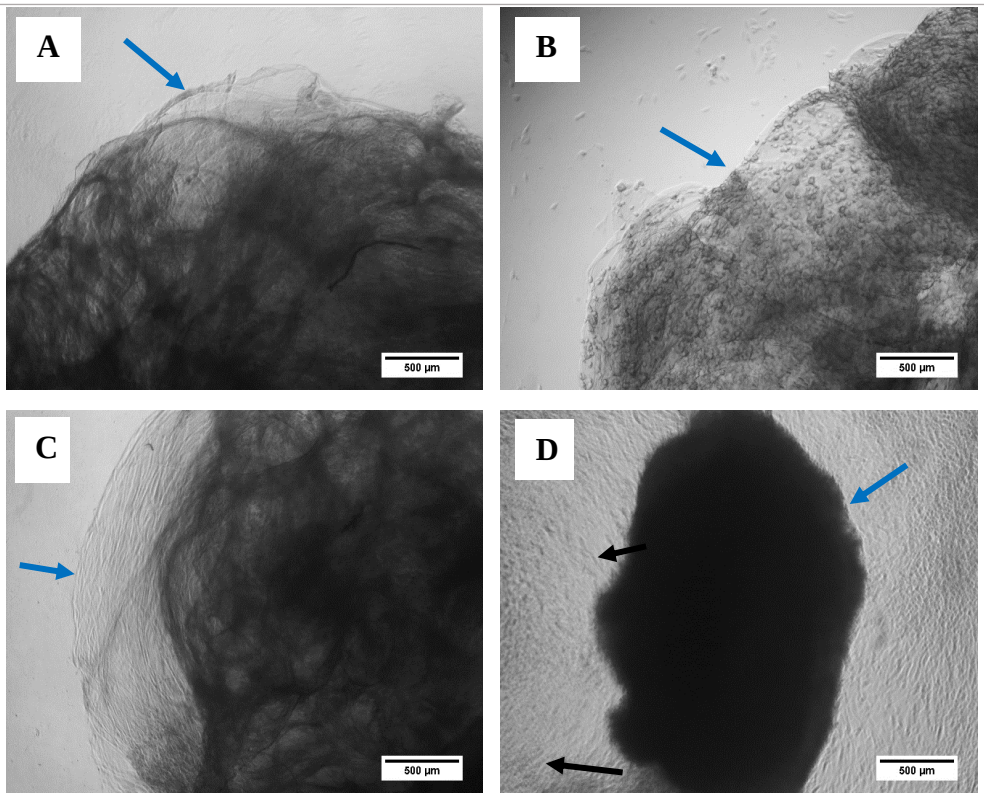

Figure 7.10 Light microscopy images of cell free (A and C) and MG63 encapsulated (C and D) FPA-fibrinogen gels formed using 0.7 mg.mL^{-1} FPA, blue arrow, at day 1 (A and B) and day 7 (C and D) of encapsulation. MG63s migrated out of the gel and this is shown by the black arrow. The images were taken at a magnification of x4. Scale bars are shown on the image.

7.1.2 Investigation of the mechanism responsible for cell migration and gel degradation

Investigations were carried out to determine the cause of FPA-fibrinogen and fibrin gel degradation and the migration of bBM-MSCs and MG63s from the FPA-fibrinogen and fibrin gels. *In vivo*, the fibrin structure of blood clots is broken down by fibrinolysis. The activation of plasminogen in the plasma is activated to a serine protease, plasmin which causes the breakdown of the fibrin clots. The *in vitro* incubations of the fibrin and FPA-fibrinogen gels was carried out in culture medium containing serum. The serum may have been a source of plasminogen which could have been activated by enzymes released by the MG63 cells and bBM-MSCs. Alternatively, the BM-MSCs and MG63 cells may have released ECM-degrading enzymes such as matrix metalloproteinases (MMP).

Two mechanisms were therefore investigated: fibrinolysis and MMP activity. Plasmin was inhibited by incubated with gels with a serine protease inhibitor, aprotinin. MMP's

were inhibited with Marimastat. Inhibition of plasmin and MMP's were therefore used to determine the cause of the gel degradation.

To determine if the activation of plasminogen was the cause of gel degradation FPA-fibrinogen gels formed from the concentration of 2.66 mg.mL^{-1} FPA and fibrin gels were encapsulated with 300,000 bBM-MSCs per gel. As described in section 4.7, these gels were incubated for 3 days in basic culture medium. After 3 days of culture, the medium was removed and replaced with serum-free medium containing 50 µM plasminogen for 24 hours. The inhibitors aprotinin and Marimastat were added to the culture medium to determine the mechanism of gel degradation.

After the incubation, gels were examined by phase contrast microscopy. Preliminary data, Figure 7.11 and Figure 7.15, showed incubation of plasminogen with cell free fibrin and FPA-fibrinogen gels formed using 2.66 mg.mL^{-1} FPA, blue arrows, had no effect on the macroscopic structure. However, incubating the FPA-fibrinogen (Figure 7.16) and fibrin (Figure 7.12) encapsulated bBM-MSCs gels with plasminogen resulted in bBM-MSC migration from the fibrinogen gels. This suggested that the bBM-MSCs produced an enzyme which either activated plasminogen to plasmin or directly degraded the fibrinogen-based gels. Gel degradation and bBM-MSC migration was investigated further by incubating the gels with aprotinin, a serine protease inhibitor, or Marimastat, a MMP inhibitor, in the serum-free culture conditions with plasminogen.

Incubation with Marimastat did not inhibit the degradation of the fibrin gels and FPA-fibrinogen gels 2.66 mg.mL^{-1} FPA as seen in Figure 7.13 and Figure 7.17, respectively. The addition of aprotinin inhibited gel degradation and reduced cell migration, shown from the crystal violet stain in fibrin and FPA-fibrinogen gels (2.66 mg.mL^{-1} FPA), shown by black arrows in Figure 7.14 and Figure 7.18, respectively. The inhibition of FPA-fibrinogen and fibrin gel degradation by incubation with aprotinin was investigated further by analysing the medium for plasmin, urokinase plasminogen activator (uPA) and tissue plasminogen activator (tPA).

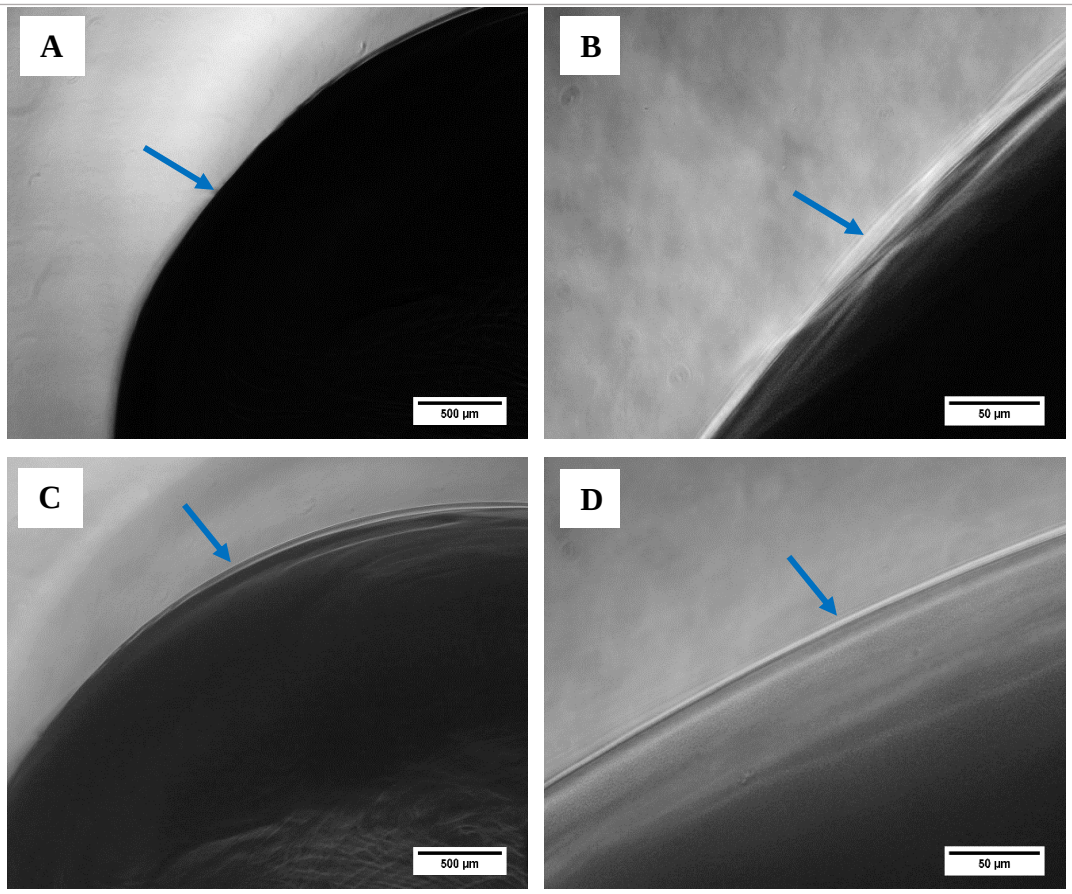

Figure 7.11 Phase contrast images of cell free fibrin gels, blue arrow, before (A and B) and after (C and D) incubation in serum free medium containing plasminogen for 24 hours. The fibrin gels did not degrade during the incubation period. Images were taken at a magnification of x4 (A and C) and x20 (B and D). Scale bars are shown on the image.

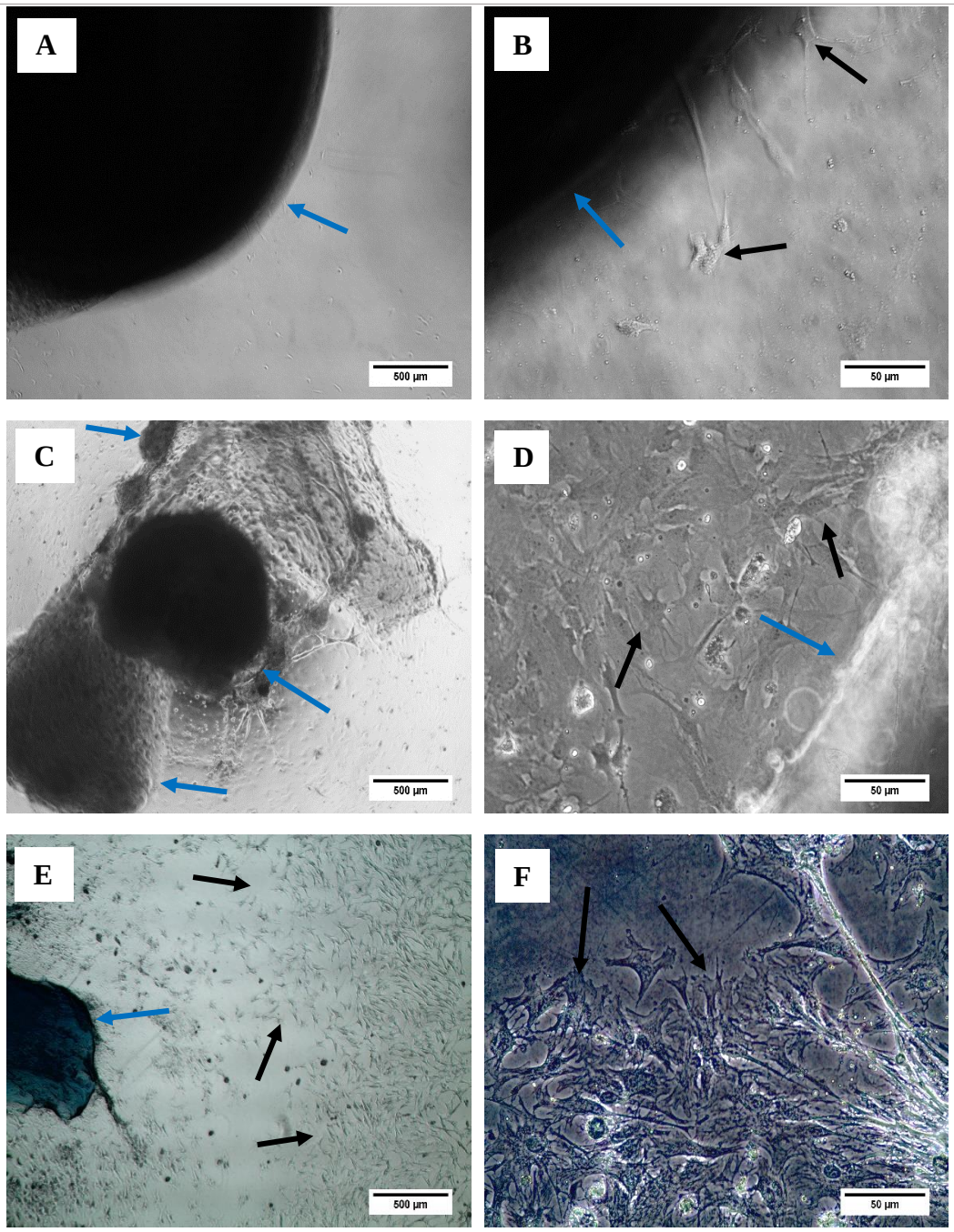

Figure 7.12 Phase contrast images of bBM-MSC encapsulated fibrin gels, blue arrows, before (A and B) and after (C and D) incubation in serum free medium containing plasminogen for 24 hours. C and D show that the fibrin gel degraded, and cell migration occurred, black arrows. Crystal violet stain on hydrogels after incubation with plasminogen (E and F) at a magnification of x4 (A, C and E) and x20 (B, D and F). Scale bars are shown on the image.

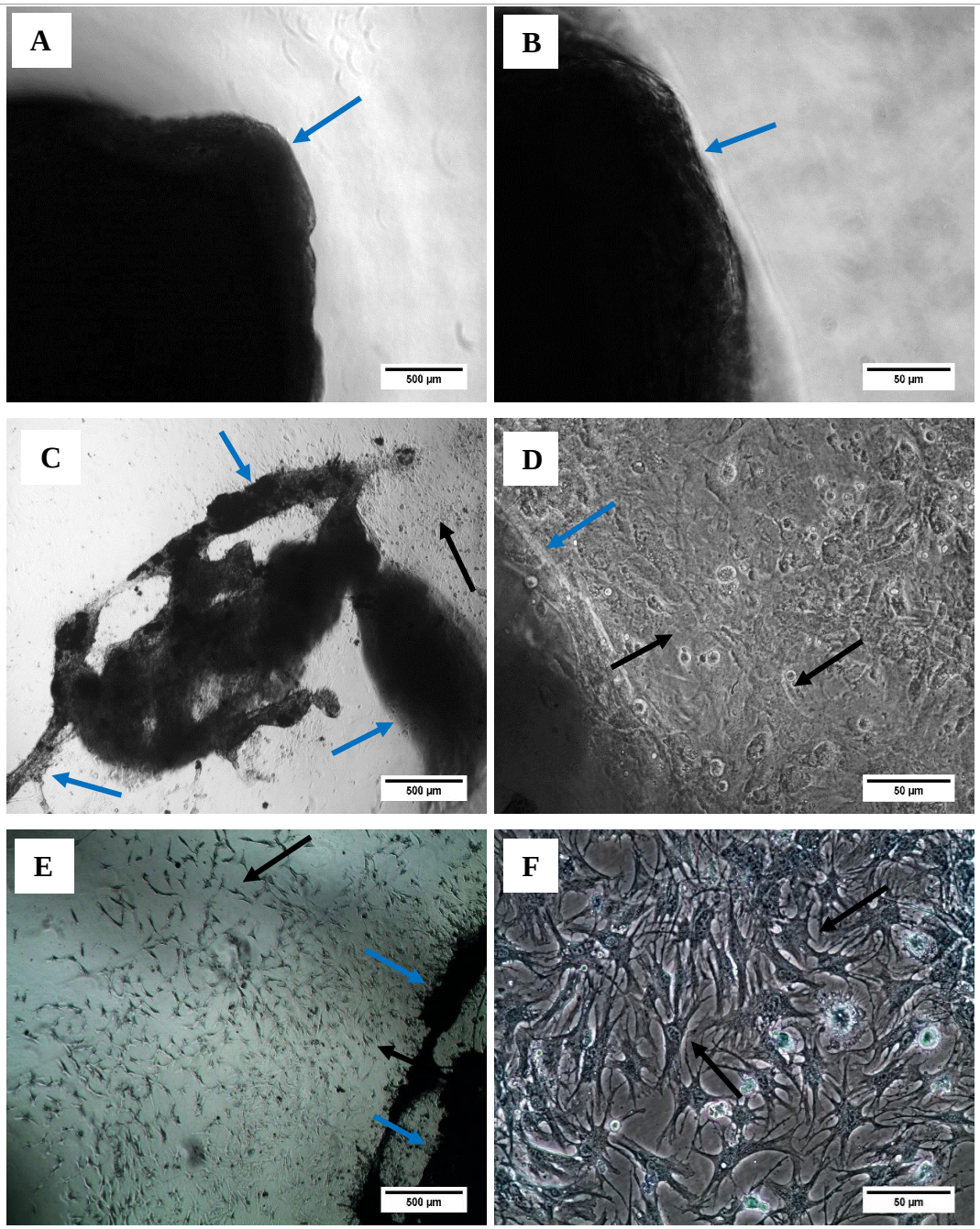

Figure 7.13 Light microscopy images of bBM-MSC encapsulated fibrin gels, blue arrows, before (A and B) and after (C and D) incubation in serum free medium containing plasminogen and Marimastat for 24 hours. C, D, E,F show that the fibrin gel degraded, and cell migration occurred, black arrows. Crystal violet stain on hydrogels after incubation with plasminogen containing Marimastat (E and F) at a magnification of x4 (A, C and E) and x20 (B, D and F). Scale bars are shown on the image.

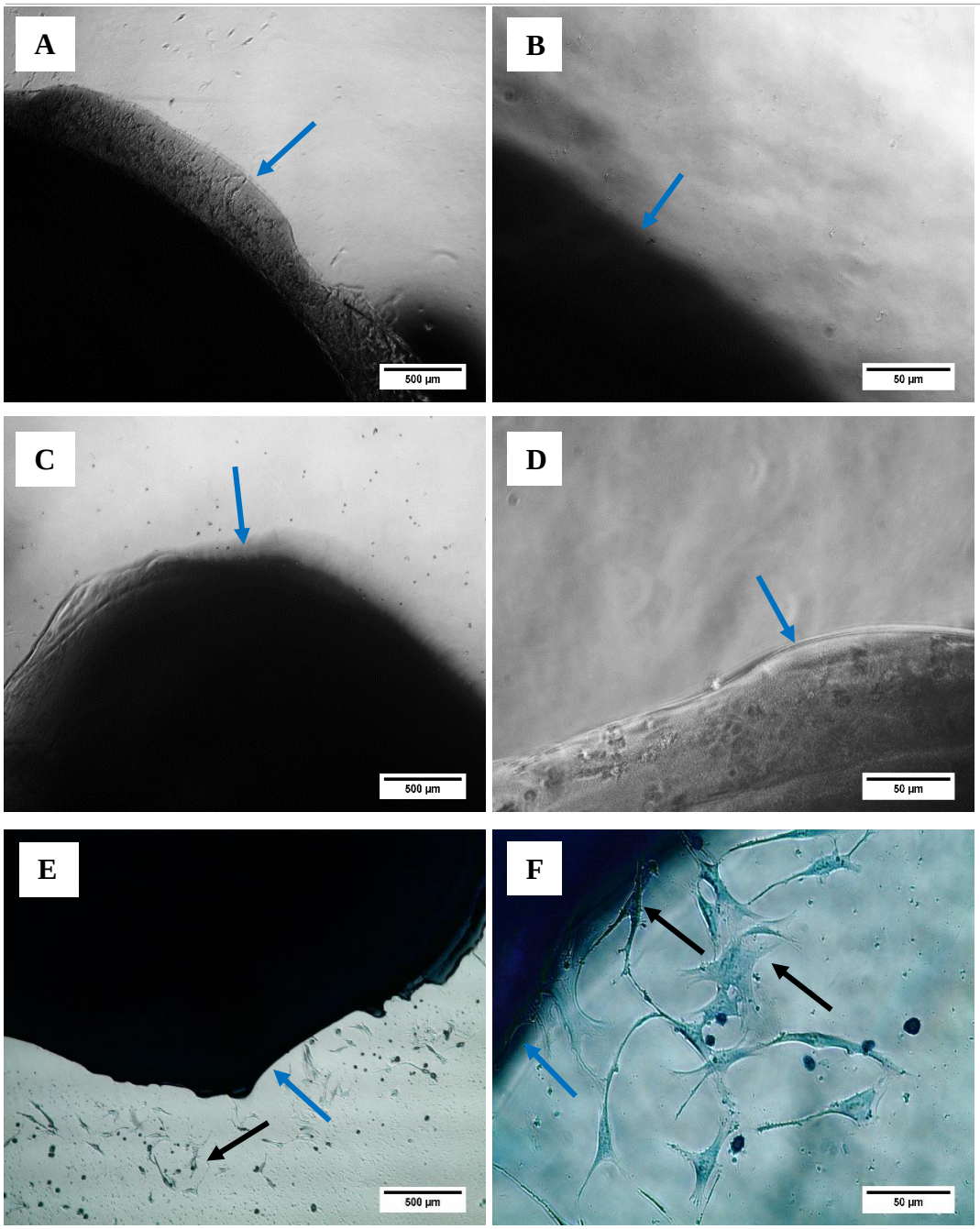

Figure 7.14 Phase contrast images of bBM-MSC encapsulated fibrin gels, blue arrows, before (A and B) and after (C and D) incubation in serum free medium containing plasminogen and 30 µM aprotinin for 24 hoursCrystal violet stain on hydrogels after incubation with plasminogen containing 30 µM aprotinin (E and F) at a magnification of x4 (A, C and E) and x20 (B, D and F). . Little cell migration was observed, black arrows. Scale bars are shown on the image.

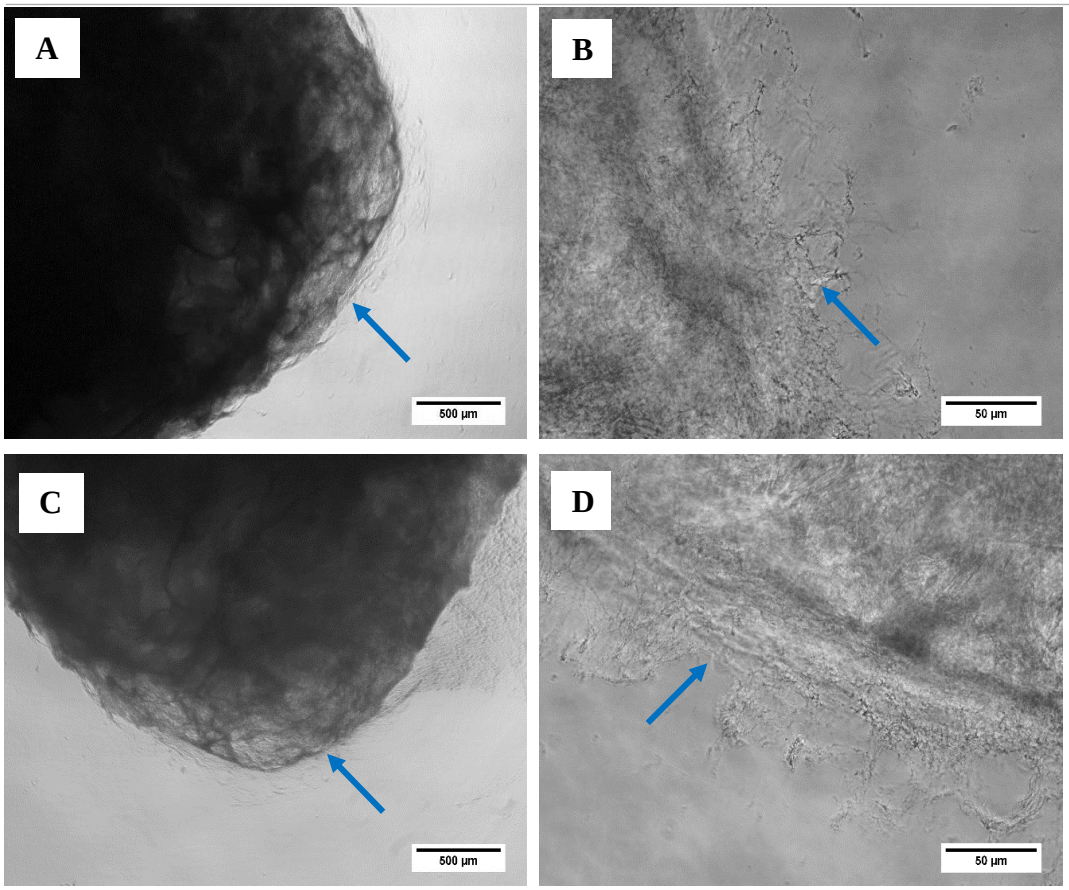

Figure 7.15 Phase contrast images of cell free FPA-fibrinogen 2.66 mg.mL^{-1} gels, blue arrows, before (A and B) and after (C and D) incubation in serum free medium containing plasminogen for 24 hours. Showing that the gels did not degrade. Images were taken at a magnification of x4 (A and C) and x20 (B and D). Scale bars are shown on the image.

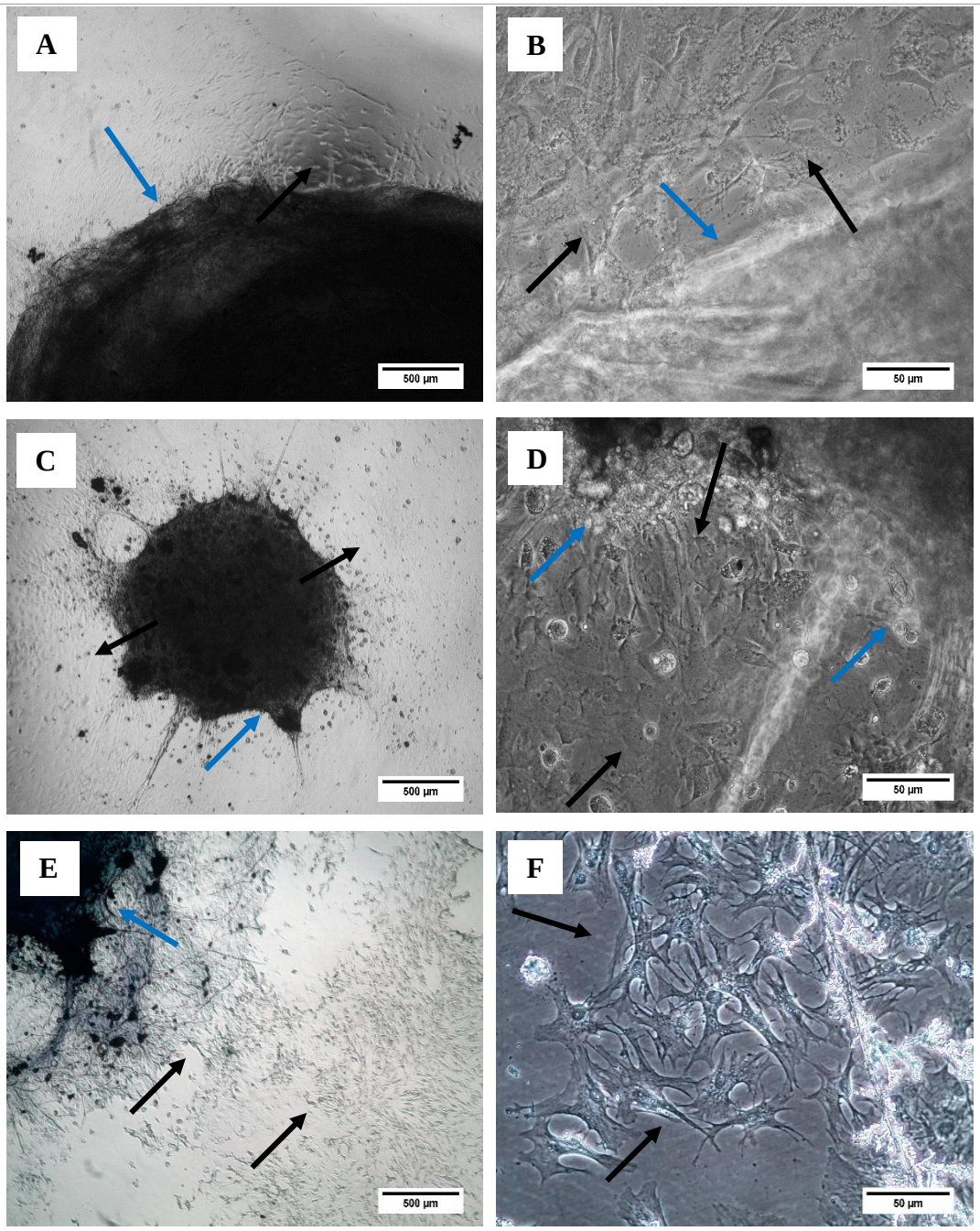

Figure 7.16 Phase contrast images of bBM-MSC encapsulated FPA-fibrinogen 2.66 mg.mL^{-1} gels, blue arrows, before (A and B) and after (C and D) incubation in serum free medium containing plasminogen for 24 hours. Crystal violet stain on hydrogels after incubation with plasminogen (E and F). Demonstrating that cell migration, black arrows, and gel degradation occurred. Images taken at a magnification of x4 (A, C and E) and x20 (B, D and F). Scale bars are shown on the image.

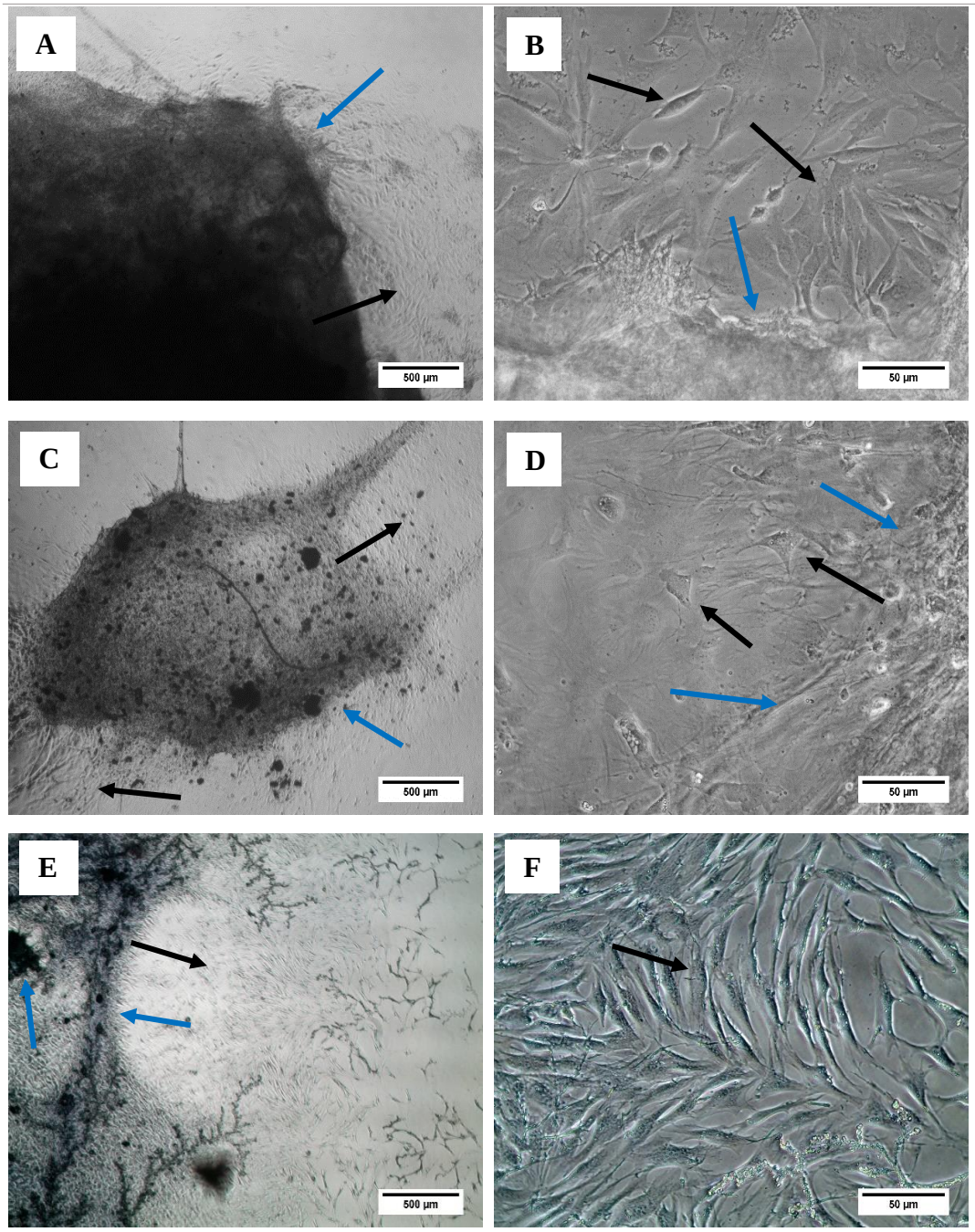

Figure 7.17 Phase contrast images of bBM-MSC encapsulated FPA-fibrinogen 2.66 mg.mL^{-1} gels, blue arrows, before (A and B) and after (C and D) incubation in serum free medium containing plasminogen and Marimastat for 24 hours. Crystal violet stain on hydrogels after incubation with plasminogen containing Marimastat (E and F) at a magnification of x4 (A, C and E) and x20 (B, D and F). Demonstrating that cell migration, black arrows, and gel degradation occurred (C,D,E,F). Scale bars are shown on the image.

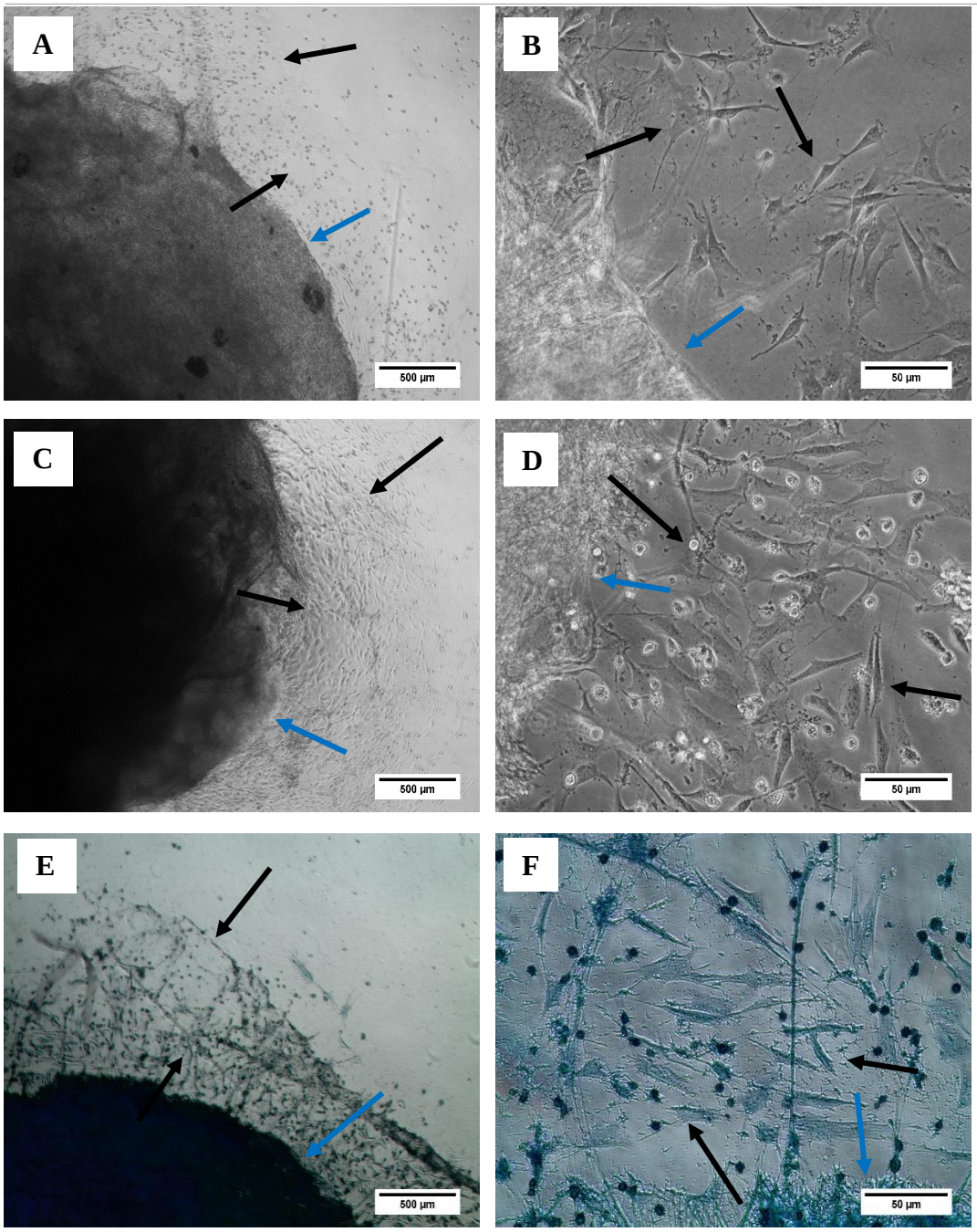

Figure 7.18 Phase contrast images of bBM-MSC encapsulated FPA-fibrinogen 2.66 mg.mL^{-1} gels, blue arrows, before (A and B) and after (C and D) incubation in serum free medium containing plasminogen and 30 µM aprotinin for 24 hours. Crystal violet stain on hydrogels after incubation with plasminogen containing 30 µM aprotinin (E and F) at a magnification of x4 (A, C and E) and x20 (B, D and F). Demonstrating that the gel did not degrade but some cell migration occurred, back arrows (C, D, E, F). Scale bars are shown on the image.

7.1.3 Plasmin, uPA and tPA detection

A serine protease inhibitor, aprotinin, inhibited FPA-fibrinogen and fibrin gel degradation and bBM-MSC migration from the gels. The gels were incubated with plasminogen for 24 hours in serum-free conditions. The medium was collected and analysed for plasmin, the presence of plasmin would suggest that bBM-MSCs are activating plasminogen to plasmin. The presence of plasmin would cause FPA-fibrinogen and fibrin gel degradation by fibrinolysis, as described previously. The medium collected from bBM-MSC encapsulated FPA-fibrinogen and fibrin gels incubated without inhibitors and with the inhibitors aprotinin and Marimastat were analysed. Figure 7.19 shows the plasmin levels of culture medium with and without plasminogen incubation, cell free FPA-fibrinogen and fibrin gels, bBM-MSC encapsulated gels with and without Marimastat or aprotinin.

Culture medium, incubated with and without plasminogen was analysed for plasmin within the samples and no plasmin was detected, see Figure 7.19 (A). This suggested that plasmin is not present in the culture medium used and therefore was not causing the fibrinogen gel degradation. The medium collected from cell free FPA-fibrinogen (2.66 $mg.mL^{-1}$ FPA) and fibrin gels incubated with plasminogen, revealed no plasmin within the samples, Figure 7.19 (A). Significantly higher levels of plasmin was detected in the medium from samples collected from the incubation of bBM-MSC encapsulated FPA-fibrinogen and fibrin gels with and without the incubation with Marimastat, Figure 7.19, (B). The bBM-MSC encapsulated FPA-fibrinogen and fibrin gels incubated with aprotinin resulted in no plasmin detection, Figure 7.19 (C). The data was significantly lower compared to bBM-MSC encapsulated FPA-fibrinogen gels (2.66 $mg.mL^{-1}$ FPA) and fibrin gels incubated without inhibitors or with Marimastat.

Due to the inhibition of gel degradation with aprotinin, there was evidence to suggest that the activation of plasminogen to plasmin was causing gel degradation. The mechanism for plasminogen activation was investigated by analysing uPA and tPA levels in the previously collected medium. uPA and tPA are serine proteases known to be secreted by some cell types and are activators of plasminogen to plasmin. tPA and uPA levels in the medium for FPA-fibrinogen (2.66 $mg.mL^{-1}$ FPA) and fibrin encapsulated with bBM-MSCs and incubated without inhibitors and in the presence of aprotinin or Marimastat. All medium collected, from all conditions was barely detectable, therefore preliminary data suggested that uPA and tPA were not activating the plasminogen, results are shown in Figure 7.20 and Figure 7.21.

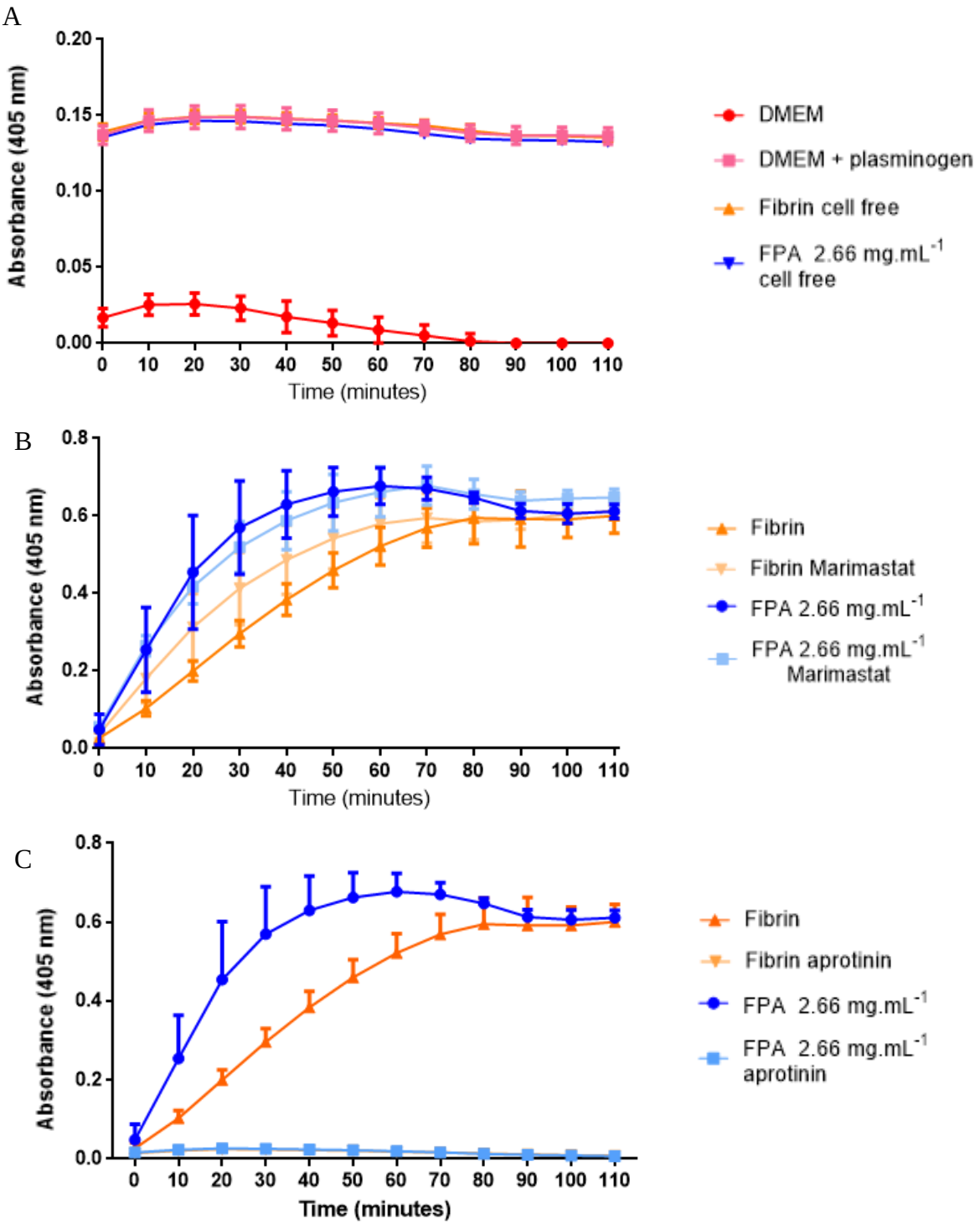

Figure 7.19 Plasmin activity in serum-free medium (DMEM) incubated with (**A**) cell free fibrin and FPA-fibrinogen 2.66 mg.mL^{-1} gels, and bBM-MSC encapsulated fibrin and FPA-fibrinogen 2.66 mg.mL^{-1} gels incubated with and without (**B**) Marimastat and (**C**) aprotinin, for 24 hours containing plasminogen, and serum free culture medium with and without plasminogen. N=2

Table 7.1 One way ANOVA with Tukey post-test comparing the group means statistical analysis of the plasmin detection assay. Significance **** P>0.0001.

Tukey's multiple comparisons test	95% CI of diff.	Summary
DMEM vs. Fibrin no inhibitors	-0.6453 to -0.5414	****
DMEM vs. Fibrin + Marimastat	-0.6556 to -0.5517	****
DMEM + plasminogen vs. Fibrin + Marimastat	-0.6367 to -0.5328	****
DMEM + plasminogen vs. Fibrin + Marimastat	-0.6470 to -0.5431	****
Fibrin cell free vs. Fibrin no inhibitors	-0.6376 to -0.5337	****
Fibrin cell free vs. Fibrin + Marimastat	-0.6478 to -0.5440	****
Fibrin no inhibitors vs. Fibrin + aprotinin	0.5491 to 0.6530	****
Fibrin Marimastat vs. Fibrin aprotinin	0.5594 to 0.6632	****
DMEM + plasminogen vs. FPA + aprotinin	-0.6571 to -0.5533	****
DMEM + plasminogen vs. FPA + Marimastat	-0.6893 to -0.5855	****
DMEM vs. FPA no inhibitors	-0.6657 to -0.5619	****
DMEM vs. FPA + Marimastat	-0.6979 to -0.5941	****
FPA cell free vs. FPA no inhibitors	-0.6610 to -0.5572	****
FPA cell free vs. FPA + Marimastat	-0.6932 to -0.5894	****
FPA no inhibitors vs. FPA + aprotinin	0.5631 to 0.6670	****
FPA + Marimastat . FPA + aprotinin	0.5953 to 0.6992	****

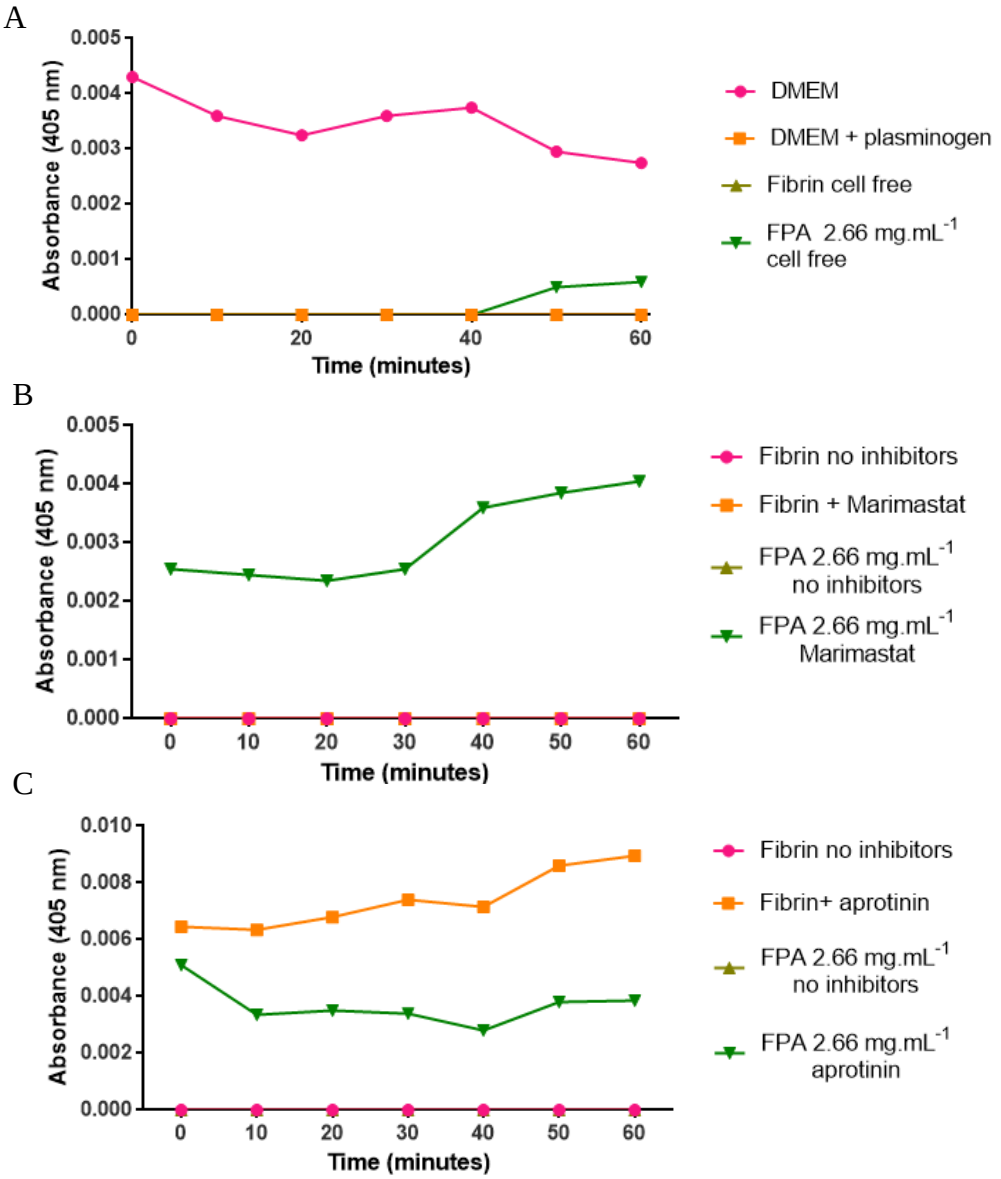

Figure 7.20 uPA activity (shown as absorbance) measured from the medium taken from the incubation of (**A**) cell free 2.66 mg.mL^{-1} FPA-fibrinogen and fibrin gels in serum-free medium (DMEM) and culture medium containing plasminogen, and 2.66 mg.mL^{-1} FPA-fibrinogen and Fibrin gels encapsulated with bBM-MSCs in serum-free medium containing plasminogen with and without (**B**) Marimastat, and (**C**) aprotinin. N=1

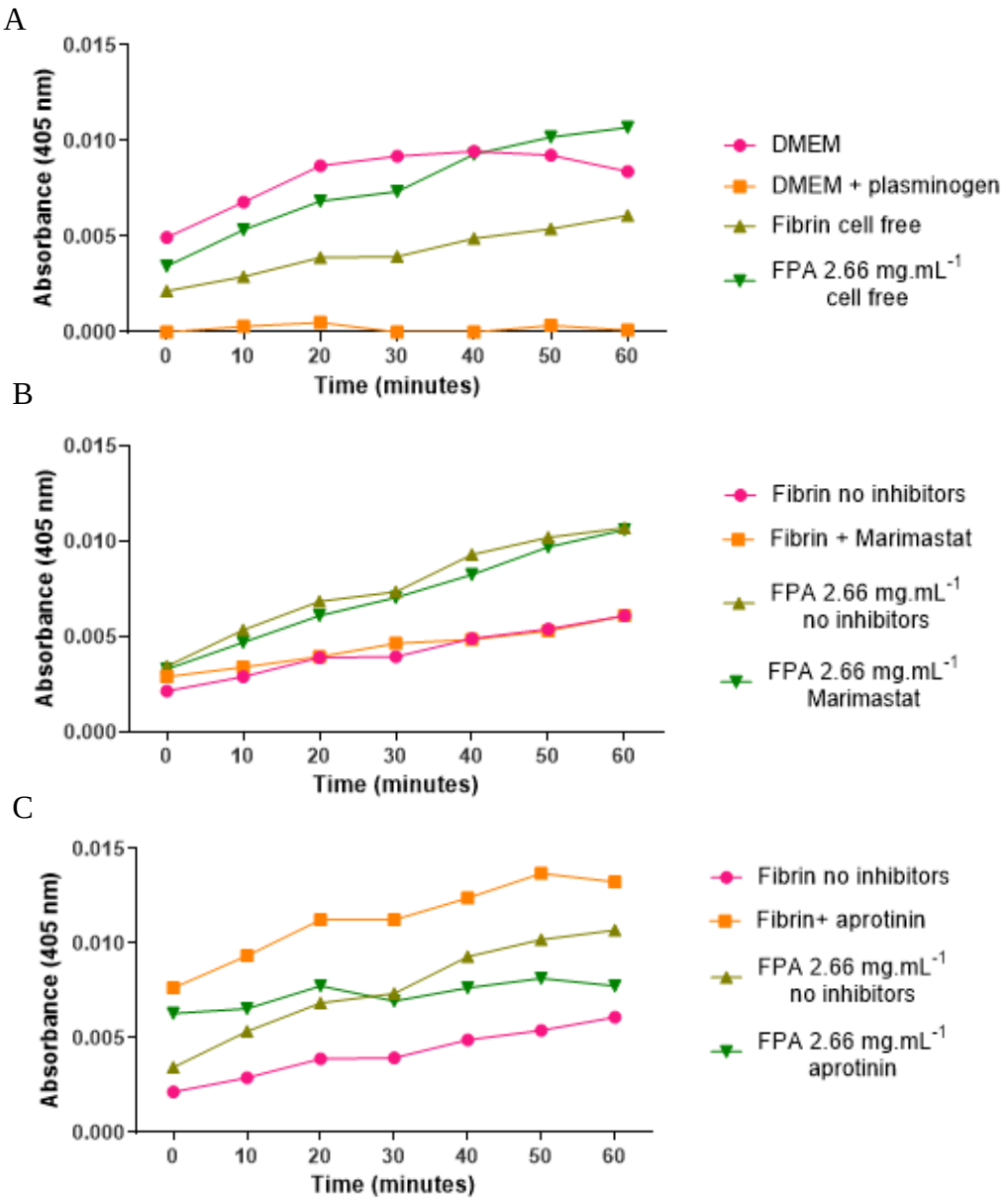

Figure 7.21 tPA activity (shown as absorbance) measured from the medium taken from the incubation of (**A**) cell free 2.66 mg.mL^{-1} FPA-fibrinogen and fibrin gels in serum-free medium (DMEM) and culture medium containing plasminogen, and 2.66 mg.mL^{-1} FPA-fibrinogen and Fibrin gels encapsulated with bBM-MSCs in serum-free medium containing plasminogen with and without (**B**) Marimastat, and (**C**) aprotinin. N=1

7.1.4 Detection of plasmin, uPA and tPA in chondrocyte encapsulated gels

It has been previously established (see section 6.2) that the chondrocytes remained in encapsulation of the FPA-fibrinogen and fibrin gels. Therefore, the activity of plasmin, uPA and tPA was investigated in chondrocyte encapsulated fibrinogen gels. This is because if plasmin was present with chondrocyte encapsulated gels, then the mechanism for gel degradation could not be due to plasmin. Therefore, cell free and chondrocyte encapsulated FPA-fibrinogen gels formed from 2.66 $mg.mL^{-1}$ FPA and fibrin gels were incubated in serum free conditions with plasminogen for 24 hours. The medium was analysed for plasmin, uPA and tPA. Figure 7.23 and Figure 7.24 suggested that uPA and tPA was barely detectable in the medium incubated with fibrin and FPA-fibrinogen 2.66 $mg.mL^{-1}$ gels encapsulated with or without chondrocytes. Plasmin levels were also investigated in the medium incubated in serum-free conditions containing plasminogen for 24 hours. Figure 7.22 shows the plasmin levels contained in the control samples: serum-free medium and serum-free medium with plasminogen, very low plasmin was detected within these samples. Figure 7.22 shows that virtually no plasmin was detected in the chondrocyte encapsulated FPA-fibrinogen 2.66 $mg.mL^{-1}$ and fibrin gels and therefore plasminogen is not being activated to plasmin, under the conditions used. This suggested that the mechanism of gel degradation is plasmin.

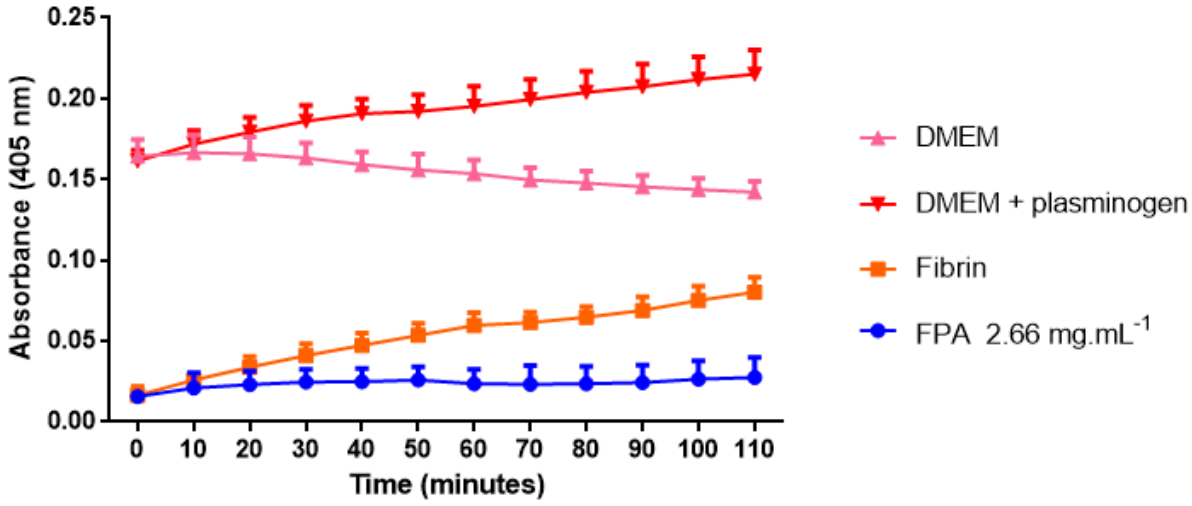

Figure 7.22 Plasmin activity (shown as absorbance) measured from serum-free medium (DMEM), serum-free medium incubated with plasminogen, the medium taken from the incubation of chondrocyte encapsulated 2.66 $mg.mL^{-1}$ FPA-fibrinogen and fibrin gels in serum-free medium containing plasminogen. N=2

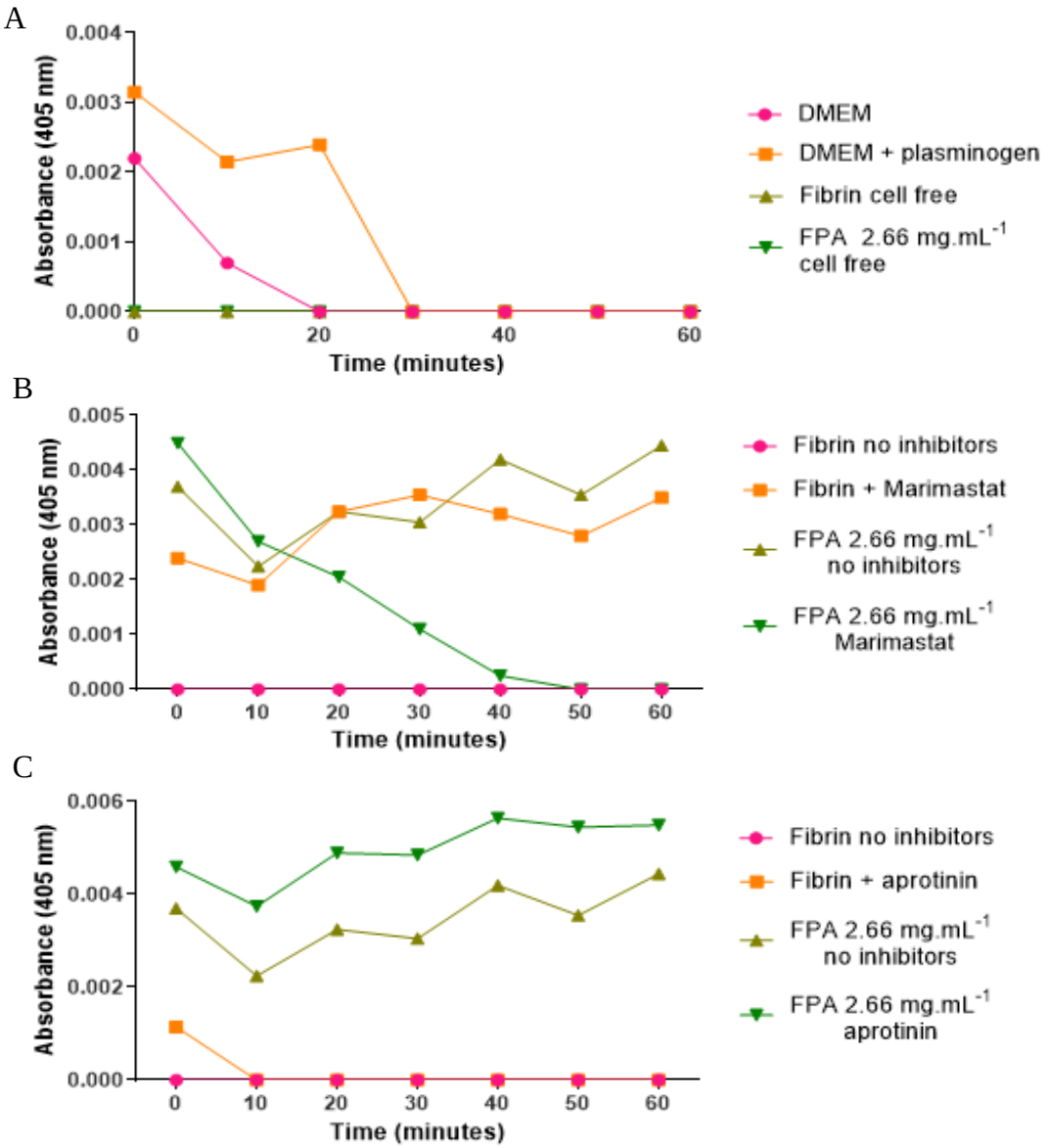

Figure 7.23 uPA levels (shown as absorbance) measured from the medium taken from the incubation of (**A**) cell free 2.66 mg.mL^{-1} FPA-fibrinogen and fibrin gels in serum-free medium (DMEM) and culture medium containing plasminogen, and chondrocyte encapsulated 2.66 mg.mL^{-1} FPA-fibrinogen and fibrin gels in serum-free medium containing plasminogen with and without (**B**) Marimastat, and (**C**) aprotinin N=1

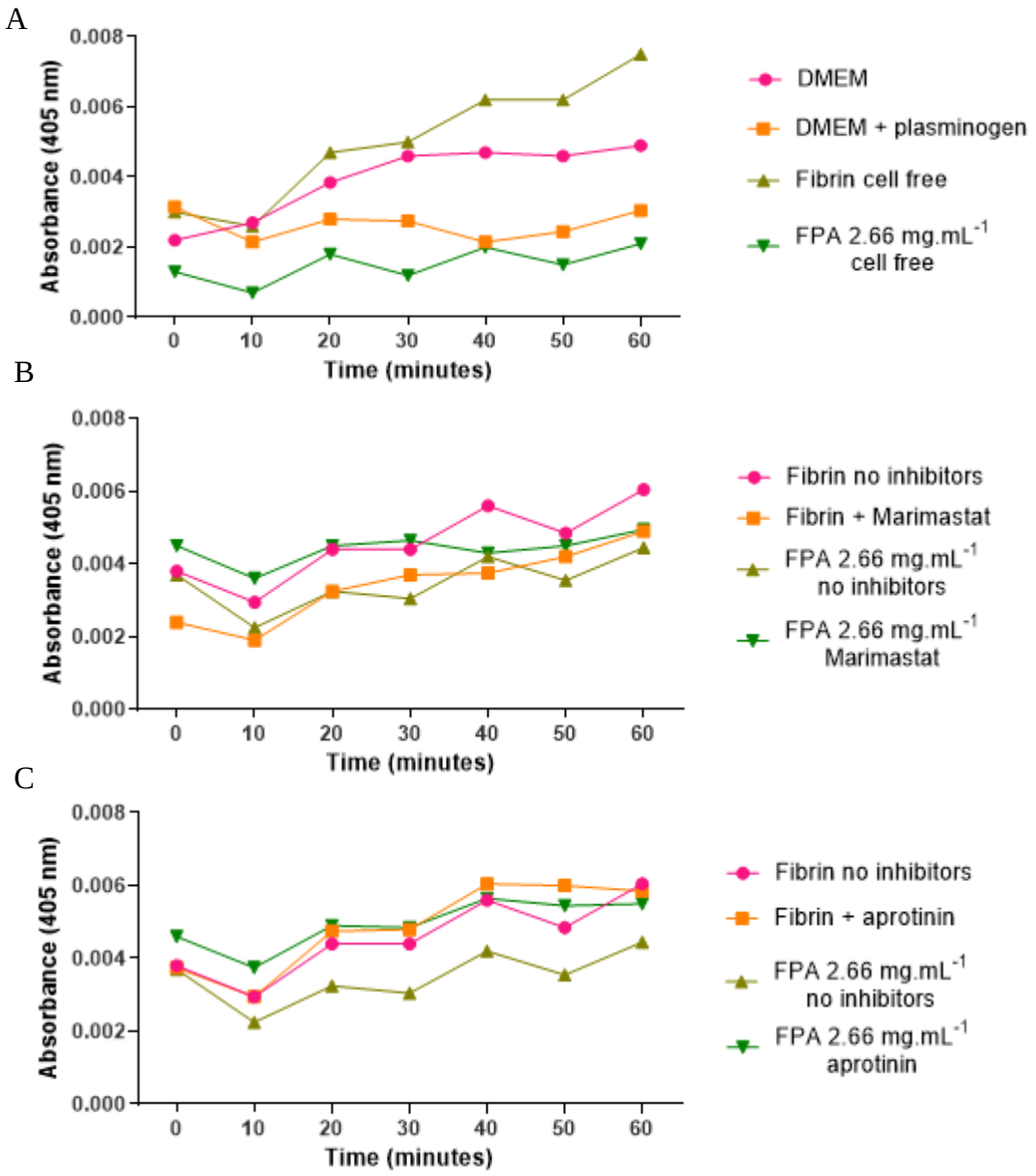

Figure 7.24 tPA activity (shown as absorbance) measured from the medium taken from the incubation of (**A**) cell free 2.66 mg.mL^{-1} FPA-fibrinogen and fibrin gels in serum-free medium (DMEM) and culture medium containing plasminogen, and chondrocyte encapsulated 2.66 mg.mL^{-1} FPA-fibrinogen and fibrin gels in serum-free medium containing plasminogen with and without (**B**) Marimastat, and (**C**) aprotinin N=1

Key Summary

- bBM-MSCs exhibited different behaviour in comparison to chondrocyte encapsulation in FPA-fibrinogen and fibrin gels.
- bBM-MSCs and MG63s migrated from the FPA-fibrinogen and fibrin gels and rapid gel degradation occurred.
- The mechanisms responsible were investigated and incubation with aprotinin reduced bBM-MSC migration and inhibited gel degradation. Inhibition of MMPs had no effect on cell migration or gel degradation.
- Plasmin was detected in all conditions that resulted in gel degradation and not in the presence of aprotinin in which no gel degradation occurred.
- Preliminary data suggested that the activation of plasminogen to plasmin is the cause for FPA – fibrinogen and fibrin gel degradation.

7.2 MSC encapsulation with serum free medium

Previous results suggested that incubation with a serine protease inhibitor, aprotinin, inhibited FPA-fibrinogen and fibrin gel degradation and reduced bBM-MSC migration from the gels, see section 7.3. This suggested that plasminogen activation to plasmin may be causing the degradation of the FPA and fibrin gels. Plasminogen is present in culture serum and is essential for cellular survival. Removing the source of plasminogen i.e. culture serum, was investigated to determine if the FPA-fibrinogen and fibrin gels would undergo degradation.

The FPA-fibrinogen 2.66 $mg.mL^{-1}$ and fibrin gels were encapsulated with 300,000 bBM-MSCs and incubated with and without aprotinin in serum-free conditions for 21 days. Cell free fibrin and FPA-fibrinogen 2.66 $mg.mL^{-1}$ did not degrade over the 21 day culture period, Figure 7.25 and Figure 7.28. The fibrin and FPA 2.66 $mg.mL^{-1}$ gels encapsulated with bBM-MSCs exhibited evidence for cell migration, illustrated by the black arrows, from the gels and FPA-fibrinogen and fibrin gel degradation over the 21 day period, Figure 7.26 and Figure 7.29. However, FPA-fibrinogen 2.66 $mg.mL^{-1}$ and fibrin gels encapsulated with bBM-MSCs and incubated with aprotinin maintained the gel structure throughout the 21 day culture period and less bBM-MSC migration was observed, Figure 7.27 and Figure 7.30.

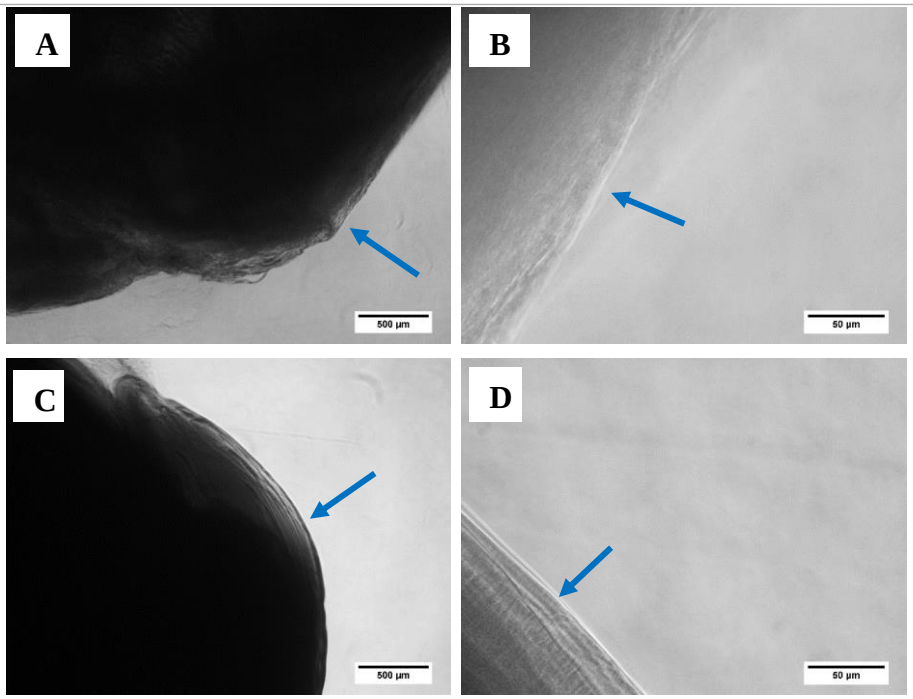

Figure 7.25 Phase contrast images of cell free fibrin gels indicated by the blue arrows. Images were taken at day 1 (A and B) and day 21 (C and D) at a magnification of x4 (A and C) and x20 (B and D). Scale bars are shown on the image.

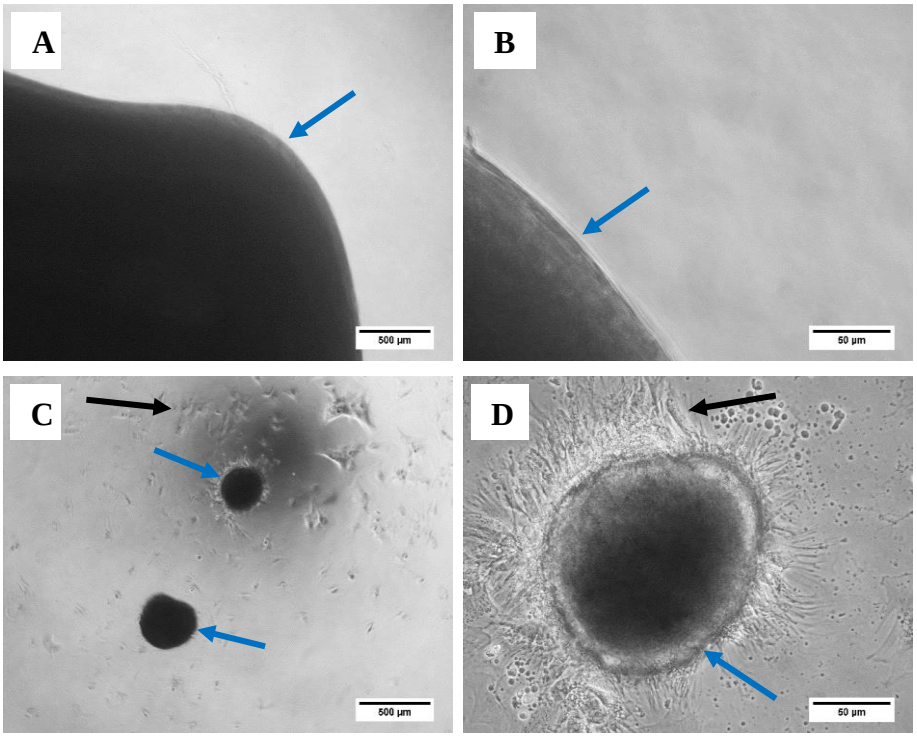

Figure 7.26 Phase contrast images of bBM-MSC encapsulated fibrin gels indicated by the blue arrows. Images were taken at day 1 (A and B) and day 21 (C and D) showing the migration of the cells from the gels, black arrows. Images were taken at a magnification of x4 (A and C) and x20 (B and D). Scale bars are shown on the images.

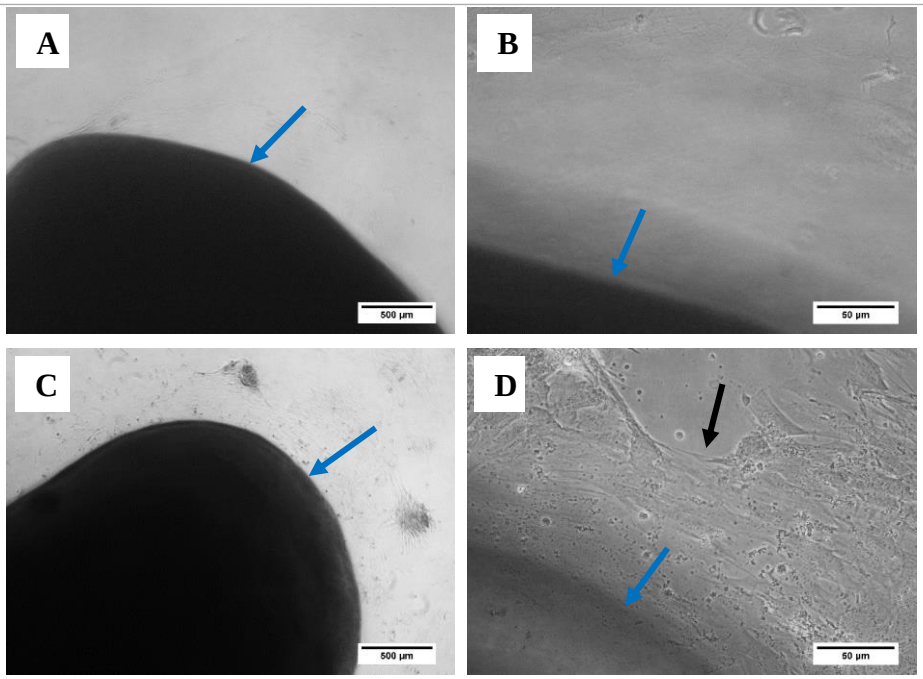

Figure 7.27 Phase contrast images of bBM-MSC encapsulated fibrin gels, blue arrows, incubated with aprotinin. Images were taken at day 1 (A and B) and day 21 (C and D) showing some cell migration from the gels, black arrow. Images were taken at a magnification of x4 (A and C) and x20 (B and D). Scale bars are shown on the image.

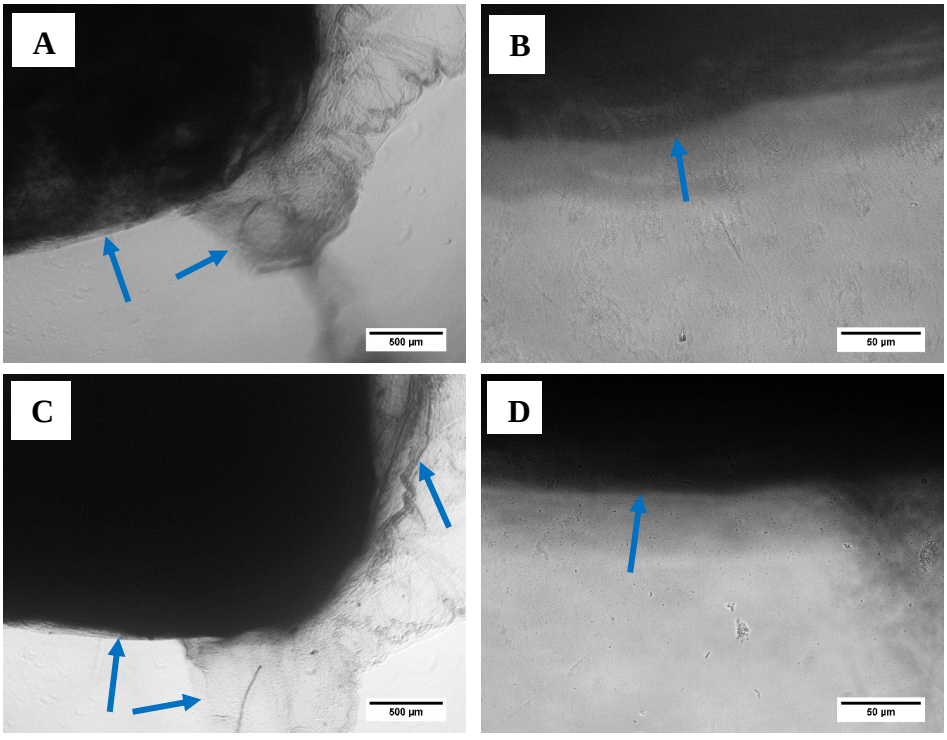

Figure 7.28 Phase contrast images of cell free FPA-fibrinogen 2.66 mg.mL^{-1} gels, blue arrows. Images taken at day 1 (A and B) and day 21 (C and D) at a magnification of x4 (A and C) and x20 (B and D). Scale bars are shown on the image.

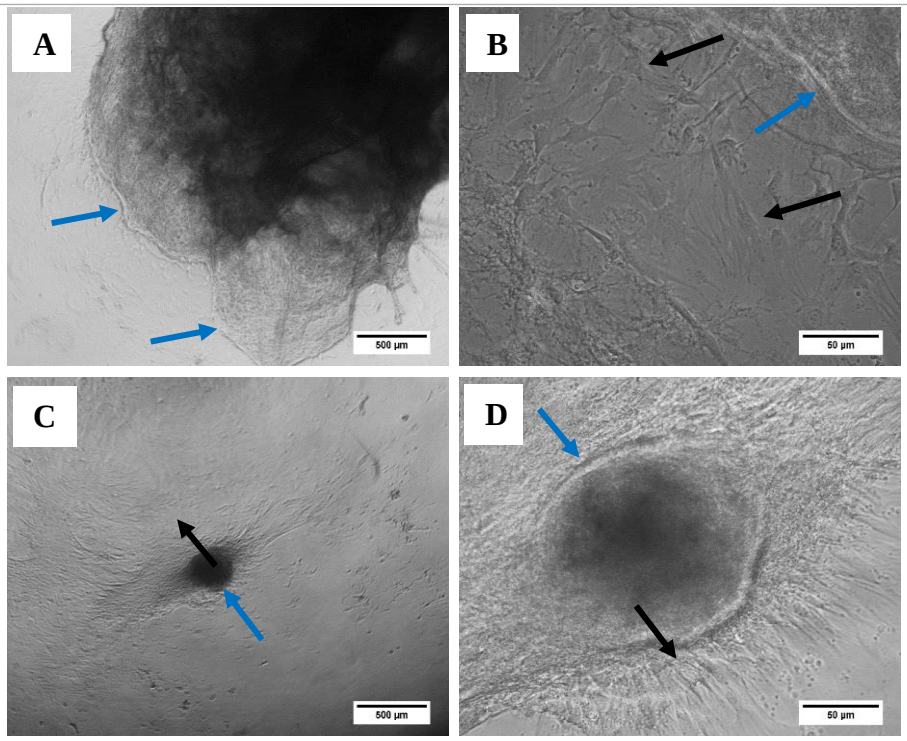

Figure 7.29 Phase contrast images of bBM-MSCs encapsulated in FPA-fibrinogen 2.66 mg.mL^{-1} gels, blue arrows. Images were taken at day 1 (A and B) and day 21 (C and D) showing gel degradation and cell migration from the gels, blue arrows. Images were taken at a magnification of x4 (A and C) and x20 (B and D). Scale bars are shown on the image.

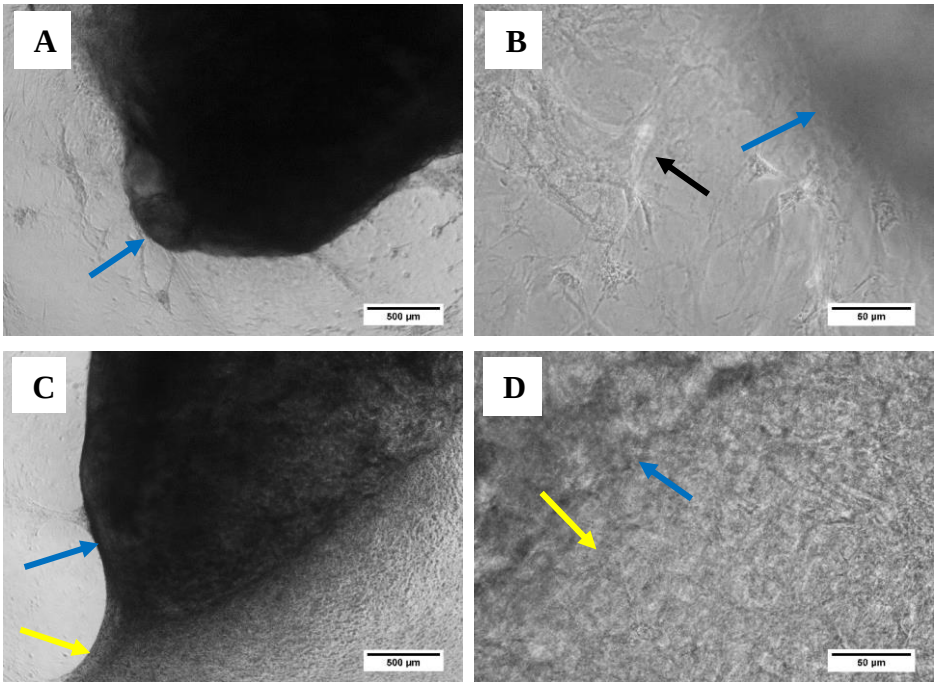

Figure 7.30 Phase contrast images of bBM-MSCs encapsulated in FPA-fibrinogen 2.66 mg.mL^{-1} gels incubated with aprotinin, blue arrows. Images were taken at day 1 (A and B) and day 21 (C and D) showing little gel degradation and gel debris in C and D, yellow arrows. Images were taken at a magnification of x4 (A and C) and x20 (B and D). Scale bars are shown on the image.

Key Summary

- It was previously established that the activation of plasminogen was causing the degradation of the FPA-fibrinogen and fibrin gels when encapsulated with bBM-MSCs. Plasmin was inhibited with aprotinin reducing bBM-MSC migration and FPA-fibrinogen and fibrin gel degradation.
- Removing the source of the plasminogen from the culture medium resulted in FPA-fibrinogen and fibrin degradation over a 21 day culture period.
- The gel degradation was slower in comparison to plasminogen present in the medium but still occurred.
- This suggested that the bBM-MSCs are producing a serine proteinase that is directly causing the degradation of the fibrin and FPA gels. The serine proteinase was inhibited with aprotinin enabling control over the degradation rate.

7.3 MSC encapsulation and culture with aprotinin

As previously shown in section 7.1, aprotinin inhibited gel degradation and reduced bBM-MSC migration from the FPA-fibrinogen and fibrin gels. Therefore, bBM-MSCs were encapsulated in FPA-fibrinogen and fibrin gels for a 21 day culture period and incubated with aprotinin. Cell viability and ECM synthesis was able to be analysed. 300,000 bBM-MSCs were encapsulated in FPA-fibrinogen gels formed from concentrations of 2.66 $mg.mL^{-1}$, 2 $mg.mL^{-1}$, 1.33 $mg.mL^{-1}$, and 0.7 $mg.mL^{-1}$ FPA, and fibrin gels, aprotinin was added to the medium to inhibit FPA-fibrinogen and fibrin gel degradation and minimise bBM-MSC migration from the gels.

Cell viability results

Figure 7.31 (B) shows the resazurin reduction from the culture medium removed from the FPA-fibrinogen and fibrin gels. Very little dye reduction was observed, however a slight peak in reduced dye was observed at day 3, and interestingly this is the time point at which the bBM-MSCs exhibited migration from the gels in the absence of aprotinin. Therefore, this may be very small numbers of cells migrating from the gel. This peak of dye reduction is very small in comparison to the rate of reduction observed from the cell encapsulated FPA-fibrinogen and fibrin gels. The cell free gels also showed very little

reduction is resazurin (Figure 7.31, (A)) suggesting that the gels or the addition of aprotinin interfered with the assay. Figure 7.32 displays the cell viability throughout the 21 days of bBM-MSC encapsulation and showed that the bBM-MSCs were metabolically active and survived in encapsulation of FPA and fibrin gels throughout the 21 day culture period. Although the results are not significantly different, it is interesting to note that there is a trend suggesting that the FPA-fibrinogen gels appeared to support cell survival to a greater extent than fibrin.

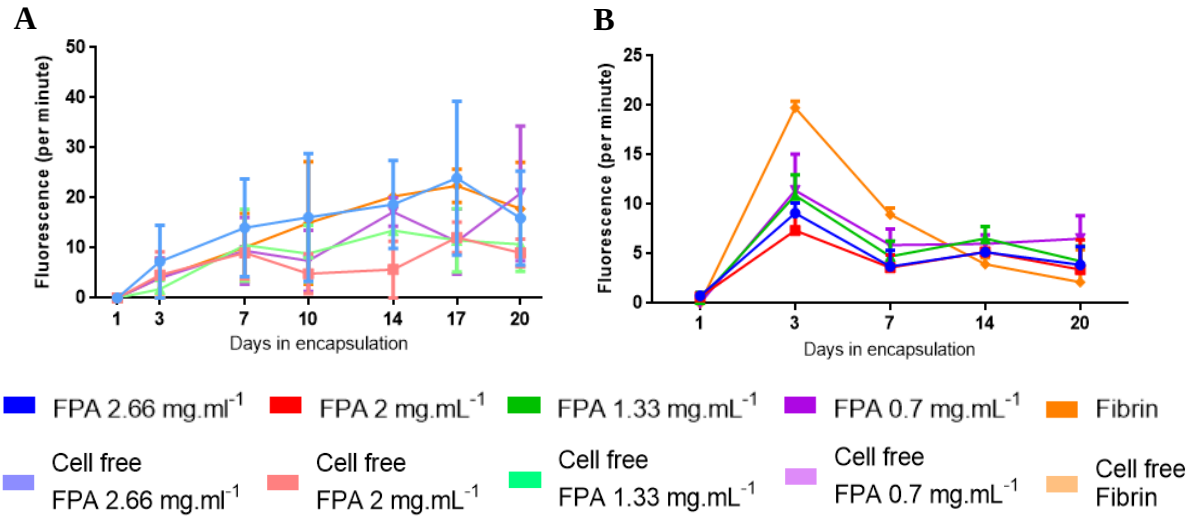

Figure 7.31 The effect of the rate of reduction from PrestoBlue® (shown as mean relative fluorescence units per minute) from cell free FPA-fibrinogen gels (A) and the culture medium (B) taken from the incubation bBM-MSC encapsulated FPA-fibrinogen and fibrin gels. The error bars represent the standard error of the mean. Statistical analysis with use of a one-way ANOVA with Tukey post test was conducted. N=3

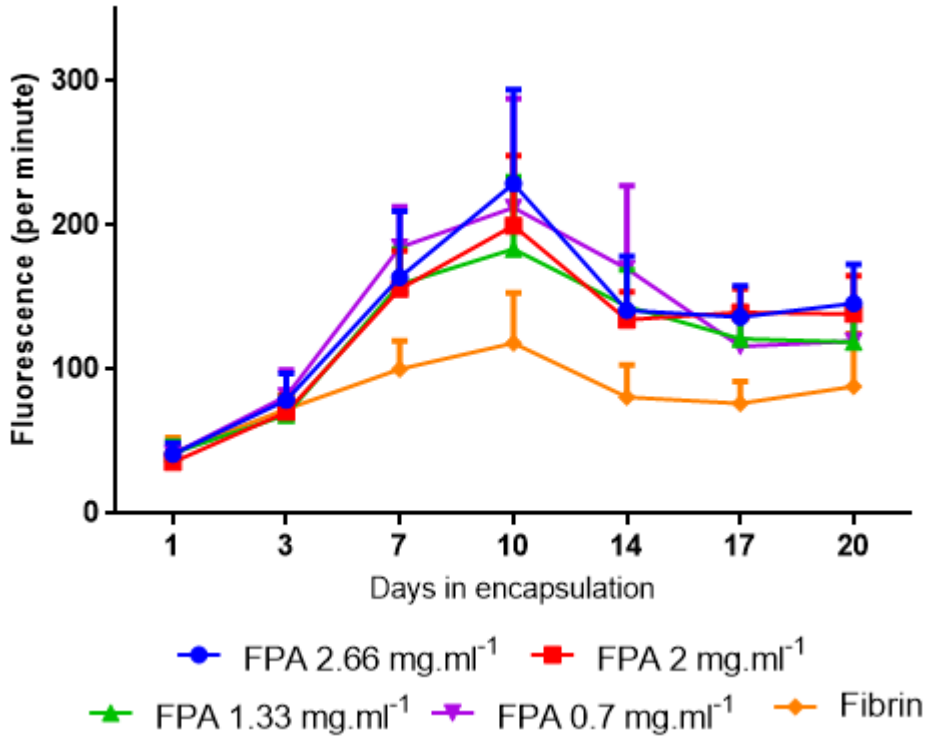

Figure 7.32 Rate of reduction of PrestoBlue (shown as mean fluorescence per minute) of bBM-MSC fibrin, and FPA-fibrinogen gels formed from 2.66 mg.mL^{-1}, 2 mg.mL^{-1}, 1.33 mg.mL^{-1}, and 0.7 mg.mL^{-1} FPA. The error bars represent the standard error of the mean. Statistical analysis with use of a one-way ANOVA with Tukey post test was conducted. N=3

Table 7.2 Statistical analysis of unpaired t-test with Welch's correction comparing fibrin and FPA-fibrinogen gels formed from 2.66 mg.mL^{-1}, 2 mg.mL^{-1}, 1.33 mg.mL^{-1}, and 0.7 mg.mL^{-1}, with their cell free equivalents from the cell viability results taken at day 1, 7, 14, 20 after encapsulation of chondrocytes refer to Figure 7.31 and Figure 7.32. Significance: * P<0.1, ** P<0.01, *** P<0.001, **** P<0.0001

	Days in encapsulation	Significance
FPA 2.66 mg.mL^{-1}	1	****
	3	***
	7	***
	10	**
	14	***
	17	*
	20	***
FPA 2 mg.mL^{-1}	1	****
	3	****
	7	****
	10	***
	14	****
	17	****
	20	***
FPA 1.33 mg.mL^{-1}	1	****
	3	****
	7	****
	10	**
	14	****
	17	***
	20	***
FPA 0.7 mg.mL^{-1}	1	****
	3	****
	7	****
	10	**
	14	**
	17	***
	20	**
Fibrin	1	***
	3	***
	7	****
	10	*
	14	**
	17	**
	20	*

Live/Dead staining

Live/dead staining and observing the surface of the gels with a confocal microscope showed live bBM-MSCs, green cells, at day 1 and day 21 of encapsulation for both fibrin Figure 7.33 and FPA-fibrinogen 2.66 $mg.mL^{-1}$ Figure 7.34 gels. Less than 10 % of the bBM-MSCs encapsulated in fibrin and FPA-fibrinogen gels were dead, red on the images, at day 1 and day 21 of encapsulation, see Figure 7.35. This suggested that the majority of cells were viable at day 21 of encapsulation. From the images and quantification of cell number, Figure 7.36, it was observed that the bBM-MSC number increased from day 1 to day 21, and therefore there is evidence to suggest cell proliferation. Cell free FPA and fibrin gels were stained and imaged. No staining was detected and therefore all staining observed was from live or dead cells on the gels.

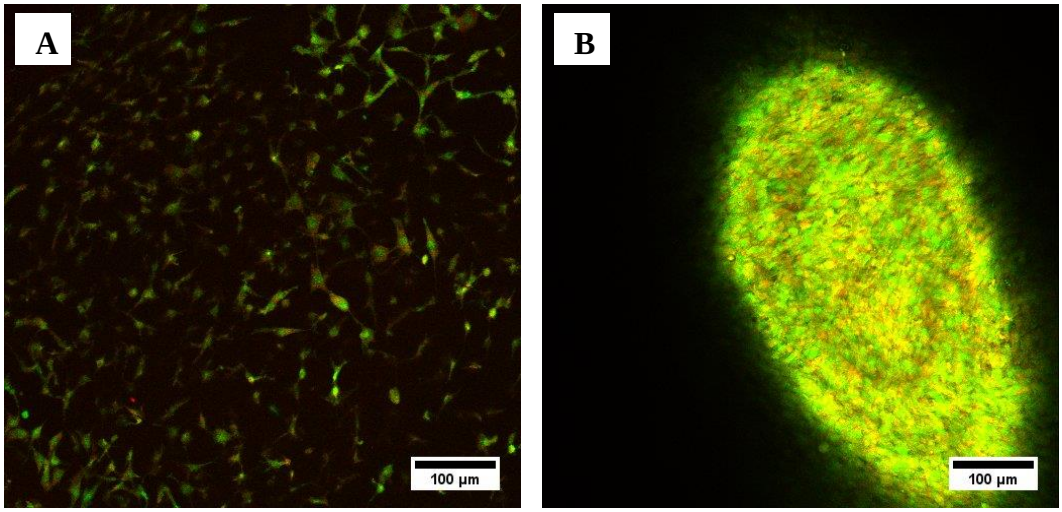

Figure 7.33 Live/Dead staining of bBM-MSC encapsulated fibrin gels at day 1 (A) and day 21 (B) of encapsulation. Images were taken using a confocal microscope

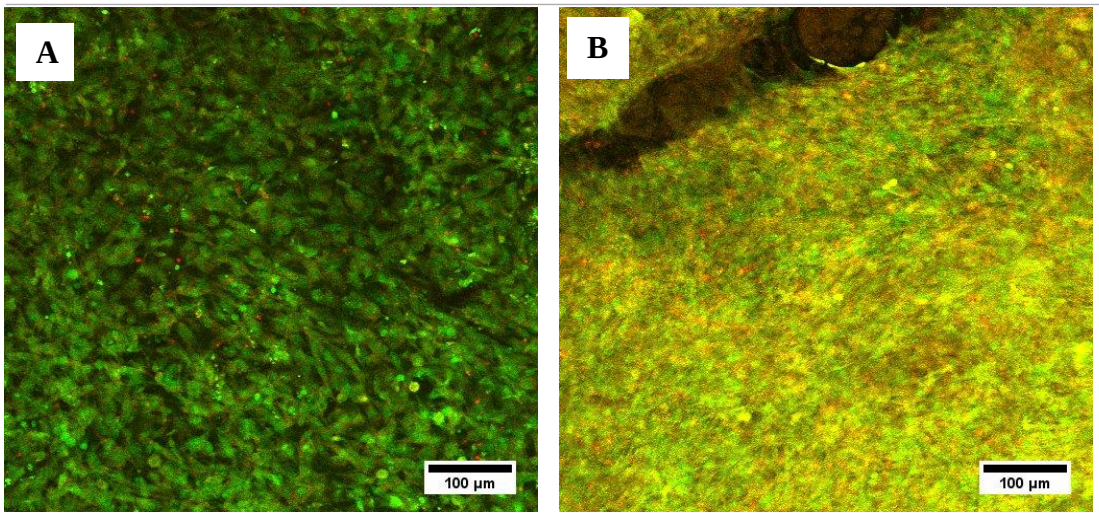

Figure 7.34 Live/Dead staining of bBM-MSCs encapsulated in FPA-fibrinogen 2.66 mg.mL^{-1} gels at day 1 (A) and day 21 (B) of encapsulation. Images were taken using a confocal microscope

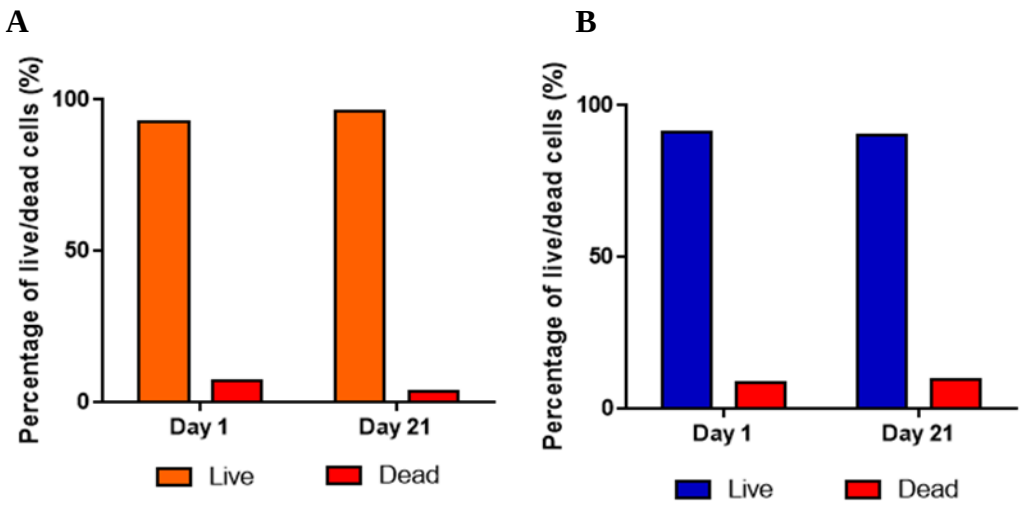

Figure 7.35 Percentage of live and dead bBM-MSCs at day 1 and 21 of encapsulation in (A) fibrin and (B) FPA-fibrinogen gels formed from 2.66 mg.mL^{-1} FPA. Cell number was quantified from live/dead stained images taken on the confocal microscope. N=1

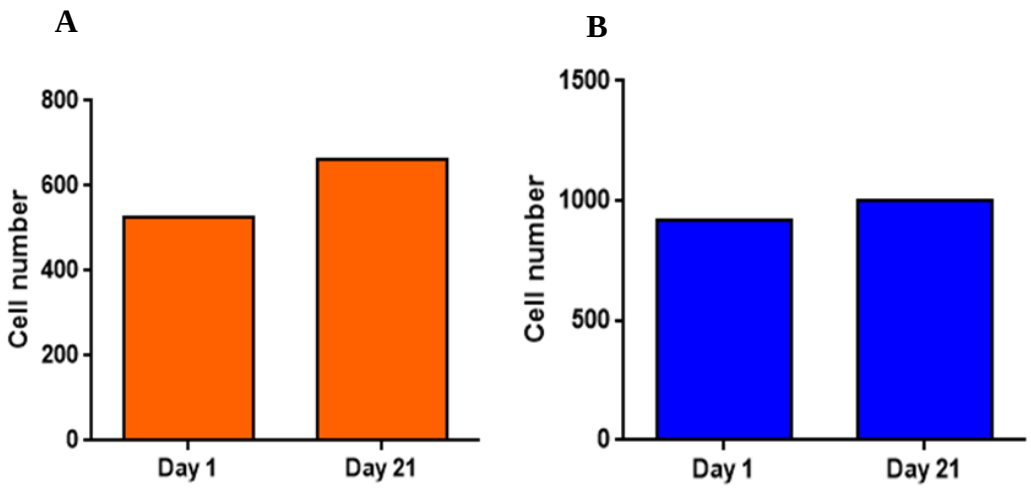

Figure 7.36 The number of live bBM-MSCs at day 1 and day 21 of encapsulation in (A) fibrin and (B) FPA-fibrinogen gel formed from 2.66 mg.mL^{-1} FPA. Cell number was quantified from live/dead stained images taken on the confocal microscope. N=1

Glycosaminoglycan content

ECM deposition was investigated by measuring GAG content of the encapsulated bBM-MSC gels. All gels contained some GAG deposition suggesting that all gels supported chondrogenic differentiation of the encapsulated bBM-MSC, shown in Figure 7.38. However, analysis of the cell free gels showed relatively high background readings for GAG, and especially for cell free fibrin gels. The data was not significantly different between bBM-MSC encapsulated FPA-fibrinogen gels 2.66 mg.mL^{-1}, and fibrin and their cell free counterparts but FPA-fibrinogen gels 2 mg.mL^{-1}, 1.33 mg.mL^{-1}, and 0.7 mg.mL^{-1} were significantly higher in comparison to their cell free counterparts, Table 7.3. These results were subtracted from the bBM-MSC encapsulated GAG content to ensure that the results were from ECM deposition alone.

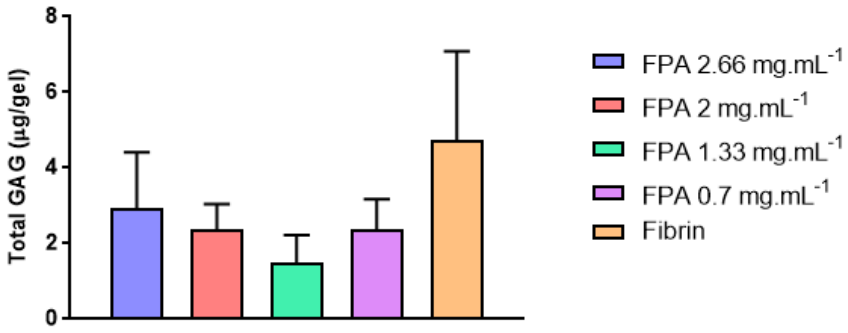

Figure 7.37 The effect of DMB (shown as Total GAG (µg/gel)) on cell free FPA-fibrinogen and fibrin gels. Measurements were taken at day 21 of culture. The error bars represent the standard error of the mean. Statistical analysis with use of a one-way ANOVA with Tukey post test was conducted. N=3

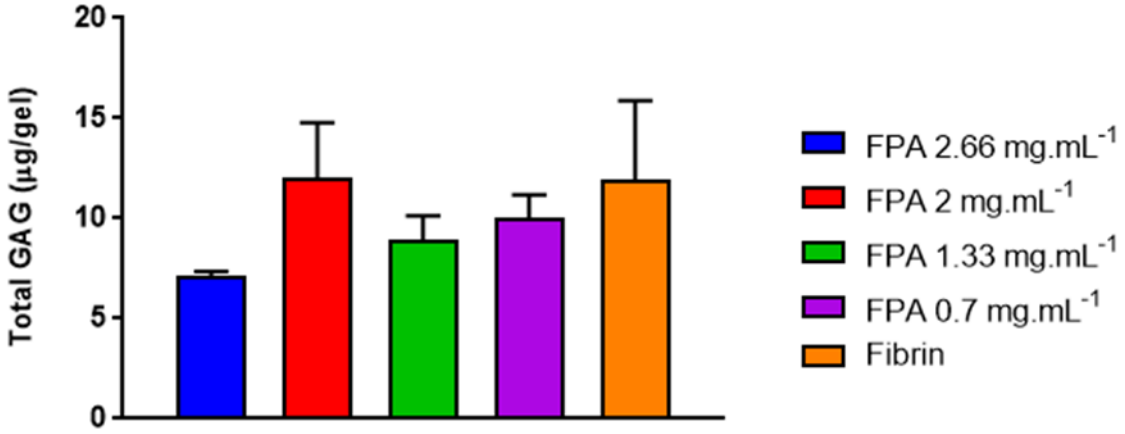

Figure 7.38 Total GAG content per from bBM-MSC encapsulated FPA-fibrinogen and fibrin gels incubated with aprotinin. Measurements were taken at day 21 of culture. The error bars represent the standard error of the mean. Statistical analysis using one-way ANOVA with Tukey post test was conducted. N=3

Table 7.3 Showing the statistical analysis of an unpaired t-test with Welch's correction comparing the GAG content of fibrin and FPA-fibrinogen gels formed from 2.66 mg.mL^{-1}, 2 mg.mL^{-1}, 1.33 mg.mL^{-1}, and 0.7 mg.mL^{-1} FPA, with their cell free equivalents. Significance: ** P<0.01, ns is no significant differences

	Significance
FPA 2.66 mg.mL	ns
FPA 2 mg.mL	*
FPA 1.33 mg.mL	**
FPA 0.7 mg.mL	**
Fibrin	ns

Haematoxylin and Eosin staining

H&E staining was carried sections taken from bBM-MSC encapsulated FPA-fibrinogen and fibrin gels. H&E staining showed dispersed cells throughout the FPA and fibrin gels, however the bBM-MSCs appear to behave differently in comparison to chondrocytes in which the bBM-MSCs congregate in pores of the gels rather than individually as the chondrocytes appeared, and this can be seen clearly on Figure 7.41 images J and H. The cell free FPA-fibrinogen and fibrin gels stained pink (Figure 7.40) and therefore ECM deposition cannot be observed. The bBM-MSC have a spherical morphology within the FPA and fibrin gels similar to that of native articular cartilage (Figure 7.39). Cell layers with ECM deposition can be seen at the edges of all fibrin and FPA gel conditions.

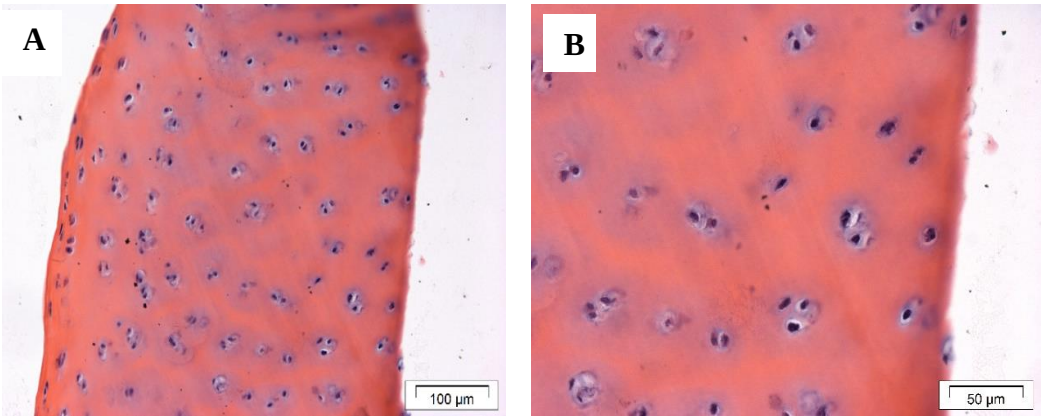

Figure 7.39 H&E staining on native articular cartilage (A and B). Images taken at a magnification of x20 (A) and x40 (B). Scale bars shown on the image.

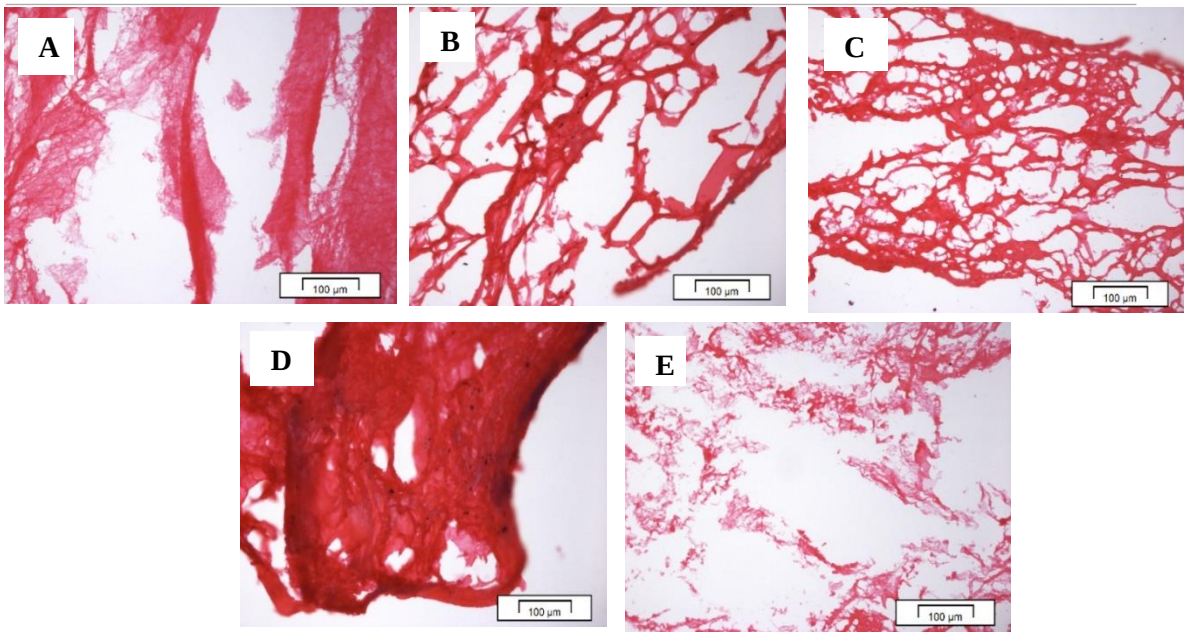

Figure 7.40 Histological H&E stained sections from cell free (A) fibrin, and FPA-fibrinogen gels formed from (B) 2.66 mg.ml^{-1} FPA, (C) 2 mg.ml^{-1} FPA, (D) 1.33 mg.ml^{-1} FPA and (E) 0.7 mg.ml^{-1} FPA. Images were taken at a magnification of x20 and scale bars are displayed on the image.

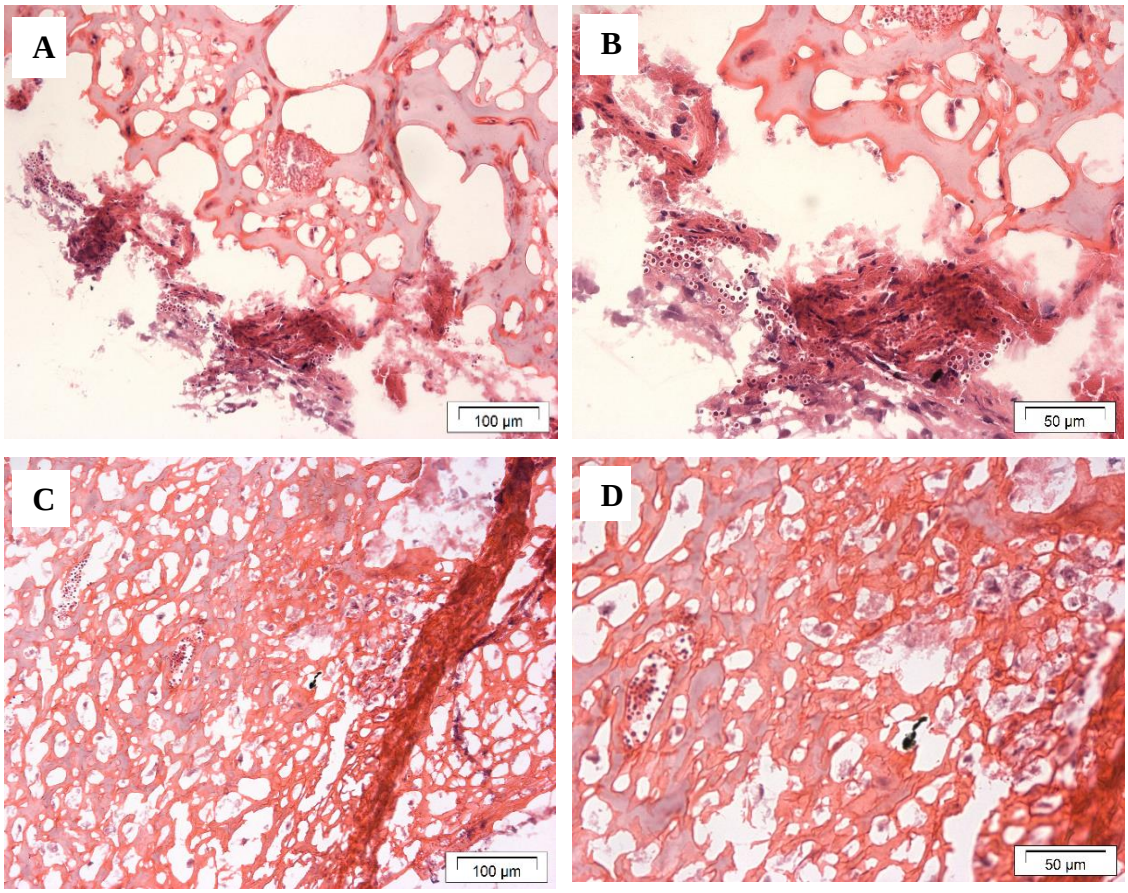

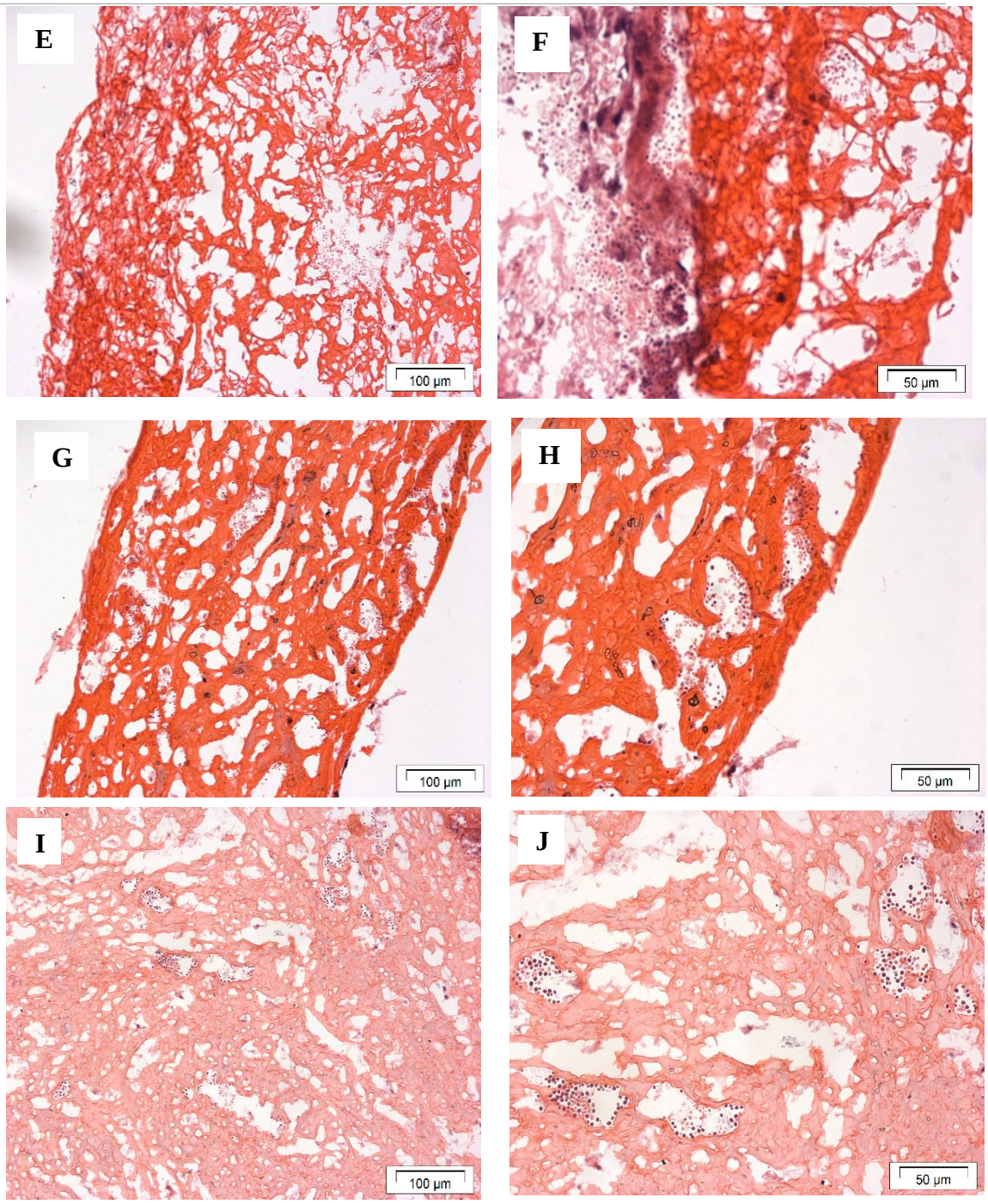

Figure 7.41 Histological H&E stained sections from bBM-MSC encapsulated (A, B) fibrin and FPA-fibrinogen gels formed from (C, D) 2.66 mg.ml^{-1} FPA, (E, F) 2 mg.ml^{-1} FPA, (G, H) 1.33 mg.ml^{-1} FPA and (I, J) 0.7 mg.ml^{-1} FPA. Images taken at a magnification of x20 (A, C, E, G, and I) and x40 (B, D, F, H and J). Scale bars shown on the image.

Toluidine blue staining

Toluidine blue staining suggested proteoglycan deposition occurred in all gels due to the purple stained areas observed throughout the stained bBM-MSC encapsulated gel sections (Figure 7.43). A cell layer at the outer gel shows higher proteoglycan formation in comparison to the centre of the gels. This was observed in histological sections from all bBM-MSC encapsulated FPA and fibrin conditions. Cell free FPA-fibrinogen and fibrin gels (Figure 7.42) did stain a dark blue colour rather than the blue-purple that is indicative of proteoglycan deposition and therefore proteoglycan deposition was observed.

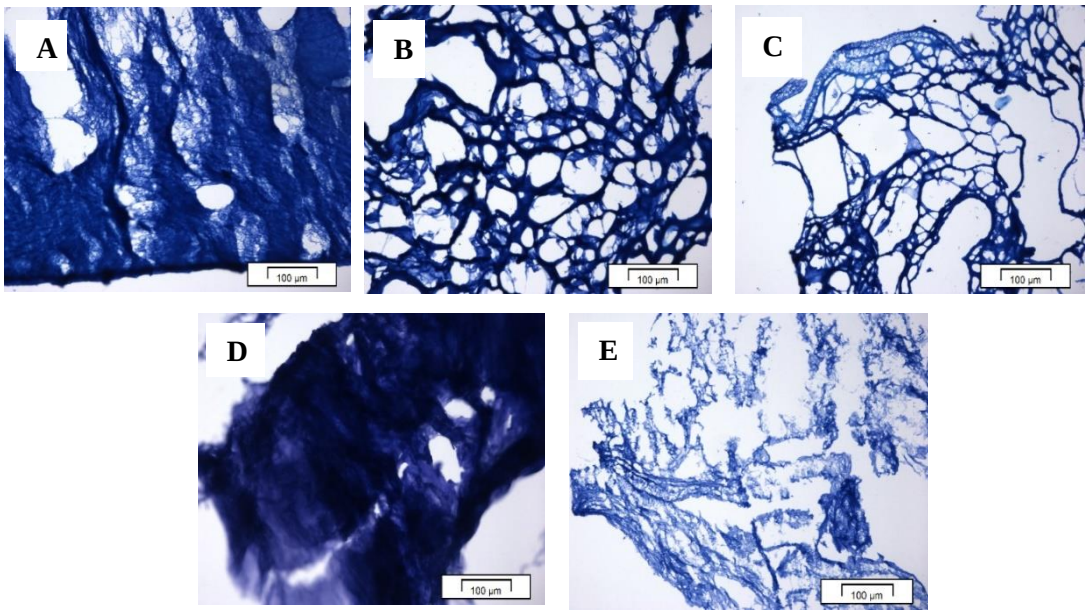

Figure 7.42 Histological Toluidine blue stained sections from cell free (A) fibrin and FPA-fibrinogen gels formed from (B) 2.66 mg.ml^{-1} FPA, (C) 2 mg.ml^{-1} FPA, (D) 1.33 mg.ml^{-1} and (E) 0.7 mg.ml^{-1} FPA. Images were taken at a magnification of x20 and scale bars are shown on the image.

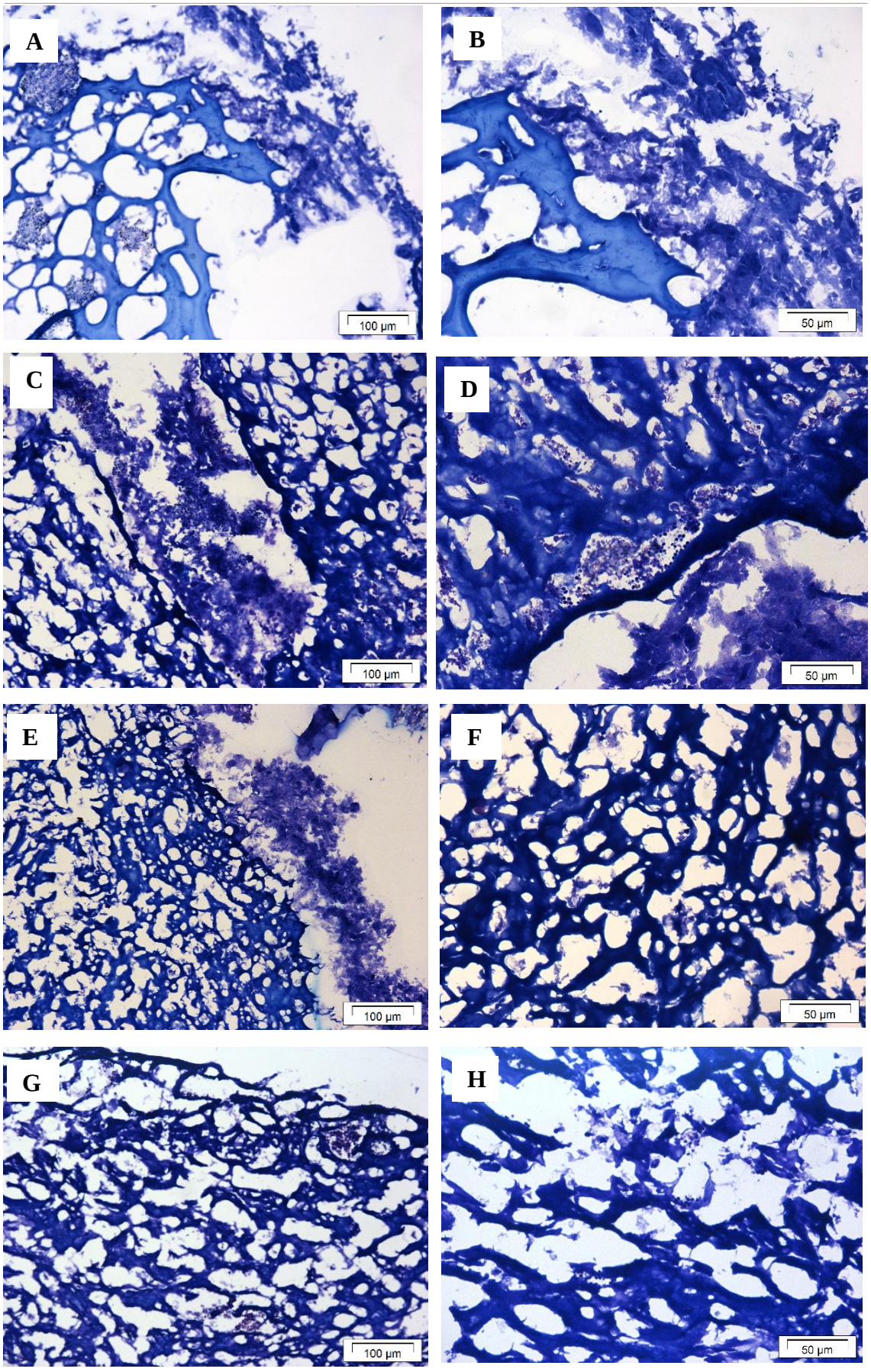
A
100 µm
B
50 µm
C
100 µm
D
50 µm
E
100 µm
F
50 µm
G
100 µm
H
50 µm

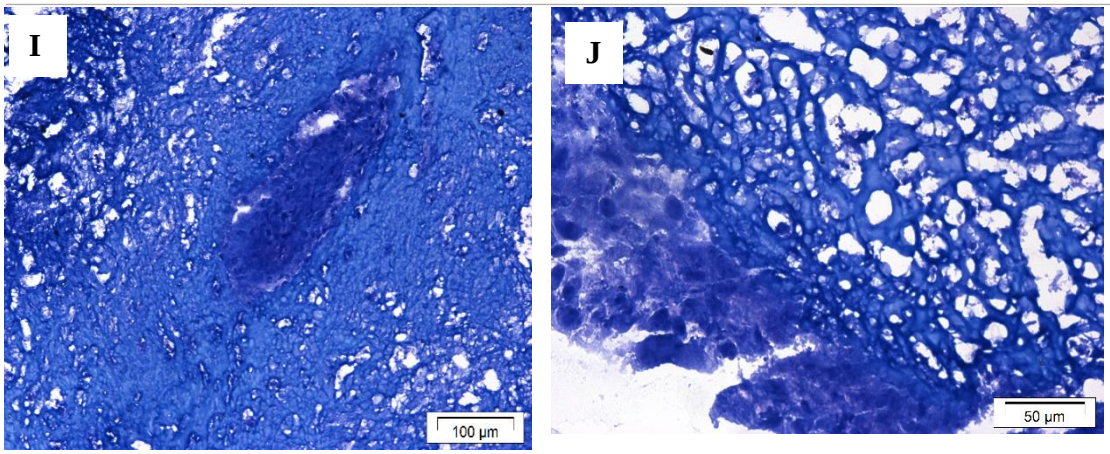

Figure 7.43 Histological Toluidine blue stained sections from bBM-MSCs encapsulated for 21 days in (A, B) fibrin and FPA-fibrinogen gels formed from (C, D) 2.66 mg.mL^{-1} FPA, (E, F) 2 mg.mL^{-1} FPA, (G, H) 1.33 mg.mL^{-1} and (I, J) 0.7 mg.mL^{-1} FPA. Images were taken at a magnification of x20 (A, C, E, G, and I) and x40 (B, D, F, H, and J). Scale bars are shown on the image.

The histological stained images were analysed for pore diameter and the average number of pores per image. Pore diameter has been shown as a box plot illustrating the minimum, maximum and median pore diameters and the interquartile range. The analysis suggested that the bBM-MSC encapsulated gels had a very similar number of pores in comparison to their cell free counterpart other than FPA-fibrinogen gel formed from 2.66 mg.mL^{-1} and fibrin (Figure 7.44, C and D). FPA-fibrinogen formed from 2.66 mg.mL^{-1} had a 4-fold increase and fibrin had a 5-fold increase in pore number with bBM-MSC encapsulated gels. From the analysis there was very little difference between cell encapsulated and cell free gels for pore diameter (Figure 7.44, A and B). Cell free fibrin had a much more closed structure with fewer pores in comparison to the FPA-fibrinogen gels.

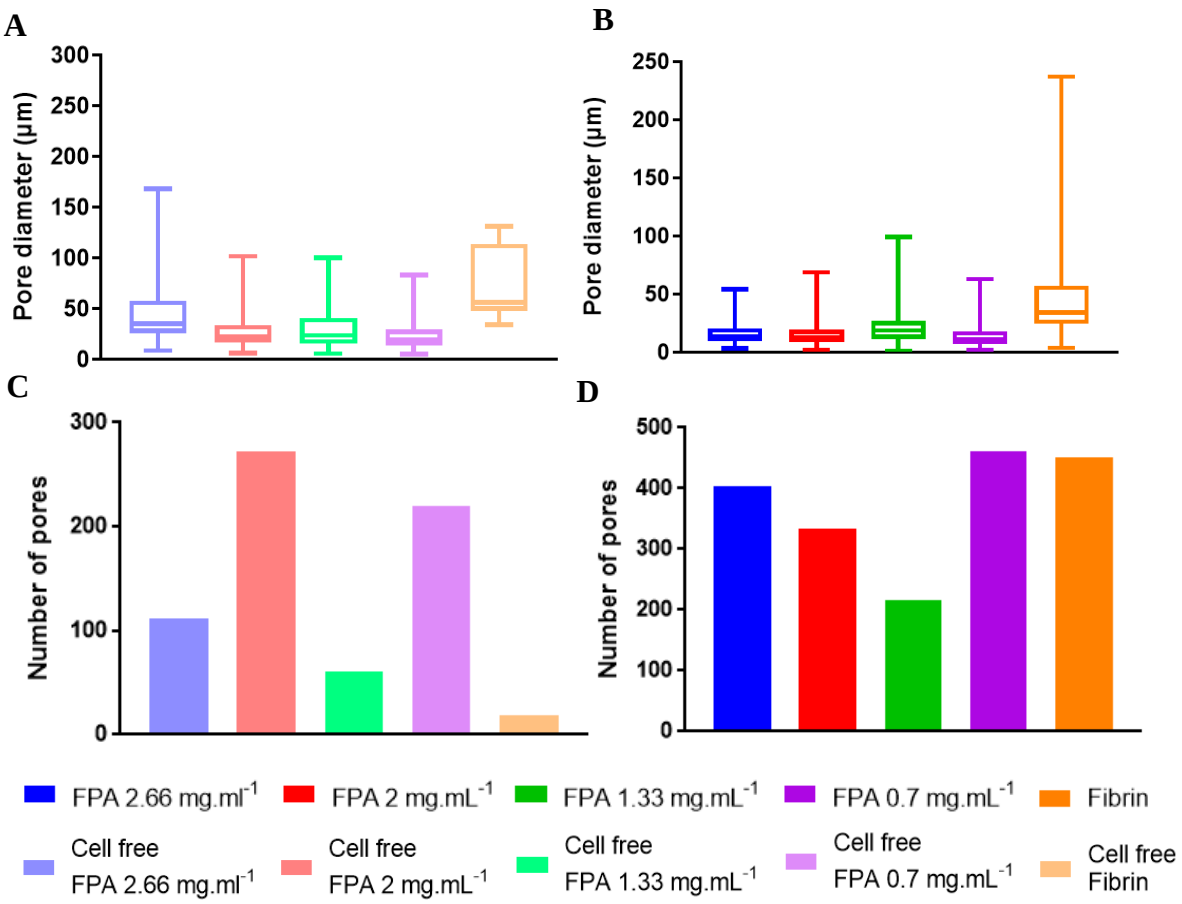

Figure 7.44 Measurements of pore diameter (A, B) and number of pores (C, D) from analysed from the histological staining of cell free (A, C) and bBM-MSC encapsulated (B, D) fibrin and FPA-fibrinogen gels formed from 2.66 mg.mL^{-1}, 2 mg.mL^{-1}, 1.33 mg.mL^{-1}, and 0.7 mg.mL^{-1} FPA. Pore diameter (A, B) is shown as a box plot indicating the minimum, median and maximum pore diameter and the interquartile range.

The H&E and Toluidine blue stained bBM-MSC encapsulated hydrogels have shown that the bBM-MSCs appear to congregate within pores. ECM formation can be observed in the centre and on the edges of the gels, suggesting that the bBM-MSCs remained viable and were differentiating and forming ECM within the gels. Analysis of the stained images showed that the FPA-fibrinogen gels had a porous structure in comparison to fibrin.

Key Summary

- In the presence of aprotinin, bBM-MSC migration and FPA-fibrinogen and fibrin gel degradation was reduced.

- bBM-MSCs survived, proliferated, and differentiated in the FPA-fibrinogen and fibrin gels.
- All FPA-fibrinogen gels were comparable to fibrin for cell activity and total GAG content per gel.
- Pore diameter and number of pores per image were similar for all FPA-fibrinogen and fibrin gels suggesting the structures of the gels were comparable.

7.4 MSC encapsulation in P15, P17 and HyStem

The volumes of the P15, P17 and HyStem fibrinogen binding peptide materials were limited in supply from Haemostatix Ltd. and therefore multiple repeats of all experiments was not possible. However, the data shown provides interesting preliminary results on how these gels functioned for MSC encapsulation. bBM-MSCs were encapsulated in fibrinogen gels formed from P15 0.75 mg.mL^{-1}, P15 0.5 mg.mL^{-1}, and P15 0.25 mg.mL^{-1}, P17 0.75 mg.mL^{-1}, P17 0.5 mg.mL^{-1}, and P17 0.25 mg.mL^{-1}, and HyStem 1 mg.mL^{-1}, and HyStem 0.75 mg.mL^{-1}, fibrin was used as a reference material. These concentrations were chosen based on previous gelation experiments with cell free gels. bBM-MSCs were encapsulated in the P15, P17, and HyStem – fibrinogen and fibrin gels at 300,000 cell per gel. All cell encapsulated gels were cultured for 9 days. Light microscopy images show that cell free P15, P17, HyStem and fibrin gels maintained their structure and exhibited no degradation, (images A and B, Figure 7.45 to Figure 7.53). However, bBM-MSC migration and gel degradation was observed in P15 0.5 mg.mL^{-1} (Figure 7.47), P15 0.25 mg.mL^{-1} (Figure 7.48), P17 0.5 mg.mL^{-1} (Figure 7.50), P17 0.25 mg.mL^{-1} (Figure 7.51), HyStem 1 mg.mL^{-1} (Figure 7.52), and HyStem 0.75 mg.mL^{-1} (Figure 7.53) encapsulated with 300,000 bBM-MSCs. Less degradation was observed in the fibrinogen gels formed with higher concentrations of P15 0.75 mg.mL^{-1} (Figure 7.46), and P17 0.75 mg.mL^{-1} (Figure 7.49). It was observed that fibrin showed the initial stages of gel degradation by day 9 of encapsulation, (Figure 7.45). Crystal violet staining showed cell migration from the gels was observed and the staining carried out at day 9 of encapsulation. It can be observed that bBM-MSC migration occurred in all P15, P17, HyStem and fibrin gels conditions, but visually, less cells appear to have migrated from the 0.75 mg.mL^{-1} concentrations of P15 (image F, Figure 7.46) and P17 (image F, Figure 7.49).

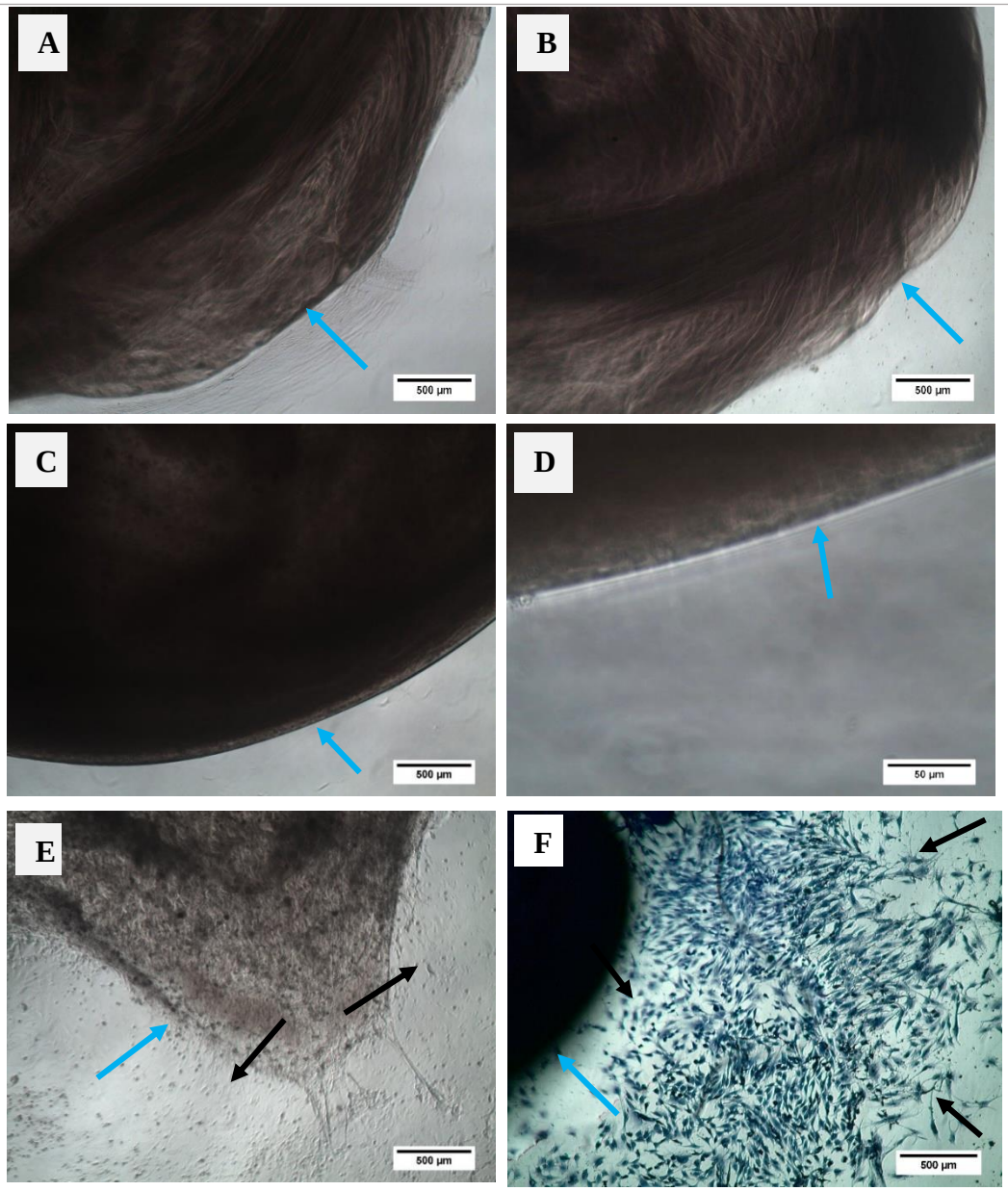

Figure 7.45 Phase contrast images of cell free (A, B) and bBM-MSC encapsulated (C, D, E, F) fibrin gels, blue arrows, images were taken at day 1 (A, C, D) and day 9 (B, E, F) and at a magnification of x4 (A, B, C, E and F) and x20 (D). Cells, black arrows, were stained with crystal violet at day 9 of encapsulation (F). Scale bars are shown on the image.

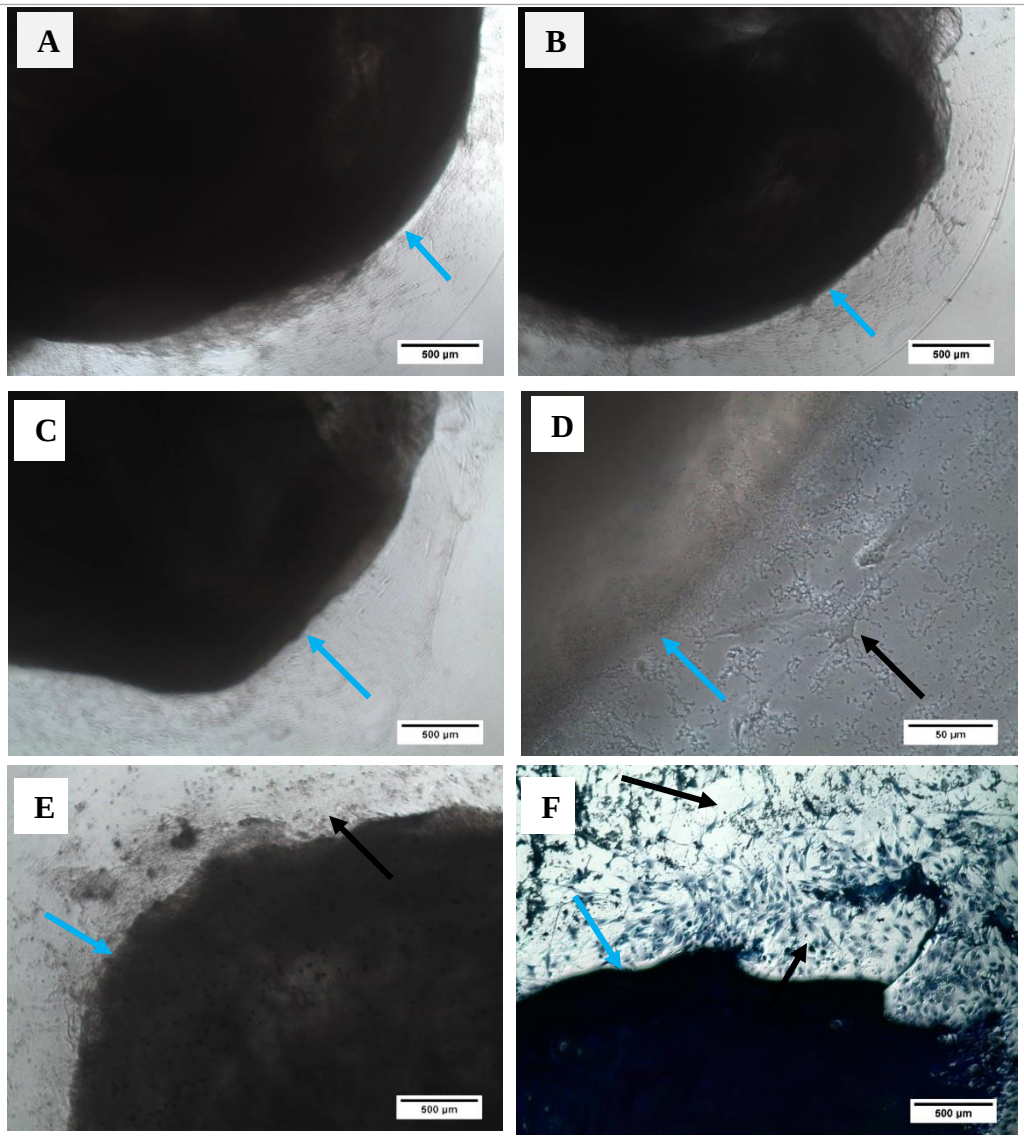

Figure 7.46 Phase contrast images of cell free (A, B) and bBM-MSC encapsulated (C, D, E, F) P15-fibrinogen 0.75 mg.mL^{-1} gels, blue arrows, images were taken at day 1 (A, C, D) and day 9 (B, E, F) at a magnification of x4 (A, B, C, E, F) and x20 (D). Cells, black arrows, were stained with crystal violet at day 9 of encapsulation (F). Scale bars are shown on the image.

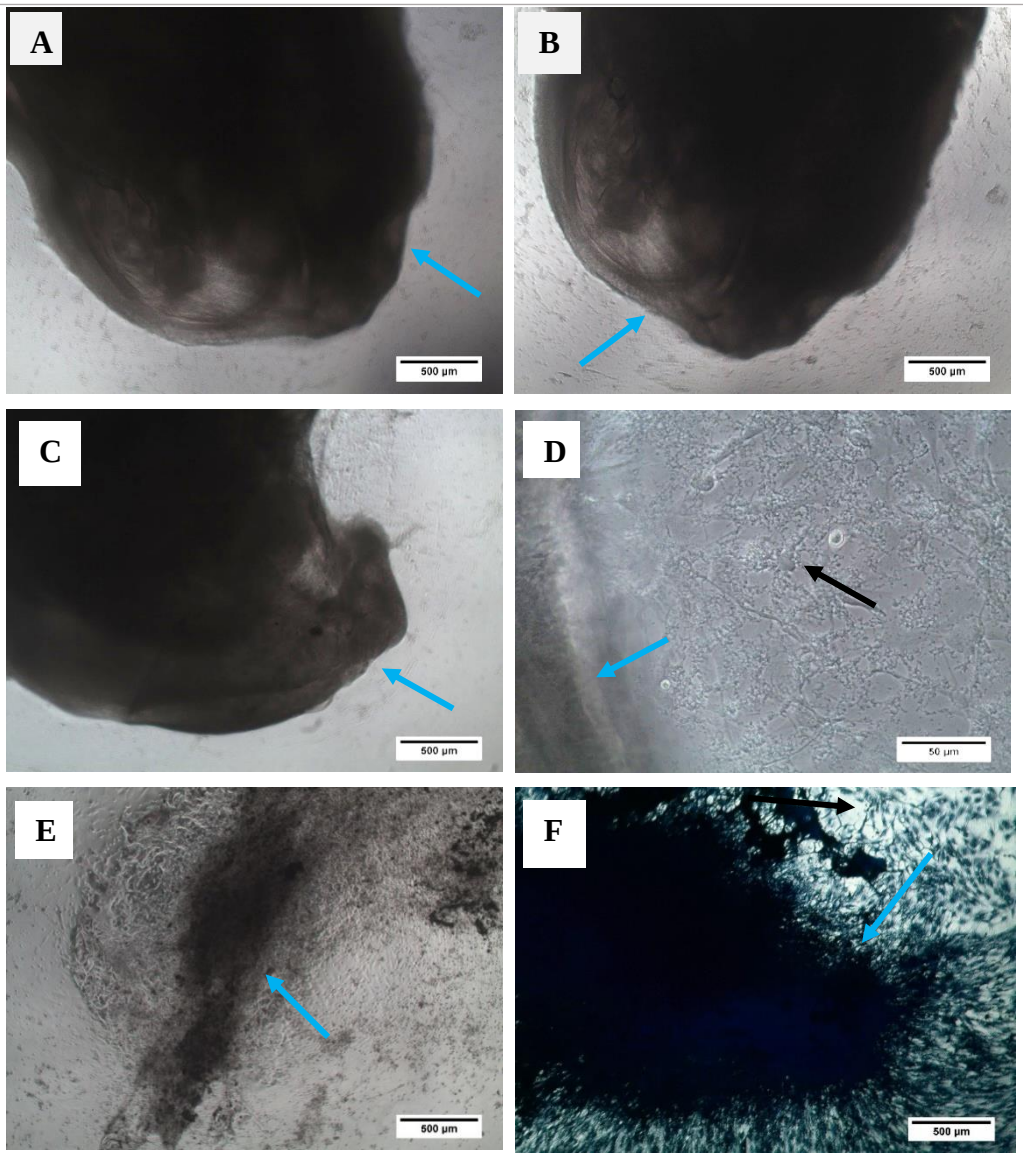

Figure 7.47 Phase contrast images of cell free (A, B) and bBM-MSC encapsulated (C, D, E, F) P15-fibrinogen 0.5 mg.mL^{-1} gels, blue arrows. Images were taken at day 1 (A, C, D) and day 9 (B, E, F) at a magnification of x4 (A, B, C, E, F) and x20 (D). Cells, black arrows, were stained with crystal violet at day 9 of encapsulation (F). Scale bars are shown on the image.

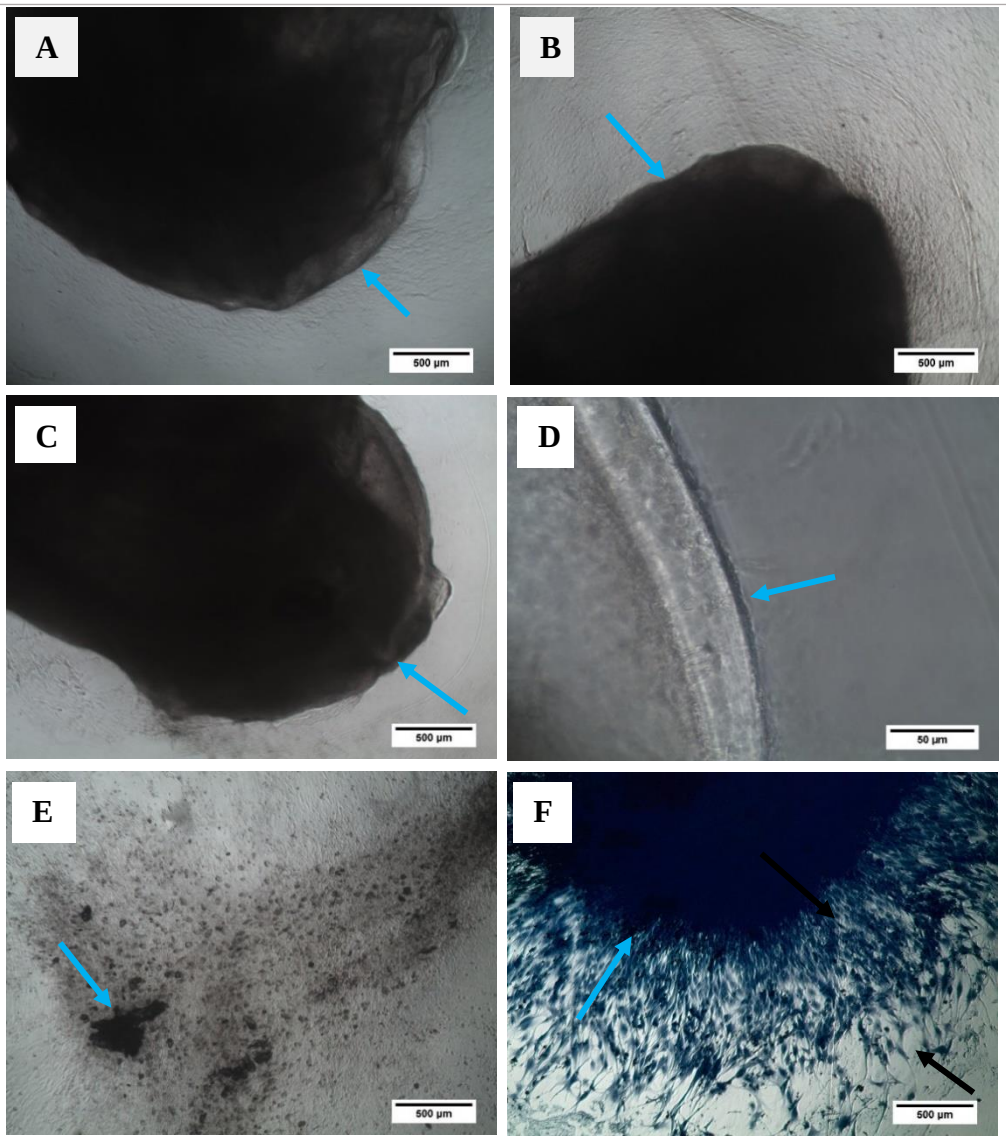

Figure 7.48 Light microscopy images of cell free (A, B) and bBM-MSC encapsulated (C, D, E, F) P15-fibrinogen 0.25 mg.mL^{-1} gels, blue arrows. Images were taken at day 1 (A, C, D) and day 9 (B, E, F) at a magnification of x4 (A, B, C, E, F) and x20 (D). Cells, black arrows, were stained with crystal violet at day 9 of encapsulation (F). Scale bars are shown on the image.

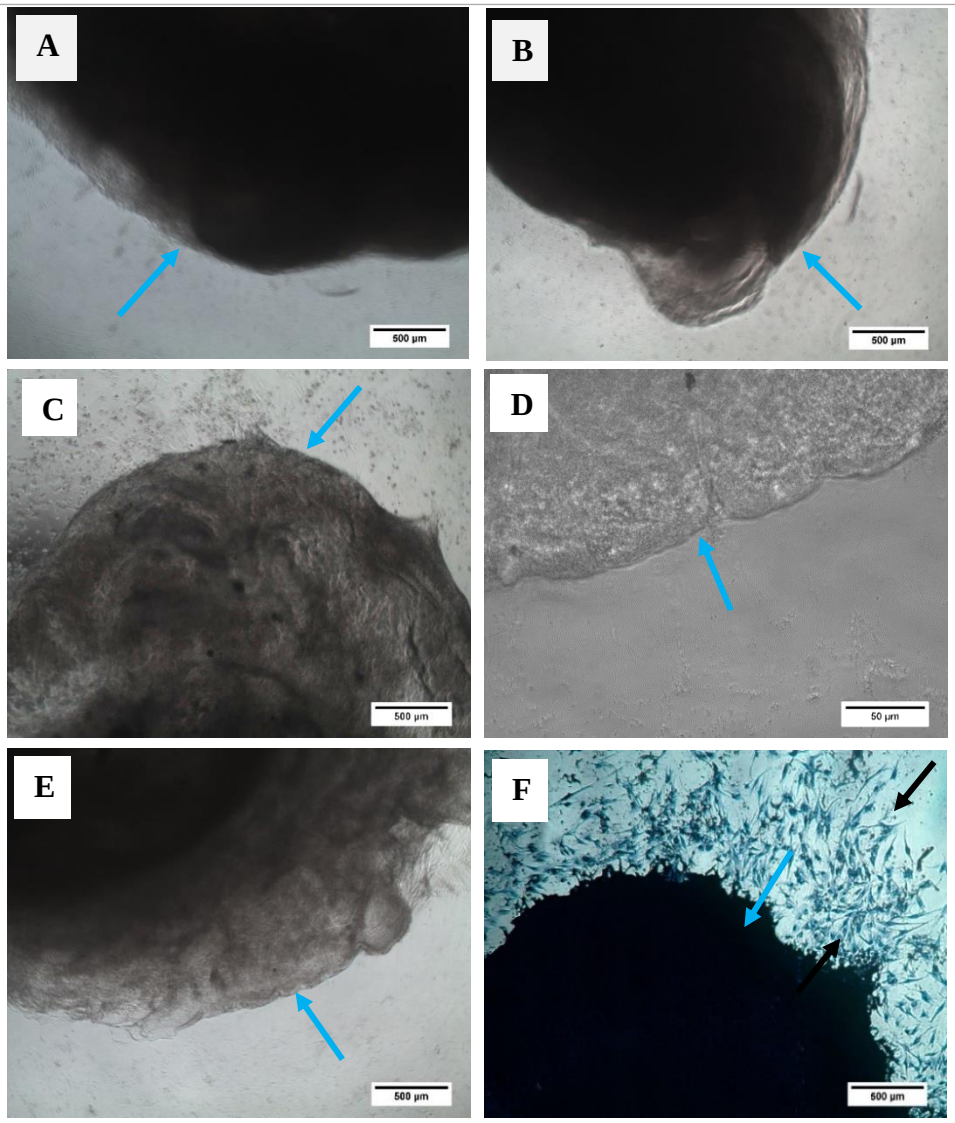

Figure 7.49 Phase contrast images of cell free (A, B) and bBM-MSC encapsulated (C, D, E, F) P17-fibrinogen 0.75 mg.mL^{-1} gels. Images were taken at day 1 (A, C, D) and day 9 (B, E, F) at a magnification of x4 (A, B, C, E, F) and x20 (D). Cells were stained with crystal violet at day 9 of encapsulation (F). Scale bars are shown on the image.

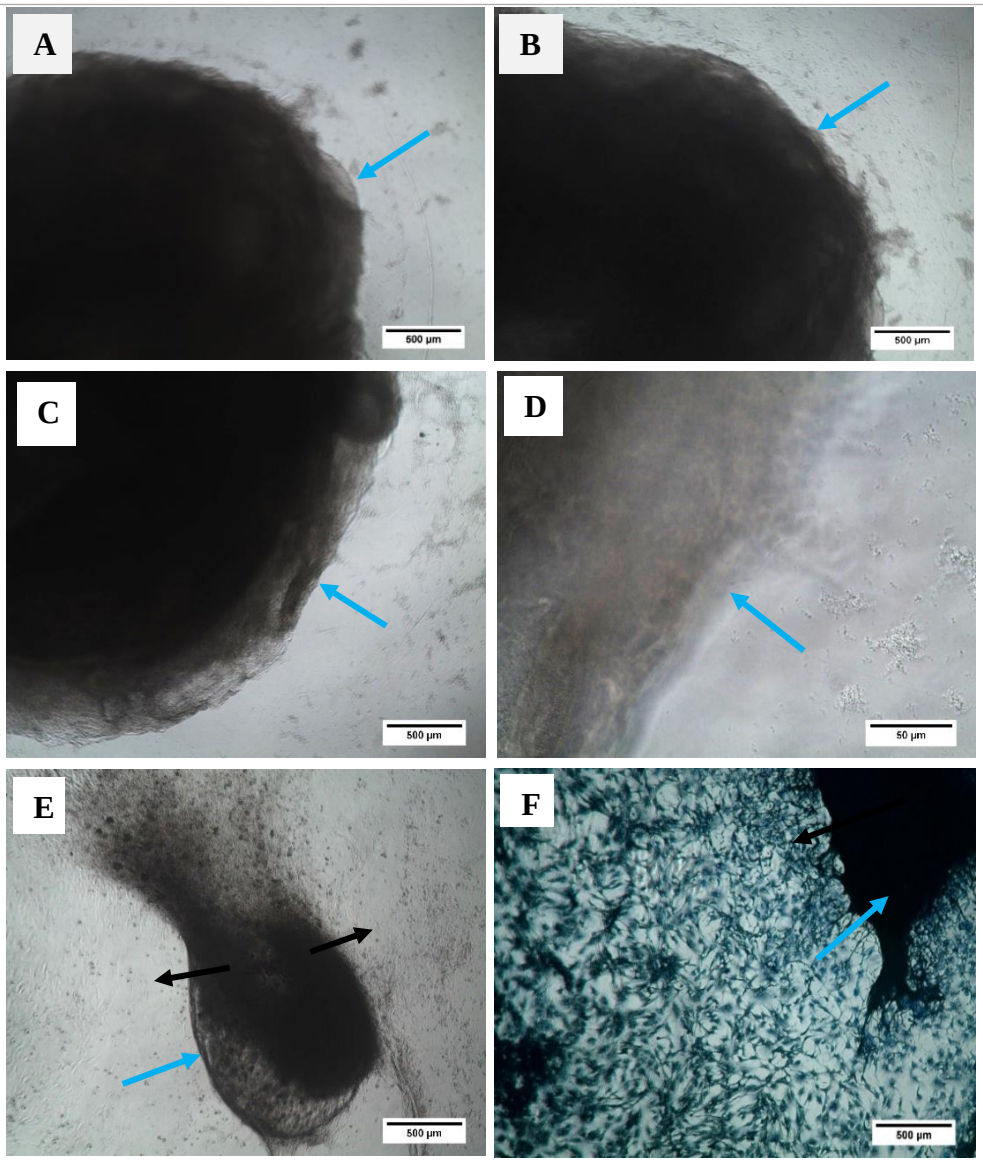

Figure 7.50 Phase contrast images of cell free (A, B) and bBM-MSC encapsulated (C, D, E, F) P17-fibrinogen 0.5 mg.mL^{-1} gels, blue arrows, images were taken at day 1 (A, C, D) and day 9 (B, E, F) at a magnification of x4 (A, B, C, E, F) and x20 (D). Cells, black arrows, were stained with crystal violet at day 9 of encapsulation (F). Scale bars are shown on the image.

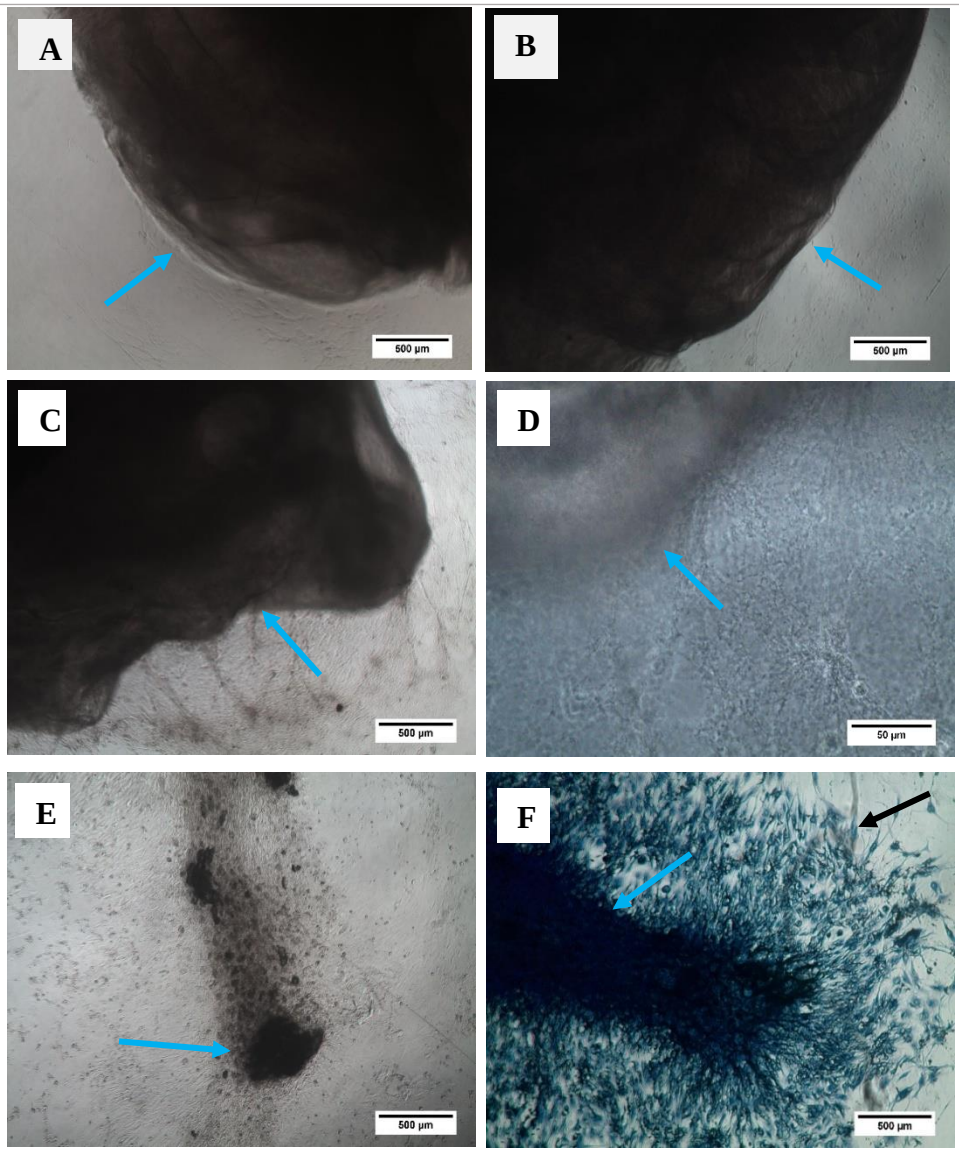

Figure 7.51 Phase contrast images of cell free (A, B) and bBM-MSC encapsulated (C, D, E, F) P17-fibrinogen 0.25 mg.mL^{-1} gels, blue arrows. Images were taken at day 1 (A, C, D) and day 9 (B, E, F) at a magnification of x4 (A, B, C, E, F) and x20 (D). Cells, black arrows, were stained with crystal violet at day 9 of encapsulation (F). Scale bars are shown on the image.

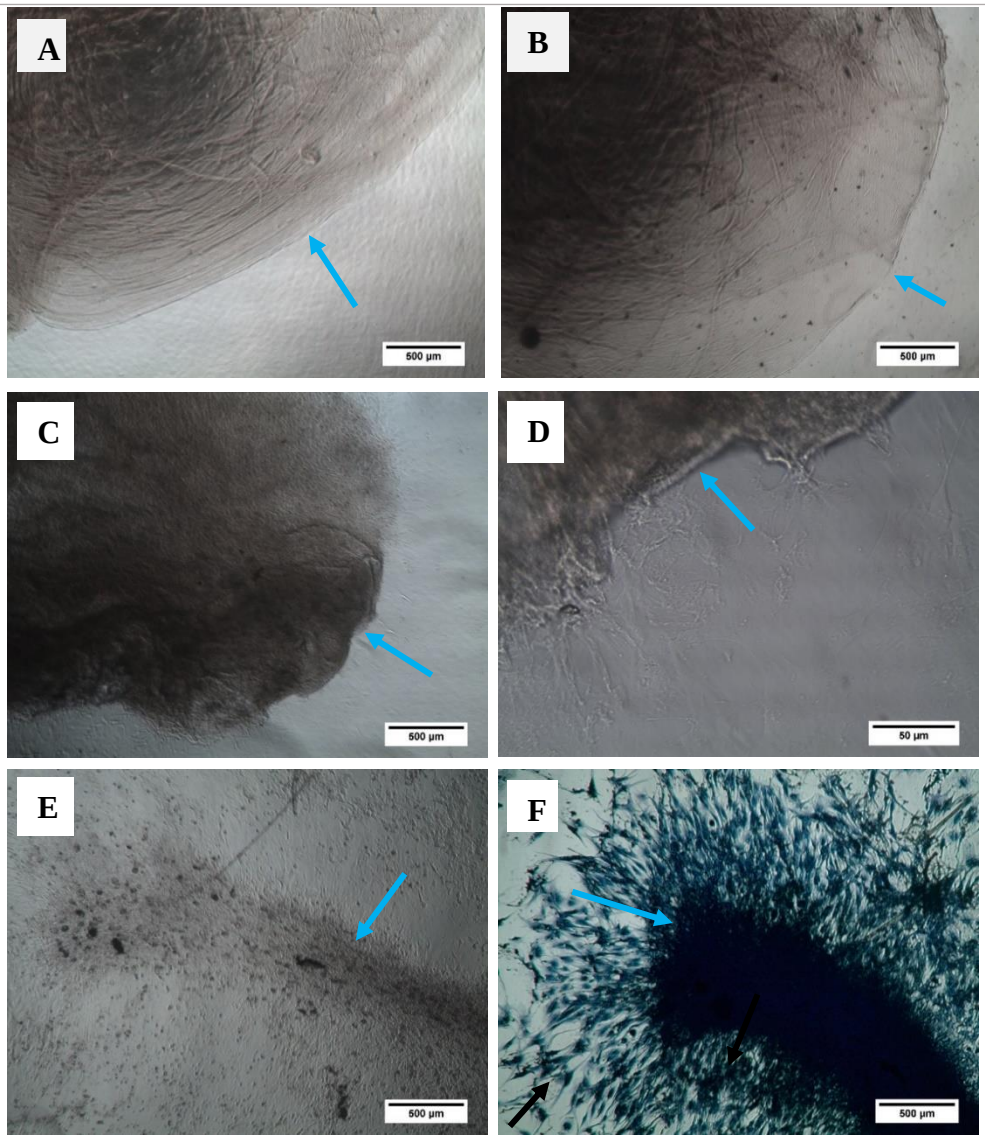

Figure 7.52 Phase contrast images of cell free (A, B) and bBM-MSC encapsulated (C, D, E, F) HyStem-fibrinogen 1 mg.mL^{-1} gels, blue arrows. Images were taken at day 1 (A, C, D) and day 9 (B, E, F) at a magnification of x4 (A, B, C, E, F) and x20 (D). Cells, black arrows, were stained with crystal violet at day 9 of encapsulation (F). Scale bars are shown on the image.

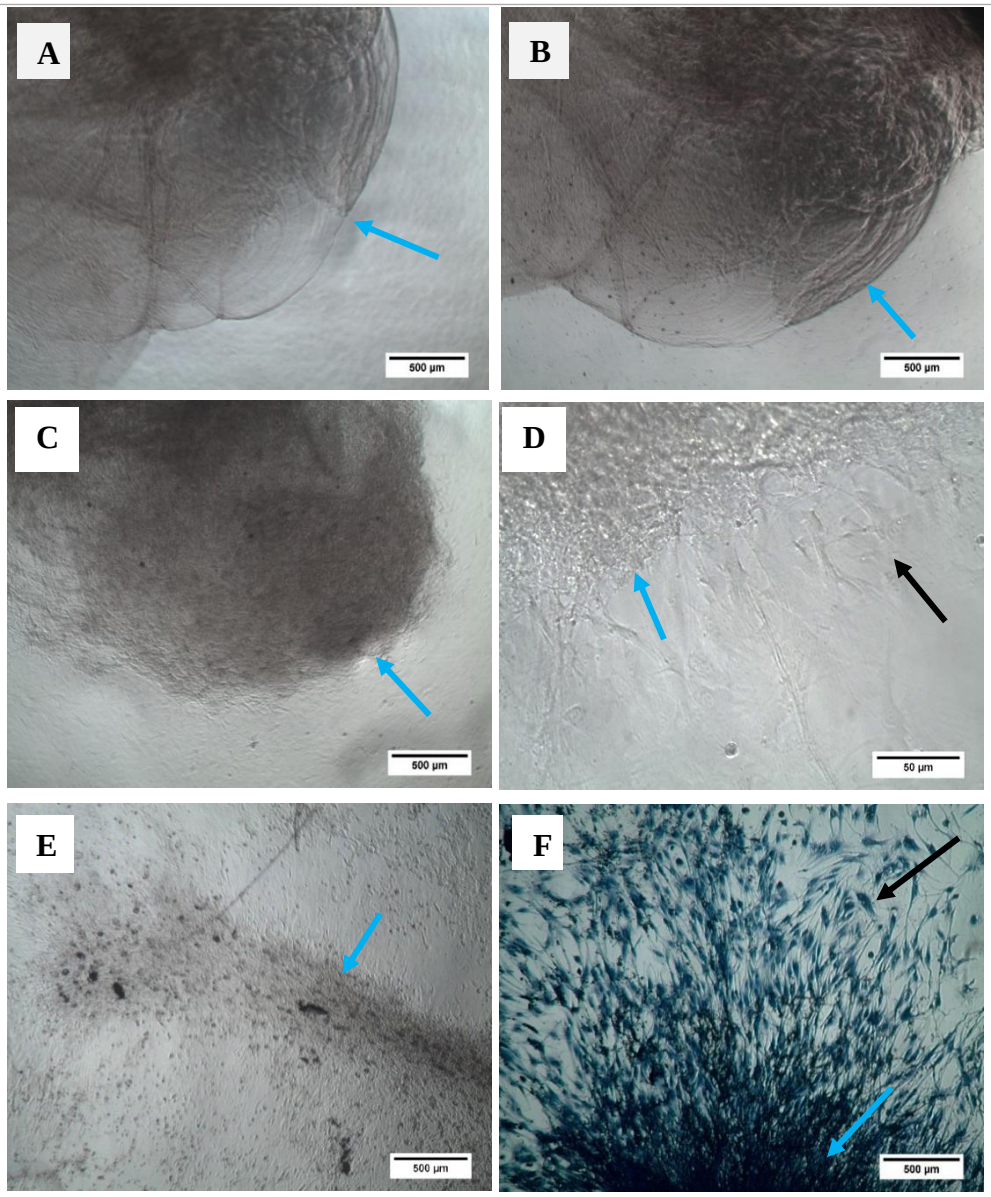

Figure 7.53 Phase contrast images of cell free (A, B) and bBM-MSC encapsulated (C, D, E, F) HyStem-fibrinogen 0.75 mg.mL^{-1} gels, blue arrows. Images were taken at day 1 (A, C, D) and day 9 (B, E, F) at a magnification of x4 (A, B, C, E, F) and x20 (D). Cells, black arrows, were stained with crystal violet at day 9 of encapsulation (F). Scale bars are shown on the image.

Key Summary

- bBM-MSC migration and gel degradation occurred in P15, P17, and HyStem – fibrinogen gels.
- P15 and P17 – fibrinogen gels formed from 0.75 mg.mL^{-1} P15 or P17, had a slower degradation rate and less cell migration in comparison to the lower concentrations of P15 and P17.

7.5 P15, P17 and HyStem gels incubated with aprotinin

Due to the degradation of the P15, P17 and HyStem gels observed in the MSC-encapsulated gels, aprotinin was added to the culture medium to inhibit gel degradation during the incubation period after the first 3 days of cell encapsulation. Previously, aprotinin inhibited FPA-fibrinogen and fibrin degradation when encapsulated with bBM-MSCs. Therefore, it was probable that the addition of aprotinin would also inhibit gel degradation and cell migration from MSC encapsulated P15, P17 and HyStem – fibrinogen gels. 300,000 bBM-MSCs were encapsulated in P15 0.75 $mg.mL^{-1}$, P15 0.5 $mg.mL^{-1}$, P15 0.25 $mg.mL^{-1}$, P17 0.75 $mg.mL^{-1}$, P17 0.5 $mg.mL^{-1}$, P17 0.25 $mg.mL^{-1}$, HyStem 1 $mg.mL^{-1}$, HyStem 0.75 $mg.mL^{-1}$, and fibrin gels. Due to experimental overlap and being unaware about the degradation of the P15, P17 and HyStem gels. Aprotinin was added on day 3 of encapsulation. The gels were then incubated in chondrogenic media with aprotinin for 21 days and ECM deposition analysis was conducted at day 24.

Cell activity

Resazrin reduction was measured from the medium incubated with the P15, P17, HyStem and fibrin gels throughout the culture period and very little reduction was observed in cell free P15, P17, HyStem and fibrin gel conditions (Figure 7.54 to Figure 7.56, A). However, a small peak of resazurin reduction was observed in culture medium that had been incubated with MSC encapsulated fibrin gels may reflect the beginning of some MSC migration from the gels, as aprotinin was only added at day 3. The cell free gels showed very little resazurin dye reduction (Figure 7.54 to Figure 7.56, B). This data suggested the gels are not interfering with the assay and therefore this data was subtracted from the cell encapsulated gels (Figure 7.57 to Figure 7.59). Preliminary data of bBM-MSC encapsulated gels showed that the cells survived in all gels throughout the 24 day culture period (Figure 7.57 to Figure 7.59). A peak of cell activity is observed at day 14 of culture, when the metabolic rate of the cells reduces in activity. This is consistent with each hydrogel condition, P15, P17, HyStem and including fibrin.

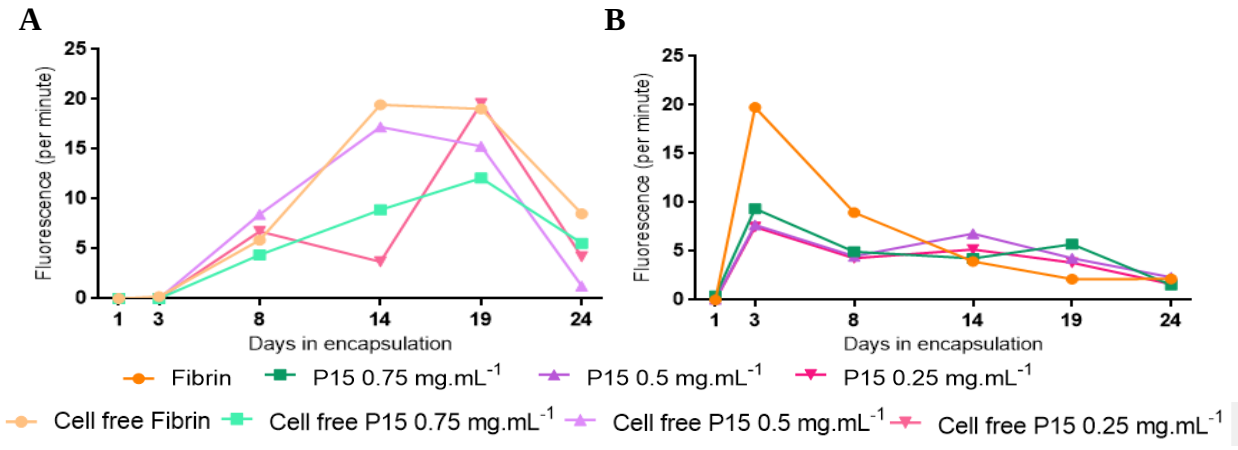

Figure 7.54 The effect of the rate of reduction of resazurin from cell free (**A**) fibrin and P15-fibrinogen gels and the culture medium (**B**) incubated with bBM-MSC encapsulated fibrin, and P15-fibrinogen gels. N=1.

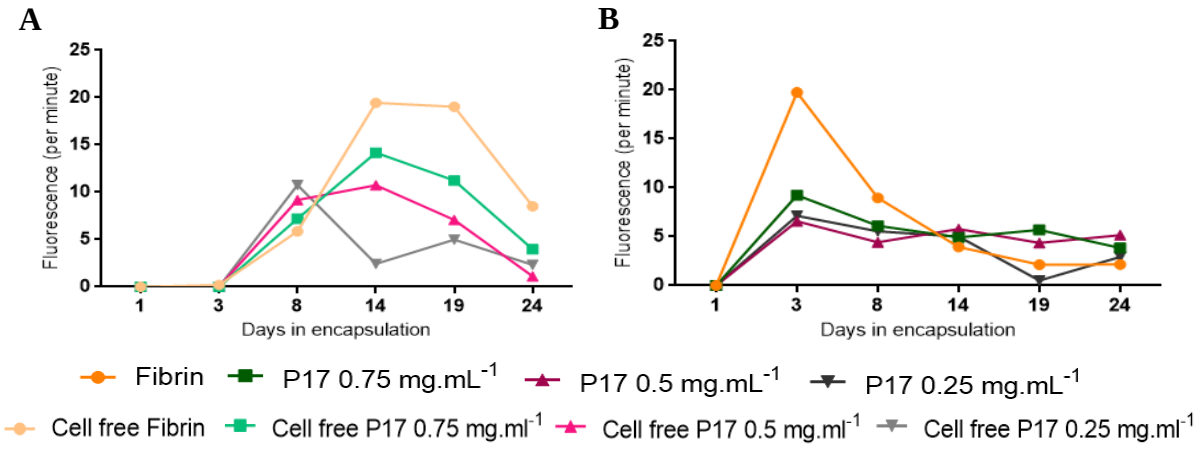

Figure 7.55 The effect of the rate of reduction of resazurin from cell free (**A**) fibrin and P17-fibrinogen gels and the culture medium (**B**) incubated with bBM-MSC encapsulated fibrin, and P17-fibrinogen gels. N=1.

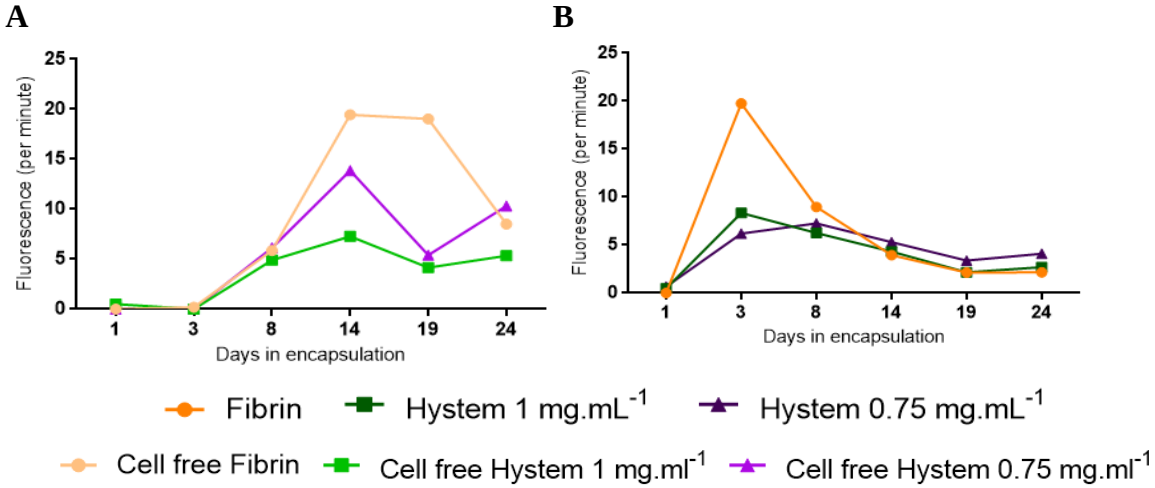

Figure 7.56 The effect of the rate of reduction of resazurin from cell free (**A**) fibrin and HyStem-fibrinogen gels and the culture medium (**B**) incubated with bBM-MSC encapsulated fibrin, and HyStem-fibrinogen gels. N=1.

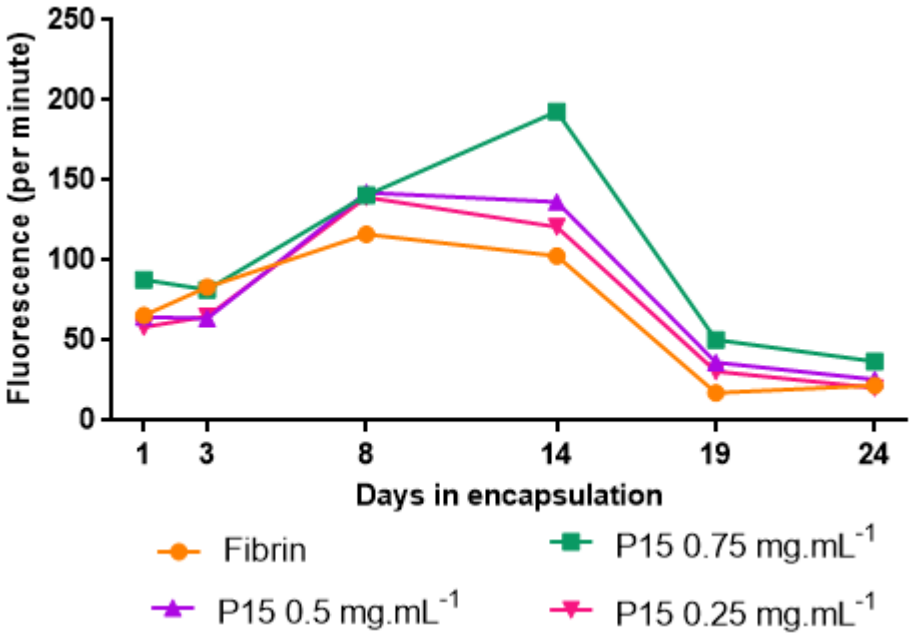

Figure 7.57 Rate of reduction of resazruin of bBM-MSCs encapsulated in fibrin, P15-fibrinogen gels. Measurements were taken at day 1, 3, 8, 14, 19, and 24 of encapsulation. N=1.

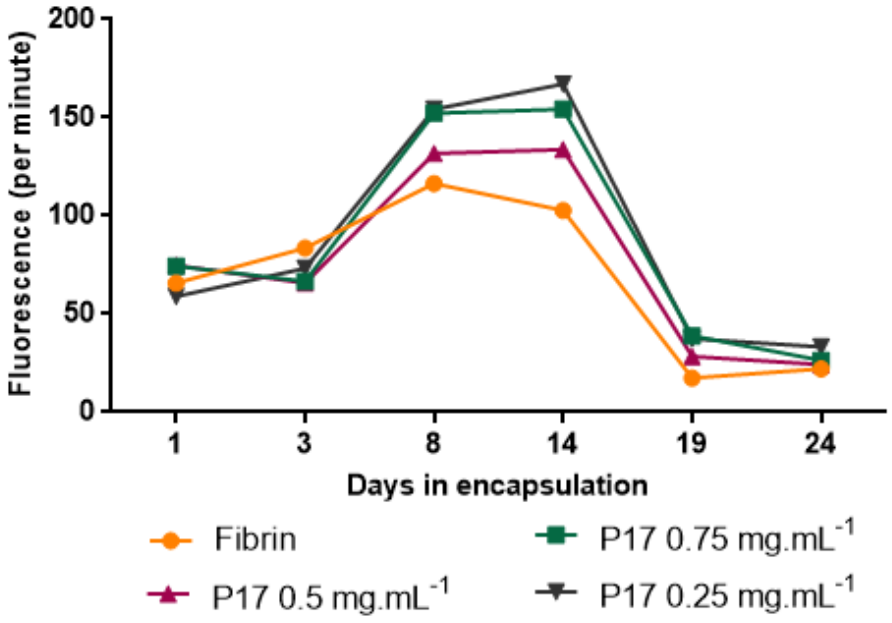

Figure 7.58 Rate of reduction of resazruin of bBM-MSCs encapsulated in fibrin, P17-fibrinogen gels. Measurements were taken at day 1, 3, 8, 14, 19, and 24 of encapsulation. N=1.

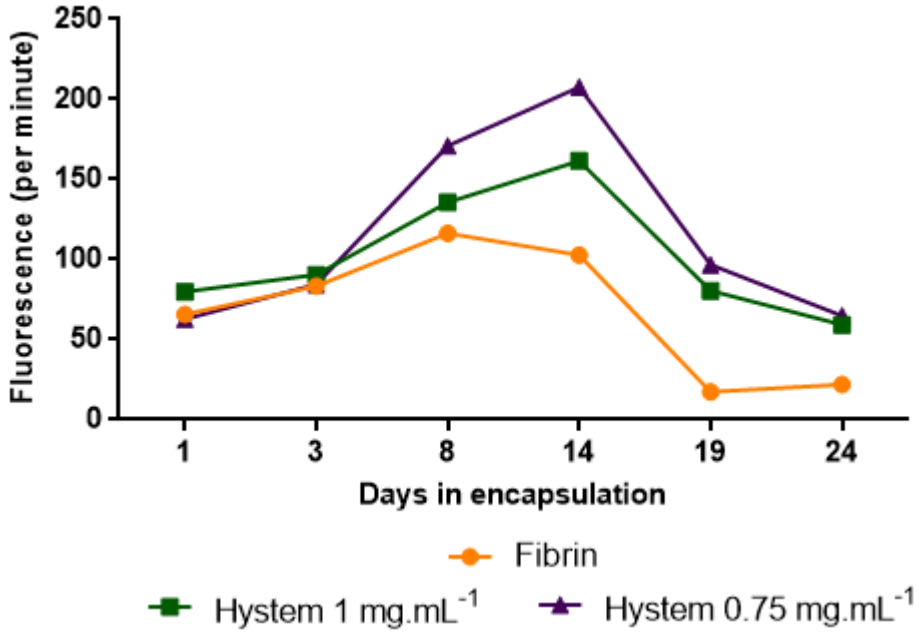

Figure 7.59 Rate of reduction of resazruin of bBM-MSCs encapsulated in fibrin, HyStem-fibrinogen gels. Measurements were taken at day 1, 3, 8, 14, 19, and 24 of encapsulation. N=1.

Glycosaminoglycan content

The effect of the cell free P15, P17, HyStem – fibrinogen and fibrin gels on DMB assay which was used to measure the total GAG content of the cell encapsulated gels was assessed. It was observed that the cell free fibrin gels gave a high reading which suggested that the fibrin gel had non-specifically affected the assay during this experiment, however all values were subtracted from the cell encapsulated data to ensure that the data shown is only from the extracellular matrix deposition from the cells, (Figure 7.60). Total GAG content per gel suggested high levels of ECM deposition in all P15, P17, HyStem and fibrin gel conditions. However the cell encapsulated fibrin gels showed a spread of values for the GAG content which is reflected in the size of the standard error of the mean bars, (Figure 7.61 to Figure 7.63). It was observed that the P15, P17, HyStem – fibrinogen and fibrin gels did undergo some gel degradation and bBM-MSC migration was observed in the culture conditions used particularly with fibrinogen gels formed from HyStem 1 $mg.mL^{-1}$ and HyStem 0.75 $mg.mL^{-1}$. To inhibit gel degradation the gels were then incubated in serum-free conditions with aprotinin.

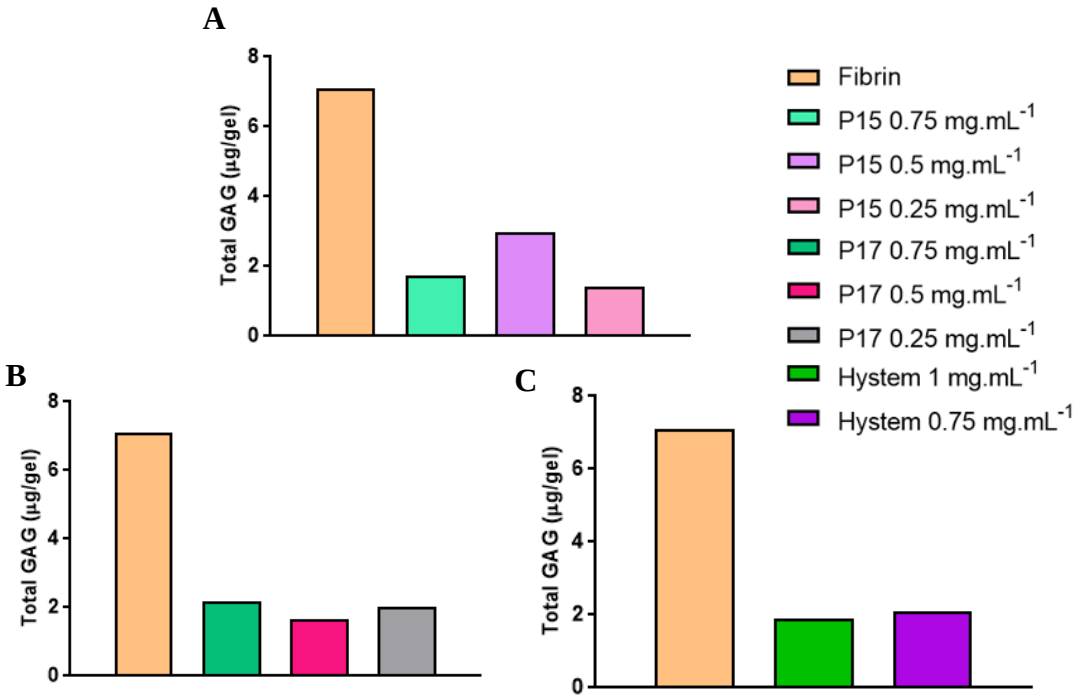

Figure 7.60 The effect of cell free fibrin, P15 (**A**), P17 (**B**), and HyStem (**C**) – fibrinogen gels on DMB assay. Measurements were taken at day 25 of encapsulation. N=1.

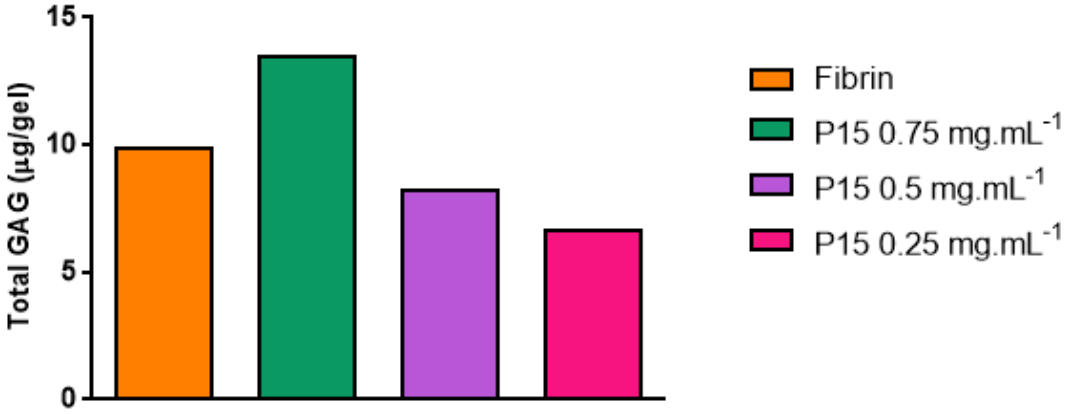

Figure 7.61 Total GAG content (µg per gel) of bBM-MSC encapsulated in fibrin, P15-fibrinogen gels. Measurements were taken at day 25 of encapsulation. N=1.

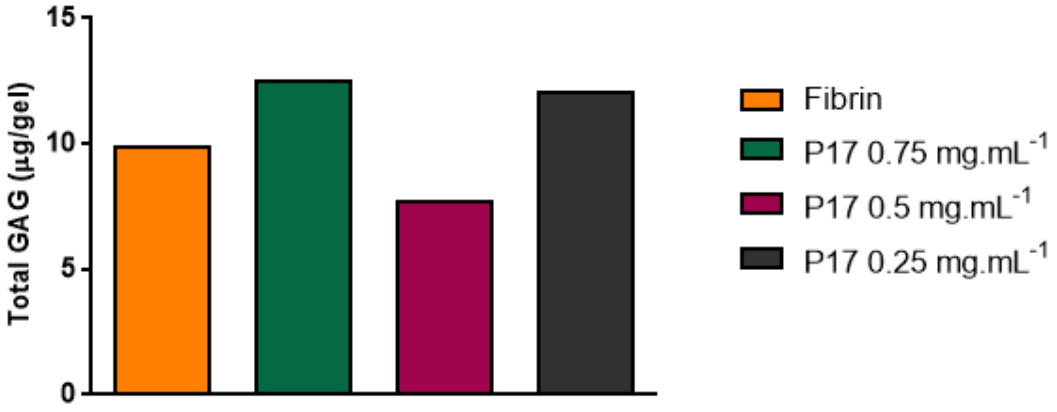

Figure 7.62 Total GAG content (µg per gel) of bBM-MSC encapsulated in fibrin, P17-fibrinogen gels. Measurements were taken at day 25 of encapsulation. N=1.

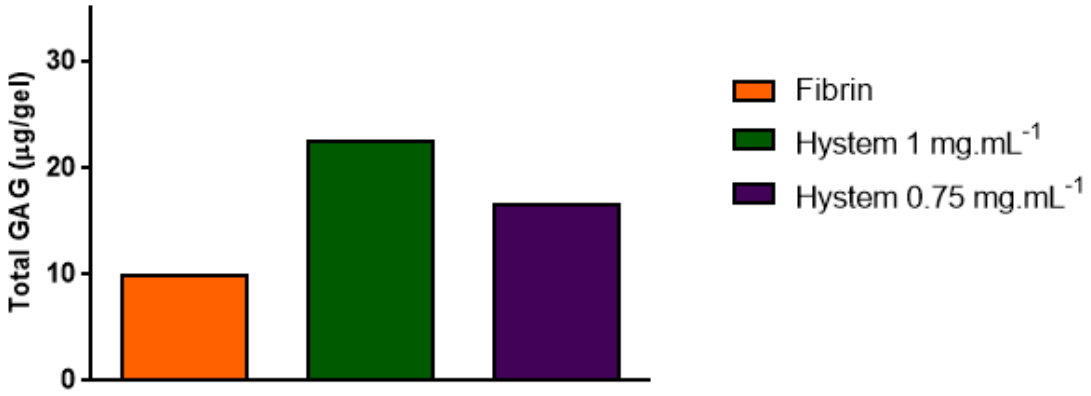

Figure 7.63 Total GAG content (µg per gel) of bBM-MSC encapsulated in fibrin, HyStem – fibrinogen gels. Measurements were taken at day 25 of encapsulation. N=1.

Key Summary

- In the presence of aprotinin, bBM-MSC encapsulated P15, P17 and HyStem – fibrinogen gels exhibited good cell survival and differentiation within the gels.
- HyStem – fibrinogen gels degraded throughout the 21 day culture period.

7.6 P15, P17 and HyStem incubation with serum-free medium and aprotinin

Previously, it had been observed that HyStem degradation occurred in the presence of serum-containing differentiation medium (section 4.4.1) and aprotinin. From previous experiments conducted with bBM-MSC encapsulation in FPA-fibrinogen and fibrin gels, serum-free conditions prolonged the time period before degradation of the gels and MSC migration was observed. Therefore, 300,000 bBM-MSCs were encapsulated in fibrinogen gels formed from P15 at concentrations of 0.75 $mg.mL^{-1}$, 0.5 $mg.mL^{-1}$, and 0.25 $mg.mL^{-1}$, P17 at concentrations of 0.75 $mg.mL^{-1}$, 0.5 $mg.mL^{-1}$, and 0.25 $mg.mL^{-1}$, and HyStem at concentrations of 1 $mg.mL^{-1}$ and 0.75 $mg.mL^{-1}$, and fibrin gels. These gels were incubated in serum-free differentiation media (section 4.4.1) with aprotinin for 21 days. However, even under these serum-free conditions it was observed that MSC encapsulated HyStem-fibrinogen gels formed using 1 $mg.mL^{-1}$ and 0.75 $mg.mL^{-1}$ HyStem had degraded during the 21 day culture period and cell migration had occurred onto the tissue culture plastic surface. In addition, cell migration was observed in all the other hydrogels but no apparent gel degradation (i.e. no decreases in cell volumes) was observed. These results are interesting, since, they show that the MSC migration from the fibrinogen gels formed with FPA, P15 or P17 could not have been due to chemical degradation as the cell-free gels remained intact and also the migration must have been independent of any influence of plasmin or other aprotinin-insensitive proteinase as there was no source of plasminogen in the serum-free culture medium and it contained the serine proteinase inhibitor, aprotinin.

Cell activity

Resazurin reduction by culture medium taken from the incubation of the cell encapsulated gels suggested very little cell activity, indicative of cells or cellular debris, within the medium, (Figure 7.64 image B to Figure 7.66 image B). Cell free gels exhibited little resarufin formation (the reduced form of resazurin) (Figure 7.64 image A to Figure 7.66 image A). Preliminary data for bBM-MSC encapsulated gels suggests that all cells survived in all P15, P17, HyStem and fibrin hydrogel conditions for the 21 day period of encapsulation (Figure 7.67 to Figure 7.69). The reduction in resazurin plateaued at day 7 of encapsulation which suggested that the cells became less metabolically active. It is possible that this lower level of cell activity is reflective of chondrogenic differentiation and that the cells were synthesising ECM.

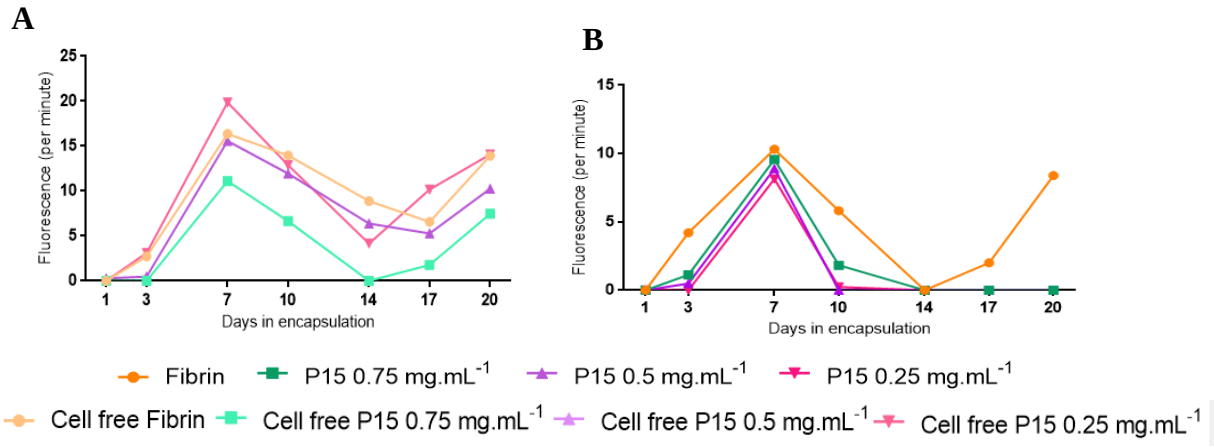

Figure 7.64 The effect of the rate of reduction of resazruin from cell free fibrin and P15-fibrinogen gels (**A**) and the culture medium incubated with bBM-MSC encapsulated fibrin and P15-fibrinogen gels (**B**). N=1.

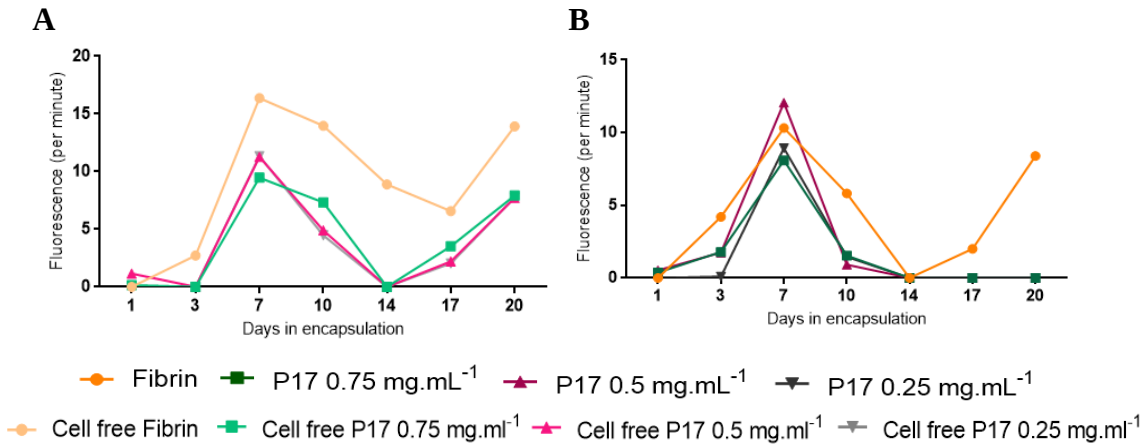

Figure 7.65 The effect of the rate of reduction of resazruin from cell free fibrin and P17-fibrinogen gels (**A**) and the culture medium incubated with bBM-MSC encapsulated fibrin and P17-fibrinogen gels (**B**). N=1.

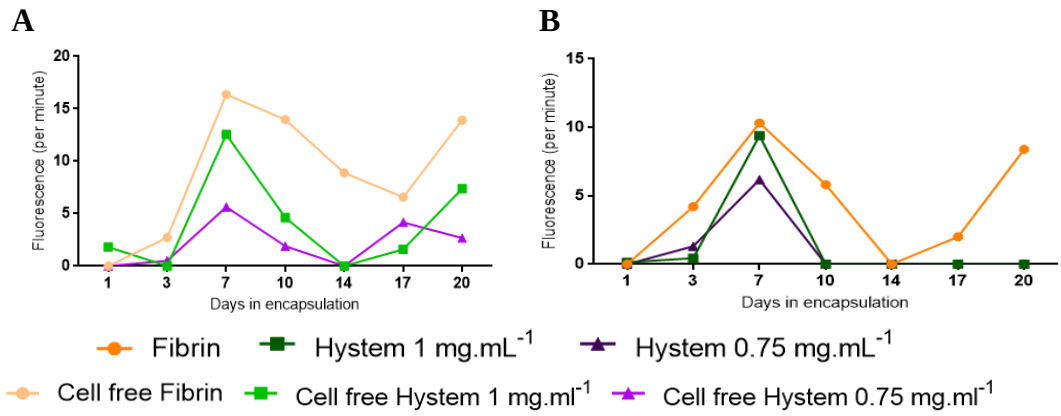

Figure 7.66 The effect of the rate of reduction of resazruin from cell free fibrin and HyStem-fibrinogen gels (**A**) and the culture medium incubated with bBM-MSC encapsulated fibrin and HyStem-fibrinogen gels (**B**). N=1.

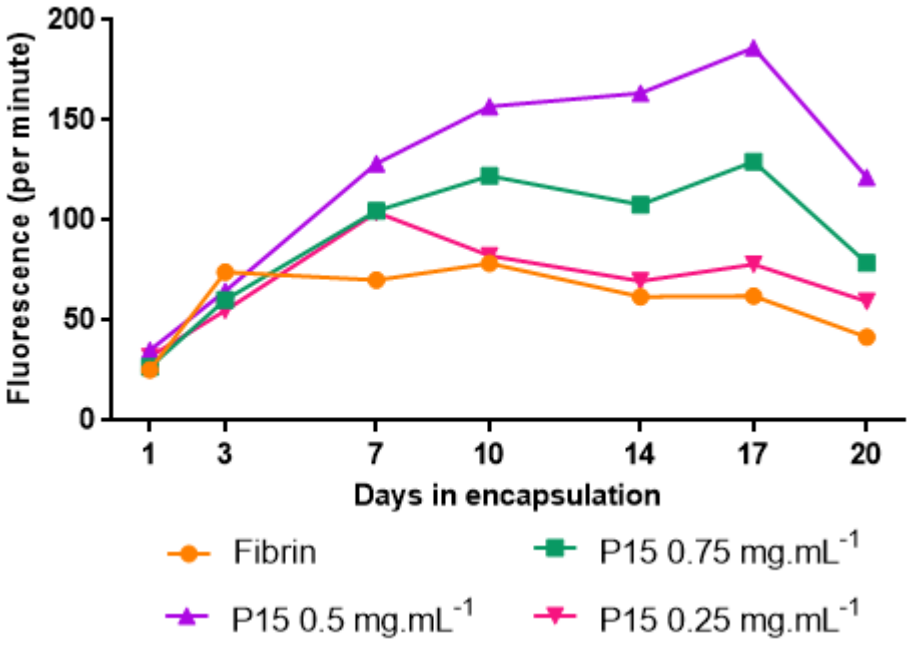

Figure 7.67 Rate of reduction of resazruin of bBM-MSCs encapsulated in P15-fibrinogen and fibrin gels. Measurements were taken at day 1, 3, 7, 14, 17, and 20 of encapsulation. N=1.

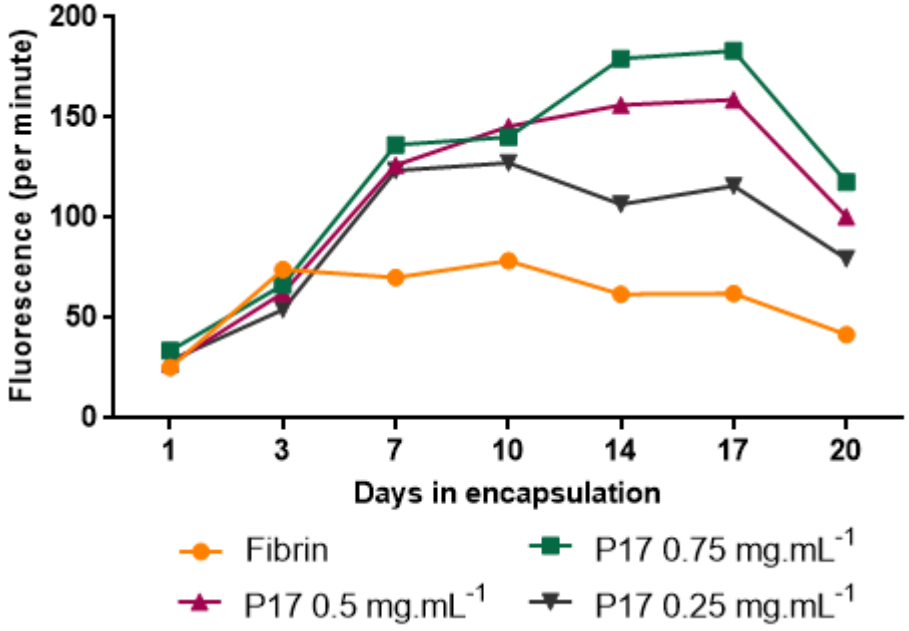

Figure 7.68 Rate of reduction of resazruin of bBM-MSCs encapsulated fibrin and P17-fibringoen gels. Measurements were taken at day 1, 3, 7, 14, 17, and 20 of encapsulation. N=1.

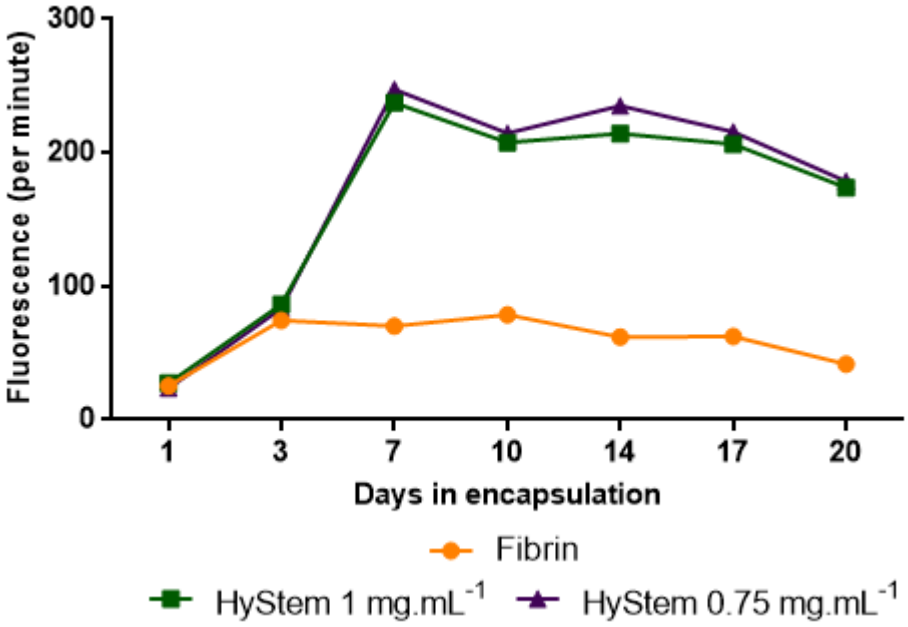

Figure 7.69 Rate of reduction of resazruin of bBM-MSC encapsulated fibrin and HyStem-fibrinogen gels. Measurements were taken at day 1, 3, 7, 14, 17, and 20 of encapsulation. N=1.

Glycosaminoglycan content

Total GAG content revealed high background values for P15 (image A Figure 7.70) and P17 (image B Figure 7.70) the cell free gels. The cell free values were subtracted from the cell encapsulated values to ensure a measure of ECM deposition. Total GAG content per gel suggests all P15, P17 and HyStem gels supported ECM synthesis (Figure 7.71 to Figure 7.73).

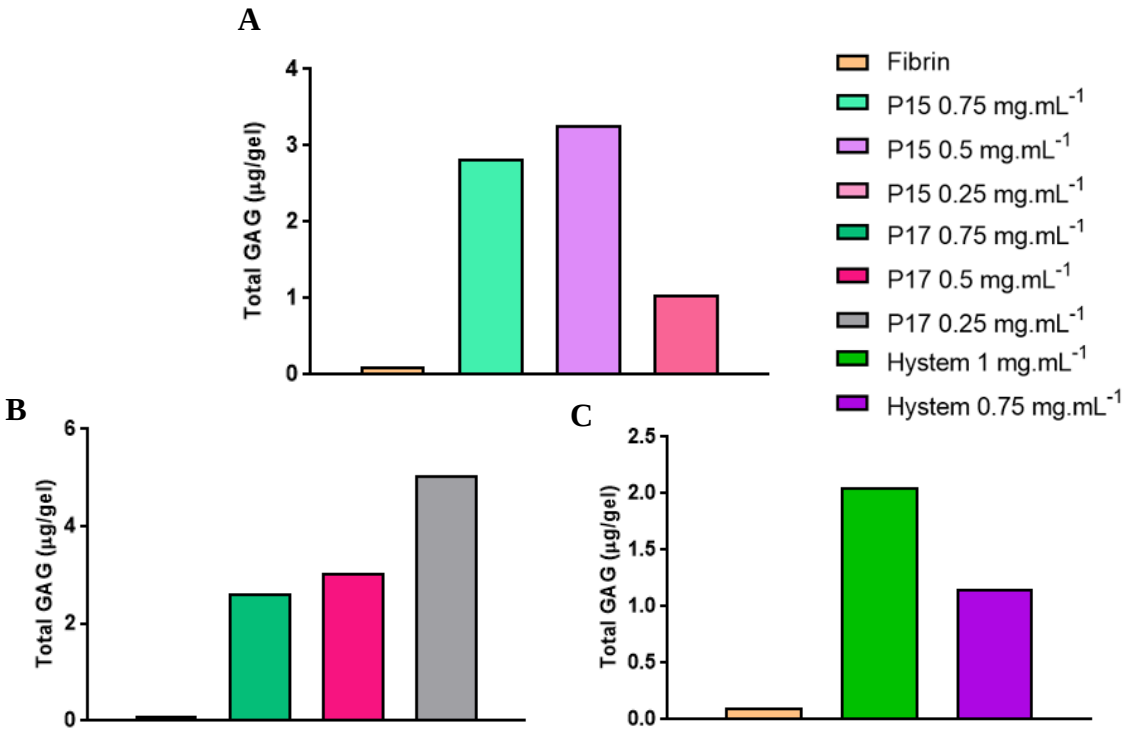

Figure 7.70 Cell free gels incubated with DMB assay. P15-fibrinogen (**A**), P17-fibrinogen (**B**) and HySem-fibrinogen gels (**C**). Fibrin was used as a reference material (A, B, C). Measurements were taken at day 21 of encapsulation. N=1.

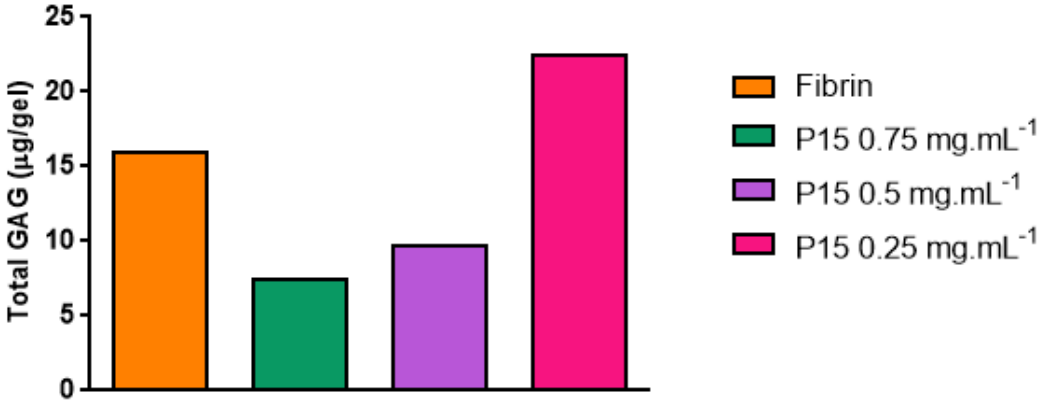

Figure 7.71 Total GAG content per gel of bBM-MSC encapsulated fibrin, P15-fibrinogen gels. Measurements were taken at day 21 of encapsulation. N=1.

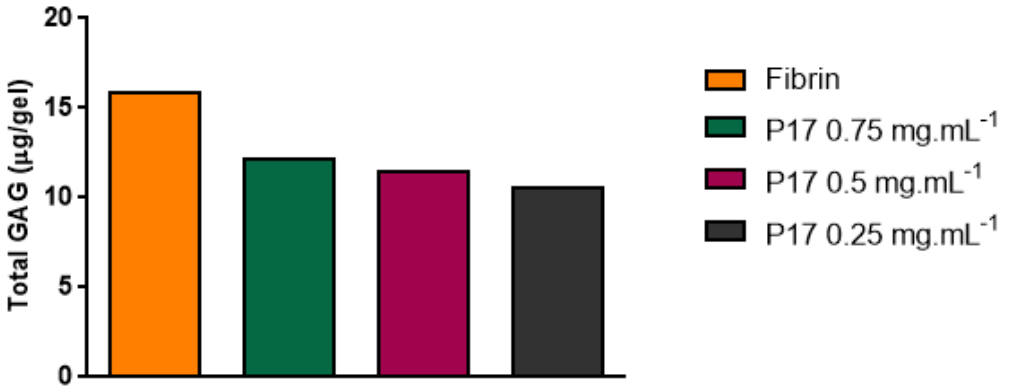

Figure 7.72 Total GAG content per gel of bBM-MSC encapsulated fibrin, P17-fibrinogen gels. Measurements were taken at day 21 of encapsulation. N=1.

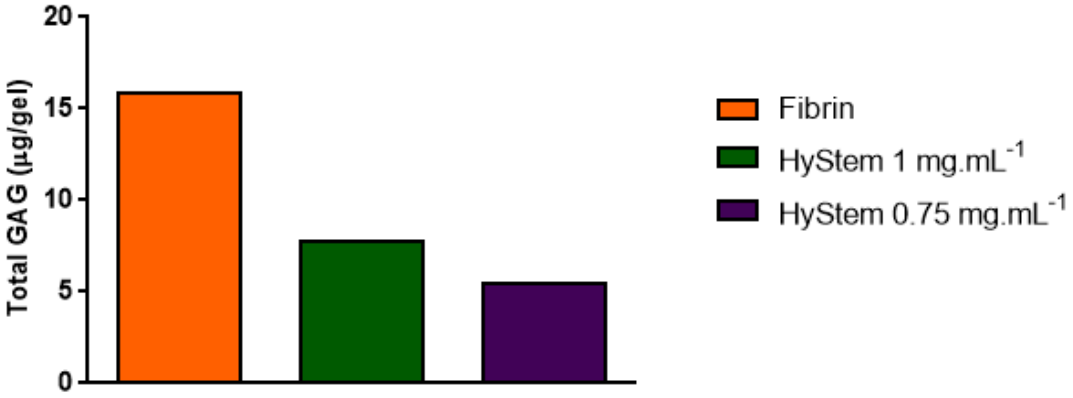

Figure 7.73 Total GAG content per gel of bBM-MSC encapsulated fibrin, and HyStem-fibrinogen gels. Measurements were taken at day 21 of encapsulation. N=1.

Haematoxylin and Eosin staining

H&E staining was carried out on cell free and bBM-MSC encapsulated hydrogels. From the cell free images (Figure 7.74) it is possible to observe that the P15, P17, and HyStem hydrogels stained pink and therefore ECM deposition cannot be fully observed (Figure 7.75 to Figure 7.77). From the H&E staining it is possible to see dense cellular and ECM deposition layers on the outer edges of the hydrogels, less ECM deposition can be observed in the centre of the gels.

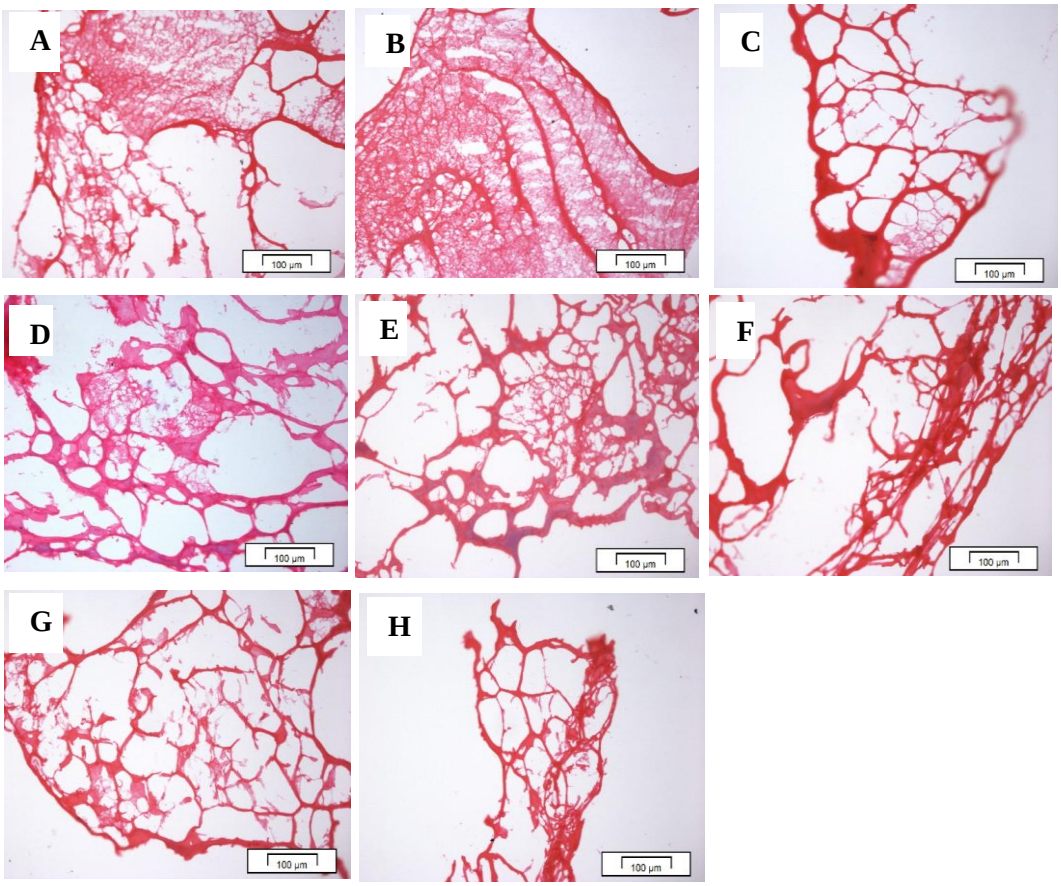

Figure 7.74 Histological H&E staining of sections taken from cell free P15-fibrinogen gels formed from (A) P15 0.75 mg.mL^{-1}, (B) P15 0.5 mg.mL^{-1}, (C) P15 0.25 mg.mL^{-1}, P17-fibrinogen gels formed from (D) P17 0.75 mg.mL^{-1}, (E) P17 0.5 mg.mL^{-1}, (F) P17 0.25 mg.mL^{-1}, and HyStem-fibrinogen gels formed from (G) HyStem 1 mg.mL^{-1} and (H) HyStem 0.75 mg.mL^{-1}. Images were taken with a magnification of x20. Scale bars are shown on the images.

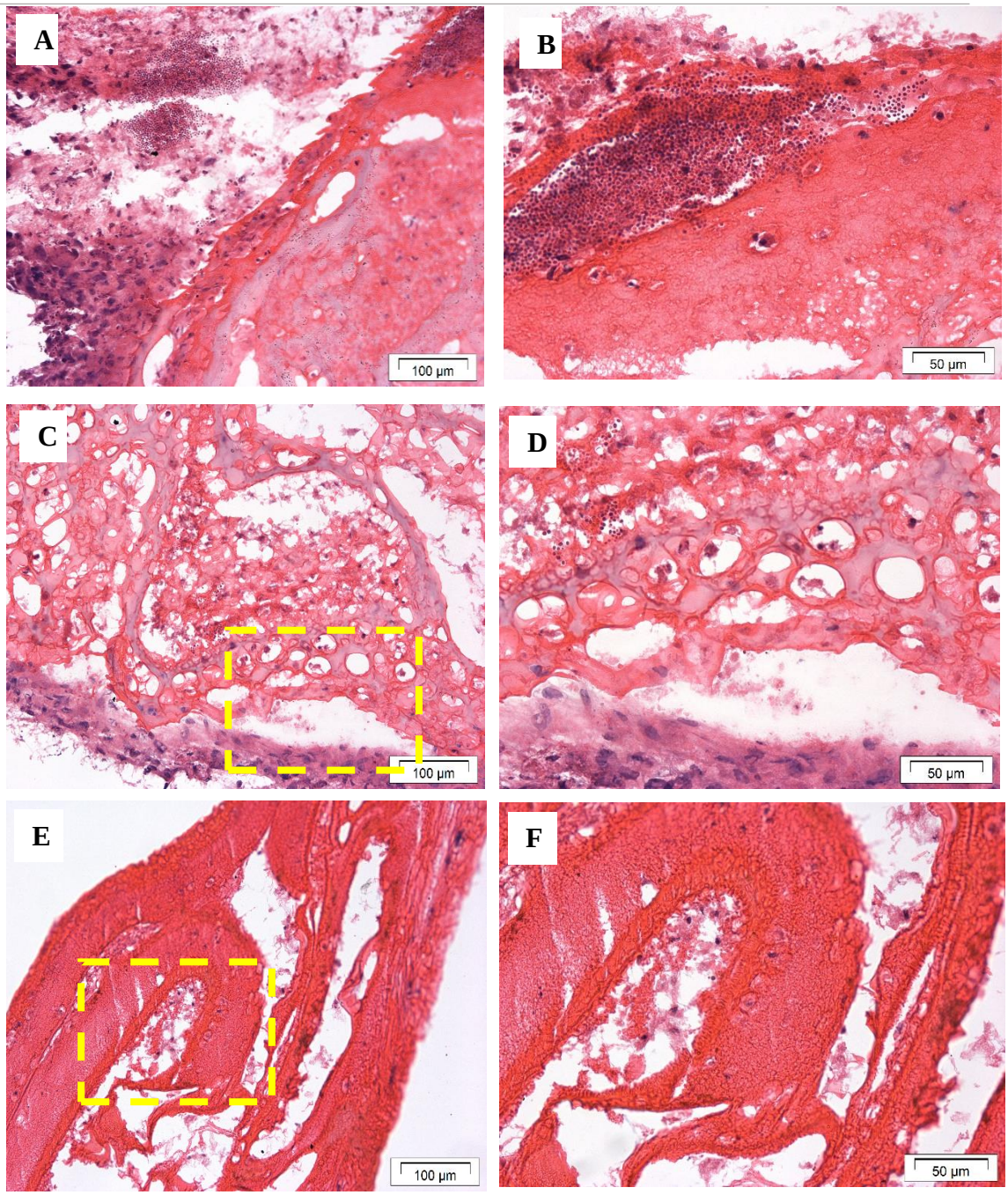

Figure 7.75 Histological H&E stained sections taken from bBM-MSC encapsulated in P15-fibrinogen gels formed from (A, B) P15 0.75 mg.mL^{-1}, (C, D) P15 0.5 mg.mL^{-1}, (E, F) P15 0.25 mg.mL^{-1}, for 21 days. Images were taken at a magnification of x20 (A, C, E) and x40 (B, D, F). Scale bars are shown on the images.

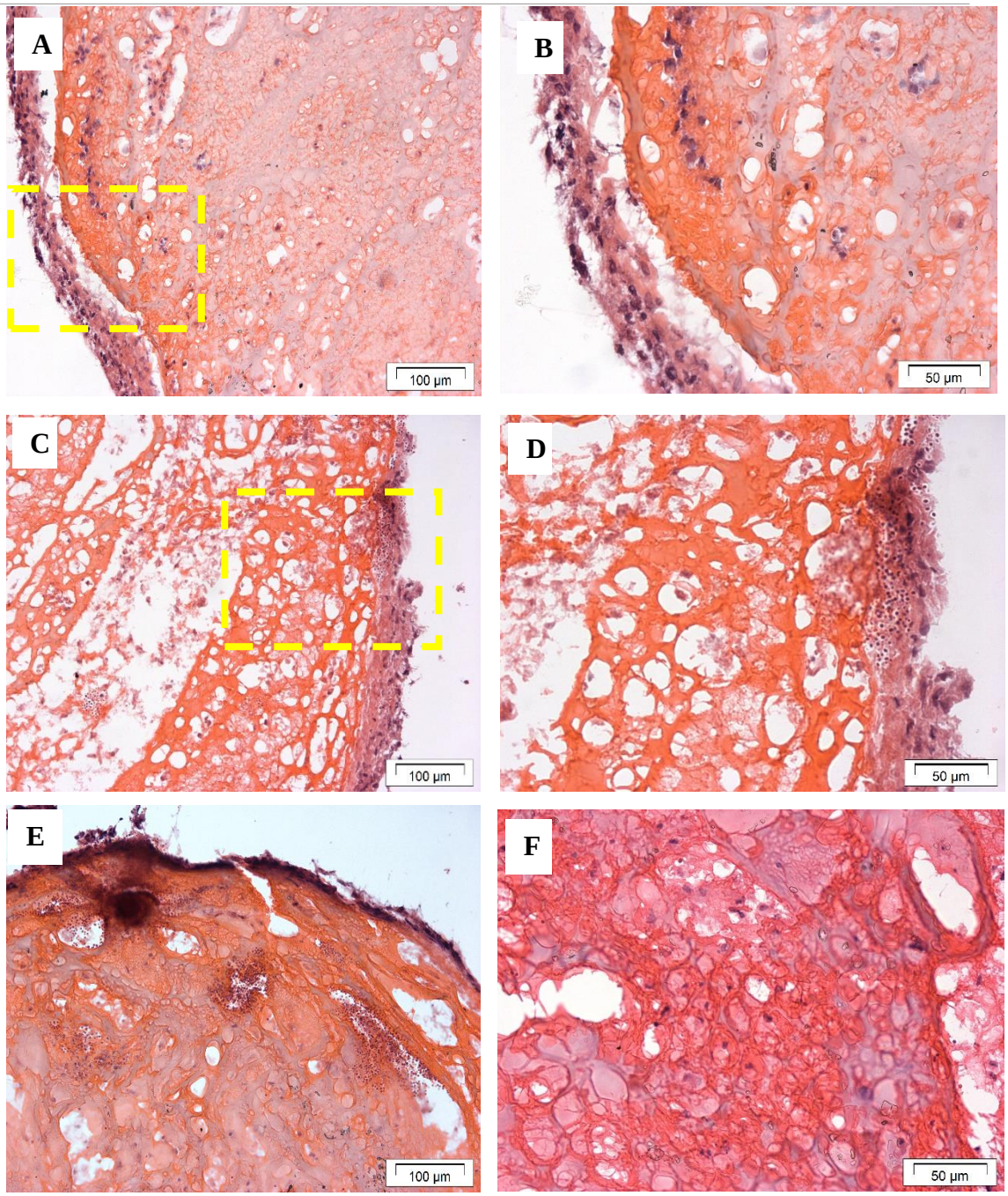

Figure 7.76 Histological H&E stained sections taken from bBM-MSC encapsulated in P17-fibrinogen gels formed from (A, B) P17 0.75 mg.mL^{-1}, (C, D) P17 0.5 mg.mL^{-1}, (E, F) P17 0.25 mg.mL^{-1}, for 21 days. Images were taken at a magnification of x20 (A, C, E) and x40 (B, D, F). Scale bars are shown on the images.

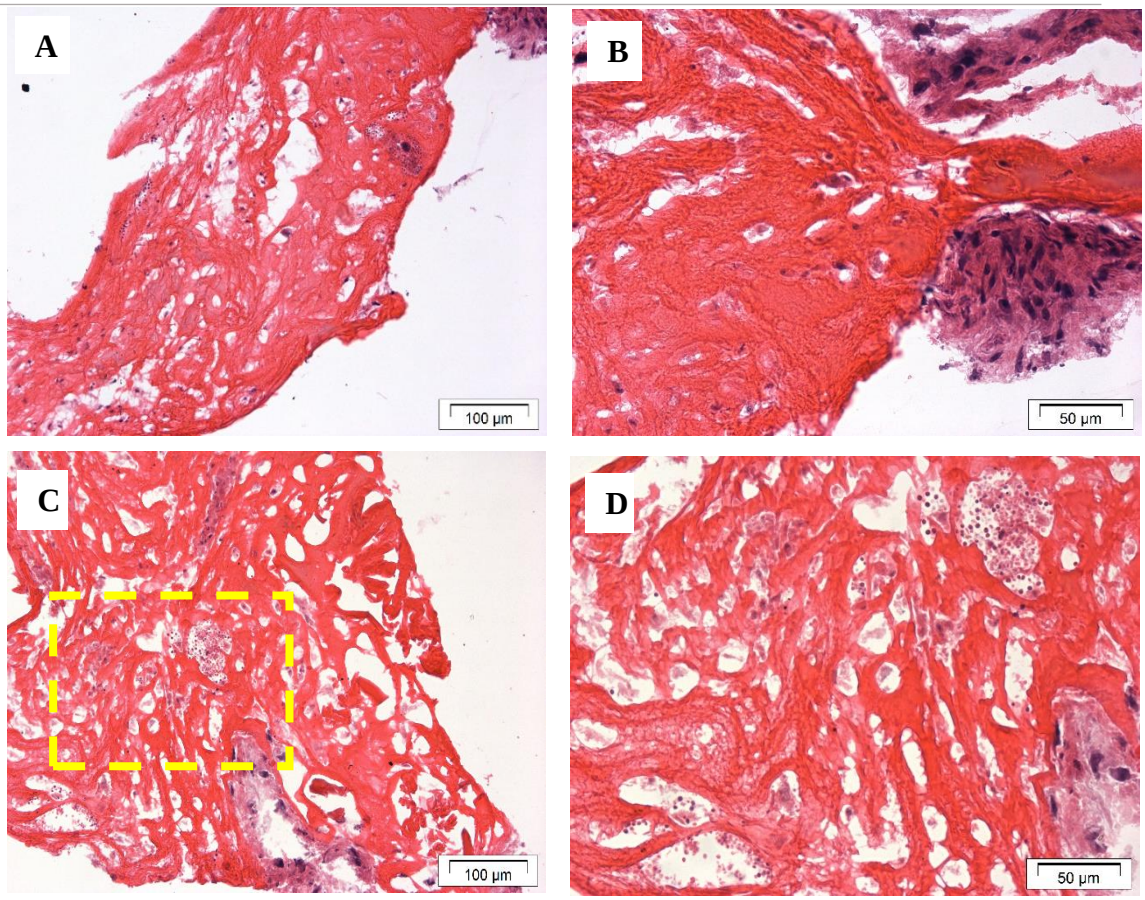

Figure 7.77 Histological H&E stained sections taken from bBM-MSC encapsulated in HyStem-fibrinogen gels formed from (A, B) HyStem 1 mg.mL^{-1}, (C, D) HyStem 0.75 mg.mL^{-1}, for 21 days. Images were taken at a magnification of x20 (A, C) and x40 (B, D). Scale bars are shown on the images.

Toluidine blue staining

Cell free gels (Figure 7.78) were stained with Toluidine blue giving the gel structure dark blue colour which made distinguishing the purple proteoglycan stain in the bBM-MSC encapsulated gels more difficult. However, P17 gels (Figure 7.80) have more areas of dark purple staining that is suggesting proteoglycan formation in these gels in comparison to the P15 (Figure 7.79) and HyStem (Figure 7.81) gels bBM-MSC encapsulated gels. It is possible to see in HyStem 0.75 mg.mL^{-1} (images C and D, Figure 7.81) more areas of bBM-MSC congregation within the pores of the gel, from the dark blue nucleic acid staining.

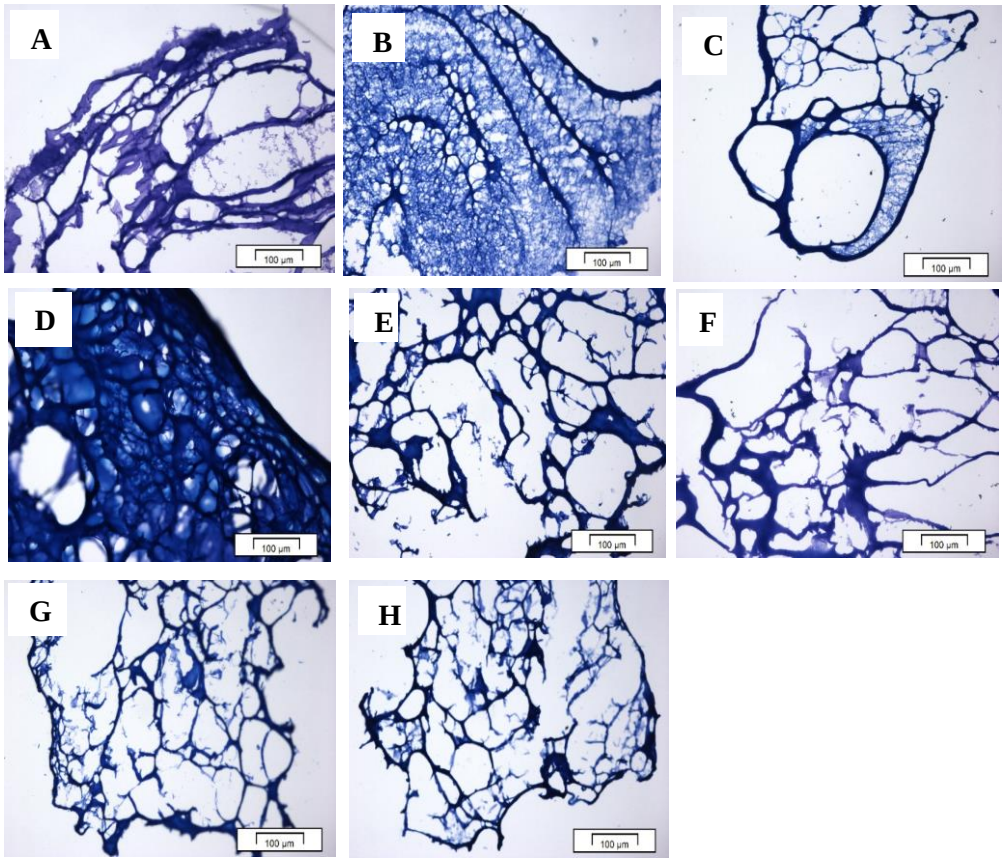

Figure 7.78 Histological Toluidine blue staining of sections taken from cell free P15-fibrinogen gels formed from (A) P15 0.75 mg.mL^{-1}, (B) P15 0.5 mg.mL^{-1}, (C) P15 0.25 mg.mL^{-1}, P17-fibrinogen gels formed from (D) P17 0.75 mg.mL^{-1}, (E) P17 0.5 mg.mL^{-1}, (F) P17 0.25 mg.mL^{-1}, and HyStem-fibrinogen gels formed from (G) HyStem 1 mg.mL^{-1} and (H) HyStem 0.75 mg.mL^{-1}. Images were taken with a magnification of x20. Scale bars are shown on the images.

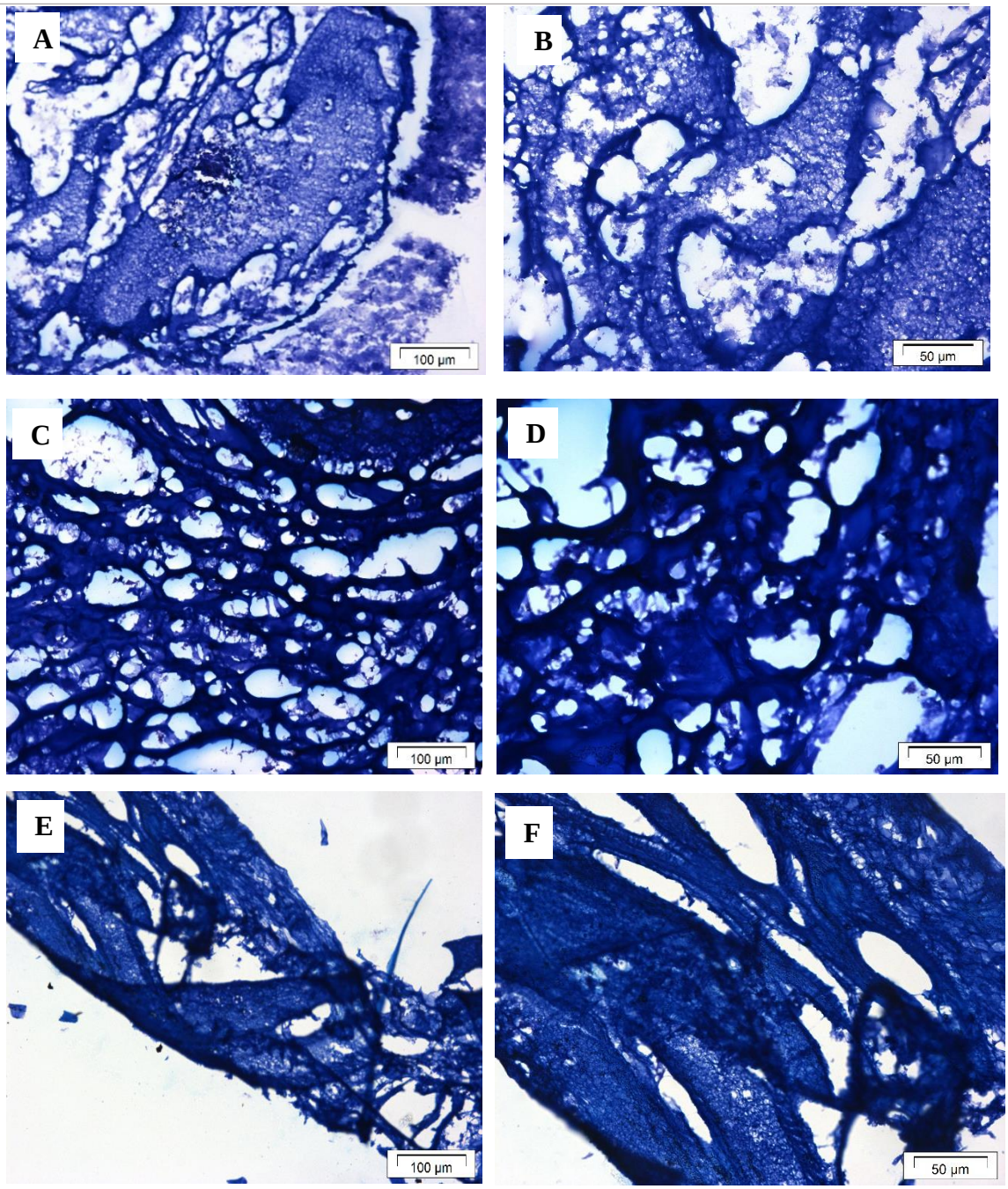

Figure 7.79 Histological Toluidine blue stained sections taken from bBM-MSC encapsulated in P15-fibrinogen gels formed from (A, B) P15 0.75 mg.mL^{-1}, (C, D) P15 0.5 mg.mL^{-1}, (E, F) P15 0.25 mg.mL^{-1}, for 21 days. Images were taken at a magnification of x20 (A, C, E) and x40 (B, D, F). Scale bars are shown on the images.

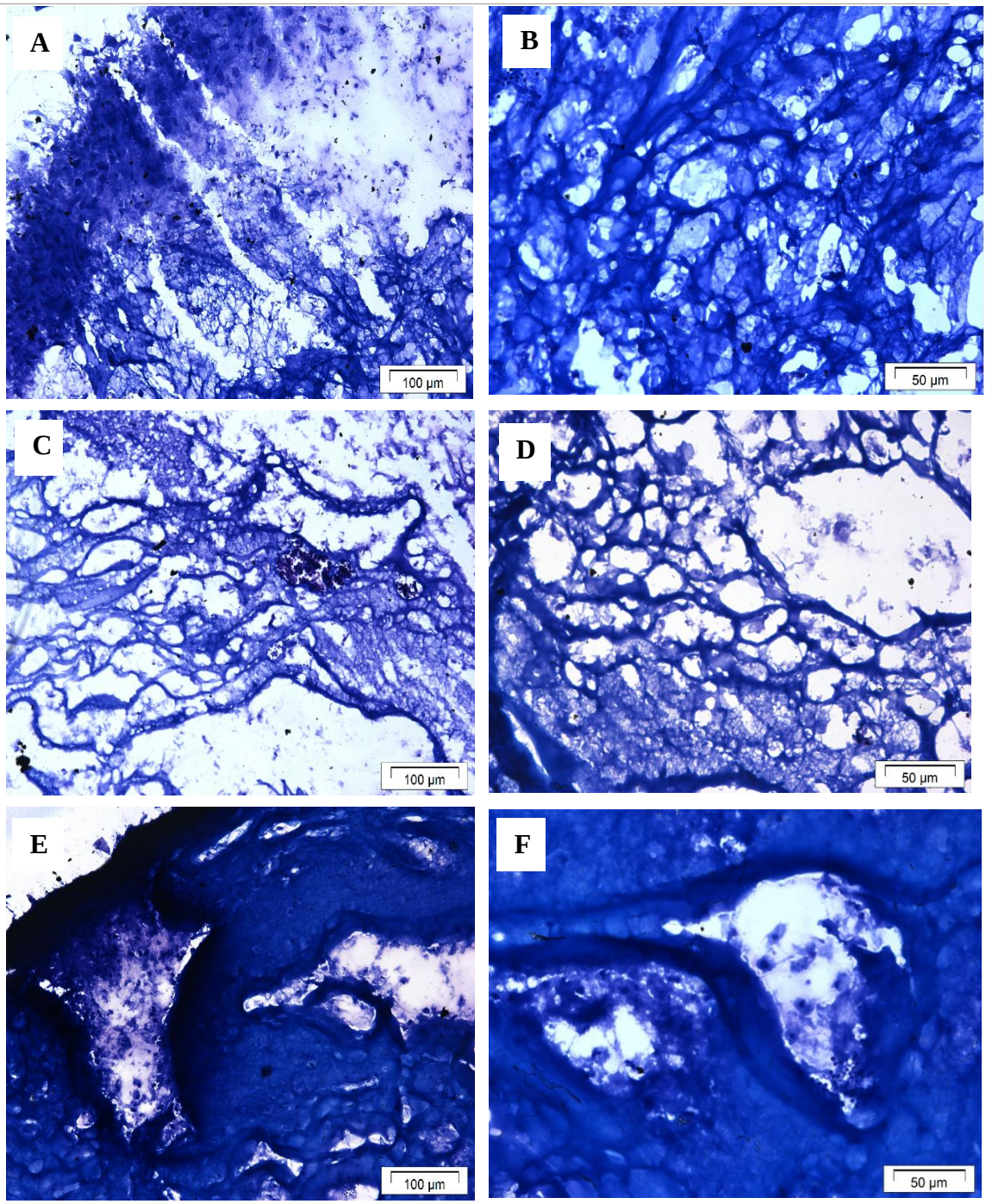

Figure 7.80 Histological Toluidine blue stained sections taken from bBM-MSC encapsulated in P17-fibrinogen gels formed from (A, B) P17 0.75 mg.mL^{-1}, (C, D) P17 0.5 mg.mL^{-1}, (E, F) P17 0.25 mg.mL^{-1}, for 21 days. Images were taken at a magnification of x20 (A, C, E) and x40 (B, D, F). Scale bars are shown on the images.

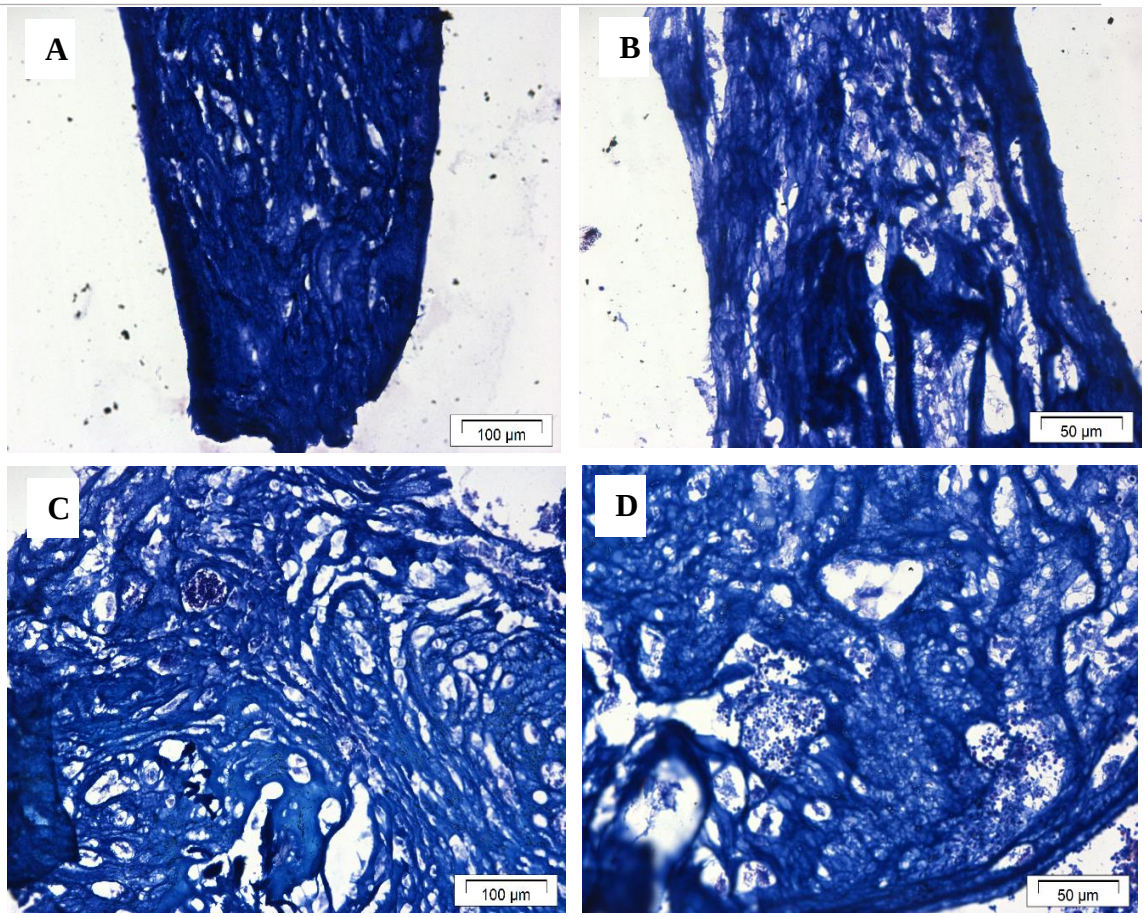

Figure 7.81 Histological Toluidine blue stained sections taken from bBM-MSC encapsulated in HyStem-fibrinogen gels formed from (A, B) HyStem 1 mg.mL^{-1}, (C, D) HyStem 0.75 mg.mL^{-1}, for 21 days. Images were taken at a magnification of x20 (A, C) and x40 (B, D). Scale bars are shown on the images.

Key Summary

- The cell activity, GAG content and histological staining suggested that bBM-MSCs survived and differentiated when encapsulated in P15, P17 and HyStem – fibrinogen gels.
- In the presence of aprotinin in serum-free conditions, HyStem – fibrinogen gels visibly degraded throughout the 21 day culture period.
- bBM-MSC migration was observed in all P15, P17 and HyStem – fibrinogen gels.
- Therefore, there is evidence to suggest that HyStem – fibrinogen gels at the concentrations investigated in this thesis, is not a suitable cell delivery system for cartilage repair.

7.7 MSC delivery to cartilage injury

An injured articular cartilage model was developed as described in section 4.2.5, Figure 4.1, in which cell encapsulated gels could be held in the cartilage defect. bBM-MSCs were encapsulated in fibrinogen -FPA 2.66 mg.mL^{-1} or fibrin gels at 300,000 cells per gel. The MSC encapsulated gels were then transferred into the cartilage defect of the cartilage injury model (1 gel per defect) and the whole cartilage model co-cultured with the MSC encapsulated gels under chondrogenic conditions for 2 weeks.

Cell activity

Cell viability determinations using the PrestoBlue® showed that the cartilage-bBM-MSC encapsulated gel systems remained viable over the 14 day incubation period. These results are shown in Figure 7.83. The culture medium removed from the cartilage – gel model showed very little resazurin dye reduction indicating that the culture medium contained little cells or cell debris from the cartilage – bBM-MSC encapsulated model, Figure 7.82.

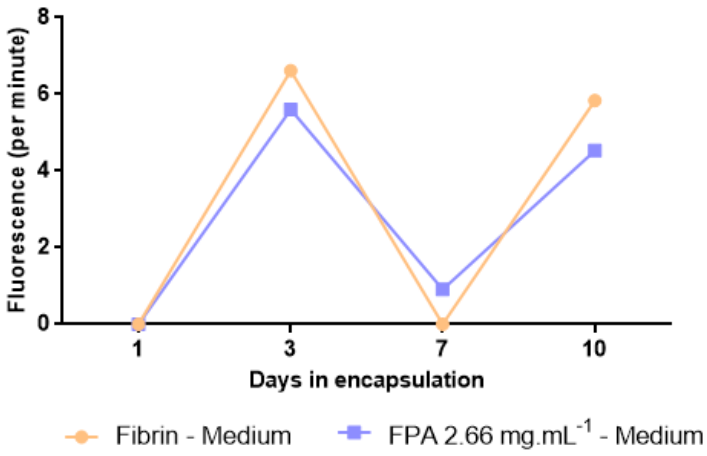

Figure 7.82 Rate of reduction of PrestoBlue® (shown as mean relative fluorescence units per minute) from the medium removed at day 1, 3, 7 and 10 from bBM-MSC encapsulated FPA-fibrinogen 2.66 mg.mL^{-1}and fibrin gels delivered to a cartilage injury model. N=1.

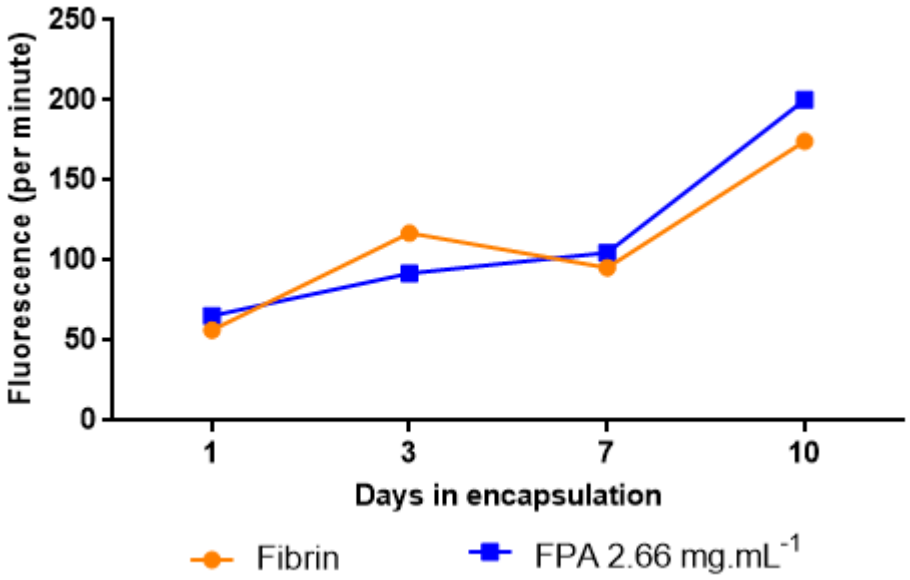

Figure 7.83 Rate of reduction of PrestoBlue® (shown as mean relative fluorescence units per minute) indicating the cell activity of bBM-MSC encapsulated FPA-fibrinogen 2.66 mg.mL^{-1}and fibrin gels delivered to a cartilage injury model. N=1.

Phase contrast images

Phase contrast images taken at day 4 of culture of the bBM-MSC encapsulated gels delivered to an injured cartilage model showed bBM-MSCs had migrated from FPA-fibrinogen 2.66 mg.mL^{-1} gels to the injured cartilage, refer to Figure 7.84 images A and B. In contrast, few bBM-MSCs appeared to migrate towards the injury site at day 4 of encapsulation in fibrin gels, refer to Figure 7.84 images C and D. However, bBM-MSC migration from the fibrin gels towards the cartilage injury occurred between day 4 and day 10 and were observed as confluent between the gel and the cartilage injury.

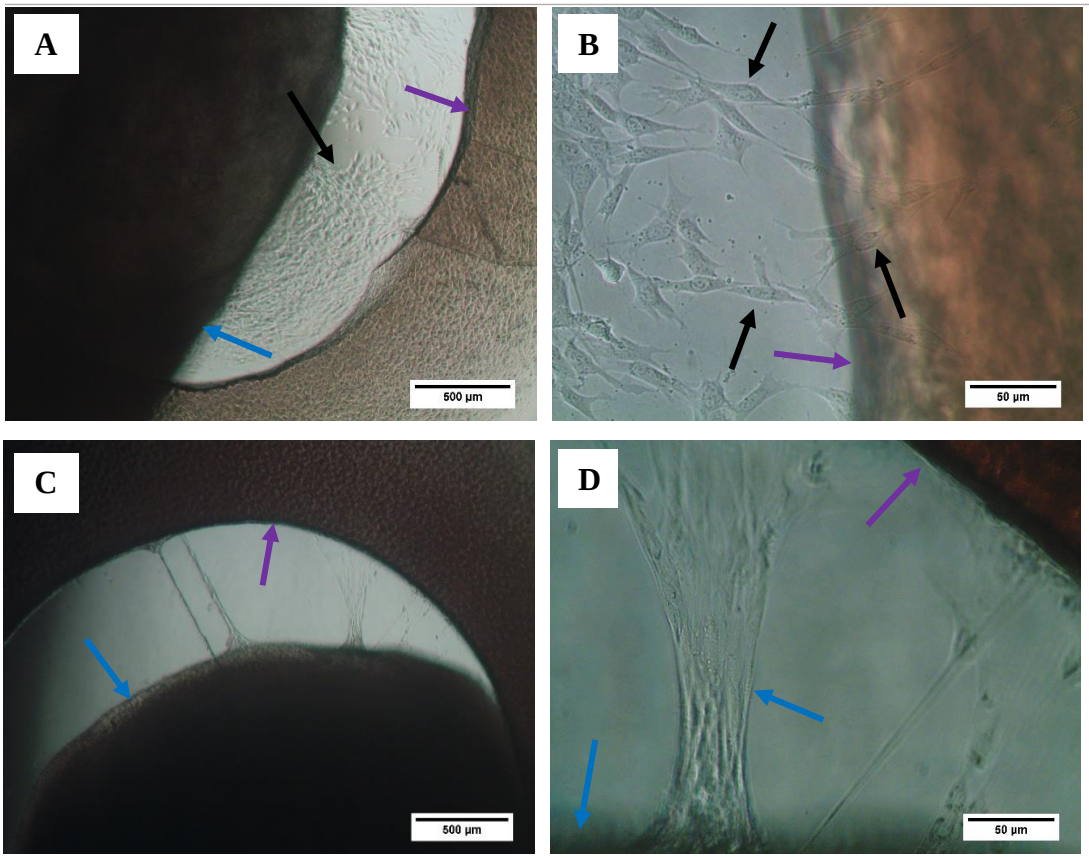

Figure 7.84 Phase contrast images of bBM MSC encapsulated in FPA-fibrinogen 2.66 mg.mL^{-1} (A and B) and fibrin (C and D) gels, blue arrows, delivered to injured articular cartilage pieces, purple arrows. Migration of bBM-MSCs are represented by black arrows. Images taken at day 4 of encapsulation at a magnification of x4 (A and C) and x20 (B and D). Scale bars are shown on the image.

Key Summary

- bBM-MSCs migrated from the FPA-fibrinogen and fibrin gels towards the injured cartilage.
- Cartilage explant injury model can be used as an *in vitro* model for cartilage repair.

8.0 Discussion

8.1 The formation and structure of gels

The gelation method and rate of the novel fibrinogen cross-linked gels is particularly important for cell survival. Gels that require external factors such as heat or photopolymerisation are adding factors which could affect cellular survival and function, and also limits the use of these gels in a clinical setting. The method of gelation for the FBP carrier molecules with fibrinogen requires the two liquid precursors to combine, rapidly forming a gel. This is a very simple and effective gelation method overcoming limitations without the addition of further techniques for gelation. The novel cross-linked fibrinogen gels therefore, are advantageous in clinical settings in comparison to gels such as agarose. The gelation rates of the novel cross-linked fibrinogen gels and fibrin were analysed using KC4 coagulation analyser; P15, P17 and FPA had a quicker gelation time with fibrinogen in comparison to fibrin, section 5.1. In clinic, the novel cross-linked fibrinogen gels would be fabricated *in situ* and a specialised syringe would be required to ensure the FBP carrier molecules and fibrinogen do not have contact before the required gelation site. The advantage to this is that the cells would become entrapped in the gel quicker providing a safe encapsulation to keep cells localised at the injury site.

The gels were fabricated using a NaCl buffer, the concentration of salt present during gelation can impact the structural properties of the gels. Davies et al found that increasing the salt concentration to 2.6 (w/v) % increased the mechanical properties of the gel and enhanced osteogenic differentiation [235]. This suggested that the gel had become much stiffer in comparison to the 0.9 (w/v) % of NaCl used during this project. Therefore, the use of higher salt concentrations may impinge chondrogenic differentiation because a softer environment is required. Also gelation in a non-physiological salt concentrations could also possibly have detrimental effects on some cell types. However, the novel cross-linked fibrinogen gels could be tailored for use in osteogenic applications by increasing the NaCl concentration present during gelation.

Cell survival and differentiation depends on the structural properties of the hydrogel in which it is encapsulated. Scanning electron microscopy (SEM) was chosen based on the success of dehydration methods and imaging of various hydrogels within the literature. Methods researched involved fixation of the gel in glutaraldehyde before the dehydration process with increased concentrations of ethanol, osmium tetroxide was used for fixing cell encapsulated gels and also provided a heavy metal stain for greater contrast

between cells and the material [194], [235], [236]. However, in this investigation it became evident that ethanol dehydration did not keep the integrity of the hydrogel structure intact. It can be seen from the SEM images in section 5.2 that clear defined fibres were not observed. Whereas, imaged gels after freeze drying enabled observations of a clear, defined structure of the gels and enabled the comparison of the FPA, P15, P17 - fibrinogen and fibrin structure. However, due to the necessary dehydration step for all SEM, the surface structure observed may not fully represent that of the hydrated fibrinogen gels. The structures of the fibrin, FPA, P15 and P17 – fibrinogen gels have distinct differences as seen on the SEM images in section 5.2. Fibrin has clear, defined fibres whereas FPA-fibrinogen gels have a more foam-like structure with defined pores. Observations suggest P15 and P17 – fibrinogen gels had similar structures and display areas of both fibres and foam-like structures throughout the gels. Haemostatix Ltd. observed areas of fibres as well as areas of foam-like structures when carrying out SEM on the FPA – fibrinogen hydrogels, however areas of fibres were not found under the conditions used for this project.

Areas of undefined fibres were observed within the FPA gels. Again, this may have been an artefact of the dehydration process. This is mostly observed on those samples dehydrated with ethanol and therefore could be a by-product of this dehydration method either an artefact or causing the structure to fuse together. This is more apparent in FPA gels at a concentration of 2 $mg.mL^{-1}$. From previous dehydration techniques, it was found that freeze-drying preserved the structure of the gel to a greater extent than ethanol dehydration and therefore the fibrinogen gels formed from the peptides P15 and P17 were freeze-dried prior to imaging. Fibrinogen gels formed from P15 and P17 were imaged using a concentration of 0.75 $mg.mL^{-1}$ of the FBP carriers because of the limited amounts of materials available. The peptide materials P15 and P17 (results shown in section 5.2) formed fibrinogen gels with a fibrous and foam-like structures within the hydrogels with both gels having very open and porous structure in comparison to the FPA-fibrinogen gel and fibrin gel structures. Also, the fibrinogen fibres appeared much bigger in the gels formed with P15 or P17 in comparison to the fibrin fibres in fibrin gels. It was observed that large areas of the fibrinogen gels formed from P15 or P17 did not have clear defined fibres and it was possible that the fibres fused together during the freeze-dried dehydration process.

The porosity and cross-linking density of hydrogels may affect cellular survival and differentiation and therefore investigating a range of porosities will determine the

optimum structural properties for different cell types. The cross-linking density and porosity of the novel cross-linked fibrinogen gels can be modified by altering the concentration of FBP present during gelation. In theory, the higher the concentration of FBP present the more cross-linked the structure becomes. This is because more fibrinogen binding peptides are present to bind to the fibrinogen molecules creating a more compact and less porous structure. If less FBPs are present then less binding will occur creating a more open porous structure. However, from the SEM images it can be observed that fibrinogen gels formed from FPA at concentrations of 2.66 $mg.mL^{-1}$, 2 $mg.mL^{-1}$ and 0.7 $mg.mL^{-1}$ had larger pores giving a more open gel structure. In contrast fibrinogen gels formed using FPA at a concentration of 1.33 $mg.mL^{-1}$ had smaller sized but a greater number of pores throughout the surface of the gel. This meant that the lowest concentration of binding peptides created a structure similar to that of the highest concentration of FPA-fibrinogen gels, providing the highest number of FBP. This phenomenon may have occurred because, as the number of FBPs was increased the number of binding peptides binding to the fibrinogen molecules plateaued. This information was provided by Haemostatix Ltd and can also be seen from the gelation times investigated using KC4 coagulation analyser, see section 5.1. It was found that the gelation rate of the FPA-fibrinogen gels plateaued giving evidence to suggest that there was a maximum number of binding peptides which could bind to the number of fibrinogen molecules present during gelation. The fibrinogen gels formed from FPA at a concentration of 0.7 $mg.mL^{-1}$ created a more open porous structure due to two binding peptides available per fibrinogen molecule during gelation. Fibrinogen gels formed from FPA gels at a concentration of 1.33 $mg.mL^{-1}$ had a more compact due to four binding peptides present per one molecule of fibrinogen during gelation. However, when the concentration of binding peptides of FPA gels is greater than 2 $mg.mL^{-1}$ a more open porous structure is observed due to the plateau of binding from the FPA. Another potential reason for this observation could be due to the artefactual structure changes of the fibrinogen gel surfaces caused by the procedure of dehydration of the hydrogels. However, the impact of the dehydration procedure needed for SEM was reduced by fixation of the novel cross-linked fibrinogen gels prior to the dehydration methods.

Due to the difficulties of measuring pore diameter with the SEM images, pore diameter was measured using the histological stained samples. The results showed that the gels had very similar pore diameters, but cell free gels had a much more open porous structure in comparison to cell encapsulated gels. Average pore diameter for cell free gels ranged

from 25 – 60 µm, whereas cell encapsulated gels ranged from 12 – 50 µm. A pore size of 3 µm – 8 µm is reported to promote chondrogenic differentiation but a smaller pore size of 0.2 µm – 1.0 µm encourages chondrocytes to attain a fibroblast morphology [237]. These pore sizes are larger than the optimum range to encourage chondrogenic differentiation, however chondrogenic differentiation and ECM formation was observed in all FPA-fibrinogen and fibrin gels as discussed in greater detail in section 8.2. Highly cross-linked structures may not allow for sufficient room for the cells to synthesise extracellular matrix but larger pore sizes may result in cell migration from and through the gel. It is important to find the optimal conditions for each cell type to allow the cells to function to their full potential. The cross-linking density of the gels can have an effect on degradation rate. Gels with a higher cross-linking density tend to have a lower degradation rate in comparison to those gels with a lower cross-linking densities. This effect of cross-linking density has been shown with various different hydrogels [238].

8.2 Chondrocyte encapsulation

To determine cell survival within the hydrogels PrestoBlue® assays were carried out. PrestoBlue® is a resazurin based dye which can enter the mitochondria of healthy cells and is reduced to resorufin mainly by NADH and NADPH produced by enzymes of an active electron transport chain found in viable cells. The dye can also be reduced by reducing agent in the cell cytoplasm. The reduced dye, resorufin is fluorescent and can be measured spectrophotometrically. The higher the fluorescence the more active the cells and this is proportional to the number of viable cells in the gels [239]. However, artefactual values can also occur by dye reduction occurring by reducing agents in incubation medium or by dye binding to scaffold materials. Cell viability methods such as MTT assays and live/dead staining require each sample to be terminated at each time point. The advantage of using resazurin dye is that it is a vital dye and most cells do not have any toxic effects at concentrations of the gel needed to determine cell viability. Therefore, the viability of the same cells (in 2 or 3D culture) can be repeatedly assessed over extended time periods. This aspect is particularly advantageous when using expensive reagents and reagent in limited supply such as the TISEEL fibrinogen used for gelation and the FBP carriers. It has also been demonstrated that PrestoBlue® is more sensitive at detected live cells in comparison to MTT assays [240].

As described in section 4.5, initial biocompatibility testing of the novel cross-linked fibrinogen gels was carried out by fabricating 100 µL gels with 50,000 chondrocytes encapsulated per gel using fibrinogen gels formed from FPA or PEG FBP carriers and fibrin gels. The gels were cast and cultured in an individual well in a 96-well culture plate. The gel formed a plug covering the entire bottom of the culture well, so that a maximum volume of 200 µL could be added on top of the gel. In this experimental style it was not possible to observe whether cells were adhering to the tissue culture plastic during the culture period. The cell viability results from the reduction of resazurin dye showed increasing levels of chondrocyte activity throughout the 21 day culture period for all novel cross-linked fibrinogen gels and fibrin gels. However, PEG 1 $mg.mL^{-1}$ was significantly higher than fibrin throughout the 21 day culture period. Whereas gels formed from FPA 2.66 $mg.mL^{-1}$ was only significantly higher than fibrin at day 7 ($P<0.0001$) and day 14 ($P<0.01$) of encapsulation. These results suggested that the fibrinogen-PEG 1 $mg.mL^{-1}$ supported the viability of chondrocytes to a greater degree than fibrin under the culture conditions used. Control experiments showed that the gels themselves did not interfere in the cell viability assay to cause artefactual results.

The results showed that the FPA gels performed better than the PEG gels in terms of GAG accumulation in the gels. Interestingly, higher levels of GAG were found in the culture medium from the PEG-fibrinogen gels, which is suggestive that chondrocytes encapsulated in these gels were synthesising the GAG components but that they may not have been incorporated to the same degree as occurred in the FPA gels. The fibrin gels were comparable to the FPA-fibrinogen gels, in terms of GAG content per gel indicating that they both performed to the same degree in term of ECM accumulation of proteoglycans. This result suggested that the natural materials are able to support cell differentiation better than synthetic co-polymers. These results indicated that the gel structure and pore sizes of the fibrinogen-FPA and fibrinogen-PEG gels was appropriate since encapsulated chondrocytes had regained their chondrogenic phenotype within the fibrinogen based gels. Chondrocytes are well known to lose their chondrogenic phenotype during the monolayer culture needed to culture a sufficient number of cells for encapsulation. However, the type of collagen in the ECM formed in the chondrocyte encapsulated hydrogels needs to be investigated. Incorporation of collagen II into the ECM would confirm the chondrogenic phenotype of the encapsulated chondrocytes

The structure of the fibrinogen gels formed with PEG and FPA would have differed, meaning that the porosity and pore sizes of the gels would likely to have been different. Differences in pore size could result in different cellular morphologies, as previously

discussed, smaller pore sizes tend to lead to a more fibroblast like morphology whereas larger pore size lead to cartilage formation and the formation of GAG's. The differences in structure of PEG gels and FPA gels have not been analysed but this may be a possible reason as to why FPA gels were outperforming PEG in terms of chondrogenic differentiation.

Interestingly, for chondrocytes encapsulated in fibrinogen gels formed from PEG analogues had higher cell viability results in comparison to FPA-fibrinogen gels. Dikovsky et al [204] created a PEGylated fibrinogen gel formed by ultraviolet light. Dikovsky et al reported that cell migration in his PEG: fibrinogen hydrogels was limited, and the higher the concentration of PEG the less the cells are able to migrate into the matrix of the gel. Not only this, but PEG may have a cytotoxic effect on cells. The cytotoxic effects reported by Dikovsky et al investigation contradict the viability data presented in this thesis. Also, other studies have shown PEG is cytocompatible and cell friendly, [203] and [141]. The main reason for the difference between Dikvosky and the results presented here is unclear and could lie within the differences in the very different structure of the PEG-fibrinogen gels. Analysis on the gel structure of PEG has not been investigated in this research. This was due to a commercial-based decision by Haemostatix Ltd. to cease all research on the PEG-fibrinogen binding peptide carrier. Therefore all further investigations were carried out continued with fibrinogen gels formed using FPA, P15, P17, HyStem fibrinogen binding peptide carriers with fibrin gels remaining as a reference material.

The initial biocompatibility testing was promising however, it was observed that cell death occurred during/immediately after encapsulation in the novel cross-linked fibrinogen gels and fibrin gels approximately one in four times during experimental repeats. Therefore, one focus of this research was to optimise the gels for chondrocyte encapsulation and to understand what was causing the cell death. Two areas were investigated to create a more reliable and 'cell friendly' gel system. The first approach was to transfer the cell-encapsulated gels into larger culture wells to increase the volume of medium to promote nutrient availability and transfer. The second approach was to investigate the minimum concentration of calcium that was needed for gelation.

The gels were originally cast and cultured in 96-well plates allowing only 200 µL of medium to be placed on the hydrogels. Cells require the exchange of nutrients and waste, nutrient depletion and waste accumulation can occur more rapidly with smaller volumes of culture medium (i.e. 200 µL) in relation to the cell number (50,000 cells per gel). The medium had to be changed daily and from day 14 onwards the medium ideally required

changing twice a day. This was not always a practical possibility and therefore nutrient depletion and waste build up could have affected chondrocyte survival and differentiation. Bioreactors were not used as a method for culture despite the added advantages of nutrient and waste exchange [241]. Due to the soft nature, the small volume of the fibrinogen gels and the difficulties with handling the gels, it was thought that the fibrinogen gels would not be able to withstand the forces in the bioreactor. Casting the gels in larger wells, for example a 24-well plate, resulted in a thin film of gel formation along the bottom of the well. As the two gel components fibrinogen and either FPA or thrombin (for fibrin gels) were combined the gelation was not fast enough to allow for a defined 3D gel pellet structure to form. The aim of the method development was to minimise handling of the gels to reduce the risk of infection and from exerting forces onto the gels that may affect cellular survival.

The first approach was to form a layer of agarose in individual culture wells and cut a 6 mm diameter wells in the agarose layer to form a mould in which to cast the fibrinogen and fibrin gels (as described in section 4.5.1). Ahearne et al also investigated the use of agarose moulds for fibrin casting, however he successfully removed the fibrin gel from the agarose well [242]. This agarose system was investigated because the cast gels would be exposed to larger volumes of culture medium (1 mL per well). The FPA-fibrinogen and fibrin gels were successfully cast in the centre of the agarose well, allowing a defined 3D gel pellet to form. However, the cell viability of chondrocytes encapsulated in the fibrinogen gels, formed and cultured in this system, suggested that the cells were not surviving when encapsulated by this method. This result was unexpected as agarose gels have been used successfully for chondrocyte encapsulation by various laboratories [243] [244] and also shown in this thesis. One possible reason for the failure to cast and culture chondrocyte encapsulated fibrinogen gels could be that 1 % agarose gels had an average pore size of 1 μm [245], this pore size may be too small to allow for sufficient nutrient transfer through the 1 % agarose gel surrounding the case gels thereby limiting nutrient and waste exchange on the sides and bottom areas of the gels. Removal of excess agarose gel after encapsulation of the chondrocytes in the FPA-fibrinogen and fibrin gels proved impractical as the gel could not be removed in one piece, leaving agarose gel pieces within the culture wells. When attempting to remove the agarose gel mould, it was noted that the FPA-fibrinogen gels were placed under stress and this may also contribute to reducing cell survival in the fibrinogen and fibrin gels. Therefore, this method of gel casting was abandoned and the use of PTFE well moulds was investigated to allow medium to surround all sides of the hydrogels to try to limit cell death.

As described in section 4.5.2, PTFE well moulds were formed from drilling 6 mm diameter holes into small, individual blocks of PTFE. PTFE was chosen due to its low friction coefficient to reduce stress placed on the gels during transfer and to encourage the gelation of the two liquid precursors. Cell free gels were tested for gelation in the PTFE wells and defined 3D gel pellets were formed within the well structures. Visually, the 3D pellet formed after gelation from this method and from casting the gels in 96-well culture plates were very similar. However, the removal of the gels from the PTFE moulds was difficult, the gels could not be transferred simply by turning the well upside down, as initially thought. Use of a sterile spatula was required to transfer the gels from the PTFE moulds into a well in a 24-well culture plate. However, after transfer 2 mL of medium was able to surround the gels in a well in a 24-well plate allowing for greater nutrient and waste exchange for the cells. This system was used successfully to cast fibrin and FPA-fibrinogen gels to investigate the effect of calcium concentration on cell survival, with successful results. However, it did become apparent that the PTFE well moulds were difficult to clean with increasing use because hydrogel residue built up in the bottom of the well. Cleaning techniques such as ultra-sonic water baths were used to remove the residue but this was unsuccessful. The PTFE moulds then became an infection risk and this method of casting was eventually abandoned.

The most efficient method tried was to cast the fibrinogen gels in individual wells in a 96-well culture plate and then transferring the gels to a well in a 24-well culture plate via a sterile spatula. These were then incubated with 2 mL of medium. This method, although labour-intensive, proved the most successful gelation method. The increased handling of the gels, increased the risk of physical damage to the gels and also increased the risk of bacterial and fungal contamination. These risks, however, outweighed the advantages of being able to incubate the cell encapsulated gels in a larger volume of medium. Gelation formed a defined 3D gel pellet in the 96-well culture plate but had the added benefits of being transferred to a larger well providing a larger volume of medium to allow for sufficient nutrient transfer. Therefore, all further investigations formed gels by using this method.

The calcium concentration used for the fibrinogen and fibrin gelation was investigated because it is known that a change in calcium ions can have an adverse effect on cells. A sudden exposure to calcium ions can trigger signalling pathways which lead to cell apoptosis [246]. Haemostatix Ltd. advised the use of 10 mM $CaCl_2$ for gelation as this had been deemed necessary for gelation of FPA gels under the conditions used. The calcium concentration of culture medium such as DMEM is 1.82 mM and therefore

investigations into using lower calcium concentrations for gelation were carried out. A range of calcium concentrations between 0 and 20 mM were tested for cell free gelation of the FPA-fibrinogen and fibrin gelation see section 6.2.4. It was observed that calcium was essential for gelation as fibrinogen-FPA and fibrin gels did not form with 0 mM $CaCl_2$ after 30 minutes of incubation at 37 ºC. However, 2 mM $CaCl_2$ enabled gelation. Davies et al found that gelation of fibrin gels occurred without the presence of calcium using 40 $mg.mL^{-1}$ fibrinogen however, the gels were too weak to be handled or analysed for cell encapsulation, [235]. The novel cross-linked fibrinogen gels fabricated with a range of calcium concentrations from 2 – 20 mM had very similar appearances and could all be handled and transferred with a sterile spatula to culture plates. Chondrocytes were encapsulated using 2 mM $CaCl_2$ with successful results and compared with gels fabricated with the original 10 mM $CaCl_2$. Cell viability results from chondrocytes encapsulated in fibrin and FPA-fibrinogen gels cast with 2 mM or 10 mM calcium did not have a detrimental effect on the gelation of the gels or chondrocyte survival within the novel cross-linked fibrinogen gels (see section 6.2.4). However, by using a calcium concentration closer to physiological levels would not expose the chondrocytes to supraphysiological calcium concentrations. It was concluded that lowering the calcium concentration to 2 mM would reduce the risk of apoptosis.

Using the 2 mM calcium for gelation and casting gels as above, the effect of the numbers of chondrocytes that could be encapsulated in the 100 µL gels was also investigated to determine the optimum number of cells for encapsulation. Cell density of 50.000 to 300, 000 cells per gel were investigated (see section 6.2.3). In all hydrogels cell densities of 300,000 chondrocytes per gel had significantly higher cell activity in comparison to 150,000 and 50,000 chondrocytes per gel. It was expected that the rate of cell activity would increase with higher cell numbers but the results showed that no significant cell death occurred with 300,000 chondrocytes encapsulated per gel over the 21 day culture period. GAG production suggested that some ECM deposition had occurred within all chondrocyte encapsulated hydrogels at all cell densities of the encapsulated cells. The results suggested that 300,000 chondrocytes per gel was the optimum for the survival of chondrocytes over a 21 day period and ECM deposition and therefore was used for further investigations.

The optimisation of the fabrication and chondrocyte encapsulation of the FPA-fibrinogen gels reduced the variation in cell death and formed a more reliable, cell friendly system where chondrocyte death was minimised (refer to results in section 6.3). Using the ‘optimised’ parameter, fibrinogen gels formed from-FPA 2.66 $mg.mL^{-1}$ were taken

forward for further investigation because from the previous results it was shown that this concentration of FPA supported chondrocyte survival and differentiation to a greater extent than the lower FPA concentrations. The FPA-fibrinogen gel formed from 2.66 mg.mL^{-1} formed a larger gel that was easier to handle in comparison to the lower concentrations of FPA, this is another reason this concentration was taken forward. Also, the 'optimised' parameters 4% agarose gels were also encapsulated with 300,000 chondrocytes per gel dispensed in 100 µL gels and used as a reference material for FPA and fibrin gels. Agarose gels were used as a comparator as is known that chondrocytes survive and differentiate in agarose gels [247].

Chondrocytes were encapsulated in fibrin and fibrinogen-FPA (refer to results section 6.3). The cells remained viable within in the fibrin and FPA-fibrinogen gels and produced GAG which indicated that the chondrocytes were synthesising proteoglycans indicative of some ECM formation. GAG formation was measured at day 21 of encapsulation and it was observed in all FPA-fibrinogen, fibrin and agarose gels (sections 6.3 and 6.4). Cell free gels exhibited high levels of GAG content suggesting interference with the assay. The total GAG content per gel had a high reading despite the background values from the cell free gels suggesting that the chondrocytes were producing GAG's and therefore synthesising ECM. FPA-fibrinogen gels formed from FPA 2.66 mg.mL^{-1} and FPA 1.33 mg.mL^{-1} were significantly higher than FPA 0.7 mg.mL^{-1}, suggesting there is a higher degree of differentiation occurring in gels formed from these concentrations of FPA. The remaining concentrations of FPA-fibrinogen gels, fibrin and agarose had no significant differences between the data suggesting that all gels are supporting ECM deposition to a similar degree other than FPA 0.7 mg.mL^{-1}. This could be due to FPA 0.7 mg.mL^{-1} formed a smaller gel in comparison to the other concentrations.

During expansion of chondrocytes to increase the cell number available for encapsulation, the cells are cultured in monolayer culture in which it is well known that the chondrocytes lose their phenotype. Dedifferentiated chondrocytes synthesise collagen I instead of collagen II and rapidly lose the ability to synthesise aggrecan, the major proteoglycan found in the ECM. The production of GAG by the encapsulated cells was also an indication that the chondrocytes had regained a chondrogenic phenotype. Confirmation of this would need the analysis of any extracellular collagen, the presence of collagen II would confirm full chondrocyte differentiation.

Interestingly, a reproducible peak in cell activity was observed at day 10 of encapsulation. However, day 10 to day 21 a decrease in chondrocyte metabolic activity was usually observed in chondrocyte encapsulated FPA gels, fibrin gels and agarose gels,

(refer to section 6.4). This diminution in cell activity may possibly be related to the time at which the chondrocytes had regained their chondrogenic phenotype and began synthesis of ECM components rather than continued proliferation. This has been observed in osteoprogenitor cells; the first four days are required for cell proliferation, differentiation begins at day 5 with cell proliferation still occurring until the cells mature and ECM deposition occurs from day 15, it is at this point when the cells stop proliferating and carry out ECM synthesis [248]. Therefore, chondrocytes may have an increase in cell activity due to proliferation up to day 10 as the chondrocytes have fully matured, the metabolic activity was reduced from day 10 as ECM synthesis occurred.

To determine whether cell death was responsible for the reduction in the cell activity at day 10, live/dead staining was carried out on fibrinogen gels formed using FPA at a concentration of 2.66 $mg.mL^{-1}$ and fibrin gels at day 1 and day 21 of chondrocyte encapsulation. In this procedure, the cytoplasm of live cells is stained with a fluorescent green stain and the nuclei of dead cells fluoresce red due to uptake of propidium iodide. Cell free gels were also tested and found not to take up any dye. Confocal microscopy showed 98 % of cells were live and viable in the chondrocyte encapsulated fibrinogen-FPA and fibrin gels both day 1 and day 21 of encapsulation, (section 6.3.1, figures 6.28 and 6.29). The gels at day 21 of encapsulation showed an increase of cell numbers in the areas of the gels nearest to the gel surface compared to day 1; suggesting that cell proliferation had occurred (see section 6.3.1, figures 6.30 and 6.31). Less than 2 % of cells were observed to be dead (i.e. red fluorescence). The gels were cut in half to observe staining in the central areas of the gels. However, no staining was observed in the inner areas of the gel suggesting that during encapsulation the chondrocytes were not dispersed in the central regions of the gel. However, H&E staining of the gels had shown that the cells are evenly dispersed throughout the gel. Therefore, it was probable that the live/dead stain did not penetrate the centre of the gel in the time period of exposure of the gels to the stain. A longer exposure time of the stain to the gel could solve this problem or exposing the centre of the gel to the stain. However, the live/dead stain had to be incubated on the cells before fixation and cutting the gels prior to staining would have created mechanical forces on the gels. This could potentially have had adverse effects on the chondrocytes and therefore an accurate representation of the live/dead staining would not be obtained from this method.

ECM deposition was further analysed by histological staining with H&E and Toluidine blue (see section 6.3, Figures 6.36 and 6.38). Haematoxylin is positively charged and binds to negatively charged areas for example DNA, of the cell nucleus. Therefore, H&E

stain was used to investigate the cell distribution throughout the gel and ECM deposition. Cell free and cell encapsulated fibrin and FPA-fibrinogen gels stained. This is because fibrinogen is a glycoprotein and therefore could bind Eosin giving hydrogels a deep pink colour. It was possible to observe the stained nuclei of the chondrocytes in purple which show that the cells appeared to be evenly dispersed throughout the gels. A cell layer was observed on the outer gel edges of all concentrations of FPA-fibrinogen and fibrin gels with a pale purple staining surrounding the cells. This suggested that the cells were synthesising ECM on the edges of the gel and filling the pores of the gel with ECM. The chondrocytes in the centre of the FPA-fibrinogen and fibrin gels did not appear to have synthesised ECM and therefore may not have been receiving appropriate nutrient transfer. However some areas of ECM formation could be observed in more central regions of fibrinogen gels formed from FPA concentrations of 1.33 $mg.mL^{-1}$ and 0.7 $mg.mL^{-1}$.

Agarose 4 % cell free gels did not stain and therefore any staining on the chondrocyte encapsulated gels is cell nuclei and ECM deposition. The chondrocytes did not look as evenly dispersed throughout the gel in comparison to FPA-fibrinogen and fibrin gels however, ECM deposition was observed in pale purple suggesting that the chondrocytes were differentiating in the agarose gels. Toluidine blue has a high affinity for acidic tissue and therefore stains nucleic acids dark blue and proteoglycans bind the dye causing a metachromic shift so that the dye appears purple. This stain was used to determine if proteoglycan formation had occurred within the fibrinogen gels providing further evidence for the GAG quantification data. The fibrin and fibrinogen gels was found to bind the toluidine blue giving a dark blue colour and therefore a high background staining. Areas of proteoglycan staining was observed in all chondrocyte encapsulated fibrinogen-FPA gels, fibrin and agarose gels (refer sections 6.3 and 6.4), however this staining was much sparser in fibrin gels compared to FPA-fibrinogen gels. FPA-fibrinogen gels at a concentration of 2.66 $mg.mL^{-1}$ had areas of very dense purple showing proteoglycan formation incorporated within the gel. The chondrocytes appear to be surrounded by proteoglycans in this area. Fibrinogen gels formed from FPA at a concentration of 0.7 $mg.mL^{-1}$ appeared to have a more compact structure in comparison to the other FPA concentrations according to the dark blue staining which is inconsistent with SEM images. Agarose 4 % cell free gels stained slightly but chondrocyte encapsulated gels have stained purple on the edges of the gel but very dark blue in the centre of the gel, this suggested proteoglycan formation within the gels, section 6.4. It is interesting to note that from both the Toluidine blue and H&E staining that fibrin has much more closed structure in comparison to the porous fibrinogen-FPA structures. Less purple ECM staining was

visible in fibrin in comparison to the fibrinogen-FPA gels. This staining is consistent with the GAG quantitative analysis.

Attempts were made to investigate the gene expression by quantitative real time polymerase chain reaction (qRT-PCR) over the 21 day incubation period for the collagen II and aggrecan which are major components of hyaline ECM. However, difficulties were found in extracting sufficient RNA from the hydrogels. TRIzol was used to extract RNA from the FPA-fibrinogen and fibrin gels with unsuccessful results. TRIzol was used due to being a popular RNA extraction method with fibrin gels having very successful results from extracted RNA from chondrocytes and MSCs with this method [249] [250] [251]. TRIzol is a phenol based extraction method and the RNA was contaminated with phenol during the extraction process this can be seen from the graphs of RNA extraction where the first peak represents phenol contamination in the sample, as described by Biomedical Genomics [252]. Contamination leads to a false RNA concentration result when analysing by NanoDrop. The phenol was removed by using a method by Krebs et al [253] to ensure minimised RNA losses from the samples. This method successfully reduced the phenol contamination yielding a purer RNA solution (section 6.3) but very low RNA yields of less than 3 $ng.mL^{-1}$ of RNA were attained. qRT-PCR required RNA concentrations of more than 50 $ng.mL^{-1}$. Therefore, three gel 'pellets' were combined for each RNA extraction and a non-phenol based Isolate II RNA mini kit was used. This RNA extraction kit used a filter centrifugation method to reduce the contaminants passing through from the hydrogel, the fibrinogen and FPA molecules should not be able to pass through the filter during centrifugation. Table 6.8 showed that with one gel per extraction 11.9 $ng.mL^{-1}$ of RNA was detected, however when three gels per extraction was carried out then 77.3 $ng.mL^{-1}$ of RNA was detected giving a high enough value for qRT-PCR. The 260/280 OD aspect ratio is a measure of how pure the sample is, this value should be as close to two as possible. This value was improved dramatically by using the Isolate II RNA mini kit in comparison to the TRIzol reagent. However, with three gels per extraction this ratio was slightly lower suggesting that the gel fragments may be contaminating the sample. Several experimental repeats were carried out using fibrinogen gels formed with FPA 2.66 $mg.mL^{-1}$ and fibrin gels with 300,000 chondrocytes encapsulated per gel. RNA was extracted at day 1, day 10 and day 21 of encapsulation. However, contamination of the extracted RNA was problematic and low yields of RNA were obtained. Unfortunately, due to limited amounts of the fibrinogen and fibrinogen binding peptides, available this area of research could not be carried on further.

Chondrocytes were encapsulated in fibrin gels and fibrinogen gels formed with FPA 2.66 mg.mL^{-1}, P15, P17 and HyStem gels. It was observed through light microscopy and Crystal violet staining, that some chondrocyte migration had occurred from the fibrinogen P15 and fibrinogen P17 during the incubation period as a 'ring' of chondrocytes had adhered to the tissue culture plastic surrounding the gels by the end of the 21 day culture period. The reasons for the migration are unknown, it could be due to breakdown of the gels, although macroscopically the gels had reduced in size. However, this could be due to chondrocytes being transferred on the outer surface of the gels on encapsulation and the chondrocytes then attached to the tissue culture plastic. Some adherence of chondrocytes was observed at day 1 of encapsulation giving some evidence for this hypothesis. The chondrocytes would then proliferate throughout the 21 day culture period on the tissue culture plastic. However, it is more probable that chondrocytes proliferating of the surface of the areas of the hydrogel in close proximity to the surface of the culture dish also became attached to the tissue culture plastic at these points.-. However, this experiment could not be repeated as the P15, P17 and HyStem materials were limited. Cell migration was not observed in previous experiments with chondrocyte encapsulated FPA gels and fibrin gels and it was not observed in future experiments. Park et al found that chondrocytes did cause degradation in fibrinogen gels and was inhibited by aprotinin [254]. The addition of hyaluronic acid into the scaffolds and in the presence of aprotinin inhibited gel degradation. However, this was not found in this study with HyStem gels and this could be due to the binding of the hyaluronic acid molecule to the fibrinogen molecule, further optimisation may be required.

Following the cell viability of the encapsulated chondrocytes over the 21 day incubation period, the level of cell activity increased throughout the 21 day culture period, suggesting some cell proliferation. This was in contrast to chondrocytes encapsulated in fibrin and fibrinogen-FPA gels in which the level of cell activity peaked at day 10 which was observed in chondrocyte encapsulated FPA gels and fibrin gels previously. The apparent increase in cell activity could possibly have been due to chondrocytes which had migrated out of the gel adhering to the tissue culture plastic. The encapsulated chondrocytes were found to have synthesised GAGs during the incubation period. However, cells encapsulated in fibrin gels and fibrinogen-FPA gels (formed with 2.66 mg.mL^{-1} FPA) had a higher mean GAG in comparison to the fibrinogen-P15 and fibrinogen-P17 gels at all concentrations and HyStem at a concentration of 1 mg.mL^{-1}.

Toluidine blue staining was not reflective of the GAG content determined by biochemical assay and no proteoglycan staining was detected. However, from all the

results obtained chondrocytes could be encapsulated in fibrinogen gels formed with P15 and P17 and HyStem with good viability for a minimum period of 21 days. However, these must be considered preliminary results as there were very limited amounts of the fibrinogen binding peptises available for this research, hence all experiments need to be repeated to ensure the validity of the preliminary findings given in this thesis.

Bovine articular cartilage pieces were removed from the metacarpophalangeal joint by using a 6 mm biopsy punch. These reproducible circular pieces of cartilage were injured by using a 3 mm biopsy punch to create a small circular defect in the centre of the cartilage, see Figure 4.1. These discs of cartilage were used as a novel cartilage injury model to deliver cells via the gels to determine if cartilage repair would occur *in vitro*. Injury models have been previously researched including the use of osteochondral plugs, in which a full thickness defect is created and attempted repair of the injury [255]. The disadvantage of using osteochondral plugs is the outgrowth of cells or release of factors into the medium which may have influenced the chondrocyte response to the injury [256]. To overcome this problem, agarose gel was used to surround the osteochondral plug. However, in this thesis cartilage only explants were used to create the injury model, to avoid the release of cells and factors from the bone explant. The cartilage – only explant injury model makes use of stiff tissue culture plastic to mimic the hardness of subchondral bone. Although this was preliminary data, chondrocyte encapsulated fibrinogen-FPA gels (FPA used at 2.66 $mg.mL^{-1}$) demonstrated very encouraging results. It can be seen from the results presented in section 6.6 that microscopic observation and histological investigation of the tissues showed that the chondrocytes were induced to migrate from the gels towards the injured cartilage surface. This is particularly interesting because chondrocytes remained in encapsulation without the presence of injured cartilage. The presence of injured cartilage also appeared to promote ECM formation to a greater extent, in just 10 days, in comparison to chondrocyte encapsulated gels, cultured for 21 days. The results from the injury model are very promising for cell delivery as a treatment to aid in the regeneration of injured cartilage. This cartilage injury model has great potential to be used *in vitro* as research model in cartilage repair.

8.2.1 Chondrocyte encapsulation summary

The gelation conditions and incubation of the 100 µL fibrin and FPA-fibrinogen gels were developed to try to maximise the viability of the encapsulated chondrocytes by ensuring the novel cross-linked fibrinogen gels and fibrin gels had sufficient nutrient and

waste exchange for survival, and by reducing the calcium concentration needed for gelation to 2 mM to prevent the risk cell apoptosis. Under the incubation conditions, 300,000 chondrocytes per gel could be encapsulated in the gels with good viability which was maintained over a period of at least 21 days. It has been shown that the chondrocytes remained in encapsulation and had survived a minimum 21 day culture period. During the incubation period the chondrocytes synthesised GAG indicating proteoglycan synthesis and probable ECM synthesis. These results showed that the FPA- fibrinogen hydrogels have great promise to be used in cell encapsulation and delivery applications. All results obtained with the FPA-fibrinogen gels were comparable to fibrin and agarose gels suggesting that the FPA-fibrinogen gels are comparable to the main competitor, fibrin in cell encapsulation and delivery applications. The successful cartilage injury model highlighted the potential for the novel cross-linked fibrinogen gels use in cell encapsulation and delivery to repair injured cartilage.

P15, P17 and HyStem – fibrinogen gels have given encouraging preliminary results for chondrocyte encapsulation and delivery. Further research is needed to confirm the consistency and reliability of the data as these reagents were in very limited supply, enabling only preliminary data to be carried out.

8.3 Mesenchymal stem cell encapsulation

bBM-MSC encapsulation, and culture was carried out using the 'optimised conditions'. 300,000 bBM-MSCs were encapsulated in fibrin and FPA-fibrinogen gels formed with 2.66 $mg.mL^{-1}$, 2 $mg.mL^{-1}$, 1.33 $mg.mL^{-1}$, and 0.7 $mg.mL^{-1}$ FPA. After 3 days of encapsulation the bBM-MSCs were observed adhering to the tissue culture plastic around the gels by phase contrast microscopy. All FPA-fibrinogen and fibrin gels showed initial signs of possible degradation, in that they appeared to be smaller. By day 15 of encapsulation the FPA-fibrinogen and fibrin gels had almost completely degraded, with high numbers of bBM-MSCs observed attached to the tissue culture plastic surrounding the gels (section 7.1). This was confirmed by using crystal violet to stain the attached cells at day 15 of encapsulation. The gels were not moved prior to staining to ensure the cells were not disturbed on the tissue culture plastic. Interestingly, gel degradation was not observed in any of the cell free FPA-fibrinogen and fibrin gels and therefore, the degradation of the fibrin and fibrinogen gels must be caused by the bBM-MSCs. Cell migration from the fibrin and fibrinogen gels was also observed when the osteoblastic-

like cells, MG63 were encapsulated in the gels (section 7.1.1.). Therefore, possible cell-based mechanisms which could lead to the hydrogel dissolution and cell migration were considered and tested using fibrin and FPA-fibrinogen encapsulated bBM-MSCs. Previous studies have demonstrated that increasing the cell number can increase the degradation rate of fibrin gels suggesting that actions from the cells are causing the degradation of the gel [257].

Cell-induced proteolytic degradation was the most likely cause of degradation of the fibrin and fibrinogen gels, and two possible types of proteinases were investigated: metalloproteinases (MMPs) and plasmin. MMP's are endopeptidases which are secreted in an inactive form and when activated can degrade ECM and play an important role in cell migration [258]. MMP-2 and MMP-9 have been found to have a role in the degradation of articular cartilage [259] [260]. Plasmin is a serine proteinase which causes the breakdown of natural fibrin clots and therefore would also cause degradation of fibrin gels *in vitro* [261]. The precursor, inactive form of plasmin is plasminogen and this is present in serum and therefore was present in the serum-containing basic culture medium. When plasminogen is enzymatically activated to plasmin (by a suitable proteinase), gel degradation may occur. Plasmin also has the ability to activate pro-MMPs including MMP-2 and MMP-9 to cause the degradation of ECM [262]. Therefore, plasminogen activation to plasmin could also lead to MMP activation.

To determine if MMPs were causing gel degradation and enabling cell migration the MMP inhibitor, Marimastat was incubated with bBM-MSC encapsulated in FPA-fibrinogen and fibrin gels. Marimastat is known to inhibit a broad spectrum of MMPs including MMP-1, MMP-2, MMP-7, MMP-9, and MMP-14. To inhibit plasmin, aprotinin, a serine proteinase inhibitor, was incubated with bBM-MSC encapsulated in fibrinogen-FPA and fibrin gels to determine if the activation of plasminogen was causing gel degradation. Aprotinin was withdrawn from clinic in 2008 by Bayer HealthCare [263] due to safety concerns reported from studies investigating the use of the serine protease inhibitor in clinic [264] [265] [266]. These concerns included: an increased risk of death after administration of aprotinin; an increase in creatinine after the surgical procedure; and a high risk of anaphylaxes after second administration [267]. The withdrawal of aprotinin led to the use of tranexamic acid and aminocaproic acid [263]. Despite this, aprotinin is regularly used *in vitro* to inhibit fibrinolysis of fibrin gels. For example, 100 KIU of aprotinin was used to supplement culture medium, cell encapsulated fibrin gels exhibited gel degradation over 7 days in culture [268]. Contradictory to the findings in

this thesis in which 204.48 KIU and 1226.48 KIU were incubated with the gels, it was observed that an activity of 130 KIU resulted in cell death, whereas a lower activity of aprotinin 65 KIU reduced degradation but enabled cells to proliferate [269]. Coffin et al reported that aprotinin activity as high as 628 KIU had no effect on MSC survival [270].

Other studies have found that gel degradation occurs when MSCs are seeded onto fibrin sutures and this was inhibited with aprotinin up to 100 $\mu g.mL^{-1}$ [271]. Mechanical testing confirmed that fibrin incubated without aprotinin is much weaker in comparison to the fibrin incubated with aprotinin at day 3 of seeding. It was also found that cell adhesion to the fibrin sutures had increased with the addition of aprotinin. There are several reports of the incubation of aprotinin with fibrin-encapsulated cells to inhibit fibrinolysis *in vitro* [272] [273] [274]. Interestingly, recombinant aprotinin was a component of the TISSEEL fibrinogen.

300,000 bBM-MSCs were encapsulated in FPA-fibrinogen (using 2.66 $mg.mL^{-1}$ FPA) and fibrin gels 24 hours and incubated with serum free medium containing 50 µM concentration of plasminogen in the presence of Marimastat or aprotinin. Gel degradation was observed in both fibrin and FPA-fibrinogen gels incubated with Marimastat (section 7.1) and the encapsulated bBM-MSC control which contained no inhibitors, with cell migration occurring from the gels onto tissue culture plastic. The gels that were incubated with aprotinin did not degrade and crystal violet stain showed that very few cells had adhered to the tissue culture plastic in comparison to those gels incubated with no inhibitors and Marimastat. Therefore, by inhibiting plasmin activity (or another serine proteinase) degradation was inhibited and cell migration was reduced dramatically. To investigate if the encapsulated bBM-MSCs could activate plasminogen to plasmin, the level of plasmin activity in the culture medium from the cell encapsulated gels was analysed. It was found that plasmin activity was detected in all bBM-MSC encapsulated medium samples incubated without aprotinin and not in the samples incubated with aprotinin. Showing that the activation of plasminogen to plasmin was occurring in all samples apart from those incubated with aprotinin.

In contrast, during incubation of the chondrocyte encapsulated fibrinogen gels, cell migration and gel degradation was not observed. Additionally, plasmin activity was not detected in the medium. However, Sitek et al found that without incubation with aprotinin or tranexamic acid to inhibit fibrinolysis, gel degradation occurred over a 28-day culture period [275]. Fibrinogen concentration for gel fabrication was 10 or 20 $mg.mL^{-1}$, a higher

fibrinogen concentration such as 34 mg.mL^{-1}, as used in this study, may decrease the rate of degradation and therefore it is not observed over the 21 day culture period. Regular microscopic examination of the encapsulated fibrin and FPA-fibrinogen gels was carried out and analysis of the culture medium from the gel cultures for resazurin reduction was performed. These experiments showed that the chondrocytes remained encapsulated in the all the fibrinogen-FPA and fibrin gels and did not migrate out of the gels. Therefore, there was evidence to suggest that plasmin was causing the bBM-MSC encapsulated fibrinogen gels to degrade.

The activation of plasminogen was investigated by determining the levels of uPA and tPA in the medium. uPA and tPA are plasminogen activators. tPA and uPA have different roles in the activation of plasminogen: tPA activates plasminogen during fibrinolysis; whereas uPA activates plasminogen during cell migration [262]. uPA and tPA was not detected in any of the medium samples suggesting that another plasminogen activation process is taking place. It would not have been surprising if uPA was present in the medium during MSC migration, however it was found that this was not the case.

Removing the source of plasminogen from the culture conditions, i.e. using serum free medium was then investigated. bBM-MSC encapsulated FPA-fibrinogen and fibrin gels incubated in serum free medium without aprotinin degraded over the 21 day culture period and cell migration occurred. However, the gels incubated with aprotinin did not degrade or exhibit signs of cell migration from the FPA-fibrinogen or fibrin gels. These results suggested that an aprotinin sensitive serine proteinase secreted by the cell surface of the bBM-MSCs caused the fibrinogen based gels to degrade. Therefore, activation of plasminogen to plasmin was not an essential requirement for fibrin and fibrinogen degradation by bBM-MSCs.

In the presence of aprotinin bBM-MSCs were encapsulated in the FPA-fibrinogen and fibrin gels. The gels were continuously incubated in chondrogenic medium with aprotinin (added freshly at each medium change) for 21 days. Cell activity and GAG formation assays were able to be carried out on the gels. It was observed that cell free and medium samples showed very little resazurin reduction indicating no effect of the gels on the assay and little release of cells into the culture medium. However, there was a slight peak in resazurin reduction in the culture medium taken at day 3 of encapsulation on the medium. Interestingly, this peak occurred at the same time that the first migration of bBM-MSC was observed from the gels cultured in the absence of aprotinin. Therefore, the peak may

potentially may be the result of a small number of cells being detected in the sample medium. However, bBM-MSCs did not migrate onto to the tissue culture plastic throughout the 21 day culture. bBM-MSC encapsulated gels showed resazurin reduction of all gels suggesting all cells were viable and metabolically active throughout the 21 day culture period. Again, a peak in cell activity was observed at day 10 of encapsulation as described for encapsulated chondrocytes. All the bBM-MSC encapsulated gels were found to have synthesised GAGs suggesting all FPA-fibrinogen and fibrin gels are able to support bBM-MSC chondrogenic differentiation. No significant differences in GAG content were observed between the different FPA-fibrinogen formulations and fibrin gels for total GAG content suggesting that all gels supporting the BM-MSCs to a similar extent and were comparable to each and the main competitor fibrin.

H&E staining showed that the bBM-MSCs behaved differently in the gels in comparison to chondrocytes. The cells appeared to congregate together in the pores of the gels rather than remaining as individual cells within the pores. Cell layers are observed on the edges of the gels but ECM formation again could not be seen due to high background staining from the gels. It was observed from the Toluidine blue staining that there were areas of congregated cells and proteoglycan formation, as well as cell layers at the edges of the gels.

On encapsulation of bBM-MSCs in fibrinogen gels formed with P15, P17 and HyStem gels, cell migration and gel degradation occurred and was observed by phase contrast light microscopy images and a crystal violet stain confirming cell adhesion to tissue culture plastic, (section 7.4). P15 contains a RGD sequence which should encourage cell adhesion, however, the shape of the peptide backbone of P15 is unknown and therefore it is not known if the RGD sequence was available to the cells. It was observed that fibrinogen gels formed with P15 and P17 at 0.75 $mg.mL^{-1}$ degraded slower and had not fully degraded by day 9 of encapsulation and less cell migration was observed whereas 0.25 $mg.mL^{-1}$ and 0.5 $mg.mL^{-1}$ for both P15 and P17 degraded within 9 days of encapsulation and exhibited high numbers of cells migrating from the gels. As previously discussed, a higher cross-linking density results in a decreased degradation rate, the results from this thesis concur. HyStem formed very weak gels with fibrinogen when encapsulated with either bBM-MSCs or chondrocytes and both concentrations 0.75 $mg.mL^{-1}$ and 1 $mg.mL^{-1}$ degraded to a thin layer on the bottom of the well plate with very high cell migration observed. To inhibit gel degradation aprotinin was incubated in the medium from day 3 of encapsulation. Aprotinin inhibited gel degradation and reduced

cell migration. Therefore, this permitted longer term incubation and enabled the cell viability and GAG accumulation to be assessed. Cell free gels and samples of medium incubated with the gels showed very little resazurin reduction and therefore did not interfere with the assay. Cell viability was observed in all fibrinogen gels formed from P15, P17 and HyStem at all concentrations of FBPs used. A peak in metabolic activity at day 14 was observed which was consistent in all gels and interestingly this peak in activity appears after the same incubation time in chondrogenic medium as with chondrocyte encapsulation in P15-fibrinogen, P17-fibrinogen, FPA-fibrinogen and HyStem-fibrinogen and bBM-MSC encapsulation in FPA-fibrinogen gels. Total GAG content was determined in all the gels and all gels showed GAG accumulation in the hydrogels. However, some cell migration was observed in the gels over the 24 day incubation period. The HyStem-fibrinogen gels degraded throughout the culture period and therefore the bBM-MSC encapsulated gels were incubated with serum-free medium and aprotinin to inhibit the degradation of the HyStem-fibrinogen gels. Snyder et al found that when crosslinking hyaluronic acid with fibrinogen concentrations of 3 $mg.mL^{-1}$ the gels would degrade within two days of encapsulating MSCs. However, when the fibrinogen concentration was increased to 6 $mg.mL^{-1}$ and in the presence of aprotinin, gel degradation did not occur [276]. This may be due to the modification of hyaluronic acid with methacrylic anhydride and the exposure to UV light creating a stronger gel. This system also incorporated aprotinin into the gel fabrication steps instead of supplementing the medium with aprotinin. This does suggested that higher concentrations of HyStem should be investigated. HyStem gels still exhibited gel degradation and cell migration meaning that the gels are too weak to enable efficient cell encapsulation of bBM-MSCs for a 21 day period. This could account for the high cell activity results because the cells had adhered to the tissue culture plastic and these were contributing to the resazurin reduction results. Total GAG content per gel suggested that all gels have supported bBM-MSC chondrogenic differentiation, however fibrin has a higher mean GAG content than all P15, P17 and HyStem gels. However, for chondrogenic differentiation to be confirmed further research must be done to determine if chondrogenic genes are expressed (such as for collagen II and aggrecan).

H&E staining showed that the bBM-MSCs congregate within the pores of the gel and this was consistent with bBM-MSC encapsulated FPA-fibrinogen gels and fibrin gels as previously discussed. Cell layers can be observed on the edges of the gels with ECM deposition suggesting that these cells had exhibited a more differentiated state in

comparison to those cells in the centre of the gel. Toluidine blue stained gels indicating proteoglycan deposition in all gels. Greater areas of proteoglycan staining was found in fibrinogen gels formed from 0.75 $mg.mL^{-1}$ concentrations of P15 and P17, suggesting that the gels formed from higher concentrations of P15 and P17 were supporting chondrogenic differentiation to a greater degree than the lower concentrations of P15 and P17. It was possible to section and stain HyStem at concentrations of 1 $mg.mL^{-1}$ and 0.75 $mg.mL^{-1}$ due to a very small gel remained after 21 days in culture. The staining suggested proteoglycan formation in 0.75 $mg.mL^{-1}$ but due to high background staining this was not observed in gels fabricated with 1 $mg.mL^{-1}$ HyStem.

8.3.1 Mesenchymal stem cell encapsulation summary

On encapsulation of bBM-MSCs it became apparent that the cells behaved differently in comparison to chondrocytes. bBM-MSC migration was observed along with gel degradation. Due to the protein nature of the fibrin and fibrinogen gels. Cell-induced proteolytic degradation was the most likely cause of degradation of the fibrin and fibrinogen gels, and two possible types of proteinases were investigated: MMPs and plasmin. Use of the MMP inhibitor Marimastat had no effect on gel degradation or cell migration. Inhibition of plasmin in serum containing medium with aprotinin was found to inhibit gel degradation and reduced cell migration. Therefore, the bBM-MSCs were able to produce a proteinase which could activate plasminogen to plasmin. Removing the source of the plasmin precursor, plasminogen, which is found in serum and incubating the bBM-MSC encapsulated gels in serum-free medium, did not stop cell migration or gel degradation. However, addition of aprotinin to these incubations inhibited cell migration and gel degradation. These results suggested the bBM-MSCs produced an aprotinin-sensitive serine protease which directly degraded the fibrinogen gels in addition to activating plasminogen to plasmin. In the presence of aprotinin, bBM-MSCs encapsulated in FPA-fibrinogen gels at all concentrations were able to survive and differentiate within the gels.

bBM-MSC encapsulated HyStem-fibrinogen gels showed gel degradation occurred in the presence of aprotinin and therefore the gels were too weak to support long-term culture. However, these gels have shown promising results despite gel degradation. P15 and P17 – fibrinogen gels had supported chondrogenic differentiation of the bBM-MSCs,

with concentrations of 0.75 mg.mL^{-1} of both fibrinogen –binding peptides showing greater promise due to a slower degradation rate.

8.4 Overall discussion

Although the novel cross-linked fibrinogen gels and fibrin gels were consistently similar when encapsulated with chondrocytes and MSCs throughout this thesis, the fibrinogen gels have added advantages which make them superior to fibrin for cell encapsulation and delivery. The FPA-fibrinogen gels were formed from reproducible synthetic carriers of the fibrinogen binding peptide sequence, removing batch to batch variation. Combined with the high quality, commercially available fibrinogen a more consistently reliable gel can be formed. The combination of synthetic and natural materials is highly advantageous to encourage cell differentiation but also has the added benefit of tailorability, as previously described. The cross-linking density of the novel fibrinogen gels can readily be modified by altering the number of fibrinogen binding peptides present during gelation. This added tailorability provides a more versatile gel suitable for many different applications. The gelation of novel cross-linked fibrinogen gels occurred by simply combining two liquid precursors (the FBP carrier and fibrinogen) and the fast gelation rate makes these novel fibrinogen gels ideal for clinical settings.

A range of gels are being developed for use in cell delivery and encapsulation for cartilage repair. It has been demonstrated by Rahman et al that combining fibrin with PLGA, an enhanced cell viability and differentiation capability was achieved than just PLGA alone, providing evidence to suggest that a combination of natural and synthetic gels is beneficial to cellular survival [277]. Sheykhhasan et al found that fibrin gels encouraged chondrogenic differentiation greater than alginate or PLGA when encapsulated with MSCs [278]. In this study cross-linking the fibrinogen with synthetic carriers of FBPs did not significantly change chondrocyte or bBM-MSC activity and differentiation in comparison to pure fibrin gels. The range of FPA-fibrinogen gels investigated appeared to have similar porosities and if lower concentrations of the FPA carriers were investigated then a bigger difference in cellular survival and chondrogenic differentiation may have been observed.

Other gel systems use a ceramic scaffold as an osteochondral plug to fill the defect and mimic the bone. Cells are then delivered on top of the plug via a gel such as fibrin to create the softer environment required for chondrogenic differentiation [279]. Successful

results have been demonstrated *in vivo* with the encapsulation of chondrocytes within the fibrin gel. Evidence suggested a hyaline-like cartilage repair. Providing further evidence for the suitability of the novel cross-linked fibrinogen gels in cell encapsulation and delivery for cartilage regeneration.

In this study the differences in cellular behaviour between chondrocytes and mesenchymal stem cells was apparent. Chondrocytes remained in encapsulation whereas MSCs migrated out of the fibrinogen based gels and the gels degraded. This behaviour is not surprising because MSCs are required to migrate out of the stem cell niche in which the MSCs are contained in an enriched ECM [280] whereas chondrocytes are required to remain in the lacunae and synthesise ECM. By these behaviours being exhibited in the novel cross-linked fibrinogen gels the cells appear to be in environments similar to that of their natural environment.

In summary, it has been demonstrated that the novel cross-linked fibrinogen gels have supported chondrocyte and MSC survival and differentiation over a 21 day culture period. Control over the degradation rate of the gels has been established with the addition of aprotinin to the culture medium reducing MSC migration. Therefore, these novel cross-linked fibrinogen gels have potential for use in cell encapsulation and delivery for cartilage repair.

9.0 Conclusions

As outlined in the literature review there is a need for cell therapies to repair injured cartilage. The research shown in this study has provided a solution with a novel cross-linked fibrinogen gel system for cell encapsulation and delivery applications. The fibrinogen based gels are formed by combining fibrinogen with novel carrier materials that have attached novel fibrinogen binding peptides. It is the interaction of the fibrinogen binding peptides with fibrinogen that leads to cross-linking of the protein to form a fibrinogen-FBP gel. A range of gels such as fibrin and agarose have been successfully investigated for cell encapsulation and delivery but have limitations. The novel cross-linked fibrinogen gels overcome these limitations and have demonstrated considerable potential for cell encapsulation and delivery throughout this research. The main conclusions from this research are outlined below:

- Confirmation of natural gel systems such as fibrin and agarose supported chondrocyte culture and therefore have potential for use in cell encapsulation and delivery despite the limitations discussed in the literature review.

- More importantly, this research has demonstrated that novel cross-linked fibrinogen gels based on different carrier molecules bound to the fibrinogen binding peptide were also able to support articular chondrocyte and MSC survival for up to 21 days in culture.

- Of these novel cross-linked fibrinogen gels, investigations into the encapsulation of FPA-fibrinogen gels was the main focus. FPA-fibrinogen gels at concentrations of 2.66 $mg.mL^{-1}$, 2 $mg.mL^{-1}$, 1.33 $mg.mL^{-1}$ and 0.7 $mg.mL^{-1}$ supported chondrocyte survival and differentiation over a 21 day culture period and are comparable to the main competitor fibrin and agarose. Chondrocytes remained in encapsulation throughout the culture period. From H&E staining fibrin has a closed structure whereas FPA has pores in which the chondrocytes appear to reside individually. Concentration of FPA present during gelation did not appear to affect chondrocyte survival or differentiation, FPA 2.66 $mg.mL^{-1}$ and FPA 1.33 $mg.mL^{-1}$ had a higher mean GAG formation compared to FPA 2 $mg.mL^{-1}$, FPA 0.7 $mg.mL^{-1}$ and fibrin. This was also consistent with the Toluidine blue staining.

- It was noted that chondrocytes remained entrapped within the novel cross-linked fibrinogen gels throughout culture whereas MSCs migrated from the gels and gel degradation was observed. MSC migration occurred at day 3 of encapsulation and by day 15 the novel cross-linked fibrinogen gels had fully degraded (see section 7.1). Gel degradation was inhibited and cell migration reduced when the fibrinogen gels were incubated with aprotinin (see section 7.3). On incubation with serum-free medium, cell migration and gel degradation also occurred but was inhibited by aprotinin. This suggested the production of an aprotinin sensitive serine protease which is able to activate plasminogen to plasmin and directly degrade the novel cross-linked fibrinogen gels. In the presence of aprotinin, FPA gels at concentrations of 2.66 $mg.mL^{-1}$, 2 $mg.mL^{-1}$, 1.33 $mg.mL^{-1}$ and 0.7 $mg.mL^{-1}$ were able to support bBM-MSC survival and chondrogenic differentiation throughout a 21 day culture period.

- The MSC-induced migration and gel degradation could focus MSC migration to a site of injury to aid in its repair, as shown from the cartilage injury model where bBM-MSCs can be observed migrating towards the injured cartilage, section 7.7.

In conclusion, the ability of being able to control the rate of cross-linking of fibrinogen by using the novel fibrinogen binding peptide analogues described in this thesis is very advantageous and enables fine tuning of the porosity of the fibrinogen gels. This refinement of porosity is not as easily or reproducibly achieved by using traditional fibrin gels. This novel cross-linked fibrinogen gel system has great promise for use in cell encapsulation and delivery applications to tissue injury sites.

10.0 Future Work

The research carried out in this thesis shows the potential for the use of novel cross-linked fibrinogen gels in cell encapsulation and delivery applications. However, further work is required to be carried out:

- P15 and P17 – fibrinogen gels at concentrations of 1 $mg.mL^{-1}$ show promise for cell encapsulation, more repeats are required to determine if the data shown is an accurate representation of the gels. Further to this P17 contains DGEA sequence, developing a collagen binding assay would determine whether this sequence was available to the cells or blocked by the shape of the peptide.
- P15, P17 and HyStem – fibrinogen gels encapsulated with chondrocytes showed inconsistent results with the GAG assay and the histological examination. This should be repeated to determine if the data shown in this thesis is an accurate representation of the encapsulation of chondrocytes in P15, P17, and HyStem – fibrinogen gels.
- Histological examination showed that the fibrinogen gels stained and therefore high backgrounds were observed. Collagen II immunostaining is more specific and would allow the observation of collagen type II production which is present in articular cartilage. This should be investigated on chondrocyte and bBM-MSC encapsulated gels.
- RNA extraction requires further optimisation to ensure phenol contamination is removed from the FPA-fibrinogen and fibrin gels, once this has been achieved qRT-PCR could be carried out to determine if chondrogenic genes are being expressed. This will also help to determine if the decrease in chondrocyte and bBM-MSC activity at day 10 of encapsulation is due to differentiation.
- The cartilage injury model has been optimised for the removal of cartilage from the metacarpophalangeal joint. The delivery of chondrocytes showed successful results. Experimental repeats for 21 days for the delivery of chondrocytes and bBM-MSC's to the injury is required for accuracy of the data.

11.0 References

[1] G. Filardo, F. Perdisa, A. Roffi, M. Marcacci and E. Kon, "Stem cells in articular cartilage regeneration," *Journal of Orthopaedic Surgery and Research,* vol. 11, no. 42, pp. 1-15, 2016.

[2] G. Leardini, F. Salaffi, R. Caporali, B. Canesi, L. Rovati and R. Montanelli, "Direct and indirect costs of osteoarthritis of the knee," *Clinical and Experimental Rheumatology,* vol. 22, no. 6, pp. 699 - 706, 2004.

[3] A. Maetzel, L. Li, J. Pencharz, G. Tomlinson and C. Bombardier, "The economic burden associated with osteoarthritis, rheumatoid arthritis, and hypertension: a comparative study," *Annals of the rheumatic diseases,* vol. 63, no. 4, pp. 395 - 401, 2004.

[4] A. UK, "Osteoathritis in general practice," Arthritis UK, Keele, 2013.

[5] A. D. Woolf and B. Pfleger, "Burden of major musculoskeletal conditions," *Bulletin of the World Health Organization,* vol. 81, no. 9, pp. 646 - 656, 2003.

[6] "Chapter 6. Priority diseases and reasons for inclusion: Osteoarthritis," in *Priority medicines for Europe and the World 2013 update,* World Health Organisation, 2013, pp. 1 - 3.

[7] S. Glyn-Jones, A. Palmer, R. Agricola, A. Price, T. Vincent, H. Weinans and A. Carr, "Osteoarthritis," *The Lancet,* vol. 386, no. 9991, pp. 367-387, 2015.

[8] A. Litwic, M. H. Edwards, E. M. Dennison and C. Cooper, "Epidemiology and burden of osteoarthritis," *British Medical Bulletin,* vol. 105, no. 1, pp. 185-199, 2013.

[9] C. Wang, K. McPherson, T. Marsh, S. L. Gortmaker and M. Brown, "Health and economic burder of the projected obesity trends in the USA and the UK," *The Lancet,* vol. 378, no. 9793, pp. 815-825, 2011.

[10] S. Z. Nawaz, G. Bentley, T. W. Briggs, R. W. Carrington, J. A. Skinner, K. R. Gallagher and B. S. Dhinsa, "Autlogous chondrocyte implantation in the knee: Mid-term to long-term results," *The Journal of Bone & Joint Surgery,* vol. 96, no. 10, pp. 824-830, 2014.

[11] E. N. Marieb and K. Hoehn, "Chapter 4. Tissue: The Living Fabric," in *Human Anatomy and Physiology,* San Francisco, Pearson Benjamin Cummings, 2007, pp. 135 - 137.

[12] A. M. Bhosale and J. B. Richardson, "Articular cartilage: structure, injuries and review management," *British medical bulletin,* vol. 87, no. 1, pp. 77-95, 2008.

[13] A. J. S. Fox, A. Bedi and S. Rodeo, "The basic science of articular cartilage: structure, composition, and function," *Sports Health: A multidisciplinary approach,* vol. 1, no. 6, pp. 461 - 468, 2009.

[14] D. R. Eyre, M. A. Weis and J.-J. Wu, "Articular cartilage collagen: An irreplaceable framework?," *European Cells and Materials,* vol. 12, pp. 57-63, 2006.

[15] M. B. Goldring, "The role of the chondrocyte in osteoarthritis," *Arthritis and Rheumatism,* vol. 43, no. 9, pp. 1916-1926, 2000.

[16] Z. Zhang, "Chondrons and the Pericellular Matrix of Chondrocytes," *Tissue engineering: Part B,* vol. 21, no. 3, pp. 267 - 277, 2015.

[17] A. C. Poole, "Articular cartilage chondrons: form, function and failure," *Journal of Anatomy,* vol. 191, no. 1, pp. 1 - 13, 1997.

[18] D. L. Bader, D. M. Salter and T. T. Chowdhury, "Biomechanical influence of cartilage homeostasis in health and disease," *Arthritis,* vol. 2011, pp. 1-16, 2011.

[19] T. S. Johnson, J.-W. Xu, V. V. Zaporojan, J. M. Mesa, C. Weinand, M. A. Randolph, L. J. Bonassar, J. M. Winograd and M. J. Yaremchuk, "Integrative repair of cartilage with articular and nonarticular chondrocytes," *Tissue Engineering,* vol. 10, no. 9 - 10, pp. 1308 - 1315, 2004.

[20] W. Widuchowskia, J. Widuchowskia and T. Trzaskab, "Articular cartilage defects: Study of 25,124 knee arthroscopies," *The Knee,* vol. 14, no. 3, pp. 177 - 182, 2007.

[21] "Review: tissue engineering for regeneration of articular cartilage," *Biomaterials,* vol. 21, pp. 431 - 440, 2000.

[22] . H. Takeda, T. Nakagawa, K. Nakamura and L. Engebretsen, "Prevention and management of knee osteoarthritis and knee cartilage injury in sports," *British journal of sports medicine,* pp. 1 - 7, 2011.

[23] K. Nakano, W. J. Whitaker, D. L. Boyle, W. Wang and G. S. Firestein, "DNA methylome signature in rheumatoid arthritis," *Annals of rheumatic diseases,* vol. 72, no. 1, pp. 110 - 117, 2012.

[24] Y. Zhu, M. Yuan, H. Y. Meng, A. Y. Wang, Q. Y. Guo, Y. Wang and J. Peng, "Basic science and clinical application of platelet-rich plasma for cartilage defects and osteoarthritis: a review," *Osteoarthritis and Cartilage,* vol. 21, no. 11, pp. 1627 - 1637, 2013.

[25] P. Panwar, G. Lamour, N. C. Mackenzie, H. Yang, F. Ko, H. Li and D. Bromme, "Changes in structural-mechanical properties and degradability of collagen during aging-associated modifications," *The journal of biological chemistry,* vol. 290, pp. 23291-23306, 2015.

[26] A. Mobasheri, C. Csaki, A. L. Clutterbuck, M. Rahmanzadeh and M. Shakibaei, "Mesenchymal stem cells in connective tissue engineering and regenerative medicine: Applications in cartilage repair and osteoarthritis therapy," *Histol Histopathol,* vol. 24, pp. 347-366, 2009.

[27] W. E. Horton, L. Feng and C. Adams, "Chondrocyte apoptosis in development, aging and disease," *Matrix Biology,* vol. 17, no. 2, pp. 107-115, 1998.

[28] M. Lotz, S. Hashimoto and K. Kuhn, "Mechanisms of chondrocyte apoptosis," *Osteoarthritis cartilage,* vol. 7, no. 4, pp. 389-391, 1999.

[29] E. A. Jones, A. Crawford, A. English, K. Henshaw , J. Mundy, D. Corscadden, T. Chapman, P. Emery , P. Hatton and D. McGonagle, "Synovial fluid mesenchymal stem cells in health and early osteoarthritis: Detection and functional evaluation at the single-cell level," *Arthritis and Rheumatism,* vol. 58, no. 6, pp. 1731 - 1740, 2008.

[30] I. Sekiya, M. Ojima, S. Suzuki, M. Yamaga, M. Horie, H. Koga, K. Tsuji, K. Miyaguchi, S. Ogishima, H. Tanaka and T. Muneta, "Human mesenchymal stem cells in synovial fluid increase in the knee with degnerated cartilage and osteoarthritis," *Journal of orthopadic research,* vol. 30, no. 6, pp. 943 - 949, 2011.

[31] K. P. Pritzker, S. Gay, S. A. Jimenez, K. Ostergaard, J. P. Pelletier, P. A. Revell, D. Salter, F. R. C. Path and W. B. van den Berg, "Osteoarthritis cartilage histopathology: grading and staging," *Osteoarthritis and Cartilag,* vol. 14, no. 1, pp. 13-29, 2006.

[32] P. M. van der Kraan and W. B. van den Berg, "Osteophytes: relevance and biology," *Osteoarthritis and Cartilage,* vol. 15, no. 3, pp. 237-244, 2007.

[33] G. Li, J. Yin, J. Gao, T. S. Cheng, N. J. Pavlos, C. Zhang and M. H. Zheng, "Subchondral bone in osteoarthritis: insight into risk factors and microstructural changes," *Arthritis research & therapy,* vol. 15, no. 6, p. 1, 2013.

[34] P. G. Conaghan, J. Dickson and R. L. Grant, "Care and management of osteoarthritis in adults: summary of NICE guidance," *British Medical Journal,* vol. 336, no. 7642, pp. 502 - 503, 2008.

[35] J. W. ijlsma, F. Berenbaum and F. P. Lafeber, "Osteoarthritis: an update with relevance for clinical practice," *The Lancet,* vol. 377, no. 9783, pp. 2115-2126, 2011.

[36] T. M. Tamer, "Hyaluronan and synovial joint: function, distribution and healing," *Interdisciplinary toxicology,* vol. 6, no. 3, pp. 111 - 125, 2013.

[37] M. Abate and V. Salini, "Hyaluronic acid in the treatment of osteoarthritis: What is new," in *Osteoartritis - Diagnosis, treatment and surgery*, Rijeka, Intech, 2012, pp. 101 - 102.

[38] W. Laupattarakasem, M. Laopaiboon, P. Laupattarakasem and C. Sumananont, "Arthroscopic debridement for knee osteoarthritis," *Cochrane Database of Systematic Reviews,* pp. 1 - 32, 2008.

[39] N. I. f. H. a. C. Excellence, "Arthroscopic knee washout, with or without debridement, for the treatment of osteoarthritis: Interventional procedure guidance," 22 08 2007. [Online]. Available: nice.org.uk/guidance/ipg230. [Accessed 05 09 2016].

[40] Y.-M. Yen, B. Cascio, L. O'Brien, S. Stalzer, P. J. Millett and R. Steadman, "Treatment of osteoarthritis of the knee with microfracture and rehabilitation," *Medicine and science in sports and exercise,* vol. 40, no. 2, pp. 200-205, 2008.

[41] G. S. E. Dowd, H. S. Somayaji and M. Uthukuri, "High tibial osteotomy for medial compartment osteoarthritis," *The Knee,* vol. 13, no. 2, pp. 87 - 92, 2006.

[42] S. Floerkemeier, A. E. Staubli, S. Schroeter, S. Goldhahn and P. Lobenhoffer, "Outcome after high tibial open-wedge osteotomy: a retrospective evaluation of 533 pateints," *Knee Surgery, Sports Traumatology, Arthroscopy,* vol. 21, no. 1, pp. 170-180, 2013.

[43] L. Hangody, J. Dobos, E. Baló, G. Pánics, L. R. Hangody and I. Berkes, "Clnical experiences with autologous ostochondral mosaicplasty in an atheletic population: A 17-year prospective multicenter study," *The american journal of sports medicine,* vol. 38, no. 6, pp. 1125-1133, 2010.

[44] N. J. R. f. E. a. Wales, "12th Annual Report," 09 2015. [Online]. [Accessed 02 09 2016].

[45] J. Fisher, "Surgery for arthritis: total hip and knee joint replacement," *Topical Reviews: Arthritis UK,* vol. 5, no. 3, pp. 1 - 8, June 2004.

[46] "Total hip replacement and resurfacing arthroplasty for end-stage arthritis of the hip," *Technology appraisal guidance,* pp. 1 - 59, 2014.

[47] N. I. f. H. a. C. Excellence, "Mini-incision surgery for total knee replacement," Excellence, National Institue for Health and Care, Manchester, 2010.

[48] M. Risbud, "Tissue engineering: implications in the treatment of organ and tissue defects," *Biogerontology,* vol. 2, no. 2, pp. 117 - 125, 2001.

[49] T. Ahmed, E. Dare and M. Hincke, "Fibrin: A versatile scaffold for tissue engineering applications," *Tissue Engineering: Part B,* vol. 14, no. 2, pp. 199 - 215, 2008.

[50] M. Brittberg, A. Lindahl, A. Nilsson, C. Ohlsson, O. Isaksson and L. Peterson, "Treatment of Deep Cartilage Defects in the Knee with Autologous Chondrocyte Transplantation," *The new England journal of medicine,* vol. 331, pp. 889 - 895, 1994.

[51] S. N. Redman, S. F. Oldfield and C. W. Archer, "Current strategis for articular cartilage repair," *S.N. Redman et al. European Cells and Materials,* vol. 9, pp. 23 - 32, 2005.

[52] K. Von Der Mark, V. Gauss, H. Von Der Mark and P. Muller, "Relationship between cell shape and type of collagen synthesised as chondrocyte lose their phenotype in culture," *Nature,* vol. 267, no. 5611, pp. 531-532, 1977.

[53] K. Pelttari, E. Steck and W. Richter, "The use of mesenchymal stem cells for chondrogenesis," *International journal of the care of the injured,* vol. S9, no. 31, pp. S58 - S65, 2008.

[54] M. Brittberg, A. Lindahl, A. Nilsson, C. Ohlsson, O. Isaksson and L. Peterson, "Treatment of deep cartilage defects in the knee with autologous chondrocyte transplantation," *The new England journal of medicine,* vol. 331, pp. 889-895, 1994.

[55] L. Peterson, M. Brittberg, I. Kiviranta, A. Lundgren and A. Lindahl, "Autologus condrocyte transplantaion: Biomechanics and long-term durability," *The american journal of sports medicine,* vol. 30, no. 1, pp. 2-12, 2002.

[56] P. Niemeyer, S. Porichis, M. Steinwachs, C. Erggelet, P. C. Kreuz, H. Schmal, M. Uhl, N. Ghanem, N. P. Sudkamp and G. Salzmann, "Long-term outcomes after first-

generation autologous chondrocyte implantation for cartilage defects of the knee," *The American journal of sports medicine,* vol. 42, no. 1, pp. 150-157, 2014.

[57] T. Minas, A. Von Keudell, T. Bryant and A. H. Gomoll, "The John Insall Award: A minimum 10-year outcome study of autologous chondrocyte implantation," *Clinical orthopaedics and related research,* vol. 472, no. 1, pp. 41-51, 2014.

[58] P. Niemeyer, G. Salzmann, M. Feucht , J. Pestka, S. Porichis, P. Ogon, N. Sudkamp and H. Schmal, "First-generation versus second-generation autologous chondrocyte implantation for treatment of cartilage defects of the knee: a matched-pair analysis on long-term clinical outcome," *International Orthopaedics,* vol. 30, no. 10, pp. 2065 - 2070, 2014.

[59] L. Peterson, H. S. Vasiliadis, M. Brittberg and A. Lindahl, "Autologous chondrocyte implantation: A long-term follow up," *The american journal of sports medicine,* vol. 38, no. 6, pp. 1117-1124, 2010.

[60] G. Knutsen, J. O. Drogset, L. Engebretsen, T. Grøntvedt, V. Isaksen, T. C. Ludvigsen, S. Roberts, E. Solheim, T. Strand and O. Johansen, "A randomized trial comparing autologous chonndrocyte implantation with microfracture. Findings at five years," *The journal of bone and joint surgery,* vol. 89, pp. 2105-2112, 2007.

[61] L. G. Peterson, T. Minas, M. Brittsberg, A. Nilsson, E. Sjogren-Jansson and A. Lindahl, "Two- to 9-year outcome after autologous chondrocyte transplantation of the knee," *Clinical orthopaedics and related research,* no. 374, pp. 212-234, 2000.

[62] W. Bertlett, J. A. Skinner, C. R. Gooding, R. Carrington, A. M. Flanagan, T. W. Briggs and G. Bentley, "Autologous chondrocyte implantation versus matrix-induced autologous chondrocyte implantation for osteochondral defects of the knee," *The bone and joint journal,* Vols. 87-B, no. 5, pp. 640-645, 2005.

[63] C. R. Gooding, W. Bartlett, G. Bentley, J. A. Skinner, R. Carrington and A. Flanagan, "A prospective, ranomised study comparing two techniques of autologous chondrocyte implantation for osteochondral defects in the knee: Periosteum covered versus type I/III collagen covered," *The Knee,* vol. 13, no. 3, pp. 203-210, 2006.

[64] T. Minas, A. H. Gomoll, R. Rosenberger, R. O. Royce and T. Bryant, "Increased failure rate of autologous chondrocyte implantation after previous treatment with marrow stimulation techniques," *The American journal of sports medicine,* vol. 37, no. 5, pp. 903-908, 2009.

[65] J. M. Pestka, G. Bode, G. Salzmann, N. P. Sudkamp and P. Niemeyer, "Clinical outcome of autologous chondrocyte implantation for failed microfracture treatment of full-thickness cartilage defects of the knee joint," *The American journal of sports medicine,* vol. 40, no. 2, pp. 325-331, 2012.

[66] A. Mobasheri, G. Kalamegam, G. Musumeci and M. E. Batt, "Chondrocyte and mesenchymal stem cell-based therapies for cartilage repair in osteoarthritis and related orthopaedic conditions," *Maturitas,* vol. 78, no. 3, pp. 188-198, 2014.

[67] A. I. Caplan, "Adult mesenchymal stem cells for tissue engineering versus regenerative medicine," *Journal of cellular physiology,* vol. 213, no. 2, pp. 341-347, 2007.

[68] F. P. Barry and J. M. Murphy, "Mesenchymal stem cells: clinical applications and biological characterization," *The international journal of biochemistry and cell biology,* vol. 36, pp. 568-584, 2004.

[69] E. Jones and D. McGonagle, "Human bone marrow mesenchymal stem cells in vivo," *Rheumatology,* vol. 47, no. 2, pp. 126 -131, 2008.

[70] T. Morito, T. Muneta, K. Hara, Y.-J. Ju, T. Mochizuki, H. Makino, A. Umezawa and I. Sekiya, "Synovial-fluid-derived mesenchymal stem cells increase after intra-articular ligament injury in humans," *Rheumatology,* vol. 47, no. 8, pp. 1137 - 1143, 2008.

[71] M. Knippenberg, N. M. Helder, B. Z. Doulabi, C. M. Semeins, P. I. Wuisman and J. Klein-Nulend, "Adipose tissue-derived mesenchymal stem cells acquire bone cell-like responsiveness to fluid shear stress on osteogenic stimulation," *Tissue Engineering,* vol. 11, no. 11-12, pp. 1780 - 1788, 2006.

[72] M. Dominici, K. Le Blanc, I. Mueller, I. Slaper-Cortenbach, F. C. Marini, D. S. Krause, R. J. Deans, A. Keating, D. J. Prockop and E. M. Horwitz, "Minimal criteria for defining multipotent mesenchymal stromal cells. The internation society for celluale therapy position statement," *Cytotherapy,* vol. 8, no. 4, pp. 315 - 317, 2006.

[73] J. M. Karp and G. S. Leng Teo, "Mesenchymal stem cell homing: the devil is in the details," *Cell Stem Cell,* vol. 4, no. 3, pp. 206 - 216, 2009.

[74] L. LI and J. Jiang, "Regulatory factors of mesenchymal stem cell migration into injured tissues and their signal transduction mechanisms," *Frontiers in medicine,* vol. 5, no. 1, pp. 33 - 39, 2011.

[75] T. Kuroda, T. Matsumoto, Y. Mifune, T. Fukui, S. Kubo, T. Matsushita, T. Asahara, M. Kurosaka and R. Kuroda, "Therapeutic strategy of third-generation autologous chondrocyte implantation for osteoarthritis," *Upsala Journal of Medical Sciences,* vol. 116, no. 2, pp. 107 - 114, 2011.

[76] A. Gregor and J. Hošek, "3D printing methods of biological scaffolds used in tissue engineering," in *Proceedings of International Conference On Innovations, Recent Trends And Challenges In Mechatronics, Mechanical Engineering And New High-Tech Products Development,* Prague, 2011.

[77] G. Nicodemus and S. Bryant, "Cell encapsulation in biodegradable hydrogels for tissue engineering applications," *Tissue Eningeering: Part B,* vol. 14, no. 2, pp. 149 - 160, 2008.

[78] J. Shi, L. Wang, F. Zhang, H. Li, L. Lei, L. Liu and Y. Chen, "Incorporating protein gradient into electrospun nanofibres as scaffolds for tissue engineering," *Applied Materials and Interfaces,* vol. 2, no. 4, pp. 1025 - 1030, 2010.

[79] C. Adelöw and P. Frey, "Synthetic hydrogel matrices for guided bladder tissue regeneration," *Tissue Engineering,* vol. 140, pp. 1543 - 1894, 2007.

[80] X. Wang, C. Han, X. Hu, H. Sun, C. You, C. Gao and Y. Haiyang, "Applications of knitted mesh fabrication techniques to scaffolds for tissue engineering and regenerative

medicine," *Journal of the mechanical behavior of biomedical materials,* vol. 4, no. 7, pp. 922 - 932, 2011.

[81] R. Silverman, D. Passaretti, W. Huang, M. Randolph and M. Yaremchuk, "Injectable tissue-engineered cartilage using a fibrin glue polymer," *Plastic and reconstructive surgery,* vol. 103, no. 7, pp. 1809 - 1818, 1999.

[82] M. Garcia-Fuentes, A. Meinel, M. Hilbe, L. Meinel and H. Merkle, "Silk fibroin/hyaluronan scaffolds for human mesenchymal stem cell culture in tissue engineering," *Biomaterials,* vol. 30, no. 28, pp. 5068 - 5076, 2009.

[83] E. Sachlos and J. Czernuszka, "Making tissue engineering scaffolds work. Review on the application of solid freeform fabrication technology to the production of tissue engineering scaffolds," *European Cells and Materials,* vol. 5, pp. 29 - 40, 2003.

[84] N. Zander, J. Orllicki, A. Rawlett and T. Beebe, "Quantification of protein incorporated into electrospun polycaprolactone tissue engineering scaffolds," *Applied Materials and Interfaces,* vol. 4, no. 4, pp. 2074 - 2081, 2012.

[85] K. Gross and L. Rodríguez-Lorenzo, "Biodegradable composite scaffolds with an interconnected spherical network for bone tissue engineering," *Biomaterials,* vol. 25, no. 20, pp. 4955 - 4962, 2004.

[86] J. Zeltinger, J. Sherwood, D. Graham, R. Müeller and L. Griffith, "Effect of pore size and void fraction on cellular adhesion, proliferation, and matrix deposition," *Tissue Engineering,* vol. 7, no. 5, pp. 557 - 572, 2001.

[87] M. Tibbitt and K. Anseth, "Hydrogels as extracellular matrix mimics for 3D cell culture," *Biothechnol Bioeng.,* vol. 103, no. 4, pp. 655 - 663, 2009.

[88] F. Pampaloni, E. Reynaud and E. Stelzer, "The third dimension bridges the gap between cell culture and live tissue," *Nature Reviews. Molecular Cell Biology,* vol. 8, no. 10, pp. 839 - 845, 2007.

[89] J. Vaquero and F. Forriol, "Knee chondral injuries: Clinical treatment strategies and experimental models," *Injury, Int. J. Care Injured,* vol. 43, no. 6, pp. 694 - 705, 2012.

[90] C. Schmidt and J. Leach, "Neural tissue engineering: strategies for repair and regeneration," *Annual review of biomedical engineering,* vol. 5, no. 1, pp. 293 - 347, 2003.

[91] K. Shalumon, K. Anulekha, K. Chennazhi, H. Tamura, S. Nair and R. Jayakumar, "Fabrication of chitosan/poly(caprolactone) nanofibrous scaffold for bone and skin tissue engineering," *International Journal of Biological Macromolecules,* vol. 48, no. 4, pp. 571 - 576, 2011.

[92] M. Schieker, H. Seitz, I. Drosse, S. Seitz and W. Mutschler, "Biomaterials as scaffold for bone tissue engineering," *European journal of trauma,* vol. 32, no. 2, pp. 114 - 124, 2006.

[93] A. Song, A. Rane and K. Christman, "Antibacterial and cell-adhesive polypeptide and poly(ethylene glycol) hydrogel as a potential scaffold for wound healing," *Acta Biomaterialia,* vol. 8, no. 1, pp. 41 - 50, 2012.

[94] S. Cartmell, "Controlled Release Scaffolds for Bone Tissue Engineering," *Journal of pharmaceutical sciences,* vol. 98, no. 2, pp. 430 - 441, 2009.

[95] S. Sahoo, L. Ang, J. Goh and S. Toh, "Growth factor delivery through electrospun nanofibers in scaffolds for tissue engineering applications," *Journal of Biomedical Materials Research Part A,* vol. 93A, no. 4, pp. 1539 - 1550, 2009.

[96] T. Dang, A. Thai, J. Cohen, J. Slosberg, K. Siniakowicz, J. Doloff, M. Ma, J. Hollister-Lock, K. Tang, Z. Gu, H. Cheng, G. Weir, R. Langer and D. Anderson, "Enhanced function of immuno-isolated islets in diabetes therapy by co-encapsulation with an anti-inflammatory drug," *Biomaterials,* vol. 34, no. 23, pp. 5792 - 5801, 2013.

[97] C. Peroni, N. de Jesus Oliveira, C. Cecchi, E. Higuti and P. Bartolini, "Different ex Vivo and Direct in Vivo DNA Administration Strategies for Growth Hormone Gene Therapy in Dwarf Animals," in *Targets in Gene Therapy,* P. Y. You, Ed., Brazil, Intech, 2011, pp. 397 - 408.

[98] G. Pierre, I. Youssef, J. Utvik, S. Florent-Bechard, V. Barthelemy, C. Malaplate-Armand, B. Kriem, C. Stenger, V. Koziel, J. Olivier, M. Escanye, M. Hanse, A. Allouche, C. Desbene, F. Yen, R. Bjerkvig, T. Oster, S. Niclou and T. Pillot, "Ciliary Neurotrophic Factor Cell-Based Delivery Prevents Synaptic Impairment and Improves Memory in Mouse Models of Alzheimer's Disease," *The journal of neuroscience,* vol. 30, no. 22, pp. 7516 - 7527, 2010.

[99] F. J. O'Brien, "Biomaterials & scaffolds for tissue engineering," *materialstoday,* vol. 14, no. 3, pp. 88 - 95, 2011.

[100] V. Saldanha and D. A. Grande, "Extracellular matrix protein gene expression of bovine chondrocytes cultured on resorbable sca!olds," *Biomaterials,* vol. 21, pp. 2427 - 2431, 2000.

[101] A. S. Badami, M. R. Kreke, M. Shane Thompson, J. S. Riffle and A. S. Goldstein, "Effect of fiber diameter on spreading, proliferation, and differentiation of osteoblastic cells on electrospun poly(lactic acid) substrates," *Biomaterials,* vol. 27, no. 4, pp. 596 - 606, 2006.

[102] R. Hynes, "Cell adhesion: old and new questions," *Biochemical Sciences,* vol. 24, no. 12, pp. M33 - M37, 1999.

[103] F. Giancotti and E. Ruoslahti, "Integrin Signalling," *Science,* vol. 285, no. 5430, pp. 1028 - 1033, 1999.

[104] M. Lutolf and J. Hubbell, "Synthetic biomaterials as instuctive extracellular microenvironments for morphogenesis in tissue engineering," *Nature biotechnology,* vol. 23, no. 1, pp. 47 - 55, 2005.

[105] A. Kloxin, A. Kasko, C. Salinas and K. Anseth, "Photodegradable hydrogels for dynamic tuning of physical and chemical properties," *Science,* vol. 324, no. 5923, pp. 59 - 63, 2009.

[106] C. Yang, P. Hillas, J. Báez, M. Nokelainen, J. Balan, J. Tang, R. Spiro and J. Polarek, "The application of recombinant human collagen in tissue engineering," *BioDrugs,* vol. 18, no. 2, pp. 103 - 119, 2004.

[107] D. Macaya and M. Spector, "Injectable hydrogel materials for spinal cord regeneration," *Biomedical Materials,* vol. 7, no. 1, pp. 1 - 22, 2012.

[108] J. Drury and D. Mooney, "Hydrogels for tissue engineering: scaffold design variables and applications," *Biomaterials,* vol. 24, no. 24, pp. 4337 - 4351, 2003.

[109] J. Hubell, "Materials as morphogenic guides in tissue engineering," *Biotechnology,* vol. 14, no. 5, pp. 551 - 558, 2003.

[110] C. Huang, P. Reuben, P. D'lppolito, P. Schiller and H. Cheung, "Chondrogenesis of human bone marrow-derived mesenchymal stem cells in agarose culture," *The Anatomical Record Part A: Discoveries in Molecular, Cellular, and Evolutionary Biology,* vol. 278, no. 1, pp. 428 - 436, 2004.

[111] G. Karoubi, M. Ormiston, D. Stewart and D. Courtman, "Single-cell hydrogel encapsulation for enhanced survival of human marrow stromal cells," *Biomaterials,* vol. 30, no. 29, pp. 5445 - 5455, 2009.

[112] R. Mauck, S. Seyhan, G. Ateshian and C. Hung, "Influence of seding density and dynamic deformational loading on the developing structure/function relationships of chondrocyte-seeded agarose hydrogels," *Annals of Biomedical Engineering,* vol. 30, no. 8, pp. 1046 - 1056, 2002.

[113] J. Shapiro, J. Lakey, E. Ryan, G. Korbutt, E. Toth, G. Warnock, N. Kneteman and G. Rajotte, "Islet transplantation in seven patients with type 1 diabetes mellitus using a glucocorticoid-free immunosuppressive regimen," *The New England Journal of Medicine,* vol. 343, no. 4, pp. 230 - 238, 2000.

[114] M. Gonen-Wadmany, L. Oss-Ronen and D. Seliktar, "Protein-polymer conjugates for forming photopolymerizable biomimetic hydrogels for tissue engineering," *Biomaterials,* vol. 28, no. 26, pp. 3876 - 3886, 2007.

[115] N. Hunt, A. Smith, U. Gbureck, R. Shelton and L. Grover, "Encapsulation of fibroblasts causes accelerated alginate hydrogel degradation," *Acta Biomaterialia,* vol. 6, no. 9, pp. 3649 - 3656, 2010.

[116] L. Andrade, K. Arcanjo, H. Martins, J. Reis, M. Farnia, R. Borojevic and M. Duarte, "Fine structure and molecular content of human chondrocytes encapsulated in alginate beads," *Cell biology international,* vol. 35, no. 3, pp. 293 - 297, 2011.

[117] A. Jonitz, K. Lochner, K. Peters, A. Salamon, J. Pasold, B. Mueller-Hiike, D. Hansmann and R. Bader, "Differentiation capacity of human chondrocytes embedded in alginate matrix," *Connective Tissue Research,* vol. 52, no. 6, pp. 503 - 511, 2011.

[118] A. Smith, J. Harris, R. Shelton and Y. Perrie, "3D culture of bone-derived cells immobilised in alginate following light-triggered gelation," *Journal of Controlled Release,* vol. 119, no. 1, pp. 94 - 101, 2007.

[119] J. Yu, K. Du, Q. Fang, Y. Gu, S. Mihardja, R. Sievers, J. Wu and R. Lee, "The use of human mesenchymal stem cells encapsulated in RGD modified alginate microspheres in the repair of myocardial infarction in the rat," *Biomaterials,* vol. 31, no. 27, pp. 7012 - 7020, 2010.

[120] E. Alsberg, K. Anderson, A. Albeiruti, R. Franceschi and D. Mooney, "Cell-interactive alginate hydrogels for bone tissue engineering," *Journal of Dental Research,* vol. 80, no. 11, pp. 2025 - 2029, 2001.

[121] M. Pannunzio, I. Jou, A. Long, T. Wind, G. Beck and G. Balian, "A new method of selecting Schwann cells from adult mouse sciatic," *Journal o Neuroscience Methods,* vol. 149, no. 1, pp. 74 - 81, 2005.

[122] M. Marenzana, N. Wilson-Jones, V. Mudera and R. Brown, "The origins and regulation of tissue tension: Identification of collagen tension-fixation process in vitro," *Experimental Cell Research,* vol. 312, no. 4, pp. 423 - 433, 2006.

[123] L. Galois, S. Hutasse, D. Cortial, C. Rousseau, L. Grossin, M. Ronziere, D. Herbage and A. Freyria, "Bovine chondrocyte behaviour in three-dimensional type I collagen gel in terms of gel contraction, proliferation and gene expression," *Biomaterials,* vol. 27, no. 1, pp. 79 - 90, 2006.

[124] K. Ahmann, J. Weinbaurn, S. Johnson and R. Tranquillo, "Fibrin degradation enhances vascular smooth muscle cell proliferation and matrix deposition in fibrin-based tissue constructs fabricated in vitro," *Tissue Engineering: Part A,* vol. 16, no. 10, pp. 3261 - 3270, 2010.

[125] M. Voigt, C. Andree, N. Cosentino, H. Bannasch, A. Wenger and G. Stark, "Keratinocytes seeded fibrin micro-carriers reconstitute an epidermis in full thickness wounds," *European Journal of Plastic Surgery,* vol. 29, no. 4, pp. 163 - 168, 2006.

[126] S. Park, S. Park, S. Chung, K. Pai and B. Min, "Tissue-engineered cartilage using fibrin/hyaluronan composite gel and its in vivo implantation," *Artificial organs,* vol. 29, no. 10, pp. 838 - 845, 2005.

[127] A. Bach, H. Bannasch, T. Galla, K. Bittner and G. Stark, "Fibrin glue as matrix for cultured autologous urothelial cells in urethral reconstruction," *Tissue Engineering,* vol. 7, no. 1, pp. 45 - 53, 2001.

[128] W. Ho, B. Tawil, J. Dunn and B. Wu, "The behaviour of human mesenchymal stem cells in 3D fibrin clots: dpendence on fibrinogen concentration and clot structure," *Tissue Engineering,* vol. 12, no. 6, pp. 1587 - 1595, 2006.

[129] S. Lien, L. Ko and T. Huang, "Effect of pore size on ECM secretion and cell growth in gelatin scaffold for articular cartilage tissue engineering," *Acta Biomaterialia,* vol. 5, no. 2, pp. 670 - 679, 2009.

[130] X. Wang, Y. Yan, Y. Pan, Z. Xiong, H. Liu, J. Cheng, F. Liu, F. Lin, R. Wu, R. Zhang and Q. Lu, "Generation of three-dimensional hepatocyte/gelatin structures with rapid prototyping system," *Tissue Engineering,* vol. 12, no. 1, pp. 83 - 90, 2006.

[131] H. Yoo, E. Lee, J. Yoon and T. Park, "Hyaluronic acid modified biodegradable scaffolds for cartilage tissue engineering," *Biomaterials,* vol. 26, no. 14, pp. 1925 - 1933, 2005.

[132] E. Horn, M. Beaumont, X. Shu, A. Harvey, G. Prestwich, K. Horn, A. Gibson, M. Preul and A. Panitch, "Influence of cross-linked hyaluronic acid hydrogels on neurite

outgrowth and recovery from spinal cord injury," *Journal of Neurosurgery,* vol. 6, no. 2, pp. 133 - 140, 2007.

[133] W. Li, K. Danielson, A. P and R. Tuan, "Biological response of chondrocytes cultured in three-dimensional nanofibrous poly(ε-caprolactone) scaffolds," *Journal of Biomedical Materials Research - Part A,* vol. 67, no. 4, pp. 1105 - 1114, 2003.

[134] D. Benoit, M. Schwartz, A. Durney and K. Anseth, "Small functional groups for controlled differentiation of hydrogel-encapsulated human mesenchymal stem cells," *Nature Materials,* vol. 7, no. 10, pp. 816 - 823, 2008.

[135] S. Bryant and K. Anseth, "Hydrogel properties influence ECM production by chondrocytes photoencapsulated in poly (ethylene glycol) hydrogels," *Journal of Biomedical Materials Research,* vol. 59, no. 1, pp. 63 - 72, 2002.

[136] W. Koh, A. Revzin and M. Pishko, "Poly(ethylene glycol) hydrogel microstructures encapsulating living cells," *Langmuir,* vol. 18, no. 7, pp. 2459 - 2462, 2002.

[137] H. Shin, C. Lee, I. Cho, Y. Kim, Y. Lee, I. Kim, K. Park, N. Yui and J. Shin, "Electrospun PLGA nanofiber scaffolds for articular cartilage reconstruction: mechanical stability, degradation and cellular responses under mechanical stimulation in vitro," *Journal of Biomaterials Science, Polymer Edition,* vol. 17, no. 1-2, pp. 103 - 119, 2006.

[138] V. Sinha, K. Bansal, R. Kaushik, R. Kumria and A. Trehan, "Poly-ε-caprolactone microspheres and nanospheres: an overview," *International Journal of Pharmaceutics,* vol. 278, no. 1, pp. 1 - 23, 2004.

[139] X. Wei, C. Gong, M. Gou, S. Fu, Q. Guo, S. Shi, F. Luo, G. Guo, L. Qiu and Z. Qian, "Biodegradable poly(ε-caprolactone) - poly(ethylene glycol) copolymers as drug delivery system," *International Journal of Pharmaceutics,* vol. 381, no. 1, pp. 1 - 18, 2009.

[140] S. Bryant, R. Bender, K. Durand and K. Anseth, "Encapsulating chondrocytes in degrading PEG hydrogels with high modulus: engineering gel structural changes to facilitate cartilaginous tissue production," *Biotechnology and bioengineering,* vol. 86, no. 7, pp. 747 - 755, 2004.

[141] C. Nuttelman, M. Tripodi and K. Anseth, "Synthetic hydrogel niches that promote hMSC viability," *Matrix biology,* vol. 24, no. 3, pp. 208 - 218, 2005.

[142] C. Lin and K. Anseth, "PEG hydrogels for the controlled release of biomolecules in regeneratice medicine," *Pharmaceutical resarch,* vol. 26, no. 3, pp. 631 - 643, 2009.

[143] J. Zhu, "Bioactive modification of poly(ethylene glycol) hydrogels for tissue engineering," *Biomaterials,* vol. 31, no. 17, pp. 4639 - 4656, 2010.

[144] C. Mangold, C. Dingels, B. Obermeier, H. Frey and F. Wurum, "PEG-based multifunctional polyethers with highly reactive vinyl-ether side chains for click-type functionalization," *Macromolecules,* vol. 44, no. 16, pp. 6326 - 6334, 2011.

[145] J. Clapper, J. Skeie, R. Mullins and A. Guymon, "Development and characterization of photopolymerizable biodegradable materials from PEG-PLA-PEG block macromonomers," *Polymer,* vol. 48, pp. 6554 - 6564, 2007.

[146] A. Metters, C. Bowman and K. Anseth, "A statistical kinetic model for the bulk degradation of PLA-b-PEG-b-PLA hydrogel networks," *The journal of physical chemistry,* vol. 104, no. 30, pp. 7043 - 7049, 2000.

[147] C. Gong, S. Shi, P. Dong, B. Kan, M. Gou, X. Wang, X. Li, F. Luo, Y. Wei and Z. Qian, "Synthesis and characterization of PEG-PCL-PEG thermosensitive hydrogel," *International journal of pharmacuetics,* vol. 365, no. 1 - 2, pp. 89 - 99, 2009.

[148] M. Kar, Y.-R. V. Shih, D. O. Velez, P. Cabrales and . S. Varghese, "Poly(ethylene glycol) hydrogels with cell cleavable groups for autonomous cell delivery," *Biomaterials,* vol. 77, pp. 186 - 197, 2016.

[149] A. Jain, Y. Kim, R. McKeon and R. Bellamkonda, "In situ gelling hydrogels for conformal repair of spinal cord defects, and local delivery of BDNF after spinal cord injury," *Biomaterials,* vol. 27, no. 3, pp. 497 - 504, 2006.

[150] M. Rinaudo, "Main properties and current applications of some polysaccharides as biomaterials," vol. 57, no. 3, pp. 397 - 430, 2008.

[151] N. Hunt and L. Grover, "Cell encapsulation using biopolymer gels for regenerative medicine," *Biotechnology Letters,* vol. 149, no. 3, pp. 209 - 224, 2010.

[152] A. Hulshoff, T. Schricker, H. Elgendy, R. Hatzakorzian and R. Lattermann, "Albumin synthesis in surgical patients," *Nutrition,* vol. 29, no. 5, pp. 703 - 707, 2013.

[153] P. Tessari, "Protein metabolism in liver cirrhosis: From albumin to muscle myofibrils," *Current Opinion in Clinical Nutrition and Metabolic Care,* vol. 6, no. 1, pp. 79 - 85, 2003.

[154] B. Elsadek and F. Kratz, "Impact of albumin on drug delivery - new applications on the horizon," *Journal of Controlled Release,* vol. 157, no. 1, pp. 4 - 28, 2012.

[155] L. Oss-Ronen and D. Seliktar, "Polymer-conjugated albumin and fibrinogen composite hydrogels as cell scaffolds designed for affinity-based drug delivery," *Acta Biomaterialia,* vol. 7, no. 1, pp. 163 - 170, 2011.

[156] W. Gombotz and S. Wee, "Protein release from alginate matrices," *Advanced drug delivery reviews,* vol. 64, pp. 194 - 205, 2012.

[157] F. Johnson, D. Craig and A. Mercer, "Characterization of the block structure and molecular weight of sodium alginates," *Journal of Pharmacy and Pharmacology,* vol. 49, no. 7, pp. 639 - 643, 1997.

[158] L. Rioux, S. Turgeon and M. Beaulieu, "Characterization of polysaccharides extracted from brown seaweeds," *Carbohydrate Polymers,* vol. 69, no. 3, pp. 530 - 537, 2007.

[159] P. Eiselt, K. Lee and J. Mooney, "Rigidity of two-component hydrogels prepared from alginate and poly(ethylene glycol) - diamines," *Macromolecules,* vol. 32, no. 17, pp. 5561 - 5566, 1999.

[160] M. George and E. Abraham, "Polyionic hydrocolloids for the intestinal delivery of protein drugs: alginate and chitosan - a review," *Journal of Controlled Release,* vol. 114, no. 1, pp. 1 - 14, 2006.

[161] A. Chan and R. Neufeld, "Tuneable semi-synthetic network alginate for absorptive encapsulation and controlled release of protein therapeutics," *Biomaterials,* vol. 31, pp. 9040 - 9047, 2010.

[162] B. Sarker, R. Singh, R. Silvia, J. A. Roether, J. Kaschta, R. Detsch, D. W. Schubert, I. Cicha and A. R. Boccaccini, "Evaluation of fibroblasts adhesion and proliferation on alginate-gelatin crosslinked hydrogel," *PLoS ONE,* vol. 9, no. 9, pp. 1 - 12, 2014.

[163] I. Sandvig, K. Karstensen, A. M. Rokstad, F. L. Aachhmann, K. Formo, A. Sandvig, G. Skjak-Braek and B. L. Strand, "RGD-peptide modified alginate by a chemoenzymatic strategy for tissue engineering applications," *Society for Biomaterials,* vol. 00A, no. 00, pp. 1 - 11, 2014.

[164] Y. Hori, A. Winans and D. Irvine, "Modular injectable matrices based on alginate solution/microsphere mixtures that gel in situ and co-deliver immunomodulatory factors," *Acta Biomaterialia,* vol. 5, no. 4, pp. 969 - 982, 2009.

[165] J. Park, S. J. Lee, S. Chung, J. H. Lee, W. D. Kim, J. Y. Lee and S. A. Park, "Cell-laden 3D bioprinting hydrogel matrix depending on different compositions for soft tissue engineering: Characterization and evaluation," *Materials Science and Engineering: C,* vol. 71, pp. 678 - 684, 2017.

[166] S. Badylak, "The extracellular matrix as a scaffold for tissue reconstruction," vol. 13, no. 5, pp. 377 - 383, 2002.

[167] J. Lee, H. Yu, G. Lee, A. Ji, J. Hyun and H. Kim, "Collagen gel three-dimensional matrices combined with adhesive proteins stimulate neuronal differentiation of mesenchymal stem cells," *Journal of the royal society interface,* vol. 8, no. 60, pp. 998 - 1010, 2011.

[168] L. Cen, W. Liu, W. Zhang and Y. Cao, "Collagen tissue engineering: development of novel biomaterials and applications," *Pediatric Research,* vol. 63, no. 5, pp. 492 - 496, 2008.

[169] M. Patino, M. Neiders, S. Andreana, B. Noble and R. Cohen, "Collagen as an implantable material in medicine and dentistry," *Journal of Oral Implantology,* vol. 28, no. 5, pp. 220 - 225, 2002.

[170] S. Srivastava, S. Gorham, D. French, A. Shivas and J. Courtney, "In vivo evaluation and comparison of collagen, acetylated collagen and collagen/glycosaminoglycan compostie films and sponges as candidate biomaterials," *Biomaterials,* vol. 11, no. 3, pp. 155 - 161, 1990.

[171] Z. Feng and T. Nakamura, "Measurements of the mechanical properties of contracted collagen gels populated with rat fibroblasts or cardiomyocytes," *The Japanese society for artificial organs,* vol. 6, no. 3, pp. 192 - 196, 2003.

[172] G. Cunniffe and F. O'Brien, "Collagen scaffolds for orthopedic regenerative medicine," *JOM,* vol. 63, no. 4, pp. 66 - 73, 2011.

[173] W. Dai, N. Kawazoe, X. Lin, J. Dong and G. Chen, "The influence of structural design of PLGA/collagen hybrid scaffolds in cartilage tissue engineering," *Biomaterials,* vol. 31, no. 8, pp. 2141 - 2152, 2010.

[174] B. Harley and L. Gibson, "In vivo and in vitro applications of collagen-GAG scaffolds," *Chemical Engineering Journal,* vol. 137, no. 1, pp. 102 - 121, 2008.

[175] V. Vicens-Zygmunt, S. Estany, A. Colom, A. Montes-Worboys, C. Machahua, A. J. Sanabria, R. Llatjos, I. Escobar, F. Manresa, J. Dorca, D. Navajas, J. Alcaraz and M. Molina-Molina, "Fibroblast viability and phenotypic changes within glycated stiffened three-dimensional collagen matrices," *Respiratory Research,* vol. 16, no. 136, pp. 1 - 15, 2015.

[176] J. Rakar, M. P. Krammer and G. Kratz, "Human melanocytes mitigate keratinocyte-dependent contraction in an in vitro collagen contraction assay," *Burns,* vol. 41, no. 5, pp. 1035 - 1042, 2015.

[177] L. Yong and D. Mooney, "Hydrogels for tissue engineering," *Chemical reviews,* vol. 101, no. 7, pp. 1869 - 1880, 2001.

[178] X. Xu, A. K. Jha, D. A. Harrington, M. C. Farach-Carson and X. Jia, "Hyaluronic Acid-Based Hydrogels: from a Natural Polysaccharide to Complex Networks," *Soft Matter,* vol. 8, no. 12, pp. 3280 - 3294, 2012.

[179] A. Strom, A. Larsson and O. Okay, "Preparation and physical properties of hyaluronic acid-based cryogels," *Journal of Applied Polymer Science,* vol. 132, no. 29, 2015.

[180] H.-S. Kim, M. Song, E.-J. Lee and U. Shin, "Injectable hydrogels derived from phosphorylated alginic acid calcium complexes," *Materials Science and Engineering,* vol. 51, pp. 139 - 147, 2015.

[181] V. K. Lai, D. S. Nedrelow, S. P. Lake, B. Kim, E. M. Weiss, R. T. Tranquillo and V. H. Barocas, "Swelling of Collagen-Hyaluronic Acid Co-Gels: An In Vitro Residual Stress Model," *Annals of Biomedical Engineering,* vol. 44, no. 10, pp. 2984 - 2993, 2016.

[182] T. N. Snyder, K. Madhavan, M. Intrator, R. C. Dregalla and D. Park, "A fibrin/hyaluronic acid hydrogel for the delivery of mesenchymal stem cells and potential for articular cartilage repair," *Journal of Biological Engineering,* vol. 8, no. 10, pp. 1 - 11, 2014.

[183] L. S. Neves, P. S. Babo, A. I. Gonçalves, R. Costa-Almeida, S. G. Caridade, J. F. Mano, R. M. A. Domingues, M. T. Rodrigues, R. L. Reis and M. E. Gomes, "Injectable Hyaluronic Acid Hydrogels Enriched with Platelet Lysate as a Cryostable Off-the-Shelf System for Cell-Based Therapies," *Regenerative Engineering and Translational Medicine,* pp. 1 - 17, 2017.

[184] J. H. Hui, S. W. Chan, J. Li, J. C. Goh, L. Li, L. X. Ren and E. H. Lee, "Intra-articular delivery of chondroitin sulfate for the treatment of joint defects in rabbit model," *Journal of Molecular Histology,* vol. 38, pp. 483 - 489, 2007.

[185] A. Khanlari, T. C. Suekama, M. S. Detamore and S. H. Gehrke, "Mimicking the Extracellular Matrix: Tuning the Mechanical Properties of Chondroitin Sulfate

Hydrogels by Copolymerization with Oligo(ethylene glycol) Diacrylates," *Materials Research Society,* vol. 1622, pp. 189 - 195, 2014.

[186] F. Anjum, A. Carroll, S. A. Young, L. E. Flynn and B. G. Amsden, "Tough, Semisynthetic Hydrogels for Adipose Derived Stem Cell Delivery for Chondral Defect Repair," *Macromolecular bioscience,* pp. 1 - 13, 2017.

[187] S. Lu, C. Gao, X. Xu, X. Bai, H. Duan, N. Gao, C. Feng, Y. Xiong and M. Liu, "Injectable and self-healing carbohydrate-based hydrogel for cell encapsulation," *Applied Materials and Interfaces,* vol. 7, pp. 13029 - 13037, 2015.

[188] P. Janmey, J. Winer and J. Weisel, "Fibrin gels and their clinical and bioengineering applications," *Journal of the Royal Society Interface,* vol. 6, no. 30, pp. 1 - 10, 2009.

[189] F. Shaikh, A. Callanan, E. Kavanagh, P. Burke, P. Grace and T. McGloughlin, "Fibrin: A natural biodegradable scaffold in vascular tissue engineering," *Cells Tissues Organs,* vol. 188, no. 4, pp. 333 - 346, 2008.

[190] M. Mosesson, K. Siebenlist and D. Meh, "The structure and biological features of fibrinogen and fibrin," *Annals of the New York Academy of Sciences,* vol. 936, no. 1, pp. 11 - 30, 2001.

[191] M. Mosesson, "Fibrinogen and fibrin structure and functions," *Journal of Thrombosis and Haemostasis,* p. 1894–1904, 2005.

[192] K. Standeven, A. Carter, P. Grant, J. Weisel, I. Chernysh, L. Masova, S. Lord and R. Ariens, "Functional analysis of fibrin y-chain cross-linking by activated factor XIII: determination of a cross-linking pattern that maximises clot stiffness," *Blood,* vol. 110, no. 3, pp. 902 - 907, 2007.

[193] M. Radosevich, H. Goubran and T. Burnouf, "Fibrin sealant: scientific rationale, production methods, properties, and current clinical use," *Vox sanguinis,* vol. 72, no. 3, pp. 133 - 143, 1997.

[194] S. Rowe, S. Lee and J. Stegemann, "Influence of thrombin concentration on the mechanical properties of cell-seeded fibrin hydrogels," *Acta Biomaterialia,* vol. 3, no. 1, pp. 59 - 67, 2007.

[195] C. Herbert, C. Nagaswami, G. Bittner, J. Hubbell and J. Weisel, "Effects of fibrin micromorphology on neurite growth from dorsal root ganglia cultured in three-dimensional fibrin gels," *Journal of Biomedical Materials Research,* vol. 40, no. 4, pp. 551 - 559, 1998.

[196] N. Peppas, Y. Huang, M. Torres-Lugo, J. Ward and J. Zhang, "Physicochemical foundations and structural desing of hydrogels in medicine and biology," *Annual Review of Biomedical Engineering,* vol. 2, no. 1, pp. 9 - 29, 2000.

[197] M. Haugh, S. Thorpe, T. Vinardell, C. Buckley and D. Kelly, "The application of plastic compression to modulate fibrin hydrogel mechanical properties," *Journal of the Mechanical Behaviour of Biomedical Materials,* vol. 16, no. 1, pp. 66 - 72, 2012.

[198] T. Aper, A. Schmidt, M. Duchrow and H. Bruch, "Autologous blood vessels engineered from peripheral blood sample," *European Journal of Vascular and Endovascular Surgery,* vol. 33, no. 1, pp. 33 - 39, 2007.

[199] J. Singelyn, J. DeQuach, S. Sief-Naraghi, R. Littlefield, P. Schup-Magoffin and K. Christman, "Naturally derived myocardial matrix as an injectable scaffold for cardiac tissue engineering," *Biomaterials,* vol. 30, no. 29, pp. 5409 - 5416, 2009.

[200] M. Kim, S. Choi, S. Kim, I. Oh and M. Won, "Autologous chondrocyte implantation in the knee using fibrin," *Knee Surgery, Sprots Traumatology, Arthroscopy,* vol. 18, no. 4, pp. 528 - 534, 2010.

[201] S. Jockenhoevel, G. Zund, S. Hoerstrup, K. Chalabi, J. Sachweh, L. Demircan, B. Messmer and M. Turina, "Fibrin gel - advantages of a new scaffold in cardiovascular tissue engineering," *Cardio - Thoracic Surgery,* vol. 19, no. 4, pp. 424 - 430, 2001.

[202] A. Amini and L. Nair, "Injectable hydrogels for bone and cartilage repair," *Biomaedical Materials,* vol. 7, no. 2, pp. 1 - 13, 2011.

[203] L. Almany and D. Seliktar, "Biosynthetic hydrogel scaffolds made from fibrinogen and polyethylene glycol for 3D cell cultures," *Biomaterials,* vol. 26, no. 15, pp. 2467 - 2477, 2005.

[204] D. Dikovsky, H. Bianco-Peled and D. Seliktar, "The effect of structural alteration of PEG-fibrinogen hydrogel scaffolds on 3-D cellular morphology and cellular migration," *Biomaterials,* vol. 27, no. 8, pp. 1496 - 1506, 2006.

[205] S. L. Vega, M. Y. Kwon and J. A. Burdick, "Recent advances in hydrogels for cartilage tissue engineering," *European Cells and Materials,* vol. 33, pp. 59 - 75, 2017.

[206] S. Dinescu, B. Galateanu, E. Radu, A. Hermenean, A. Lungu, I. C. Stancu, D. Jianu, T. Tumbar and M. Costache, "A 3D Porous Gelatin-Alginate-Based-IPN Acts as an Efficient Promoter of Chondrogenesis from Human Adipose-Derived Stem Cells," *Stem Cells International,* pp. 1 - 17, 2015.

[207] Y. Wen, F. Li, C. Li, Y. Yin and J. Li, "High mechanical strength chitosan-based hydrogels cross-linked with poly(ethylene glycol)/polycaprolactone micelles for the controlled release of drugs/growth factors," *Journal of Materials Chemistry B,* no. 5, pp. 961 - 971, 2017.

[208] H.-f. Y. C.-a. G. J. L. X.-h. G. T. F. S. L. W.-s. F. X.-m. M. a. Z.-q. Y. Jian-feng Pan, "One-step cross-linked injectable hydrogels with tunable properties for space-filling scaffolds in tissue engineering," *Royal Society of Chemistry,* vol. 5, pp. 40820 - 40830, 2015.

[209] J. L. Holloway , H. Ma, R. Rai and J. A. Burdick, "Modulating hydrogel crosslink density and degradation to control bone morphogenetic protein delivery and in vivo bone formation," *Journal of Controlled Release,* vol. 191, pp. 63 - 70, 2014.

[210] M. Patenaude, S. Campbell, D. Kinio and T. Hoare, "Tuning Gelation Time and Morphology of Injectable Hydrogels Using Ketone−Hydrazide Cross-Linking," *Biomacromolecules,* vol. 15, no. 3, pp. 781 - 790, 2014.

[211] J. Guo, Z. Xie, R. T. Tran, D. Xie and J. Yang , "Click chemistry plays a dual role in biodegradable polymer design," *Advanced Materials,* vol. 26, no. 12, pp. 1906 - 1911, 2014.

[212] M. N. Moghadam and D. P. Pioletti, "Biodegradable HEMA-based hydrogels with enhanced mechanical properties," *Journal of Biomedical Materials Research,* vol. 104, no. 6, pp. 1161 - 1169, 2015.

[213] C. P. Chukwuemeka, J. Cupp and J. R. Sanders, "Using a Radial Diffusion Method to Investigate the Role of Plasmin Degradation of Fibrin in a Physical Model of an Early-phase Wound," *Wounds,* pp. 122 - 123, 2017.

[214] B. R. Hamlin, A. M. DiGioia, A. Y. Plakseychuk and T. J. Levison, "Topical versus intravenous tranexamic acid in total knee arthroplasty," *The Journal of Athroplasty,* vol. 30, no. 3, pp. 384 - 386, 2015.

[215] T. C. Gamboa-Martınez, V. Luque-Guillen, C. Gonzalez-Garcıa, J. L. G. Ribelles and G. G. Ferrer, "Crosslinked fibrin gels for tissue engineering: Two approaches to improve their properties," *Journal of Biomedical Materials Research A,* vol. 103A, no. 2, pp. 614 - 621, 2015.

[216] B. Balakrishnan, N. Joshi, A. Jayakrishnan and R. Banerjee, "Self-crosslinked oxidized alginate/gelatin hydrogel as injectable, adhesive biomimetic scaffolds for cartilage regeneration," *Acta Biomaterialia,* vol. 10, pp. 3650 - 3663, 2014.

[217] M. Nieto-Suárez, M. A. López-Quintela and M. Lazzari, "Preparation and characterization of crosslinked chitosan/gelatin scaffolds by ice segregation induced self-assembly," *Carbohydrate Polymers,* vol. 141, p. 175–183, 2016.

[218] L. Cai, R. E. Dewi and S. C. Heilshorn, "Injectable Hydrogels with In Situ Double Network Formation Enhance Retention of Transplanted Stem Cells," *Advanced Functional Materials,* vol. 25, pp. 1344 - 1351, 2015.

[219] E. J. Kim, J. S. Choi, J. S. Kim, Y. C. Choi and Y. W. Cho, "Injectable and Thermosensitive Soluble Extracellular Matrix and Methylcellulose Hydrogels for Stem Cell Delivery in Skin Wounds," *Biomacromolecules,* vol. 17, no. 1, pp. 4 - 11, 2016.

[220] H. C. Kolb, M. G. Finn and K. B. Sharpless, "Click Chemistry: Diverse Chemical Function from a Few Good Reactions," *Angewandte Chemie International Edition,* vol. 40, no. 11, pp. 2004 - 2021, 2001.

[221] M. Fan, Y. Ma, J. Mao, Z. Zhang and H. Tan, "Cytocompatible in situ forming chitosan/hyaluronan hydrogels via a metal-free click chemistry for soft tissue engineering," *Acta Biomaterialia,* vol. 20, pp. 60 - 68, 2015.

[222] H. Shih and C.-C. Lin, "Photoclick Hydrogels Prepared from Functionalized Cyclodextrin and Poly(ethylene glycol) for Drug Delivery and in Situ Cell Encapsulation," *Biomacromolecules,* vol. 16, pp. 1915 - 1923, 2015.

[223] V. Truong, K. Tsang, G. Simon, R. Boyd, R. Evans, H. Thissen and J. Forsythe, "Photodegradable gelatin-based hydrogels prepared by bioorthogonal click chemistry

for cell encapsulation and release," *Biomacromolecules,* vol. 16, no. 7, pp. 2246 - 2253, 2015.

[224] S. Middleton and B. Nichols, "PeproStat," Haemostatix Ltd, [Online]. Available: http://www.haemostatix.com/products/PeproStat.aspx. [Accessed 12 July 2013].

[225] S. Middleton and B. Nichols, "Topical Haemostatic Technology," Haemostatix Ltd, [Online]. Available: http://www.haemostatix.com/technology/topicalHaemostats.aspx. [Accessed 12 July 2013].

[226] L. A. Hidalgo-Bastida and S. H. Cartmell, "Mesenchymal Stem Cells, Osteoblasts and Extracellular Matrix Proteins: Enhancing Cell Adhesion and Differentiation for Bone Tissue Engineering," *Tissue engineering: Part B,* vol. 16, no. 4, pp. 405 - 412, 2010.

[227] C.-W. Huang, Z. Li, H. Cai, K. Chen, T. Shahinian and P. Conti, "Design, synthesis and validation of integrin α2β1-targeted probe for microPET imaging of prostate cancer," *European Journal of Nuclear Medicine and Molecular Imaging,* vol. 38, no. 7, pp. 1313 - 1322, 2011.

[228] "Alpha2beta1 integrin is the major collagen-binding integrin expressed on human Th17 cells," *European Journal of Immunology,* vol. 40, no. 10, pp. 2710 - 2719, 2010.

[229] S. R. Caliari and J. A. Burdick, "A practical guide to hydrogels for cell culture," *Nature Methods,* vol. 13, pp. 405-414, 2016.

[230] J. Schense and J. Hubbell, "Cross-linking exogenous bifunctional peptides into fibrin gels with factor XIIIa," *Bioconjugate Chemistry,* vol. 10, no. 1, pp. 75 - 81, 1999.

[231] B. Mann, A. Gobin, A. Tsai, R. Schmedlen and J. West, "Smooth muscle cell growth in photopolymerizd hydrogels with cell adhesive and proteolytically degradable domains: synthetic ECM analogs for tissue engineering," *Biomaterials,* vol. 22, no. 22, pp. 3045 - 3051, 2001.

[232] M. Mehta, C. M. Madl, S. Lee, G. N. Duda and D. J. Mooney, "The collagen I mimetic peptide DGEA enhances an osteogenic phenotype in mesenchymal stem cells when presented from cell-encapsulated hydrogels," *Journal of biomdical materials research. Part A,* vol. 103, no. 11, pp. 3516 - 3525, 2015.

[233] E. Liao, M. Yaszemski, P. Krebsbach and S. Hollister, "Tissue-Engineered Cartilage Constructs Using Composite Hyaluronic Acid/Collagen I Hydrogels and Designed Poly(Propylene Fumarate) Scaffolds," *Tissue Engineering,* vol. 13, no. 3, pp. 537 - 550, 2007.

[234] R. W. Farndale, D. J. Buttle and A. J. Barrett, "Improved quantitation and discrimination of sulphated glycosaminoglycans by use of dimethylmethylene blue," *Biochima et biophysica acta.,* vol. 883, no. 2, pp. 173 - 177, 1986.

[235] H. E. Davis, S. L. Miller, E. M. Case and J. K. Leach, "Supplementation of fibrin gels with sodium chloride enhances physical properties and ensuring osteogenic response," *Acta Biomaterialia,* vol. 7, pp. 691 - 699, 2011.

[236] M. S. Ventura Ferreira, W. Jahnen-Dechent, N. Labude, M. Bovi, T. Heironymus, M. Zenke, R. Schneider and S. Neurs, "Cord blood-hematoppoietic stem cell expansion

in 3D fibrin scaffolds with stromal support," *Biomaterials,* vol. 33, pp. 6987 - 6997, 2012.

[237] S. Lee, Y. Lee, C. Han, H. Lee and G. Khang, "Response of human chondrocytes on polymer surfaces with different micropore sizes for tissue-engineered cartilage," *Journal of Applied Polymer Science,* vol. 92, no. 5, pp. 2784 - 2790, 2004.

[238] J. L. Holloway, H. Ma, R. Rai and J. Burdick, "Modulating hydrogel crosslink density and degradation to control bone morphogenetic protein delivery and in vivo bone formation," *Journal of Controlled Release,* vol. 191, pp. 63 - 70, 2014.

[239] H. G. Yu, H. Chung, Y. S. Yu, J. M. Seo and J. W. Heo , "A new rapid and non-radioactive assay for monitoring and determining the proliferation of retinal pigment epithelial cells," *Korean journal of ophthalmology,* vol. 17, no. 1, pp. 29 - 34, 2003.

[240] M. Xu, D. J. McCanna and J. G. Sivak, "Use of the viability reagent PrestoBlue in comparison with alamarBlue and MTT to assess the viability of human corneal epithelial cells," *Journal of Pharmacological and Toxicological Methods,* vol. 71, pp. 1 - 7, 2015.

[241] L. A. Hidalgo-Bastida, S. Thirunavukkarasu, S. Griffiths, S. H. Cartmell and S. Naire, "Modeling and design of optimal flow perfusion bioreactors for tissue engineering applications," *Biotechnology and Bioengineering,* vol. 109, no. 4, pp. 1095 - 1099, 2012.

[242] M. Ahearne and D. J. Kelly, "A comparison of fibrin, agarose and gellan gum hydrogels as carriers of stem cells and growth factor delivery microspheres for cartilage regeneration," *Biomedical Materials,* vol. 8, no. 3, pp. 1 - 10, 2013.

[243] T. Toyoda, B. B. Seedhom, J. Q. Yao, J. Kirkham, S. Brookes and W. A. Bonass, "Hydrostatic pressure modulates proteoglycan metabolism in chondrocytes seeded in agarose," *Arthritis & Rheumatology,* vol. 48, no. 10, pp. 2865 - 2872, 2003.

[244] A. Guaccio, C. Borselli, O. Oliviero and P. A. Netti, "Oxygen consumption of chondrocytes in agarose and collagen gels: A comparative analysis," *Biomaterials,* vol. 29, no. 10, pp. 1484 - 1493, 2008.

[245] N. Stellwagen, "Electrophoresis of DNA in agarose gels, polyacrylamide gels and in free solution," *Electrophoresis,* vol. 30, no. S1, pp. S188 - S195, 2009.

[246] P. Nicotera and S. Orrenius, "The role of calcium in apoptosis," *Cell Calcium,* vol. 23, no. 2/3, pp. 173 - 180, 1998.

[247] M. Buschmann, Y. Gluzband, A. Grodzinsky, J. Kimura and E. Hunziker, "Chondrocytes in agarose culture synthesize a mechanically functional extracellular matrix," *Journal of Orthopaedic Research,* vol. 10, no. 6, pp. 745 - 758, 1992.

[248] Z. Huang, E. R. Nelson, R. L. Smith and S. B. Goodman, "The sequential expression profiles of growth factors from osteoprogenitors to osteoblasts in vitro," *Tissue Engineering,* vol. 13, no. 9, pp. 2311 - 2320, 2007.

[249] C. Vinatier, O. Gauthier, M. Masson, O. Malard, A. Moreau, B. H. Fellah, M. Bilban, R. Spaethe, G. Daculsi and J. Guicheuxx, "Nasal chondrocytes and fibrin sealant for

cartilage tissue engineering," *Journal of Biomaedical Research Part A,* vol. 89, no. 1, pp. 176 - 185, 2009.

[250] J. S. Park, M.-S. Shim, S. H. Shim, H. N. Yang, S. Y. Jeon, D. G. Woo, R. D. Lee, T. K. Yoon and K.-H. Park, "Condrogenic potential of stem cells derived from amniotic fuid, adipose tissue, or bone marrow encapsulated in fibrin gels containing TGF-B3," *Biomaterials,* vol. 32, pp. 8139 - 8149, 2011.

[251] H. D. Kim, J. Heo, Y. Hwand, S.-Y. Kwak, O. K. Park, H. Kim, S. Varghese and N. S. Hwang, "Extracellular-Matrix-Based and Arg-Gly-Asp–Modified Photopolymerizing Hydrogels for Cartilage Tissue Engineering," *Tissue Engineering. Part A,* vol. 21, no. 3 - 4, pp. 757 - 766, 2014.

[252] "RNA Quality Control," Biomedical Genomics, 2007. [Online]. Available: http://biomedicalgenomics.org/RNA_quality_control.html. [Accessed 25 April 2016].

[253] S. Krebs, M. Fischaleck and H. Blum, "A simple and loss-free method to remove TRIzol contaminations from minute RNA samples," *Analytical Biochemistry,* vol. 387, pp. 136 - 138, 2009.

[254] S. H. Park, S. R. Park and B. H. Miin, "Reinforcement Fibrin-Hyaluronic Acid Composite Gel for Tissue Engineering Cartilage Genesis," *Key Engineering Materials,* Vols. 342 - 343, pp. 12586 - 12592, 1986.

[255] M. K. Boushell, E. B. Hunziker and H. H. Lu, "Characterization of a Full Thickness Bovine Cartilage Defect Model," in *Orthopaedic Research Society,* New Orleans, Louisiana, 2014.

[256] M. L. de Vries-van Melle, E. W. Mandl, N. Kops, W. J. L. M. Koevoet , J. A. N. Verhaar and G. J. V. M. van Osch, "An Osteochondral Culture Model to Study Mechanisms Involved in Articular Cartilage Repair," *Tissue Engineering. Part C, Methods,* vol. 18, no. 1, pp. 45 - 53, 2012.

[257] S. Willerth, K. Arendas, D. Gottlieb and S. Sakiyama-Elbert, "Optimization of Fibrin Scaffolds for Differentiation of Murine Embryonic Stem Cells into Neural Lineage Cells," *Biomaterials,* vol. 27, no. 36, pp. 5990 - 6003, 2006.

[258] M. D. Sternlicht and Z. Werb, "How matrix metalloproteinases regulate cell behavior," *Annual review of cell and developmental biology,* vol. 17, no. 1, pp. 463 - 516, 2001.

[259] R. Srinivas, T. Sorsa, L. Tjaderhane, E. Niemi, A. Raustia, H. Pernu, O. Teronen and T. Salo, "Matrix metalloproteinases in mild and severe temporomandibular joint internal derangement of synovial fluid," *Oral surgery, oral medicine, oral pathology, oral radiology and endodontology,* vol. 91, no. 5, pp. 517 - 525, 2001.

[260] K. Yoshida, S. Takatsuka, E. Hatada, H. Nakamura, A. Tanaka, K. Ueki, K. Nakagawa, Y. Okada, E. Yamamto and R. Fukuda, "Expression of matrix metalloproteinases and aggrecanase in the synovial fluid of patients with symptomatic temporomandibular disorders," *Oral Surgery, Oral Medicine, Oral Pathology, Oral Radiology, and Endodontology,* vol. 102, no. 1, pp. 22 - 27, 2006.

[261] O. Castillo, Z. Dominguez, E. Angles-Cano and R. Marchi, "Endothelial fibrinolytic response onto an evolving matrix of fibrin," *BMC Hematology,* vol. 16, no. 9, pp. 1 - 9, 2016.

[262] B. Heissig, D. Dhahri, S. Eiamboonsert, Y. Salama, H. Shimazu, S. Munakata and K. Hattori, "Role of mesenchymal stem cell-derived fibrinolytic factor in tissue regeneration and cancer progression," *Cellular and Molecular Life Sciences,* vol. 72, pp. 4759 - 4770, 2015.

[263] A. D. Sharma, A. Al-Achi, D. Bahrend and J. F. Seccombe, "Adult cardiac surgery blood/blood product utilization in the post aprotinin era: an 855 patient, community hospital, retrospective experience," *Indian Journal of Thoracic and Cardiovascular Surgery,* vol. 32, no. 2, pp. 87 - 96, 2016.

[264] A. D. Shaw, M. Stafford-Smith, W. D. White, B. Phillips-Bute, M. Swiminathan, C. Milano, I. J. Welsby, S. Aronson, J. P. Matthew, E. D. Peterson and M. F. Newman, "The effect of aprotinin on outcome after coronary-artery bypass grafting," *The New England Journal of Medicine,* vol. 358, pp. 784 - 793, 2008.

[265] D. T. Mangano, I. C. Tudor and C. Dietzel , "The Risk Associated with Aprotinin in Cardiac Surgery," *The New England Journal of Medicine,* vol. 354, pp. 353 - 365, 2006.

[266] S. Schneeweiss, J. D. Seeger, J. Landon and A. M. Walker, "Aprotinin during coronary-artery bypass grafting and risk of death," *The New England Journal of Medicine,* vol. 358, pp. 771 - 783, 2008.

[267] D. Royston, "The current place of aprotinin in the management of beeding," *Anaesthesia,* vol. 70, no. s1, pp. 46 - e17, 2015.

[268] Y. Zhang, P. Heher, J. Hilborn, H. Redl and D. A. Ossipov, "Hyaluronic acid-fibrin interpenetrating double network hydrogel prepared in situ by orthogonal disulfide cross-linking reaction for biomedical applications," *Acta Biomaterialia,* vol. 38, pp. 23 - 32, 2016.

[269] J. Kim, B. Wu, S. M. Niedzielski, M. T. Hill, R. M. Coleman, A. Ono and A. Shikanov, "Characterizing natural hydrogel for reconstruction of three-dimensional lymphoid stromal network to model T-cell interactions," *Journal of Biomedical Materials Research,* vol. 103, no. 8, pp. 2701 - 2710, 2015.

[270] S. T. Coffin and G. R. Gaudette, "Aprotinin extends mechanical integrity time of cell-seeded fibrin sutures," *Journal of Biomedical Materials Research,* vol. 104, no. 9, pp. 2271 - 2279, 2016.

[271] S. Coffin and G. Gaudette, "Aprotinin extends mechanical integrity time of cell-seeded fibrin sutures," *Journal of Biomedical Materials Research Part A,* vol. 104, no. 9, pp. 2271 - 2279, 2016.

[272] Q. Ye, G. Zund, P. Benedikt, S. Jockenhoevel, S. Hoerstrup, S. Sakyama, J. Hubbell and M. Turina , "Fibrin gel as a three dimensional matrix in cardiovascular tissue engineering," *European Journal of Cardio-Thoracic Surgery* , vol. 5, no. 587 - 591, p. 17, 2000.

[273] P. Zilla, R. Fasol, P. Preiss, M. Kadletz, M. Deutsch, H. Schima, S. Tsangaris and P. Groscurth, "Use of fibrin glue as a substrate for in vitro endothelialization of PTFE vascular grafts," *Surgery,* vol. 105, no. 4, pp. 515 - 522, 1989.

[274] O. Cakmak, S. Babakurban, H. Akkuzu, S. Bilgi, E. Ovali, M. Kongur, H. Altintas, B. Yilmaz, B. Bilezikci, Z. Celik, M. Yakicier and F. Sahin, "Injectable tissue-engineered cartilage using commercially available fibrin glue," *Facial Plastics and Reconstructive Surgery*, vol. 123, no. 12, pp. 2986 - 2992, 2013.

[275] P. Sitek, A. Wysocka-Wycisk, F. Kepski, D. Krol, H. Bursig and S. Dylag, "PRP-fibrinogen gel-like chondrocyte carrier stabilized by TXA-preliminary study," *Cell and tissue banking,* vol. 14, no. 1, pp. 133 - 140, 2013.

[276] T. Synder, K. Madhavan, M. Intrator, R. Dregella and D. Park, "A fibrin/hyaluronic acid hydrogel for the delivery of mesenchymal stem cells and potential for articular cartilage repair," *Journal of biological engineering,* vol. 8, no. 10, pp. 1 - 11, 2014.

[277] R. A. Rahman, N. M. Sukri, N. M. Nazir, M. Aa'zamuddin , A. Radzi, . A. H. Zulkifly, A. C. Ahmad, . A. A. Hashi, S. A. Rahman and M. Sha'ban, "The potential of 3-dimensional construct engineered from poly(lactic-co-glycolic acid)/fibrin hybrid scaffold seeded with bone marrow mesenchymal stem cells for in vitro cartilage tissue engineering," *Tissue and Cell,* vol. 47, no. 4, pp. 420 - 430, 2015.

[278] M. Sheykhhasan, R. T. Qomi, N. Kalhor, M. Mehdizadeh and M. Ghiasi, "Evaluation of the ability of natural and synthetic scaffolds in providing an appropriate environment for growth and chondrogenic differentiation of adipose-derived mesenchymal stem cells," *Indian journal of orthopaedics,* vol. 49, no. 5, pp. 561 - 568, 2015.

[279] C. Ossendorf, C. Kaps, P. C. Kreuz, G. R. Burmester, M. Sittinger and C. Erggelet, "Treatment of posttraumatic and focal osteoarthritic cartilage defects of the knee with autologous polymer-based three-dimensional chondrocyte grafts: 2-year clinical results," *Arthritis research and therapy*, vol. 9, no. 2, p. R41, 2007.

[280] M. P. Lutolf and H. M. Blau, "Artificial Stem Cell Niches," *Advanced Materials,* vol. 21, no. 32-33, pp. 3255 - 3268, 2009.

[281] Z.-H. Kim, Y. Lee, S.-M. Kim, H. Kim, C.-K. Yun and Y.-S. Choi, "A Composite Dermal Filler Comprising Cross-Linked Hyaluronic Acid and Human Collagen for Tissue Reconstruction," *Journal of Microbiology and Biotechnology*, vol. 25, no. 3, pp. 399 - 406, 2015.

[282] V. X. Truong, K. M. Tsang, G. P. Simon, R. L. Boyd, R. A. Evans, H. Thissen and J. S. Forsythe, "Photodegradable Gelatin-Based Hydrogels Prepared by Bioorthogonal Click Chemistry for Cell Encapsulation and Release," *Biomacromolecules*, vol. 16, pp. 2246 - 2253, 2015.